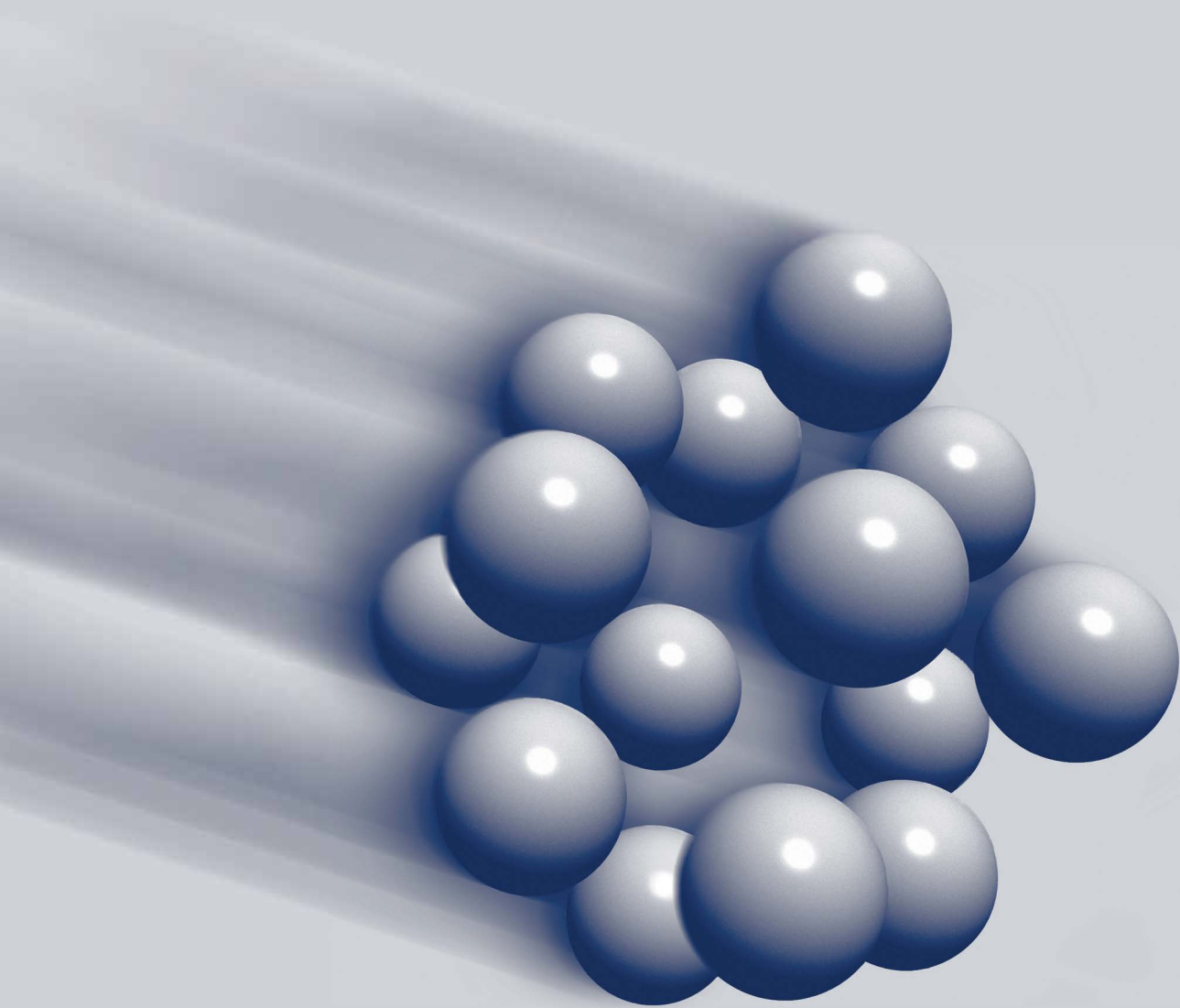


# General Particle Tracer



User Manual  
Version 3.43

**About GPT**

The General Particle Tracer GPT is developed, written and maintained by:

Dr. S.B. van der Geer

Dr. M.J. de Loos

For questions about GPT, please contact:

Pulsar Physics tel.: +31 40 2930585

Burghstraat 47 info@pulsar.nl

NL-5614 BC Eindhoven www.pulsar.nl

The Netherlands

**Acknowledgements**

The GPT code could never have matured without the constant flow of suggestions and constructive criticism of the GPT user community. It is slightly unfair to single out individuals, but it would be even more unfair not to mention anyone. We would like to express our thanks to Wim van Amersfoort and Andy Sessler for their confidence in and support of the first version of GPT. Furthermore, we would like to thank Gisela Pöplau for sharing her fast multigrid poisson solver and Marnix van der Wiel for his decade-long support of the GPT project as a whole. Many of the built-in components of GPT were originally developed by GPT users from universities, research institutions and the industry. We would like take this opportunity to thank them all for generously sharing their work with us.

# Preface .

Particle tracing is a very powerful tool in the design of charged-particle accelerators and beam lines. However, the computers used to be too slow to trace the number of particles needed to obtain reliable statistics in a reasonable amount of computing time. Therefore the particle tracing method was often abandoned and especially matrix/optical methods became popular. These alternative methods however are limited because they fail to simulate an actual beam. Most of these methods yield inaccurate results or cannot be applied at all when space-charge effects are dominant and/or paraxial approximations can not be used.

Currently it is possible to trace millions of particles through complex electromagnetic fields. Because of the enormous advances in computer technology all 3D effects and space-charge forces can be taken into account. This offers much more accurate results compared to matrix and paraxial codes. The General Particle Tracer (GPT) code offers all of these capabilities in a user-friendly and easy-to-customize package.

In order to be able to read this manual, basic knowledge of electromagnetism theory and the special theory of relativity is required. Experience with accelerator or beam-line design is useful, but is not necessary. For information about how to write custom GPT code, we refer to the GPT Custom Elements documentation.

# Table of contents

<b>Preface</b>	<b>iii</b>
<b>Table of contents</b>	<b>iv</b>
<b>Introduction</b>	<b>1</b>
<b>1 The GPT code</b>	<b>7</b>
1.1 The GPT inputfile .....	7
1.2 Running GPT .....	9
1.3 Error messages .....	11
1.4 Coordinate Systems .....	12
1.5 Space charge .....	14
1.6 Initial particle distribution .....	16
1.7 Equations of motion .....	24
1.8 Runge-Kutta .....	25
1.9 Output .....	26
1.10 GDF .....	28
1.11 Collector design .....	29
1.12 Automatic solving .....	31
<b>2 Tutorial</b>	<b>41</b>
2.1 Quadrupole focusing .....	42
2.2 The GPTwin user interface .....	46
2.3 Scanning the beam energy .....	52
2.4 Automatic solving .....	54
2.5 Electrostatic accelerator .....	62
2.6 Accuracy .....	64
2.7 Magnetic mirror .....	66
2.8 Element Coordinate System .....	68
2.9 Initial particle distribution .....	71
2.10 Photo-cathode, starting particles as function of time .....	74
2.11 Collector design .....	77
<b>3 GDF</b>	<b>83</b>
3.1 Basics .....	84
3.2 ASCI2GDF .....	85
3.3 ASTRA2GDF .....	86
3.4 FISH2GDF .....	87
3.5 FISHFILE .....	89
3.6 GDF2A .....	90
3.7 GDF2DXF .....	91
3.8 GDF2GDF .....	92
3.9 GDF2HIS .....	93
3.10 GDF2SDDS .....	94
3.11 GDF2VTP .....	95
3.12 GDFA .....	97
3.13 GDFFLATTEN .....	103
3.14 GDFMGO .....	104
3.15 GDFSELECT .....	109
3.16 GDFSOLVE .....	110
3.17 GDFTRANS .....	114
3.18 MR .....	115
3.19 RAW2GDF .....	117
<b>4 GPT Reference</b>	<b>119</b>
4.1 Inputfile syntax .....	120
4.2 Initial particle distribution .....	123
4.3 Timestep and output control .....	139
4.4 Accelerating structures .....	147
4.5 Static electric fields .....	155

4.6	Static magnetic fields .....	159
4.7	Field maps .....	174
4.8	Spacecharge.....	188
4.9	Scattering.....	203
4.10	Remove particles .....	210
4.11	Miscellaneous.....	212
4.12	Free Electron Laser (FEL), Wakefields, and CSR .....	216
4.13	Obsolete elements.....	223
<b>References</b>		<b>231</b>
<b>Index</b>		<b>233</b>



# Introduction

The General Particle Tracer (GPT) code is a well-established simulation platform for the study of charged particle dynamics in electromagnetic fields. The code is completely 3D, including the space-charge model. GPT can be conveniently customized without compromising its ease of use, accuracy or simulation speed, because of its modern implementation.

The first chapter of this manual describes the GPT kernel in detail. The second chapter is a tutorial introduction to GPT where simplified but practical examples are discussed. Although we recommend reading the first chapter first, some may prefer to start directly with the tutorial. Chapter three gives an overview of all pre- and postprocessing commands, many of which are also covered in the tutorial. Chapter four describes all the built-in GPT elements and keywords that can be used in the inputfile.

Customizing GPT is the subject of a separate manual, the GPT Programmer's Reference.

## Overview

The General Particle Tracer (GPT) is a software package developed to study 3D charged-particle dynamics in electromagnetic fields. Its purpose is to aid in the design of accelerators and beam lines by using modern, particle tracking techniques.

Over the past decade the GPT code has become a well-established simulation tool for the design of accelerators and beam lines. The General Particle Tracer (GPT) is based on 3D particle-tracking techniques, providing a solid basis for the study of all 3D and non-linear effects of charged-particles dynamics in electromagnetic fields. An embedded fifth order Runge-Kutta driver with adaptive stepsize control ensures accuracy while computation time is kept to a minimum. GPT provides various space-charge models, ranging from 1D interaction to fully 3D point-to-point calculations. Most standard beam-line components are represented in GPT. Users of GPT can easily extend the code to perform highly specialized calculations for specific applications. Hierarchical data analysis, automatic parameter scans and graphical output allow for fast and detailed interpretation of simulation results.

The GPT package consists of the GPT executable, which performs the actual calculations, and an extensive set of pre- and post-processing tools including data analysis tools and a graphical user interface.



## The GPT executable

A schematic of the GPT executable is shown in the figure below. The following subsections describe the individual components in detail.

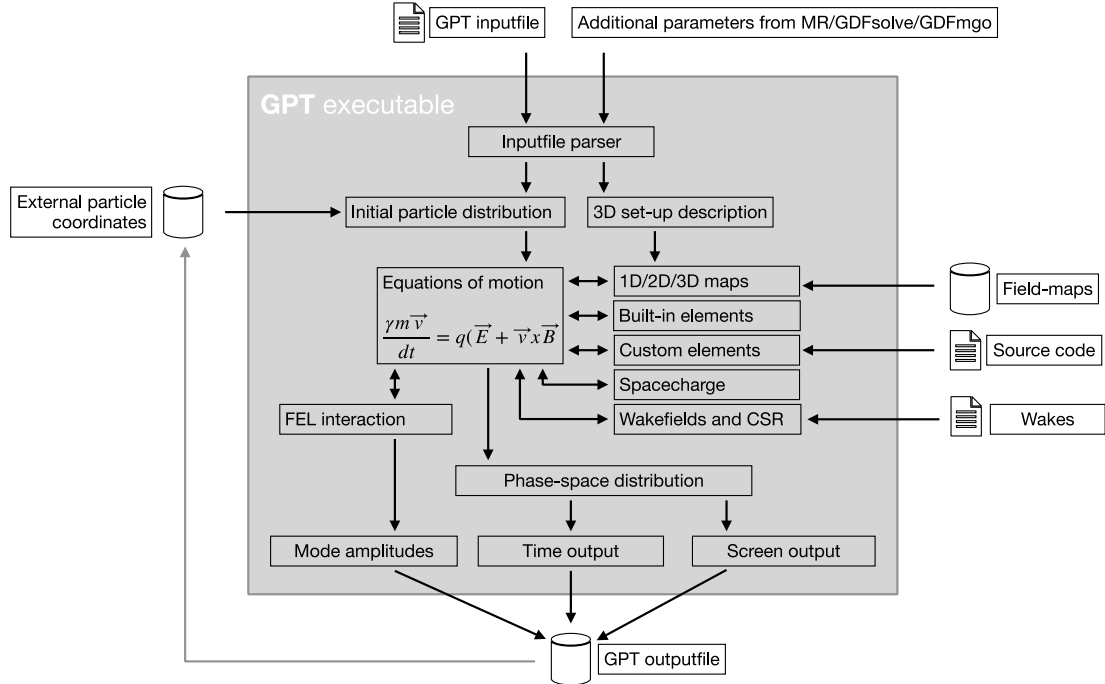


Figure 1: Schematic of the GPT executable.

The GPT executable starts by reading one or more ASCII inputfile(s) describing the simulation to perform. The inputfile specifies the initial particle distribution, the 3D electromagnetic field configuration (set-up), the required accuracy of the calculations and the output method. Standard expressions, functions and user-defined variables can be used for convenience. Optionally, a MR file (Multiple Run) can be used to automatically scan any number of parameters.

The initial particle distribution consists of a number of macro-particles, each typically representing a large number of elementary particles. Hammersley sequences are employed to minimize statistical errors due to the finite number of particles. Each projection of the initial distribution can be specified using the built-in particle generators or can be read from an external file. Complicated particle distributions can consist of any number of separate particle distributions, e.g. a beam with a halo or a mixture of different ion species each having their own distribution in position-momentum space.

The set-up defines the 3D electromagnetic field configuration as generated by the beam-line components. It can be composed of any number of built-in elements, external 2D or 3D field maps and user-defined expressions in custom elements. There is no limit to the number, location and orientation of the elements. The field-map elements can read electromagnetic field configurations calculated by external programs like TOSCA and the SUPERFISH set of codes. Measured field information can be used in the calculations as well. Furthermore, GPT users can easily write their own elements for specific configurations. The interface for writing custom elements is very broad and covers the development of user-defined electromagnetic field configurations, custom initial particle distributions, interfaces to other codes and additional differential equations. All GPT elements are developed in their own coordinate system and written in separate source files. These files are platform independent and allow users to freely exchange elements with each other without having to modify the GPT kernel. When an element is positioned in 3D space, the GPT kernel takes care of all required coordinate transformations.

The self-fields of the particles often form a crucial part of the electromagnetic fields through which these particles are tracked. Space-charge effects can be calculated using various depending on the type of simulation. The 3D space-charge routines include a fully 3D relativistic point-to-point interaction model, a fast hierarchical model and a very fast mesh-based PIC routine based on solving Poisson's equation in the rest frame of the bunch. For the simulation of (semi)continuous beams a 2D space-charge model can be used calculating relativistic point-to-ray interactions. Space-charge effects in cylindrical symmetric beams can be modeled using a relativistic 2D point-to-circle routine.

The equations of motion for the macro-particles are solved relativistically in the time domain using a 5<sup>th</sup> order embedded Runge-Kutta integrator with adaptive stepsize control. When required, the individual particle coordinates can be obtained with an accuracy of  $10^{-10}$ . The adaptive timestep mechanism modifies the stepsizes according to the gradients of the electromagnetic fields to ensure that all output satisfies the user-specified accuracy. Optionally, the equations of motion are combined with additional differential equations. This mechanism can be used to calculate beam-loading or FEL interaction completely self-consistently.

GPT has two available output modes: time and position output. Time output writes all particle coordinates at user specified time(s). Position output writes all particle coordinates passing any plane in 3D space. This output mode is also known as ‘nondestructive screen’ output. Time and position output can be freely mixed and any number of time and position outputs can be specified. Optionally, the electric and magnetic fields at the particle coordinates are also output, which greatly helps in understanding particle dynamics.

## Pre- and post-processing

Being able to simulate charged-particle dynamics in time-dependent 3D electromagnetic field configurations is usually far from sufficient for serious accelerator and beam-line design. The simulation data must be analyzed, parameters must be scanned and typically a comparison must be made between different scenarios. GPT is accompanied by a number of pre- and postprocessing programs as well as interfaces to other software packages to ease this step in the design process. These tools are combined with GPT and integrated into the MS-Windows graphical user interface, GPTwin. GPT on Linux machines uses command-line versions of these programs. The typical data flow within GPTwin is shown in Figure 2. The following subsections describe the individual components in detail.

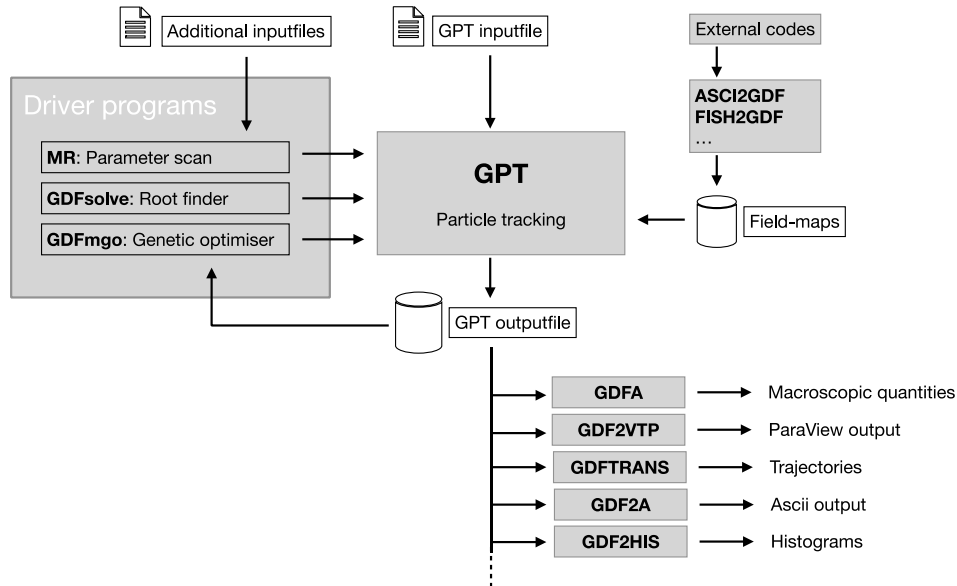


Figure 2: Typical data flow within GPTwin.

GPTwin is the all-integrated MS-Windows user interface for GPT. It provides a standard editor with on-line help capabilities for editing the inputfile. Inputfiles can be run and combined with any number of pre- and post-processing tools. GPTwin is able to directly plot the output of GPT as well as the results of data analysis tools like GDFA. Any number of plots can be shown in separate windows within the GPTwin user interface. When more windows show different views of the same outputfile, the hierarchy between the different views always remains synchronized.

The GPT results are written to a binary file for off-line analysis and interpretation. This file is written in the General Datafile Format (GDF), a multi-purpose, hierarchical file format specifically designed for efficiently storing large quantities of numerical data. It allows the post-processing components to easily extract information. The GDF format is used throughout the GPT kernel, the analysis tools and the GPT elements to keep the code compact and efficient. As shown in figure 2, various conversion utilities are available to convert to and from the GDF format.

The main analysis program for GPT output is GDFA. It calculates macroscopic beam parameters as function of simulation time, position or any scanned parameter. Typical macroscopic quantities like emittance, bunch length, average energy and beam radius can be obtained. GDFA is capable of calculating many other useful quantities as well. When needed, the list of GDFA programs can be extended with custom code to calculate the beam parameter of interest. GDFA maintains the original hierarchy in the GDF file when more parameters are simultaneously scanned simultaneously.

The MR and GDFSOLVE utilities can be used to instruct GPT to run a sequence of simulations with one or more parameters varying. The MR program scans over a pre-defined multi-dimensional parameter range while GDFSOLVE automatically optimizes a design until user-defined criteria are met.



# 1 The GPT code

## 1.1 The GPT inputfile

The crucial part of every GPT simulation consists of an ASCII inputfile describing the simulation to be performed. Apart from describing the set-up, this file also specifies the initial particle distribution, the calculation accuracy and when/where to write output. If desired, the inputfile can be split separated into a number of individual files. The extension of a GPT inputfile is `.in` by convention. A typical inputfile is shown in Listing 1-1 sending a very basic 6 nC, 2 MeV bunch of electrons through a single solenoid. The formal specification of the GPT inputfile syntax is given in section 4.1.

Listing 1-1: **Experi.in**: A simple GPT experiment.

```
1. # Basic beam parameters
2. Eo   = 2e6 ;                               # Energy [eV]
3. G    = 1+|qe|*Eo/(me*c^2) ;                # Corresponding Lorentz factor G
4. Beta = sqrt(1-G^-2) ;                      # Corresponding normalized velocity
5. rxy  = 5e-3 ;                               # Bunch radius [m]
6. zlen = 1e-3 ;                               # Bunch length [m]
7. Qtot = -6e-9 ;                             # Total charge in tlen [C]
8.
9. # Simulation parameters
10. nps  = 50 ;                                # Number of particles
11.
12. # Start bunch
13. setparticles("beam",nps,me,qe,Qtot) ;
14. setrxydist("beam","u", rxy/2, rxy) ;
15. setphidist("beam","u", 0, 2*pi) ;
16. setzdist("beam","u", 0, zlen) ;
17. setGdist("beam","u", G, 0) ;
18.
19. # Space-charge
20. if( Qtot!=0 ) spacecharge3D() ;
21.
22. # Set-up
23. solenoid("wcs","z",0.2, 0.1, 40000) ;
24.
25. # Output
26. tout(0,1.3e-9,0.02e-9) ;
```

The first section of this file defines the basic beam parameters. In this example, the bunch is cylindrically symmetric with an energy of 2 MeV. The bunch length is 1 mm, the beam radius is 5 mm and the total bunch charge is 6 nC. All parameters are in SI units, except when specified otherwise. None of the user variables have a special meaning; They are just for convenience to make the inputfile more readable.

The simulation parameters typically define the number of particles and the simulation accuracy. As the **accuracy** keyword, see section 4.3.2, is not specified in this case, the default timestep mechanism is used.

The electron bunch is started using the start elements as explained in section 1.6. The **setparticles** element fills the particle set "beam" with **nps** particles carrying a total charge **Qtot**. The predefined variables **me** and **qe** are the mass and charge of an electron respectively. After the particles are created, the following keywords each modify part of the real- or velocity-space of the set, allowing full control over the initial particle distribution. In this example, the real-space is defined as a uniform cylinder with a 5 mm radius and 1 mm longitudinal length. Transverse velocity is not defined here which means that this component is zero. Longitudinal velocity is introduced by setting the Lorentz factor  $\gamma$  without spread.

After the initial particle distribution is specified, the space-charge model must be chosen. In this case, a fully 3D treatment is requested with the **spacecharge3D** element as described in section 4.8.3. Because the beam

is cylindrically symmetric, the **spacecharge2Dcircle** element, see section 4.8.6, could be used as an alternative. The **if** statement removes the space-charge calculation altogether if the total charge is set to zero.

This set-up consists of only one solenoid, see section 4.6.15, positioned at longitudinal position  $z=0.2$  m. As explained in section 1.4.2 it is possible to position any element anywhere in 3D space in any orientation. A realistic set-up typically consists of more beam-line components, modeled as built-in elements, field maps or custom elements.

GPT is a time-domain particle tracer, as explained in section 1.7. Therefore, the most natural form of output is a list of all particle coordinates at specific times. This can be specified with a **tout** statement. Alternatively, interpolated particle coordinates can be calculated at specific positions using the **screen** element. Both forms of output are described in section 1.9.

## 1.2 Running GPT

The formal syntax of GPT is:

```
gpt [-hHv] [-o outfile] [-a outfile] infile [var=value] [GPTLICENSE=N]
```

<b>-h</b>	Print a short usage line.
<b>-H</b>	Print a usage line and a brief explanation of all options.
<b>-v</b>	Verbose mode: Various information about the progress of the simulation is written to <b>stderr</b> . Furthermore, the following numbers are printed at each timestep: <ul style="list-style-type: none"> <li>• The number of particles simulated in the current timestep.</li> <li>• The simulation time <math>t</math> [s].</li> <li>• The timestep <math>h</math> [s].</li> </ul>
<b>-j nCPU</b>	Run simultaneously over <b>nCPU</b> processors in a multi-processor system. When not specified, all cores in the system are used.
<b>-o outfile</b>	Write the result of the calculations to <b>outfile</b> . If not specified output is written to <b>stdout</b> . We refer to sections 1.9 and 1.10 for more information about GPT outputfiles.
<b>-a outfile</b>	Append to <b>outfile</b> . This option is for internal use only.
<b>infile</b>	The name of the file that describes the experiment to be simulated. A dash - can be specified to force GPT to read from <b>stdin</b> . It is possible to list more than one inputfile.
<b>var=value</b>	Assign a value to a variable used but not defined in the inputfile.
<b>GPTLICENSE=N</b>	Sets the GPT license number to <b>N</b> . Linux and standalone MS-Windows only.

GPTwin, the MS-Windows-based user interface for GPT, allows users to run a batch file containing the instructions to run GPT. Error messages and diagnostic output are shown in the message window. Linux users are advised to create a shell script.

The GPT executable reads the ASCII inputfile(s) describing the initial particle distribution, the calculation accuracy, the locations and parameters of all beam-line components and when/where output is required. Inputfiles typically have extension **.in**. The output of GPT is in the General Data Format (GDF), an hierarchical binary database specifically developed for the GPT project. Outputfiles typically have extension **.gdf**.

For an experiment named **experi**, the GPT inputfile is typically named **experi.in**. The correct instruction to run GPT is:

```
gpt [-v] -o experi.gdf experi.in [GPTLICENSE=N]
```

where the bracket notation indicates that these parameters are optional.

The **[-v]** notation means that **-v** can be optionally specified. When specified, verbose output is written in the message window in GPTwin and written to the terminal on Linux machines.

On Linux machines it is recommended to specify your GPT license number in the **GPTLICENSE** environment variable. Alternatively, it can be listed on the GPT command-line. On MS-Windows machines the license number is automatically set by the graphical user interface.

The command to run GPT is typically placed in a batch file named **experi.bat**. GPTwin users can open the batch file and click the Run button on the toolbar. GPTwin does not allow GPT inputfiles to be run directly. Linux users specify **sh experi.bat**, or any other instruction to run a sequence of commands. Especially when pre- or post-processing tools are required, such a batch file or shell script is very convenient. For example, the above GPT command is typically followed by an instruction to calculate particle trajectories and average beam parameters as shown in Figure 1-1:

```
gpt -o experi.gdf experi.in
gdftrans -o traj.gdf experi.gdf time x y z G
gdffa -o avgs.gdf experi.gdf time avgr avgz avgG
```

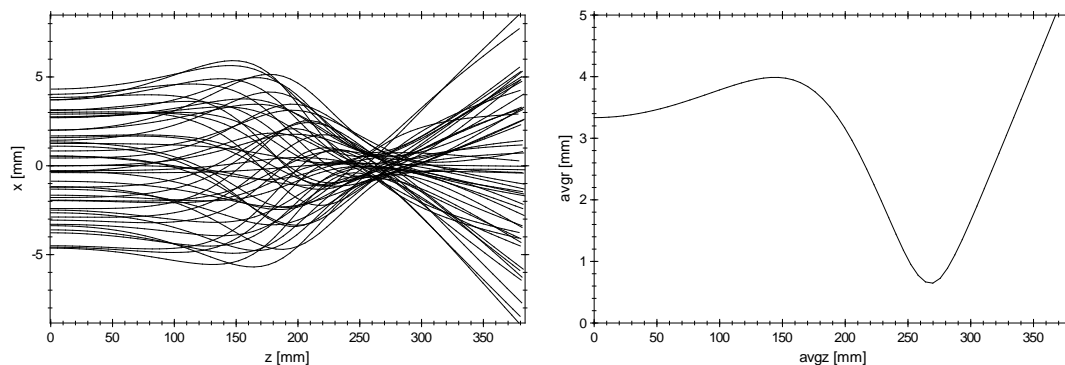


Figure 1-1: Particle trajectories and average beam parameters for the **experi.in** file as plotted by GPTwin. The experiment is a very strong solenoid lens at  $z=200$  mm. Strong aberrations are present.

It is possible to omit variables in the inputfile, and specify them on the command line instead. For example, if **rxxy** would not have been defined in the inputfile, the following line would produce correct results:

```
gpt [-v] -o experi.gdf experi.in [GPTLICENSE=N] rxxy=5e-3
```

It is also possible to pass string variables, for example to specify system dependent pathnames. For this to work, the string must be surrounded by double quotes escaped by a backslash: **mystring="\pathname"**.

**stderr** is Synonym for *Standard error*. This output is shown in the messages window of GPTwin. On Linux machines, it can be redirected using the operator **>&**. For example:

```
gpt -o test.gdf test.in >& logfile
```

**stdout** is Synonym for *Standard output*. This output is shown in the messages window of GPTwin, but can also serve as input to other applications using the operator **|**. For example:

```
gpt test.in | gdf2a
```

**stdin** is Synonym for *Standard input*. It can be the output of some other program using the operator **|** as shown in the example above.



## 1.3 Error messages

A message is displayed when something in the inputfile or in a datafile is incorrect. Such a message typically looks like one of the following lines:

```
filename(linenumbe)r: Warning: warningmessage.  
filename(linenumbe)r: Error: errormessage.
```

GPT continues execution after a warning but terminates after an error (with exit code 1). The difference between warnings and errors is sometimes vague and we prefer to give an error during initialization and a warning during simulation. When the program displays nothing, there are no errors or warnings. No news is good news! Continuous information can be specified with the `-v` option as described before.

Linux users can stop GPT during the simulation by pressing the interrupt key, usually Ctrl-C. The current timestep is completed and the program terminates with exit code 2. Results up to that point are saved in the outputfile. If you don't have enough patience to wait for a timestep to be completed you can press the interrupt key again. The timestep is not completed and the outputfile may be corrupted.

MS-Windows users can stop GPT by clicking the Stop button in GPTwin, or by ending the process with the Task Manager. You can activate the Task Manager by pressing the Delete key while holding down Ctrl and Alt. The current timestep is not saved and the simulation results may be lost.

## 1.4 Coordinate Systems

### 1.4.1 Element Coordinate System (ECS)

Elements in the set-up need to be positioned. The parameters of a single-turn solenoid for example are obvious: the radius, the current and the location. The code for a solenoid however is location independent; It is centered around the origin with the  $z$ -axis as its normal. The GPT kernel handles all necessary coordinate transforms needed to interface between the code for a solenoid and the actual solenoid positioned in the set-up.

The base coordinate system of GPT, the World Coordinate System or WCS, is a standard orthonormal right-handed Cartesian coordinate system. The GPT kernel assigns a private coordinate system to all elements of the inputfile. This coordinate system, the Element Coordinate System or ECS, is also right-handed orthonormal Cartesian. The various methods to specify such a coordinate system are described in later sections. Because both WCS and ECS are Cartesian, their relation can be defined by an orthonormal matrix  $\mathbf{M}$  and an offset  $\mathbf{o}$  as follows:

$$\mathbf{r}_{WCS} = \mathbf{M} \mathbf{r}_{ECS} + \mathbf{o} \quad [1.1]$$

or

$$\mathbf{r}_{ECS} = \mathbf{M}^{-1}(\mathbf{r}_{WCS} - \mathbf{o}) \quad [1.2]$$

where  $\mathbf{r}$  is a coordinate measured in either WCS or ECS.

Because the base GPT coordinate system is WCS, all particle positions are stored relative to this coordinate system. To obtain the electromagnetic fields generated by an element, the following actions are needed:

- Convert the particle coordinates to the ECS using [1.2].
- Calculate the electromagnetic fields using the code of the element.
- Transform these fields back to WCS.

To transform the fields to WCS, the following transformations are used:

$$\begin{aligned} \mathbf{E}_{WCS} &= \mathbf{M} \mathbf{E}_{ECS} \\ \mathbf{B}_{WCS} &= \mathbf{M} \mathbf{B}_{ECS} \end{aligned} \quad [1.3]$$

Because of the superposition principle, the electromagnetic fields of all the elements in the set-up can be added to obtain the total field at the position of a particle. This can be a time-consuming process when hundreds of elements are present. Therefore the kernel differentiates between two kinds of elements: global elements and local elements.

Global elements have a relatively long working range. The typical example is a large solenoid, possibly even around an accelerator section. The fields of all the global elements are added to obtain the total field generated by the global elements.

Local elements however have a relatively short working range. Their ranges are required to not extend past the centers of neighbouring local elements, and this is used internally to speed up the tracking. The `overlaptest` element can be used to check if any local elements are violating the rules.

### 1.4.2 Specifying an Element Coordinate System (ECS)

The first parameter of almost all GPT elements is the Element Coordinate System. For example, the syntax of a solenoid is:

```
solenoid(ECS,R,I) ;
```

The specification of an ECS consists of the following two parts:

- The name of the coordinate system relative to which the element is located. This usually is "**wcs**", but can also be the name of a previously defined Custom Coordinate System, CCS, see section 1.4.3.
- The offset  $\mathbf{o}$  and matrix  $\mathbf{M}$  as defined in [1.1].

Various methods are available for specifying an ECS. They all specify  $\mathbf{o}$  and  $\mathbf{M}$ , but the simple methods have restrictions. The transformation most commonly used is the "**z**" transformation. It moves an element in the  $z$ -direction without performing any rotations. Another useful coordinate system is the "**I**" transformation, the identity transformation. All methods available to specify an ECS are listed in Table 1-A.

Table 1-A: Element coordinate system specifications

ECS specification	<b>o</b>	<b>M</b>
"name", "I"	(0,0,0)	Identity
"name", "z", oz	(0,0,oz)	Identity
"name", ox, oy, oz, xx, xy, xz, yx, yy, yz	(ox,oy,oz)	See below

The columns of the matrix **M** are the unit vectors of the coordinate system to be specified. Those unit vectors, named **x**, **y** and **z**, are calculated from the specified parameters by:

$$\begin{aligned}
 \mathbf{x}' &= (\mathbf{xx}, \mathbf{xy}, \mathbf{xz}) \\
 \mathbf{y}' &= (\mathbf{yx}, \mathbf{yy}, \mathbf{yz}) \\
 \mathbf{x} &= \frac{\mathbf{x}'}{|\mathbf{x}'|} \\
 \mathbf{y} &= \frac{\mathbf{y}' - \mathbf{x} \cdot \mathbf{y}'}{|\mathbf{y}' - \mathbf{x} \cdot \mathbf{y}'|}
 \end{aligned} \tag{1.4}$$

By normalizing the  $\mathbf{x}'$  to obtain the unit  $x$ -vector and by subtracting the  $\mathbf{x}$  part from  $\mathbf{y}'$  while normalizing, the specified vectors need not to be of unit length nor orthogonal. The  $z$ -direction is calculated by the cross product:

$$\mathbf{z} = \mathbf{x} \times \mathbf{y} \tag{1.5}$$

### 1.4.3 Custom Coordinate System (CCS)

When a large set-up needs to be modeled, additional coordinate systems can be defined. Consider for example a number of beam-line components downstream a bending magnet. Determining the position and orientation of the elements after the first bending magnet is difficult in the WCS system. Especially in the design phase of a project when elements are relocated on a regular basis, specifying the element positions relative to a custom coordinate system can be convenient. In our example, the needed coordinate system would have a  $z$ -axis in the direction of the beam after the bend and an origin at the intersection of the axes.

For performance reasons, particles hold a reference to a Coordinate System, and only beamline components defined relative the particle's coordinate system are visible. The initial Coordinate system for all particles is "**wcs**". Defining a new CCS and positioning beamline components relative to this CCS will result in invisible beamline components: Particles need to be transferred to this new CCS, and only the **sectormagnet**, and last-resort **ccsflip**, elements can do this.

Any number of additional coordinate systems can be defined provided they are orthonormal and Cartesian. The coordinate transformations relating the particle coordinates between WCS and a Custom Coordinate System, CCS, are similar to [1.1] and [1.2]. See section 4.11.1 for the reference of CCS.

The ECS to WCS transforms are calculated by the GPT kernel by multiplying the transform from WCS to CCS and the transform from CCS to ECS:

$$\begin{aligned}
 \mathbf{M} &= \mathbf{M}_{\text{CCS}} \mathbf{M}_{\text{ECS}} \\
 \mathbf{o} &= \mathbf{M}_{\text{CCS}} \mathbf{o}_{\text{ECS}} + \mathbf{o}_{\text{CCS}}
 \end{aligned} \tag{1.6}$$

They are used as in [1.1] and [1.2].

Because matrix-vector multiplications are costly in terms of CPU time, they are not performed for identity transformations. The code checks for these identity transformations during the initialization, thus eliminating the coordinate transformation overhead for straight beam-line sections completely.

## 1.5 Space charge

The GPT code has a number of built-in elements to calculate Coulomb interactions, each optimized for a different application. All routines have certain characteristics that make them suitable for a subset of parameter space, but they can be very inefficient or even wrong if used incorrectly. To obtain correct simulation results, it is important to understand the assumptions made in every routine before selecting one. A summary of all built-in space-charge models in GPT is listed in Table 1-B.

Reference section 4.8 of this manual describes the inputfile syntax and the equations of each routine individually. This section focuses on the differences between the various models and gives guidelines for selecting one. Independent on the model selected, we strongly advise to regularly scan the number of particles using the MR/GDFA program combinations and to test convergence by plotting the parameters of interest as function of the logarithm of the number of particles.

Table 1-B: Summary of all GPT space charge elements. Complexity is in terms of the number of particles  $N$ .

Name	Complexity	Granularity effects	Dim	Description
<b>spacecharge3Dmesh</b>	$\mathcal{O}(N^{\sim 1.1})$	No	3D	PIC in rest frame
<b>spacecharge3Dtree</b>	$\mathcal{O}(N \log N)$	Yes	3D	Barnes-Hut in rest frame
<b>spacecharge3D</b>	$\mathcal{O}(N^2)$	Yes	3D	All pair-wise relativistic interactions
<b>spacecharge3Dclassic</b>	$\mathcal{O}(N^2)$	Yes	3D	All pair-wise interactions
<b>spacecharge2Dcircle</b>	$\mathcal{O}(N^2)$	No	2D	Cylindrically symmetric
<b>spacecharge2Dline</b>	$\mathcal{O}(N^2)$	No	2D	Continuous beam

All routines in GPT dealing with Coulomb interactions are derived from the electric field at the position of particle  $i$  due to Coulomb interaction with all particles  $j$ :

$$\mathbf{E}_i = \sum_{j \neq i} \frac{q_j}{4\pi\epsilon_0} \cdot \frac{\mathbf{r}_j - \mathbf{r}_i}{|\mathbf{r}_j - \mathbf{r}_i|^3} \quad [1.7]$$

Space charge is usually defined as the collective effect only, governed by long-range interactions with charge *density*. The summation hereby changes into an integration. This implies a smooth, fluidlike charge distribution, where the point-like nature of charge can be ignored. In that case, assuming the electrostatic case only, Coulomb interactions can be rewritten in terms of Poisson's equation:

$$-\nabla^2 V = \frac{\rho}{\epsilon_0} \quad [1.8]$$

where  $\rho$  is the charge density and  $V$  the electrostatic potential. This equation is numerically much easier to solve compared to the previous point-to-point calculation. However, it is plainly wrong in the case where granularity/stochastic effects play a dominant role. For example, random emission processes start bunches with excess electrostatic potential energy, which is subsequently converted via Coulomb interactions into additional momentum spread (heat). This process is not included in Poisson's equation. To determine if stochastic effects are important, one can use the following argument: A particle bunch with number density  $n$  [ $\text{m}^{-3}$ ] and no initial momentum will heat up to a temperature  $T_f$  given by:

$$k T_f = \frac{q^2}{4\pi\epsilon_0 a} \quad [1.9]$$

where  $a = (4\pi n/3)^{-1/3}$  is the Wigner-Seitz radius. This final temperature is reached on a timescale of the order of the inverse plasma frequency  $\omega_p^{-1} = \sqrt{m\epsilon_0/nq^2}$ . Consequently, stochastic effects are important if the initial temperature of the bunch is below  $T_f$ , and if the total simulation time is larger than  $\omega_p^{-1}$ . For typical thermionic and photo-emission processes this is typically not at all a concern.

We realize that the title of this section is confusing because the term space charge is used to denote all Coulomb interactions, including stochastic effects. For historical reasons the confusion is also present in the names of the GPT elements, all having **spacecharge** in their names. Some of them include granularity effects, some don't.

The **spacecharge3Dmesh** routine, see section 4.8.1, is GPT's workhorse space-charge routine. It is based on solving Poisson's equation in 3D in the rest frame of the bunch. It is by far the fastest space-charge model in the GPT code, but unsuitable for the calculation of granularity/stochastic effects. The method scales  $\mathcal{O}(N)$  in terms of CPU time and allows millions of particles to be tracked on a normal PC due to a tailor-made non-isotropic multi-grid solver

A single Lorentz transformation is used to convert the calculated electrostatic fields in the co-moving frame into both electric and magnetic fields for the tracking engine. Consequently, the model cannot be used if there is so much energy spread that velocities in the zero-momentum frame approach the speed of light. This is very unusual.

The **spacecharge3Dtree** routine, see section 4.8.2, calculates *all* Coulomb interactions from first principles, thus including space charge *and* granularity effects. It employs a Barnes-Hut method to hierarchically group particles together. This reduces the computational effort from  $\mathcal{O}(N^2)$  to  $\mathcal{O}(N \log N)$ , but the prefactor is considerably larger compared to the mesh version described above. Use this routing if granularity effects are expected to be significant.

Analogous to the PIC **spacecharge3Dmesh** method, a single Lorentz transformation is used to calculate the magnetic field in the laboratory frame.

The **spacecharge3D** element also calculates *all* Coulomb interactions from first principles. However, **spacecharge3D** uses Lorentz transforms for *each* pair-wise interaction, where **spacecharge3Dtree** transforms the bunch as a whole (analogous to the PIC **spacecharge3Dmesh** method). This approach makes this routine the 'best' with respect to physics included, but the drawback is significant: The computational cost is  $\mathcal{O}(N^2)$ , compared to  $\mathcal{O}(N \log N)$  for **spacecharge3Dtree**, limiting the amount of particles that can be tracked in practice to the order of a few thousand. Use this routine for cases with several ten percent relative energy spread, where particles are relativistic in the co-moving frame. Because of its 'from-first-principles' approach, this routine provides a great benchmarking opportunity for both **spacecharge3Dmesh** and **spacecharge3Dtree** for people with patience.

The **spacecharge3Dclassic** routine, see section 4.8.4, models non-relativistic point-to-point interaction. Because this routine scales  $\mathcal{O}(N^2)$  in terms of CPU time its use is restricted to simulations with just a few particles. In all other cases, **spacecharge3Dtree** is the best choice.

The **spacecharge2Dcircle** routine, see section 4.8.6, is a cylindrically-symmetric version of **spacecharge3D**. It also scales  $\mathcal{O}(N^2)$  in terms of CPU time, but because it uses one dimension less, the number of particles required before convergence is reached is reduced significantly. Longitudinal Lorentz transformations are applied to every binary interaction, allowing bunches with very large longitudinal energy spread to be simulated correctly. Bunches with extremely high azimuthal velocity, or relativistic transverse velocities cannot be modeled.

The **spacecharge2Dline** routine, see section 4.8.8, is a version of **spacecharge3D** written for continuous beams. It also scales  $\mathcal{O}(N^2)$  in terms of CPU time, but far less particles are required compared to full 3D modeling with any of the other space-charge models. Although no Lorentz transformations are applied, the model is relativistically correct. Bunches with large longitudinal velocity spread and extreme divergence cannot be modeled.

The GPT Custom Elements documentation describes how to extend GPT with a custom space-charge model in case none of the built-in routines are suitable for your application.

## 1.6 Initial particle distribution

Before GPT can start tracking the particle trajectories, the initial particle distribution must be specified. The initial particle distribution contains the initial position, momentum, mass, charge and release time of all particles. The start elements provide a very flexible method to start all kinds of initial particle distributions, ranging from GeV positron beams to less than eV electrons leaving a photo-cathode surface. Different ion species with different phase-space distributions can be specified using the same elements. All space-charge calculations are compatible with multiple particle species.

The GPT code uses particle-sets to store any number of initial particle distributions. Each set contains a number of initial particles and each set can be freely manipulated by the start elements before the simulation starts. For example, particles can be added to a set and the initial positions of the particles in a set can be modified according to a specified distribution. Different sets can contain different particle species, providing precise control over the initial distribution per particle species.

The philosophy behind the start elements is to use a number of keywords to specify the initial particle distribution, where each keyword only sets a certain projection of the distribution. For example, **setzdist** modifies the  $z$ -distribution of the particles, without affecting the  $xy$ -position coordinates and the velocity distribution.

It is possible to specify a uniform, Gaussian, linear, quadratic or cosine distribution for all one-dimensional projections of the initial phase-space distribution. Alternatively, if none of these distributions is applicable, it is possible to read the distribution from a separate file.

In two dimensions, a Gaussian distribution in the  $xy$ -plane can be obtained by specifying a Gaussian distribution in  $x$  with **setxdist**, followed by a Gaussian distribution in  $y$  with **setydist**. The result is shown in the left plot of Figure 1-2. However, in general a transverse distribution can not be set by setting the  $x$ - and  $y$ -projections independently. For example a uniform hard-edged cylinder in the  $xy$ -plane can not be produced by any combination of  $x$  and  $y$ -projections. Such transverse distributions require **setrxydist** to specify the distribution of particle radius and **setphidist** to set the angular distribution. To obtain a uniform distribution in the  $xy$ -plane, the radial distribution must be uniform between 0 and the beam radius, whereas the angular distribution must be uniform between 0 and  $2\pi$ . The result is shown in the right plot of Figure 1-2.

It is important to note that a uniform transverse (Cyl) distribution differs from a uniform one-dimensional (1D) distribution. To obtain a uniform distribution in the  $xy$ -plane, a linearly increasing number of particles must be launched as function of radius. In both cases, the user must specify a Uniform distribution, and GPT takes care of the difference.

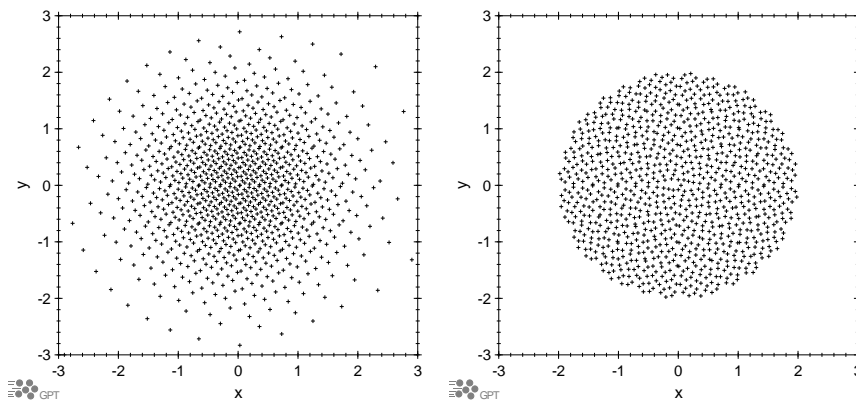


Figure 1-2: Gaussian distribution in the  $xy$ -plane (left) and uniform distribution in the  $xy$ -plane (right) with Hammersley sequences.

It is apparent that the points in Figure 1-2 are not drawn randomly from the underlying distribution. The reason for this is the following: Typically, GPT uses less particles in the simulations than are present in the actual experiment. Statistical fluctuations of a random creation process, also known as shot noise, scale as  $N^{-1/2}$  with  $N$  being the number of particles. Consequently, if both the actual and the simulated particles are created randomly, then the statistical noise of the small number of simulated particles is much larger than the actual shot noise. This is not desirable and GPT uses Hammersley sequences [1] to artificially reduce the

shot noise to  $1/N$ . This results in ordered patterns that provide a good tradeoff between ‘smooth’ distributions in both real and Fourier space. These low-discrepancy sequences reduce CPU time because less particles are needed compared to a random distribution for the same final accuracy.

It is important to realize that these Hammersley sequences should *not* be used when the number of macro-particles in the simulation matches the number of actual particles in the experiment. The combination of random starting conditions and one of the point-to-point space-charge models is essential for example for the investigation of disorder-induced heating, trajectory displacement and Boersch effect. To illustrate the difference, Figure 1-3 shows the same distributions as shown in Figure 1-2 but now without making use of Hammersley sequences.

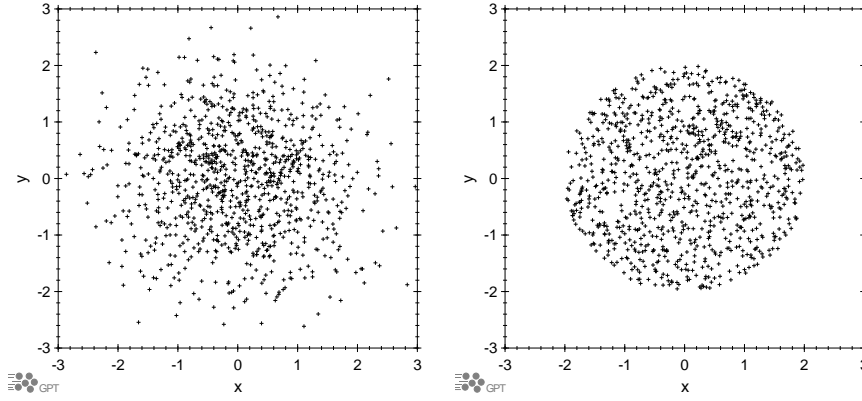


Figure 1-3: Gaussian distribution in the xy-plane (left) and uniform distribution in the xy-plane (right) drawn from a random distribution.

The Hammersley sequence samples  $N$  points with an  $r$ -dimensional uniform distribution quasi-randomly as:

$$x_i = \left\{ \left( i - \frac{1}{2} \right) / N, \Phi_2(i), \Phi_3(i), \dots, \Phi_r(i) \right\} \quad [1.10]$$

where  $i = 1 \dots N$ . The function  $\Phi_r(i)$  is the radical inversion function in the base of prime number  $r$ . It is obtained by first inverting the base  $r$  representation of an integer  $i$ , given as

$$i = a_0 + a_1 r + a_2 r^2 + \dots \quad [1.11]$$

and then computing

$$\Phi_r(i) = a_0 r^{-1} + a_1 r^{-2} + a_2 r^{-3} + \dots \quad [1.12]$$

Each coordinate of a Hammersley sequence is uniformly distributed between 0 and 1. To prevent correlations, every GPT element modifying a particle distribution uses the next prime number for the generation of the Hammersley sequence. To further illustrate the Hammersley sequences, the top row of Figure 1-4 shows the particle histograms for a Gaussian distribution centered around 0 with a sigma of 1 sampled with 1000 particles. The first plot shows a distribution based on the first equidistant Hammersley sequence, resulting in a perfect histogram. The next plots show the next Hammersley sequences, calculated from the prime bases 3, 5 and 7. The bottom row of Figure 1-4 shows the corresponding correlation between particle position and particle ID. The first plot shows the ascending equidistant case. The next plots show the typical ‘interference’ pattern between position and particle ID, getting slowly more profound for each next sequence. For a particle tracking application with typically 6 or 7 dimensions, this poses no problem.

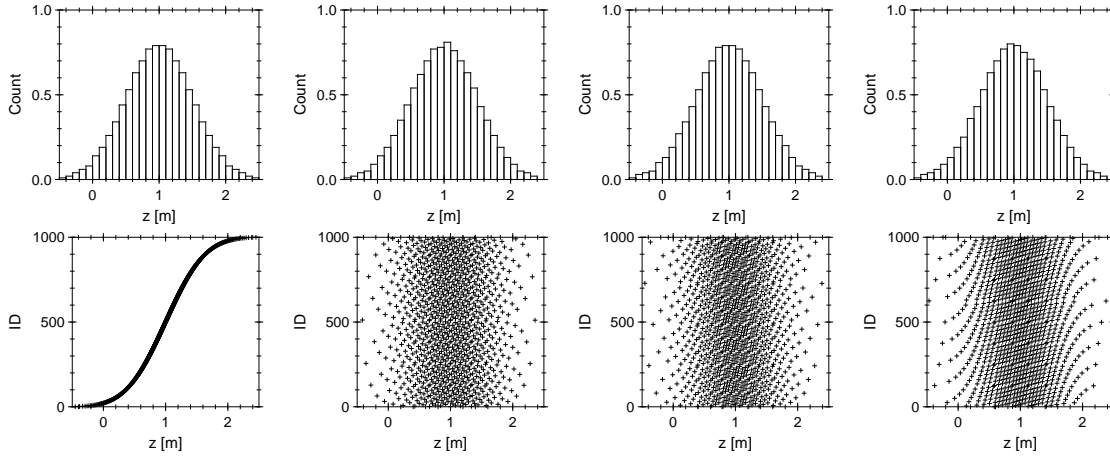


Figure 1-4: Histograms (top) and position versus particle ID correlation (bottom) for a Gaussian distribution based on the first four Hammersley sequences. The first equidistant and the next sequences based on prime numbers 3, 5 and 7 are shown.

### 1.6.1 Syntax

Before a specific particle distribution can be defined, first the number and type of particles must be specified using the **setparticles** keyword:

```
setparticles(set,N,m,q,Qtot) ;
```

The keyword **setparticles** defines a particle set name, for example **"beam"**, and generates **N** particles with all initial coordinates at zero. The total charge **Qtot** is uniformly distributed among all particles. To start 1000 electron macro-particles at the origin without velocity having a total charge of 100 pC one could use the line:

```
setparticles("beam",1000,me,qe,-100e-12) ;
```

**me** and **qe** are built-in constants having the mass and charge of an electron in [kg] and [C] respectively.

After all these 1000 particles are initialized, the initial distributions can be specified. This is done using a number of keywords, each setting only a particular aspect of the distribution. For example the longitudinal particle distribution, the *z*-coordinates of the particles, can be specified using the **setzdist** keyword.

```
setzdist(set,distribution) ;
```

The particle set must be **"beam"** again to match the **set** parameter of **setparticles**. The distribution is specified as a character indicating the distribution type, followed by its specific parameters. Examples are:

```
setzdist("beam","u",1,2) ; Uniform centered on  $z=1$  m having width 2 m.
```

```
setzdist("beam","g",1,1,2,2) ; Gaussian centered on  $z=1$  m,  $\sigma=1$  m and cut-off left and right at 2 sigma.
```

To switch off the Hammersley sequences, the distribution specifier must be prepended by a tilde **~** character. This results in a set of pseudo-random points, where it should be noted that each GPT run uses the same random number sequence. The **randomize** keyword must be used explicitly to instruct GPT to use a new random number sequence at each run.

The plots in Figure 1-2 are created using:

```
sigma=1 ;  
setxdist("beam","g",0,sigma,3,3) ;  
setydist("beam","g",0,sigma,3,3) ;  
and  
R=2 ;  
setrxydist("beam","u",R/2,R) ;  
setphidist("beam","u",0,2*pi) ;
```

The plots in Figure 1-3 are created using:

```
sigma=1 ;  
setxdist("beam","~g",0,sigma,3,3) ;  
setydist("beam","~g",0,sigma,3,3) ;  
and  
R=2 ;  
setrxydist("beam","~u",R/2,R) ;  
setphidist("beam","~u",0,2*pi) ;
```

Table 1-C lists the possible distribution types and their parameters. The columns 1D, Cyl and Sphere correspond to Cartesian, Cylindrical and Spherical coordinates used in some of the start elements.

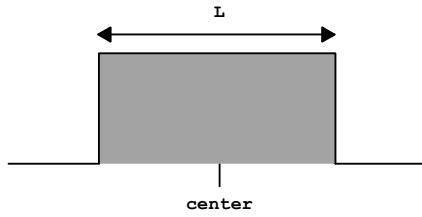


Table 1-C: Distributions, availability and parameters

Specifier	Type	1D	Cyl	Sphere	Parameters	Shape
"u"	Uniform	√	√	√	center, L	1
"g"	Gaussian	√	√		center, sigma, left, right	$e^{-x^2}$
"l"	Linear	√	√		center, L, hstart, hend	$x$
"q"	Quadratic	√			center, L	$1 - x^2$
"c"	Cosine	√			center, L, alpha	$\cos(x)$
"s"	Sphere		√		center, R	$\sqrt{1 - x^2}$
"f"	File	√	√		"filename", "x", "P(x)", scale, offset	Tabulated

### 1.6.2 Uniform distribution: "u", center, L

The uniform distribution is independent on its variable in the interval:  $[\text{center} - \frac{1}{2}L, \text{center} + \frac{1}{2}L]$



"u" Uniform distribution.  
**center** Center of the distribution.  
**L** Width of the distribution.

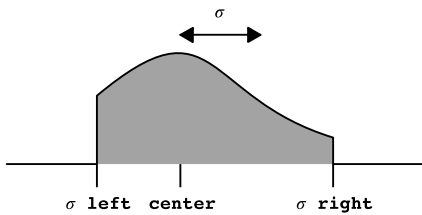
The probability  $P$  is given by:

$$P = \begin{cases} 1/L & \text{1D distribution in } x \\ r/(\text{center} \cdot L) & \text{Cylindrical distribution in } r \\ \sin(\theta) & \text{Spherical distribution in } \theta \\ 2 \sin(\text{center}) \sin(\frac{1}{2}L) & \end{cases} \quad [1.13]$$

in range  $[\text{center} - \frac{1}{2}L, \text{center} + \frac{1}{2}L]$  and 0 otherwise.

### 1.6.3 Gaussian distribution: "g", center, sigma, left, right

The Gaussian distribution models a truncated normal distribution in the interval:  $[\text{center} - \sigma \cdot \text{left}, \text{center} + \sigma \cdot \text{right}]$



"g" Gaussian distribution.  
**center** Center of the distribution.  
**sigma** RMS width  $\sigma$  of the distribution.  
**left** Left span of distribution relative to  $\sigma$ . A value of 10 effectively makes this parameter  $\infty$ . For cylindrical distributions this parameter must be set such that all radii are nonnegative, i.e.  $\text{left} < \text{center}/\sigma$ .  
**right** Right span of distribution relative to  $\sigma$ . A value of 10 effectively makes this parameter  $\infty$ .

The probability  $P$  in the range  $[\text{center} - \sigma \cdot \text{left}, \text{center} + \sigma \cdot \text{right}]$  is given by

$$P(x) = \frac{\sqrt{\frac{2}{\pi}} \exp\left(-\frac{(x - \text{center})^2}{2\sigma^2}\right)}{\sigma \left( \text{erf}\left(\frac{\text{left}}{\sqrt{2}}\right) + \text{erf}\left(\frac{\text{right}}{\sqrt{2}}\right) \right)} \quad [1.14]$$

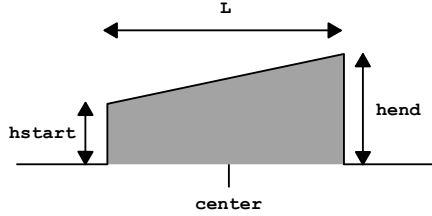
for 1D distributions in  $x$ . For cylindrical distributions in  $r$  it is given by

$$P(r) = \frac{r \exp\left(-\frac{(r - \text{center})^2}{2\sigma^2}\right)}{\sigma^2 \left(\exp\left(-\frac{\text{left}^2}{2}\right) - \exp\left(-\frac{\text{right}^2}{2}\right)\right) + \frac{\sqrt{2\pi} \text{center} \sigma}{2} \left(\text{erf}\left(\frac{\text{left}}{\sqrt{2}}\right) + \text{erf}\left(\frac{\text{right}}{\sqrt{2}}\right)\right)} \quad [1.15]$$

where  $P$  is zero outside the given range.

#### 1.6.4 Linear distribution: "l", center, L, hstart, hend

The linear distribution models a linearly increasing probability in the interval:  $[\text{center} - \frac{1}{2}L, \text{center} + \frac{1}{2}L]$



"l"	Linear distribution.
center	Center of the distribution.
L	Width of the distribution.
hstart	Start value of the distribution at $x = \text{center} - \frac{1}{2}L$ .
hend	End value of the distribution at $x = \text{center} + \frac{1}{2}L$ .

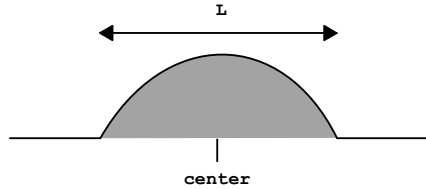
The probability  $P$  is given by:

$$P = \begin{cases} \frac{(2x - 2\text{center} + L)\text{hend} - (2x - 2\text{center} - L)\text{hstart}}{L^2 (\text{hend} + \text{hstart})} & \text{1D distribution in } x \\ \frac{6r ((2r - 2\text{center} + L)\text{hend} - (2r - 2\text{center} - L)\text{hstart})}{6L^2 \text{center} (\text{hend} + \text{hstart}) + L^3 (\text{hend} - \text{hstart})} & \text{Cylindrical distribution in } r \end{cases} \quad [1.16]$$

in range  $[\text{center} - \frac{1}{2}L, \text{center} + \frac{1}{2}L]$  and 0 otherwise.

#### 1.6.5 Quadratic distribution: "q", center, L

The quadratic distribution models a parabolic probability in the interval:  $[\text{center} - \frac{1}{2}L, \text{center} + \frac{1}{2}L]$



"q"	Quadratic (parabolic) distribution.
center	Center of the distribution.
L	Width of the distribution.

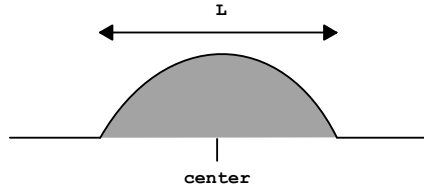
The probability  $P(x)$  for 1D distributions is given by:

$$P(x) = \frac{3}{2L^3} (L^2 - 4(x - \text{center})^2) \quad [1.17]$$

in range  $[\text{center} - \frac{1}{2}L, \text{center} + \frac{1}{2}L]$  and 0 otherwise.

### 1.6.6 Cosine distribution: "c", center, L, alpha

The cosine distribution models a cosine-shaped probability in the interval:  $[\text{center} - \frac{1}{2}L, \text{center} + \frac{1}{2}L]$



"c"	Cosine distribution.
center	Center of the distribution.
L	Width of the distribution.
alpha	Opening angle $\alpha$ [rad] between 0 and $2\pi$ selecting which part of the cosine to use.

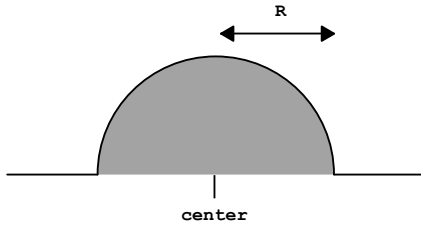
The probability  $P(x)$  for 1D distributions is given by:

$$P(x) = \frac{\cos\left(\frac{\alpha}{2}\right) - \cos\left(\frac{(x - \text{center})\alpha}{L}\right)}{L \cos\left(\frac{\alpha}{2}\right) - \frac{2L}{\alpha} \sin\left(\frac{\alpha}{2}\right)} \quad [1.18]$$

in range  $[\text{center} - \frac{1}{2}L, \text{center} + \frac{1}{2}L]$  and 0 otherwise.

### 1.6.7 Sphere distribution: "s", center, R

The sphere distribution models a half-circle in the interval:  $[\text{center} - R, \text{center} + R]$ .



"s"	Sphere (half circle) distribution.
center	Center of the distribution, must be 0 in the current implementation.
R	Radius of the distribution.

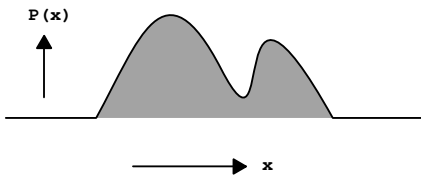
The probability  $P(r)$  for cylindrical distributions is given by:

$$P(r) = \frac{3r}{R^2} \sqrt{1 - \frac{r^2}{R^2}} \quad [1.19]$$

in the range  $0 < r < R$  and 0 otherwise.

### 1.6.8 File distribution: "f", "filename", "x", "P(x)", scale, offset

The file distribution reads a probability curve from a user-specified GDF file. This is particularly useful if the distribution can not be set by one of the built-in functions listed above.



"f"	File distribution.
"filename"	Name of the GDF file containing the tabulated probability curve.
"x"	Name of the array containing the $x$ variables.
"P(x)"	Name of the array containing the probability for each $x$ value.
scale	Scale for the $x$ values. Typically 1.
offset	Offset for the $x$ values. Typically 0.

The probability distribution is interpolated linearly between the specified  $(x, P_x)$  points on the probability curve. The  $x$ -coordinates are scaled by  $x \cdot \text{scale} + \text{offset}$  to accommodate a parametric linear coordinate transform. If this is not desired, set **scale** to 1 and **offset** to 0.

The  $x$  array can be of arbitrary length, where all  $x$  values must be in ascending order. The probability  $P(x)$  array must be of equal length and negative probabilities are not allowed. It is the responsibility of the user to specify sufficient points to model the desired curve with sufficient accuracy.

The distribution is implemented for 1D distributions and cylindrical distributions.

Example: Triangular z-distribution.

To set a triangular distribution between 4 and 8 for the initial z-coordinates, first a GDF file containing such a distribution must be created. The easiest way to do so is to first create an ASCII file containing the desired distribution **dist.txt** and subsequently convert this file to the GDF format. The latter can easily be done with the ASCII2GDF utility program in a batch file:

```
ascii2gdf -o dist.gdf dist.txt
```

```
1.  z    Pz
2.  4    0
3.  5    1
4.  6    2
5.  7    1
6.  8    0
```

Listing 1-2: File **dist.txt** specifies a triangular distribution between 4 and 8.

The produced **dist.gdf** can subsequently be used to set the desired distribution in a GPT inputfile:

```
setzdist("f", "dist.gdf", "z", "Pz", 1, 0) ;
```

### 1.6.9 Advanced syntax

To distribute a number of points along a given distribution  $f(x)$ , first the cumulative distribution  $F(x)$  is defined by:

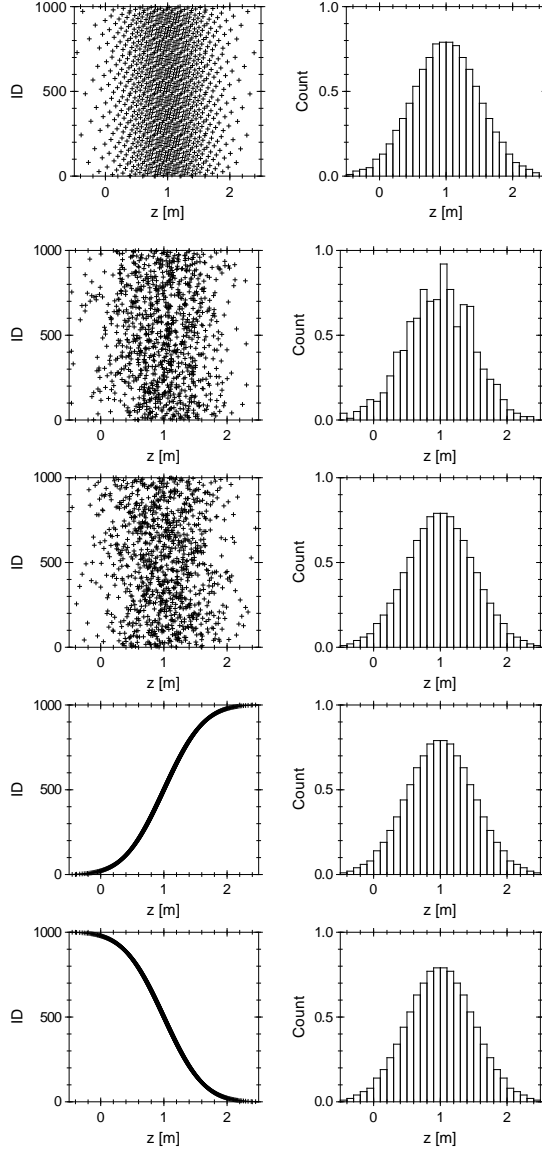
$$\begin{aligned} F(x) &\propto \int_{x'=-\infty}^x f(x') dx' && \text{For 1D distributions} \\ F(r) &\propto \int_{r'=0}^r f(r') 2\pi r dr' && \text{For cylindrical distributions} \\ F(\theta) &\propto \int_{\theta'=0}^{\theta} f(\theta') \sin(\theta') d\theta' && \text{For spherical distributions} \end{aligned} \quad [1.20]$$

In all cases,  $F$  is normalized by imposing  $F(\infty) = 1$ . Statistically it can be shown that  $F^{-1}$  maps a homogeneous distribution in the interval between 0 and 1 to a distribution following  $f$ .

The default GPT approach is to apply  $F^{-1}$  to a Hammersley sequence between 0 and 1. This results in a quasi-random set of low discrepancy points, following the distribution  $f$ . Alternatively,  $F^{-1}$  can be applied to a number of points randomly distributed in the interval between 0 and 1. This results in a pseudo-random set of points, as can be obtained by prepending the distribution specifier with a tilde  $\sim$  in the GPT inputfile. These two options are shown in the top rows of Table 1-D, where a gaussian distribution is approximated by 1000 points. Despite the low number of sample points, the Hammersley sequence results in a smooth histogram. The random distribution shows the actual fluctuations of 1000 randomly positioned particles.

Also shown in Table 1-D are three other methods to create a distribution. When a star  $\star$  is prepended to the distribution type, the distribution is created by applying  $F^{-1}$  to a randomized set of equidistant points. When a plus  $+$  respectively minus  $-$  sign is prepended to the distribution type, the same distribution is added in ascending respectively descending order. The latter two options result in either a monotonically rising or falling correspondence between the coordinate of interest and the particle number. The  $+$  order is identical to the first Hammersley sequence.

Table 1-D: Example of distribution modifiers.



Specifier: **h** or none

Example:

**setzdist("beam", "g", 1, .5, 3, 3) ;**

Description: Hammersley order following a specified distribution.

The 3<sup>rd</sup> sequence with prime base 5 is shown.

Specifier: **~**

Example:

**setzdist("beam", "~g", 1, .5, 3, 3) ;**

Description: Fully random set of points following a specific distribution.

Specifier: **\***

Example:

**setzdist("beam", "\*g", 1, .5, 3, 3) ;**

Description: Random order of an optimized sequence of points following a specified distribution.

Specifier: **+**

Example:

**setzdist("beam", "+g", 1, .5, 3, 3) ;**

Description: Ascending order of an optimized sequence of points following a specified distribution.

Specifier: **-**

Example:

**setzdist("beam", "-g", 1, .5, 3, 3) ;**

Description: Descending order of an optimized sequence of points following a specified distribution.

## 1.7 Equations of motion

The relativistic equations of motion of the individual macro-particles are solved by GPT. The position  $\mathbf{x}$  and the momentum  $\mathbf{p} = \gamma m \mathbf{v}$  are used as the coordinates of a particle. The equations of motion for particle  $i$  are given by:

$$\begin{aligned} \frac{d\mathbf{p}_i}{dt} &= \mathbf{F}_i \\ \frac{d\mathbf{x}_i}{dt} &= \mathbf{v}_i = \frac{\mathbf{p}_i c}{\sqrt{\mathbf{p}_i^2 + m_i^2 c^2}} \end{aligned} \quad [1.21]$$

The force on particle  $i$  is calculated using:

$$\mathbf{F}_i = q(\mathbf{E}_i + \mathbf{v}_i \times \mathbf{B}_i) \quad [1.22]$$

These equations of motion can not be solved for each particle individually because, due to the spacecharge, the force on each particle depends on the position of all other particles. Therefore we introduce the vector  $\mathbf{y}(t)$  containing the six coordinates of all the particles as a function of time  $t$ . The equations of motion [1.21] can then be rewritten as:

$$\frac{d\mathbf{y}(t)}{dt} = \mathbf{f}(t, \mathbf{y}(t)) \quad [1.23]$$

where  $\mathbf{f}(t, \mathbf{y}(t))$  is a combination of the equations [1.21] and [1.22] for every particle. The only boundary conditions are the initial particle coordinates at a specified time.

When additional differential equations are added, the variables are added to  $\mathbf{y}(t)$  and the differential equations are added to  $\mathbf{f}$ . The extra differential equations can be a function of all the particle coordinates, time and the variables of other differential equations. The boundary condition, the initial value of the variables, must be supplied for each value individually. Because GPT solves particles coordinates and extra variables simultaneously, the results are always self-consistent. The method used to solve [1.23] is described in the following section.

## 1.8 Runge-Kutta

In this section we describe the method GPT uses to solve equation [1.23]. This method is known as fifth-order embedded Runge-Kutta with adaptive stepsize control. The algorithm is efficient and has the capability to specify the accuracy of the calculations. For a detailed description we refer to Numerical Recipes [2] but we will briefly explain the algorithm here.

Basically the algorithm consists of a fifth-order Runge-Kutta step. It advances  $\mathbf{y}(t)$  to  $\mathbf{y}(t+h)$  by performing the following steps:

$$\begin{aligned} \mathbf{k}_1 &= h\mathbf{f}(t, \mathbf{y}) \\ \mathbf{k}_2 &= h\mathbf{f}(t + a_2h, \mathbf{y} + b_{21}\mathbf{k}_1) \\ &\vdots \\ \mathbf{k}_6 &= h\mathbf{f}(t + a_6h, \mathbf{y} + b_{61}\mathbf{k}_1 + \dots + b_{65}\mathbf{k}_5) \\ \mathbf{y}(t+h) &= \mathbf{y}(t) + c_1\mathbf{k}_1 + c_2\mathbf{k}_2 + c_3\mathbf{k}_3 + c_4\mathbf{k}_4 + c_5\mathbf{k}_5 + c_6\mathbf{k}_6 + \mathcal{O}(h^6) \end{aligned} \quad [1.24]$$

The values of the constants  $a$ ,  $b$  and  $c$  can be found in Table 1-E. To be able to monitor the accuracy of  $\mathbf{y}(t+h)$  each step is calculated again using an embedded fourth-order formula:

$$\mathbf{y}^*(t+h) = \mathbf{y}(t) + c_1^*\mathbf{k}_1 + c_2^*\mathbf{k}_2 + c_3^*\mathbf{k}_3 + c_4^*\mathbf{k}_4 + c_5^*\mathbf{k}_5 + c_6^*\mathbf{k}_6 + \mathcal{O}(h^5) \quad [1.25]$$

The error estimate  $\Delta$  is given by:

$$\Delta \equiv \mathbf{y}(t+h) - \mathbf{y}^*(t+h) = \sum_{i=1}^6 (c_i - c_i^*) \mathbf{k}_i \quad [1.26]$$

It is an indicator of the error made in the timestep. It is this difference that is kept to a specified degree of accuracy. Not too large, because this indicates an insufficient precision of the result. Not too small either, because a higher accuracy than needed is a waste of CPU time. Keeping the difference to the specified accuracy is done by adjusting the stepsize  $h$ .

$\Delta$  is a vector of all the coordinates of all the particles. The maximum absolute values for the position and momentum coordinates are defined as  $x_{\max}$  and  $mcy\beta_{\max}$  respectively. They are compared with  $x_{\text{err}}$  and  $\gamma\beta_{\text{err}}$ , set in the in the inputfile to define the desired accuracy. The error indicator  $\Lambda$  is defined as the largest of the two following ratios:

$$\Lambda = \max\left(\frac{\gamma\beta_{\max}}{\gamma\beta_{\text{err}}}, \frac{x_{\max}}{x_{\text{err}}}\right) \quad [1.27]$$

If  $\Lambda > 1$ , thus  $\gamma\beta_{\max} > \gamma\beta_{\text{err}}$  or  $x_{\max} > x_{\text{err}}$ , the step is not accepted and will be retried with:

$$h_{\text{new}} = \begin{cases} S \Lambda^{\frac{1}{4}} h_{\text{old}} & \text{if } S \Lambda^{\frac{1}{4}} > 0.10 \\ 0.10 h_{\text{old}} & \text{otherwise} \end{cases} \quad [1.28]$$

where  $h_{\text{new}}$  is chosen in such a way that for the next timestep  $\Lambda$  will approximately equal the safety parameter  $S$ .  $S$  is default set to 0.85. The timestep can decrease by no more than a factor of 10.

If  $\Lambda \leq 1$  the step is accepted with  $\mathbf{y}(t+h)$ . The next timestep is performed with:

$$h_{\text{new}} = \begin{cases} S \Lambda^{\frac{1}{5}} h_{\text{old}} & \text{if } S \Lambda^{\frac{1}{5}} < 5.0 \\ 5 h_{\text{old}} & \text{otherwise} \end{cases} \quad [1.29]$$

This ensures that no more than a factor of 5 increase in the stepsize is possible.

Table 1-E: Cash-Karp constants for embedded Runge-Kutta method.

$i$	$a_i$	$b_{ij}$					$c_i$	$c_i^*$
1							$\frac{37}{378}$	$\frac{2825}{27648}$
2	$\frac{1}{5}$	$\frac{1}{5}$					0	0
3	$\frac{3}{10}$	$\frac{3}{40}$	$\frac{9}{40}$				$\frac{250}{621}$	$\frac{18575}{48384}$
4	$\frac{3}{5}$	$\frac{3}{10}$	$-\frac{9}{10}$	$\frac{6}{5}$			$\frac{125}{594}$	$\frac{13525}{55296}$
5	1	$-\frac{11}{54}$	$\frac{5}{2}$	$-\frac{70}{27}$	$\frac{35}{27}$		0	$\frac{277}{14336}$
6	$\frac{7}{8}$	$\frac{1631}{55296}$	$\frac{175}{512}$	$\frac{575}{13824}$	$\frac{44275}{110592}$	$\frac{253}{4096}$	$\frac{512}{1771}$	$\frac{1}{4}$
$j =$		1	2	3	4	5		

## 1.9 Output

The output of GPT mainly consists of the position and normalized velocity coordinates of all the macro-particles and optionally the electromagnetic fields at the positions of the particles. The output is written in GPT Datafile Format, GDF, explained in detail in section 1.10. Three output mechanisms are currently implemented: Snapshot, Position and Field output.

The GPT code solves the differential equations of motion in time-domain. Consequently, the most efficient output mechanism is output at specific simulation times. This can be done with the **snapshot** keyword that writes the phase-space coordinates of all particles to the GPT outfile at arbitrary simulation time. Because the **snapshot** keyword does not affect the stepsizes taken by the ODE solver it produces no overhead, apart from disk I/O, and it does not affect the overall accuracy. Its syntax is described in detail in section 4.3.11.

To obtain electromagnetic field information, output can be generated with the **tout** keyword. This writes the electromagnetic fields at all particle positions to the outfile. Internally, **tout** instructs the GPT ODE solver to decrease its stepsizes in such a way that the particle coordinates are calculated exactly at the specified times. The used algorithm looks ahead and starts to make small adjustments to the stepsizes ahead of the requested output time in order to end correctly. As a result, **tout** slows down the ODE solver. Furthermore, because stepsizes can be decreased but are never increased, **tout** increases the overall accuracy of the simulations. Relying on such a side-effect is not wise and we strongly suggest using the **accuracy** keyword to specify the overall simulation accuracy. For the exact syntax of the **tout** keyword please see reference section 4.3.15.

Position output can be requested using the **screen** keyword. The particle coordinates are recorded when they pass a specified non-destructive plane in 3D space. Any number of planes with any orientation can be specified. Starting from GPT version 3.10, the screen implementation in GPT is 'perfect' in the sense that the interpolation error is always smaller or equal compared to the tracking error. Screens need to buffer particle coordinates and involve high-order interpolations. Consequently they are slower and more resource intensive compared to snapshots. For more information we refer to reference section 4.3.10.

The coordinates of all the particles and optionally the electromagnetic fields are written as individual arrays in the GPT outfile. For example, **x** is an array of all the x-coordinates of all the particles. A description of the arrays written to the outfile is given in Table 1-F. How the outfile is structured is explained in the next section.

Table 1-F: Description of the particle array columns in the GPT outfile.

Name	Snapshot	Screen	Tout	Description
<b>ID</b>	✓	✓	✓	Particle identification numbers
<b>x</b>	✓	✓	✓	$x$ coordinate [m]
<b>y</b>	✓	✓	✓	$y$ coordinate [m]
<b>z</b>	✓	✓	✓	$z$ coordinate [m]
<b>Bx</b>	✓	✓	✓	Normalized velocity $\beta_x$
<b>By</b>	✓	✓	✓	Normalized velocity $\beta_y$
<b>Bz</b>	✓	✓	✓	Normalized velocity $\beta_z$
<b>G</b>	✓	✓	✓	Lorentz factor $\gamma$
<b>rxy</b>	✓	✓	✓	Distance to $z$ -axis [m]
<b>t</b>		✓		Time when particles cross the screen [s]
<b>fEx</b>			✓	$E_x$ field at the particle coordinates [V/m].
<b>fEy</b>			✓	$E_y$ field at the particle coordinates [V/m].
<b>fEz</b>			✓	$E_z$ field at the particle coordinates [V/m].
<b>fBx</b>			✓	$B_x$ field at the particle coordinates [T].
<b>fBy</b>			✓	$B_y$ field at the particle coordinates [T].
<b>fBz</b>			✓	$B_z$ field at the particle coordinates [T].

Within a user element, the GPT kernel can be instructed to call a specified routine at every time output. Typically this mechanism is used to write the parameters of custom differential equations in the outfile, but it can also be very helpful for debugging purposes. For more information about this feature, we refer to the GPT Custom Elements documentation.



At the end of the simulation the variable **cputime** is written. It contains the CPU time, measured in seconds, between the previous and current time output. It can be used to track where most of the CPU time is spent. The variable **cputime** not listed in a time group is the total CPU time used by GPT.

## 1.10 GDF

The raw output of GPT consists of arrays containing the coordinates of the macro-particles and the electromagnetic fields. To efficiently accommodate additional output variables and parameter scans, the General Datafile Format (GDF) was developed. A GDF file consists of a number of GDF blocks, where every block contains binary data with a name. The  $x$ -coordinates of the particles for example are all written in a single block named **x**. Because all particle coordinates need to be written for every time output and every screen output, the GDF database is hierarchical. The blocks can be grouped together, where the groupname is itself a GDF block with name and data. For time output, the block name is **time** and the data is the simulation time itself. The GDF equivalent of such a structure is shown in Figure 1-5. Screen output is analogous, with block name **position** and the data the  $z$ -coordinate in the local coordinate system of the screen.

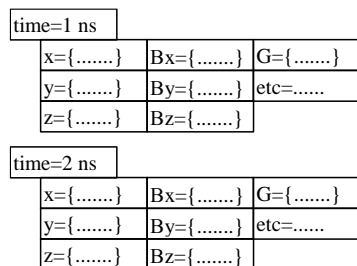


Figure 1-5: GDF representation of the outputfile. The blocks represent a GDF-object and its data. The indentation represents the internal hierarchy.

Although studying particle coordinates at consecutive output times can be very useful, generally macroscopic quantities like bunchlength, emittance and standard deviations are needed as well. The GDFA program is written to extract such information directly from the GPT outputfile.

When the effect of any parameter needs to be studied, the Multiple Run (MR) facility can be used. MR instructs GPT to run with one varying parameter and creates one outputfile containing the results of all the simulations. Such an outputfile is schematically shown in Figure 1-6 where the effects of different settings for the variable **phi** are calculated.

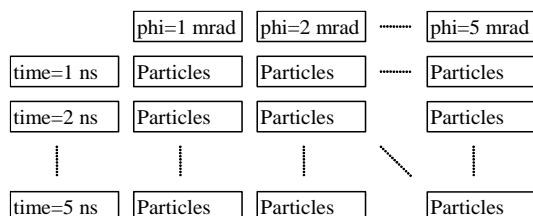


Figure 1-6: MR Output when multiple time output is written for various settings of the parameter **phi**.

GDFA needs extra information before such a file can be processed. When for example the average  $z$ -coordinate versus the standard  $z$  deviation, a measure for bunch length, need to be studied, there are two possibilities.

1. For every value of **phi**: Calculate average  $z$  and bunchlength. Every point is calculated at a different time.
2. For every time: Calculate average  $z$  and bunchlength. Every point is calculated for a different setting of **phi**.

One option is not arguably better than/preferable over the other, as depends on what needs to be studied. Therefore GDFA needs an additional parameter, which is named **group\_by**. This parameters pecifies which level of hierarchy collapses. The first of the two options mentioned above groups by **time**, the second groups by **phi**. The **group\_by** parameter itself is always output as an array in the produced outputfile.

For a complete description of all the GDF programs we refer to chapter 3. Table 1-E lists the description of the names in the GPT outputfile

## 1.11 Collector design

GPT can be used for the design of collectors and other beam-line elements in which scattering on the surface has to be taken into account. The main difference between collector design and normal beam-line simulations is found in the fact that scattered particles, generated when a particle hits a surface, play an important role.

The scattering process is modeled as two separate steps in GPT:

- Boundary elements calculate if, where and at what angle a particle hits a surface. Many basic surfaces like plates, cones, spheres, pipes, irises and toruses are built into GPT and custom shapes can be defined when needed.
- The physical properties of the surface material are defined by a scatter element. When a hit is detected, the corresponding scatter element removes the incident particle and optionally creates one or more new scattered particles with an energy and angle distribution as function of the incident energy and angle.

The separation between boundary elements and scatter elements allows the user to apply any material to any boundary.

The GPT kernel stores all raw scatter statistics to the GPT outputfile for subsequent analysis. The position, energy, charge and angle of incidence of both the incoming and scattered particle are recorded. For the design of a collector consisting of several plates, the FISHFILE program described in section 3.5 reads the raw scatter statistics and writes the statistics per collector plate. The electrostatic field inside the collector is typically calculated by Superfish and imported in GPT as a 2D field-map. To keep the GPT inputfile and the Superfish file consistent, it is possible to generate the boundary description required in the GPT inputfile automatically from the Superfish file.

### 1.11.1 Boundary elements

GPT boundary elements, like a hollow pipe or sphere, calculate 2D surfaces in 3D space. They determine if a particle trajectory crosses the boundary and, if so, calculate the intersection point, angle of incidence and interpolated momentum. The applied scatter model, as described in section 1.11.2, determines the fate of the incident particle. Typically it is removed and optionally (back) scattered particles are generated.

A 2D boundary in 3D space can be defined by:

$$f(x, y, z) = 0 \quad [1.30]$$

For example, the boundary of a hollow sphere with radius  $r$  is:

$$f(x, y, z) = x^2 + y^2 + z^2 - r^2 = 0 \quad [1.31]$$

All boundary elements implemented in GPT and their corresponding boundary equation are listed in section 4.9. The cone, iris, pipe, sphere and torus elements are used to model cylindrically symmetric geometries. The plate element can be used to model asymmetric geometries.

To detect if a particle trajectory crosses a boundary, the trajectory is first approximated by straight line segments between consecutive successful Runge-Kutta steps. As an optimization, the bounding-boxes of all elements are first used to determine if a line segment makes any chance of crossing the boundary. For example, a line segment running from  $(x_1, y_1, z_1)$  to  $(x_2, y_2, z_2)$  with positive  $z_1$  and positive  $z_2$  can never intersect with a plate at  $z=0$  and a line with  $x_1 > R$  and  $x_2 > R$  can never intersect with a pipe with radius  $R$ . If the bounding-box tests does not rule out an intersection, the line segment is parameterized to a single variable  $\lambda$ :

$$\mathbf{P}(\lambda) = \begin{pmatrix} x_1 + \lambda \Delta x \\ y_1 + \lambda \Delta y \\ z_1 + \lambda \Delta z \end{pmatrix} \quad [1.32]$$

where  $\Delta = (x_2 - x_1, y_2 - y_1, z_2 - z_1)$ . To stay between the start- and endpoint of the line segments,  $\lambda$  must always be between 0 and 1. Solving the intersection point  $\mathbf{P}(\lambda)$  is identical to solving  $\lambda$  from:

$$f(\mathbf{P}(\lambda)) = 0 \text{ where } 0 < \lambda < 1 \quad [1.33]$$

In the case of a sphere, this yields the following second-order equation:

$$a\lambda^2 + b\lambda + c = 0 \quad [1.34]$$

where

$$\begin{aligned} a &= \Delta x^2 + \Delta y^2 + \Delta z^2 \\ b &= 2(\Delta x x_1 + \Delta y y_1 + \Delta z z_1) \\ c &= x_1^2 + y_1^2 + z_1^2 - r^2 \end{aligned} \quad [1.35]$$

We could have expected the boundary test for a sphere to be a second-order equation because a line and a hollow sphere can have a maximum of two intersections. Using the same argument, testing a plate intersection results in a first-order expression and a torus intersection test requires solving a fourth-order equation.

When more boundaries are present, they must all be tested. When more boundaries are crossed, the boundary with the smallest positive  $\lambda$  is the nearest and the one actually hit. When the intersection point of the nearest boundary is calculated, the surface normal  $\mathbf{n}$  at the intersection point  $\mathbf{P}$  is determined using the gradient of  $f$ :

$$\mathbf{n}(x, y, z) = \nabla f \quad [1.36]$$

When the surface normal is known, the angle of incidence  $\alpha$  is given by:

$$\alpha = \cos^{-1} \left( \frac{\mathbf{n} \cdot \Delta}{|\mathbf{n}| |\Delta|} \right) \quad [1.37]$$

### 1.11.2 Scatter elements

Whenever a boundary element detects a particle hitting its surface, the corresponding scatter element is called into action. This element defines the physical properties of the surface material. It is responsible for removing the incident particle and optionally generating one or more scattered particles. Just like regular GPT elements, a scatter element can have one or more parameters allowing a broader range of materials to be modeled using the same element.

Apart from removing the incident particles and optionally generating one or more scattered particles, scatter elements also write detailed information of every particle-boundary intersection to the GPT outputfile. These ‘hits’ are recorded for direct plotting, or for further analysis with the FISHFILE program described in section 3.5. Table 1-G gives the scatter arrays written in the GPT outputfile.

Table 1-G: Description of the scatter arrays in the GPT outputfile.

Name	Description
<b>scat_x</b>	Array of the $x$ coordinates of the ‘hits’ [m]
<b>scat_y</b>	Array of the $y$ coordinates of the ‘hits’ [m]
<b>scat_z</b>	Array of the $z$ coordinates of the ‘hits’ [m]
<b>scat_Qin</b>	Corresponding total charge of incident particle [C]
<b>scat_Qout</b>	Corresponding total charge of scattered particle(s) [C]
<b>scat_Qnet</b>	<b>scat_Qin</b> – <b>scat_Qout</b>
<b>scat_Ein</b>	Corresponding total kinetic energy of incident particle [J]
<b>scat_Eout</b>	Corresponding total kinetic energy of scattered particle (s) [J]
<b>scat_Enet</b>	<b>scat_Ein</b> – <b>scat_Eout</b>
<b>scat_inp</b>	Cos(angle of incidence)

The simplest GPT scatter element is forwardscatter, described in section 4.9.1. It scatters a particle in the forward direction with user-defined probability  $P$ . A reflected macro-particle is generated with the same energy as the incident particle in the forward direction. The new number of elementary particles this macro-particle represents is  $P*N$ , where  $N$  is the number of elementary particles represented by the incident particle. When  $P*N$  is smaller than a user-defined threshold the new particle is not created to avoid the simulation running forever. A more realistic scatter element for a copper surface is described in section 4.9.2.

## 1.12 Automatic solving

Typical use of GPT is to use MR to scan a variable and use GDFA to aggregate the result. This allows plots of for example spotsize versus lens strength to be obtained fully automatically. The GDFsolve program goes one step further: It can for example automatically find the current that you need to get a desired spotsize. GDFMGO (Multi-objective Global Optimization) can do the same thing, but it can also show you tradeoffs between conflicting objectives such as spotsize and pulse-duration.

Both GDFsolve and GDFMGO are multi-dimensional solvers that can be used as a 'driver-programs' for GPT simulations: Any number of variables in the GPT inputfile can be varied, and both GDFsolve and GDFMGO allow a non-equal number of variables and constraints as well as external boundary conditions for all variables. The objectives are all calculated by standard GDFA data-analysis, allowing both built-in and custom GDFA programs to be used.

To understand how to use these solvers we first need to distinguish between three different use cases. They are summarized below, where  $f(\mathbf{x})$  implies a GPT run with variables  $x_1 \dots x_N$ .

Use case	Program	Description	Algorithm
Find multi-dimensional root with multiple objectives	GDFsolve	Solve $\mathbf{x}$ given $f(\mathbf{x})=a$ Solve $\mathbf{x}$ given $f(\mathbf{x})=a, g(\mathbf{x})=b, \dots$	Newton-Raphson
Find nearest minimum with multiple objectives	GDFsolve	Find $\mathbf{x}$ that minimizes $f(\mathbf{x})$ Find $\mathbf{x}$ that minimizes $a \cdot f(\mathbf{x}) + b \cdot g(\mathbf{x}) + \dots$	Powell
Find global minimum with multiple objectives	GDFMGO	Find $\mathbf{x}$ that minimizes $f(\mathbf{x})$ Find tradeoff between $f(\mathbf{x})$ and $g(\mathbf{x})$	Genetic evolution

GDFsolve, either used as a root-finder or as optimizer, assumes that the target objective(s) are smooth with respect to the variables. The program starts from a single point in variable space and calculates the derivate(s) by one or more extra function evaluation at a fixed but finite distance away from the selected point. These derivatives are subsequently used to create a better initial estimate and the process is repeated until convergence. GDFMGO on the other hand does not make any assumptions about how the objectives relate to the variables. It does not start with a single point in variable space, but with a population of such points. The objectives are calculated for all these points, and the best ones are genetically combined to improve the population as a whole.

In theory GDFMGO is the best algorithm. It can solve, optimize, and it is not very sensitive to local minima. In practice however we need to take into account that GDFMGO is intrinsically slow. Although there is an MPI version that can launch thousands of GPT runs simultaneously, typically a few hundred iterations are needed before convergence. Consequently, wall-clock time is, even with a supercomputer at your disposal, at least the time it takes to run hundreds of GPT runs. GDFsolve on the other hand can be much faster, especially when used as root-finder. The underlying Newton-Raphson algorithm doubles the number of significant digits at each iteration and given a good starting position it is possible to find roots in just a few iterations.

Our advice is to first try to cast a problem into a form that is suitable for the *root-finder* and provide good starting position(s) for the variable(s). In that case GDFsolve will be the fastest method.

For the optimization of a *single objective*, one should take into account that numerically calculating a derivative is sensitive to noise. Where the root-finder only needs the first derivative, the optimizer needs the second derivative to find the optimum. This makes it difficult to select the correct distance in variable space: On the one hand the stepsize should be rather large to prevent numerical noise, while on the other hand it should be quite small to get good accuracy. Finding the right balance can be tricky, but as long as the global optimization properties of GDFMGO are not needed using GDFsolve is recommended.

For the optimization of *multiple objectives*, we recommend the use of GDFMGO. It has been specifically designed to handle that case, and the result is a plot giving the tradeoff between the objectives known as the Pareto front. This gives much more information about the underlying problem than the single output of GDFsolve, and it is an ideal tool for decision making.

The following sections describe the internal algorithms of GDFsolve and GDFMGO. More practical information can be found in tutorial section 2.4 and reference sections 3.14 and 3.14 respectively.

### 1.12.1 Using GDFsolve as root finder

GDFsolve used as root finder tries to find a simultaneous solution to the following set of non-linear equations:

$$\begin{aligned} f_1(x_1, x_2, \dots) - ft_1 &= 0 \\ f_2(x_1, x_2, \dots) - ft_2 &= 0 \\ &\vdots \end{aligned} \quad [1.38]$$

Or in vector notation:

$$\mathbf{f}(\mathbf{x}) - \mathbf{ft} = 0 \quad [1.39]$$

The very simple vector notation in [1.39] is misleading because the components of  $\mathbf{f}$  can represent completely unrelated physical quantities. Solving them simultaneously is in general a very difficult problem.

When the dimensions of  $\mathbf{f}$  and  $\mathbf{x}$  are equal, a relatively simple solution can be obtained by writing a multi-dimensional Taylor-series expansion of  $\mathbf{f}$  around a start value  $\mathbf{x}_0$ :

$$\mathbf{f}(\mathbf{x}) \approx \mathbf{f}(\mathbf{x}_0) + \left. \frac{d\mathbf{f}}{d\mathbf{x}} \right|_{\mathbf{x}_0} (\mathbf{x} - \mathbf{x}_0) \quad [1.40]$$

Subsequent solving of [1.40] provides a first order estimate for a new trial  $\mathbf{x}_{n+1}$  based on previous guess  $\mathbf{x}_n$ :

$$\mathbf{x}_{n+1} = \mathbf{x}_n + \mathbf{M}^{-1}(\mathbf{ft} - \mathbf{f}(\mathbf{x}_n)) \text{ where } M_{ij} = \frac{df_i}{dx_j} \quad [1.41]$$

Iterating the above procedure is known as multidimensional Newton-Raphson and works very well in the vicinity of a root. As shown in Figure 1-7, the derivative of the function is extrapolated to produce the next trial. Sufficiently near a root convergence is quadratic, i.e. the number of significant digits in  $\mathbf{x}$  doubles at each step.

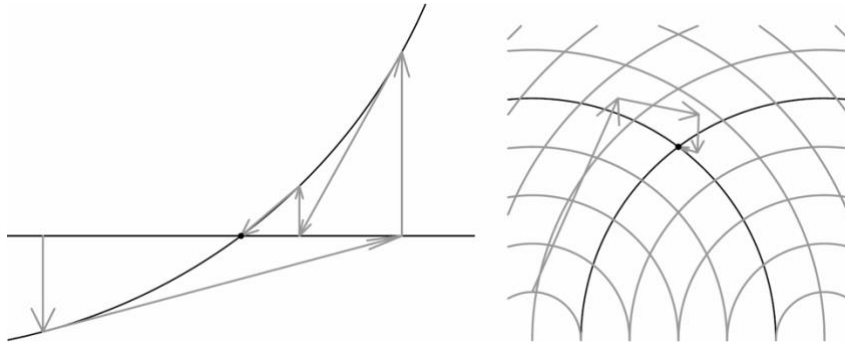


Figure 1-7: Typical Newton-Raphson iteration sequence in one and two dimensions.

There are however a number of problems with this approach:

- Typical variables  $x$  can have very different scaling. When one column in  $\mathbf{M}$  denotes total bunch charge in [C] while the next is beam energy in [eV], inverting that matrix can result in unacceptable truncation errors.
- When the Jacobian matrix  $\mathbf{M}$  can not be evaluated directly, it must be estimated numerically by a finite difference approach  $M_{ij} \approx \Delta f_i / \Delta x_j$ . This not only reduces the order of convergence, but also imposes a new question: How large should  $\Delta x$  be chosen?
- There are a large number of situations where basic Newton-Raphson sends the solution to outer space in the first iterations or where the method does not converge at all.
- Not all matrices  $\mathbf{M}$  can be inverted. This is obvious when the number of variables and the number of constraints are not equal. But the same problem arises when one variable does not have any effect on  $\mathbf{f}$ , or when one constraint is not affected by changing any  $x$ .
- Almost all variables are bounded by external constraints. For example, variables can be limited by specifications of existing hardware, budget restrictions or the location of other beam line components.
- The number of function evaluations required to obtain  $\mathbf{M}$  is equal to the number of free parameters. This is very costly in terms of CPU time because every function evaluation needs a complete GPT run.

The following sections present solution(s) used to approach these problems.

### 1.12.1.1 Scaling and initial stepsizes

To avoid truncation error problems when the matrix  $d\mathbf{f}/d\mathbf{x}$  is inverted, it is made dimensionless by dividing both  $\mathbf{f}$  and  $\mathbf{x}$  by a typical set of scale-factors:  $d\mathbf{f}$  and  $d\mathbf{x}$  respectively. The user can specify the appropriate scaling as a constant value, a relative fraction or both. The total scaling is given by the vector length:

$$\begin{aligned} df_i &= \sqrt{dfabs_i^2 + (f \cdot dfrel_i)^2} \\ dx_i &= \pm \sqrt{dxabs_i^2 + (x \cdot dxrel_i)^2} \end{aligned} \quad [1.42]$$

The sign for the steps in  $\mathbf{x}$  is determined by the external boundary conditions, as explained in section 1.12.1.4.

Although it is possible to automatically detect appropriate scaling, this will always result in more function evaluations. Especially because  $\mathbf{f}$  can be a numerically noisy function depending on the number of particles and accuracy settings of the corresponding GPT run, we have decided not to implement dynamic scaling.

To simplify the equations we directly subtract the target value  $\mathbf{f}_t$  from  $\mathbf{f}$  such that the new function  $\mathbf{F}$  must be zero at the solution. As a convention, both the scaled dimensionless function components  $\mathbf{F}$  and the dimensionless variables  $\mathbf{X}$  are written in uppercase. Now that the variables are properly scaled, the first step to obtain derivative information  $\mathbf{M}$  can be chosen simply as  $\Delta\mathbf{X} = 1$ . This leads us to the following new set of equations:

$$\begin{aligned} \mathbf{F}(\mathbf{x}) &= (\mathbf{f}(\mathbf{x}) - \mathbf{f}_t)/d\mathbf{f} \\ \mathbf{X} &= \mathbf{x}/d\mathbf{x} \\ \mathbf{M} &= \Delta\mathbf{F}/\Delta\mathbf{X} = \mathbf{F}(\mathbf{x}_N + d\mathbf{x}) - \mathbf{F}(\mathbf{x}_N) \\ \mathbf{x}_{N+1} &= \mathbf{x}_N - (\mathbf{M})^{-1}\mathbf{F}(\mathbf{x}_0)d\mathbf{x} \end{aligned} \quad [1.43]$$

The scaling  $d\mathbf{x}$  is a crucial parameter because it is directly related to the stepsize in the determination of  $\mathbf{M}$ . It is our experience that almost all problems with GDFsolve are related to an incorrect scaling of the variables. Figure 1-8 shows a typical too small, good and too large  $dx$ . A too small  $dx$  is smaller than the simulation noise on the constraints. A too large  $dx$  sends the constraints into a non-linear regime. When no correct scaling can be found, the tracing accuracy of GPT must be increased or more particles must be added to the simulation.

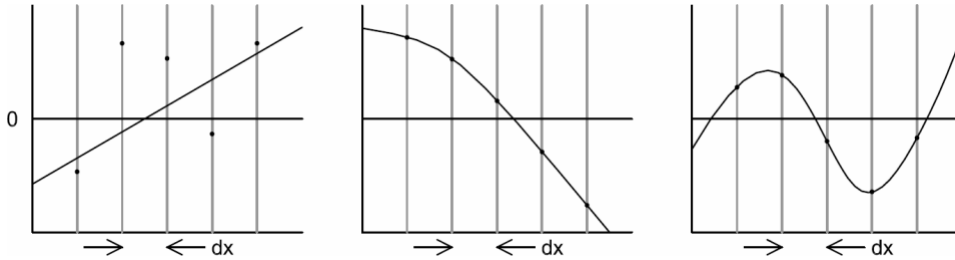


Figure 1-8: Too small, good and too large  $dx$ .

### 1.12.1.2 Backtracking

One of the problems with the proposed scheme is that it can send a solution to outer space when the first estimate of  $\mathbf{x}$  is not sufficiently near a root in  $\mathbf{F}$ . A related problem can occur when the sequence simply does not converge. As shown in Figure 1-9 a very small difference in start position for  $\mathbf{x}$  can change a convergent solution into a cyclic or even divergent scheme.

To solve these convergence problems, we first have to detect that the algorithm is not working. Because  $\mathbf{F}$  is scaled, its vector length can be used as convergence indicator:

$$|F(x_{n+1})| \geq (1 - \alpha)F(x_n) \quad [1.44]$$

When [1.44] is not satisfied with sufficiently small  $\alpha$ , convergence problems may occur. A typical convergence factor  $\alpha$  is a few percent. Not meeting [1.44] usually indicates that the used step is too large. In that case the stepsize is reduced by a factor of 2, for three iterations if necessary, in an attempt to find a smaller  $\mathbf{F}$ . If this fails, GDFsolve is unable to find a solution and terminates.

### 1.12.1.3 Singular Value Decomposition

Matrix inversion of the Jacobian  $\mathbf{M}$  is numerically a dangerous process. Because the CPU time in all practical applications is dominated by the evaluation of  $\mathbf{F}$ , it is in our opinion better to use Singular Value Decomposition (SVD). A full treatment of the method is beyond our scope here, but basically the method is as follows:

The matrix  $\mathbf{M}$  is written as the product of three matrices<sup>1</sup>:

$$\mathbf{M} = \mathbf{U} \cdot \text{diag}(w_1, w_2, \dots) \cdot \mathbf{V}^T \quad [1.45]$$

where the columns of both  $\mathbf{U}$  and  $\mathbf{V}$  are orthonormal. For our application the columns of  $\mathbf{V}$  define an orthonormal set of directions of the variables  $\mathbf{X}_i$  and the columns of  $\mathbf{U}$  define the corresponding change in the constraints  $\mathbf{F}_i$ . The diagonal matrix containing  $w_i$ , the singular values, defines the scaling between these two.

Once the Singular Value Decomposition is calculated, inverting  $\mathbf{M}$  is simple:

$$\mathbf{M}^{-1} = \mathbf{V} \cdot \text{diag}(1/w_1, 1/w_2, \dots) \cdot \mathbf{U}^T \quad [1.46]$$

Numerically you run into trouble when one or more of the  $w_i$ 's is much smaller than the others. A relatively small  $w_j$  indicates a change in  $\mathbf{X}$  that does not affect  $\mathbf{F}$ . So if you want to change  $\mathbf{F}$  in that direction, you need a very large change in  $\mathbf{X}$ . Typically, such giant steps lead you away from the solution rather than put you on top of it. Therefore the pragmatic approach is simple: Because you can not change  $\mathbf{F}$  in the direction of a small  $w_i$ , do not try. Numerically, this means that in the inversion process all  $1/w_i$  must be set to zero when  $w_i$  is sufficiently small.

When  $\mathbf{M}$  is not square, the matrix  $\mathbf{U}$  is not square either, but all observations still apply. In other words, the number of variables and constraints does not need to be equal. Thus we can use more variables, or even more constraints when desired.

Summarizing the advantages of SVD over matrix inversion:

- When  $\mathbf{M}$  is ill conditioned, one or more  $w_i$ 's are very small,  $\mathbf{F}$  is very insensitive to one or more directions in  $\mathbf{X}$ . Instead of sending the solution to near infinity, these directions can be ignored by setting the corresponding singular values to zero in the inversion process.
- When  $\mathbf{X}$  has more dimensions than  $\mathbf{F}$ , the matrix  $\mathbf{M}$  is under-conditioned. This results in a nullspace of  $\mathbf{M}$  where a change in  $\mathbf{X}$  does not affect  $\mathbf{F}$ . The new trial value for  $\mathbf{X}$  will not move in the nullspace.
- When  $\mathbf{F}$  has more dimensions than  $\mathbf{X}$  the matrix  $\mathbf{M}$  is over-conditioned. The new trial value for  $\mathbf{X}$  is fitted in a least-squares sense in an attempt to solve for too many constraints.

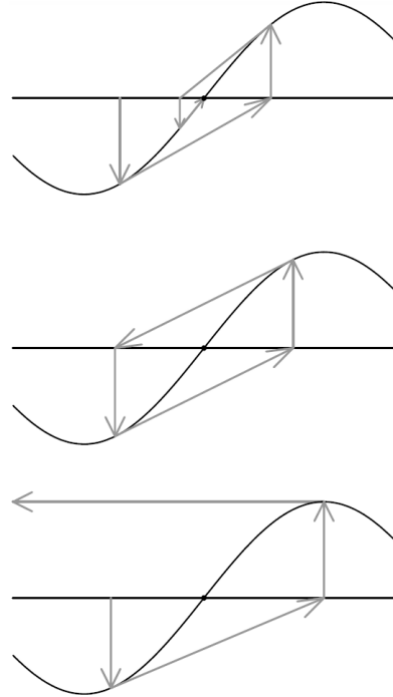


Figure 1-9: Convergent, cyclic and divergent iterations.

<sup>1</sup> In literature, sometimes  $\mathbf{V}$  is defined without the transpose.



One question remains: How small can  $w_i$  be before that direction must be ignored? This depends on correct scaling between the variables  $\mathbf{x}$  and  $\mathbf{X}$  and between the constraints  $\mathbf{f}$  and  $\mathbf{F}$ . Furthermore, it depends on the accuracy of the underlying GPT simulation. Finally, it depends on the machine precision but this is never a real concern for double-precision calculations. Specific situation-dependent experience is needed, but it appears that the method is not particularly sensitive: A typical range between  $10^{-2}$  and  $10^{-6}$  compared to the maximum  $w_i$  can be used as criteria for smallness.

#### 1.12.1.4 External boundary conditions

In many design scenario's, the variables  $x_j$  can not be chosen freely. They are restricted to boundary conditions such as the location of other beam-line components. In our implementation all variables are bounded by a minimum and maximum value, forming a hypercube of free space.

When a new trial value  $\mathbf{x}_{n+1}$  lies outside the hypercube, an attempt is made to move it inside by changing  $\mathbf{x}_{n+1}$  in the nullspace of  $\mathbf{M}$ . This corresponds to a move for any  $\boldsymbol{\lambda}$  of the form:

$$\mathbf{x} \leftarrow \mathbf{x} + \mathbf{V}' \cdot \boldsymbol{\lambda} \quad [1.47]$$

where only the columns of  $\mathbf{V}$  corresponding to small  $w_i$  are used in  $\mathbf{V}'$ .

The additional unknown vector  $\boldsymbol{\lambda}$  can be solved from:  $\mathbf{x}\mathbf{b} = \mathbf{x} + \mathbf{V}'' \cdot \boldsymbol{\lambda}$  where  $\mathbf{V}''$  contains only the rows of  $\mathbf{V}'$  corresponding to the component of  $x$  that must be moved into the boundary hypercube, given by a corresponding  $x\mathbf{b}$ . A unique solution for  $\boldsymbol{\lambda}$  exists when there is an equal number of dimensions in the nullspace of  $\mathbf{M}$  as there are unsatisfied boundary conditions. This process is illustrated in Figure 1-10 where nullspace of  $\mathbf{M}$  is used to solve a boundary condition.

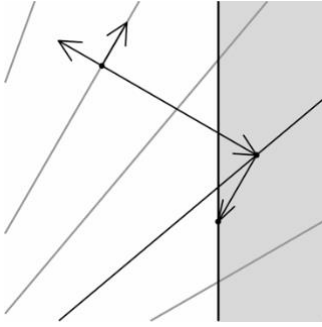


Figure 1-10: A boundary condition is solved by moving the new estimate in the nullspace of  $\mathbf{M}$ .

Solving for one boundary condition might sometimes trigger a new boundary condition. Therefore, the complete boundary-solving process must be iterated until all boundary conditions are satisfied, or until no boundary condition can be solved anymore. Because the dimensions of the nullspace and the number of boundary conditions are not always equal, SVD is used again to solve for  $\boldsymbol{\lambda}$ . This does not necessarily satisfy all boundary conditions, and they sometimes need to be enforced with a warning message as a result.

When a parameter is near the maximum of a boundary condition, the step to obtain the derivative information may violate the boundary condition. In that case, a negative step will be used.

#### 1.12.1.5 Broydens method

Obtaining the Jacobian  $\mathbf{M}$  requires as many function evaluations, complete GPT runs, as free parameters. This is expensive in terms of CPU time. However, it is possible to use the function information from the previously successful step to make an estimate of  $\mathbf{M}$  without any additional function evaluations. This requires only one Jacobian to be calculated in the first step to start the process. The update method according to Broyden [2] is given by:

$$\mathbf{M}_{N+1} \approx \mathbf{M}_N + \frac{(\delta\mathbf{F}_i - \mathbf{M}_i \cdot \delta\mathbf{X}_i) \otimes \delta\mathbf{X}_i}{\delta\mathbf{X}_i \cdot \delta\mathbf{X}_i} \quad [1.48]$$

where  $\delta\mathbf{F}$  is the difference in  $\mathbf{F}$  in a step with size  $\delta\mathbf{X}$ .

The method might fail to produce a good representation of the actual Jacobian. In that case, the backtracking algorithm will not find a solution and GDFsolve must reinitialize  $\mathbf{M}$  by calculating a full Jacobian. Especially when there is no solution to be found, Broydens Method can increase the number of function evaluations significantly. Furthermore, the method is not advisable when the number of variables is larger than the number of constraints. The algorithm can be switched on and off as required.

### 1.12.2 Using GDFsolve as optimizer

GDFsolve as optimizer tries to find the minimum of any function  $g(\mathbf{x})$  by varying all components of  $\mathbf{x}$ . The used algorithm is Powell and described in [2]. Our implementation is very close to [2] with the following modifications: Function evaluations with identical parameters are not repeated, one-dimensional optimization properly generalizes to a single-line minimization and relative termination detection is changed to an absolute value. Qualitatively, the algorithm is as follows:

The first steps find the minimum in the direction of the first component of  $\mathbf{x}$ . Starting from there, the second component of  $\mathbf{x}$  is varied until a minimum is found. This process is repeated as many times as there are dimensions in  $\mathbf{x}$ . To improve the efficiency of the algorithm, the average direction resulting from these iterations is also used as minimization direction, replacing the direction of the largest function decrease. The complete process is iterated until a stable solution is found.

The line-minimization routine takes larger and larger steps downhill until a minimum is bracketed. That is three points where the middle point has the lowest function value. Then the actual minimum is found by either parabolic interpolation or golden section search.

#### 1.12.2.1 Required number of iterations

Any smooth function  $g$  can be approximated as a second-order Taylor series around  $\mathbf{x}_0$  by:

$$f(\mathbf{x}) \approx \mathbf{f}(\mathbf{x}_0) + \left. \frac{dg}{d\mathbf{x}} \right|_{\mathbf{x}_0} (\mathbf{x} - \mathbf{x}_0) + \frac{1}{2} (\mathbf{x} - \mathbf{x}_0) \mathbf{H}(\mathbf{x}_0) (\mathbf{x} - \mathbf{x}_0) \quad [1.49]$$

where the components of the Hessian matrix  $\mathbf{H}$  are defined as:

$$H_{ij}(\mathbf{x}_0) = \left. \frac{d^2 g}{d x_i d x_j} \right|_{\mathbf{x}_0} \quad [1.50]$$

Solving for an extremum in  $g$  yields:

$$\mathbf{x} = \mathbf{x}_0 - \mathbf{H}^{-1}(\mathbf{x}_0) \cdot \left. \frac{dg}{d\mathbf{x}} \right|_{\mathbf{x}_0} \quad [1.51]$$

Because solving  $\mathbf{x}$  requires knowledge of all components of  $\mathbf{H}$ , at least  $N^2$  functions evaluations are required to find a minimum. Compared to the  $N$  evaluations required to find a root, optimization typically takes much more iterations than root-finding.

#### 1.12.2.2 Optimizing more functions simultaneously

In real life one typically wants to have it all. For example both the best emittance and the shortest bunch-length. This is not possible with any single-valued  $g$  as required by GDFsolve. Some tradeoff must be made between the two separate functions. Using GDFsolve this is accomplished by using individual weight factors  $m_i$  for a number of independent functions  $g_i$  to optimize. Making use of the same scaling  $df_i$  as defined in [1.42], the total  $g$  to minimize is then given by:

$$g = \sum_i m_i \frac{g_i}{df_i} \quad [1.52]$$

As expected, a negative weight factor automatically maximizes the corresponding component. Please note that if this tradeoff is not a priori known GDFsolve cannot be used. In that case, the multi-objective solver GDFMGO must be used.

#### 1.12.2.3 Additional constraints

Apart from wanting to optimize a function, ideally a number of additional constraints must be met. For example: Make sure that “all charge must come through”. To accomplish this, the scaled mismatch between the constraints and the function value is added as penalty to  $g$ .

$$g = \sum_i m_i \frac{g_i}{df_i} + \sqrt{\sum_i \left( \frac{f_i - f_{t_i}}{df_i} \right)^2} \quad [1.53]$$

We realize that this does not result in the most elegant algorithm for a number of reasons: Depending on the scaling the constraints will be met or not. And perhaps even worse, improper scaling of the constraints can move the location of the found optimum off the actual solution. The reason we choose this algorithm is that with proper scaling the method is very fast because it does not require any additional function evaluations. When robust constraint handling is required, the slower GDFMGO program is most likely a better choice.

#### 1.12.2.4 Boundary conditions

Just as with the root finder, not all parameters  $x_i$  can be chosen freely. Space restrictions or budget reasons can impose maximum possible values. All variables are bounded again by a minimum and maximum value, forming a hypercube of free space.

### 1.12.3 GDFMGO

GDFMGO is a multi-objective global optimizer. Its internal algorithm evolves a population of candidate solutions towards the so-called Pareto-front. This front is defined as the set of points where it is impossible to improve one objective without making at least one other objective worse. The final result is a set of points equally spaced at or near the Pareto front, where each point is fully optimized in all its variables.

The Pareto front samples, for the given objectives, the optimal combination of variables. For two objectives and ten variables, the Pareto front is a line through two dimensional objective space and ten dimensional variable space. In other words, the original problem of having to choose the best combination of ten variables has been reduced to the one dimensional problem of selecting where on the line you want to be. This collapse of dimensionality makes multi-objective optimization such a powerful tool for decision making. Its power does not come from providing the ‘the best’ solution, but from reduction of the dimensionality of the problem and simultaneously providing insight in tradeoffs between the different objectives. Tutorial section 2.4.4 shows this in practice.

GDFMGO starts with a fixed size population of candidate solutions with variables either chosen randomly in a user specified interval or read from file. Typically this initial population is very poor in terms of the objectives, and probably in violation of a number of constraints if present. The idea is to create improved candidate solutions based on the solutions already present, while gradually removing the worst ones. This process is repeated over and over again, and slowly the population as a whole evolves in the desired direction. Global convergence properties come from the fact that the population is pushed gently towards the Pareto front instead of steepest descent into a potential local minimum. Although there are plenty of pathological cases where this does not work, in practice the algorithm finds the global optimum in a impressively large number of cases with the default parameters.

The key ingredients of the algorithm are a) creation of new candidate solutions based on the existing ones, b) ranking the solutions such that the worst can be removed and c) a stopping criterion. They are described in detail below.

#### 1.12.3.1 New species

New random samples are created from the existing population. The mechanism we use is known as ‘differential evolution’. To create a new combination of variables  $\mathbf{p}$ , first *four* random species from the population are selected. We denote them  $\mathbf{u}$ ,  $\mathbf{v}$ ,  $\mathbf{w}$  and  $\mathbf{x}$ . Subsequently, an intermediate point  $\mathbf{t}$  is calculated from  $\mathbf{u}$ ,  $\mathbf{v}$  and  $\mathbf{w}$  using:

$$\mathbf{t} = \mathbf{w} + s(\mathbf{u} - \mathbf{v}) \quad [1.54]$$

The idea is that the new point is close to the existing  $\mathbf{w}$ , but offset with the direction from  $\mathbf{v}$  to  $\mathbf{u}$ . To speed up convergence, the direction is slightly reduced by a scale factor  $s$  that must be below 1. In practice using this intermediate point  $\mathbf{t}$  as the new point already works very well. However, when the entire candidate solution lies on a hyperplane in all variables there is no escape from this plane thereby stalling the algorithm. This is where the last selected point  $\mathbf{x}$  comes into play, where there is a mutation probability  $(1 - \rho)$  that variables are selected from  $\mathbf{x}$  instead of from  $\mathbf{t}$ . To avoid duplicating  $\mathbf{x}$  at least one of the variables must come from  $\mathbf{t}$ . In equations:

$$cr = \text{random\_int}[1, n] \\ p_i = \begin{cases} t_i & \text{random}[0,1] < \rho \quad \vee \quad i = cr \\ x_i & \text{otherwise} \end{cases} \quad [1.55]$$

A lower  $\rho$  increases global convergence properties at the cost of a slower convergence rate. In practice neither the scale factor  $s$  nor the mutation rate  $\rho$  are critical parameters and the defaults of 0.6 and 0.9 respectively work fine in most cases.

New candidate solutions are added until the population size is doubled. Then the population is ranked and trimmed to the original size again. How this is done is the subject of the next section.

### 1.12.3.2 Ranking procedure: NSGA

The initial population is based on a random selection in all variables. Obviously, such random start conditions give poor results in terms of the objectives. The idea is to slowly improve this population, but to do this a ranking procedure is needed that defines which points are ‘better’ and which ones are ‘worse’. In case of a single objective this is trivial, since we can simply sort all candidate solutions: If the objective needs to be minimized, an ascending sorting order gives a natural rank and the ‘worse’ ones can simply be defined as an upper fraction.

In the case of multiple and conflicting objectives things become more complicated. When a candidate solution has, compared to another one, shorter pulse-duration (good) but larger emittance (bad) it is not immediately clear if this one is better or worse. The idea followed in GDFMGO is based on the NSGA algorithm, where the ranking is based on domination: A point dominates another if it is better in at least one objective, and not worse in all other objectives. All points that are not dominated by any other point are given rank 0. This is the set that lies closest to the Pareto front, and these are the ‘best’ points in our set. The ones with rank 1 are the ones that are not dominated by any other point, not taking into account points with rank 0. They are the ‘next best’. And so forth and so on. The final result is a candidate set that is fully ranked based on all objectives. An example is shown in Figure 1-11 where *stdx* and *stdy* are conflicting objectives to be minimized. Points with small *stdx* but large *stdy* are correctly assigned the same rank as points with large *stdx* but small *stdy*.

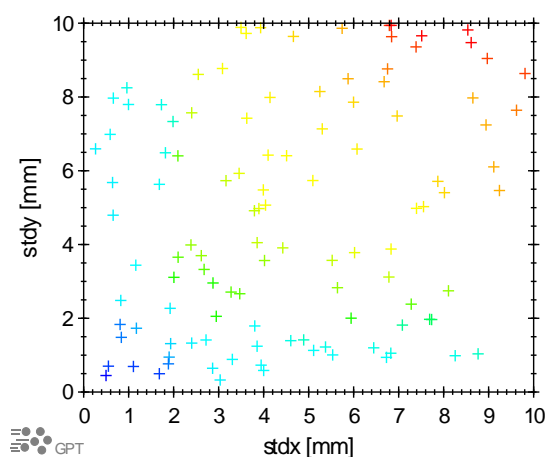


Figure 1-11: Multi-objective ranking shown in colors ranging from blue, via green and yellow, to red.

The ranking procedure is used to trim the candidate solution. Initially points with the highest rank are removed since they are furthest away from the Pareto front. When more than 50% of the points have rank 0, also particles with rank 0 are removed. This is done in such a way that the front is sampled as uniformly as possible by removing points with near neighbours.

### 1.12.3.3 Additional constraints

An extra complication in the ranking procedure is that in many cases there are additional constraints. An example is a spot size as small as possible, under the condition that the total charge is larger than 1 pC. With just one extra constraint, an intuitive ranking procedure is that all candidates that violate the constraint are dominated by candidates that do not violate the constraint. This allows the rest of the procedure to remain identical, and indeed this works just fine. The optimizer essentially first optimizes the entire population to not violate the constraint, and when this is established it continues the optimization in the constrained subset of variable space.

With more constraints however, we have to be careful: It is impossible to define something like the sum of all violations. If the spotsize must be smaller than 10 micron and we are 1 micron off, and if the charge must be larger than 1 pC and we are 0.1 pC off, then the total violation is 1 micron plus 0.1 pC. These can only be added with additional scaling factors, and these typically cannot easily be defined. The solution is to not do any summation, but only count the *number* of violations. This works very robustly in practice, but there is still one problem.

Tough optimization problems have almost all initial candidates in violation of several constraints. This results in too much evolutionary pressure on the initial set because the elitist nature of the algorithm will not temporarily give up on one constraint to fulfill another one. That fully undermines the global optimization

properties of the algorithm. To solve this problem GDFMGO uses dynamic constraints: The actual constraints are relaxed until at most half the population violates the constraint. This causes a much more gentle evolutionary push towards zero constrained violations, restoring the global convergence properties.

#### **1.12.3.4 Stop criterion**

GDFMGO stops the optimization when the worst solution has rank 1, i.e. when there are only two fronts. Furthermore GDFMGO stops the optimization after  $N$  generations, where one generation is defined as doubling the initial population size and trimming back to the original size. In practice, this combination works reasonably well, but we have to admit that these criteria need some experimenting on a case by case basis.



## 2 Tutorial

This chapter gives a tutorial introduction to the GPT package. All the files in the tutorial can be found in the GPT distribution in the **tutorial** directory. Within that directory, a subdirectory or folder exists for every section in the tutorial containing the described files.

2.1	Quadrupole focusing .....	42
2.2	The GPTwin user interface.....	46
2.3	Scanning the beam energy.....	52
2.4	Automatic solving .....	54
2.5	Electrostatic accelerator .....	62
2.6	Accuracy.....	64
2.7	Magnetic mirror.....	66
2.8	Element Coordinate System .....	68
2.9	Initial particle distribution .....	71
2.10	Photo-cathode, starting particles as function of time .....	74
2.11	Collector design.....	77

## 2.1 Quadrupole focusing

In this section we will simulate a rectangular beam with Lorentz factor  $\gamma=100$  through two quadrupole lenses. The first quadrupole lens focuses the beam in the  $y$ -direction and defocuses the beam in the  $x$ -direction. The second quadrupole lens does just the opposite. The net result is a focusing force in both directions and the length and strength of both quadrupoles is chosen so that the beam is sent through a focus in both directions at  $z=1$  meter.

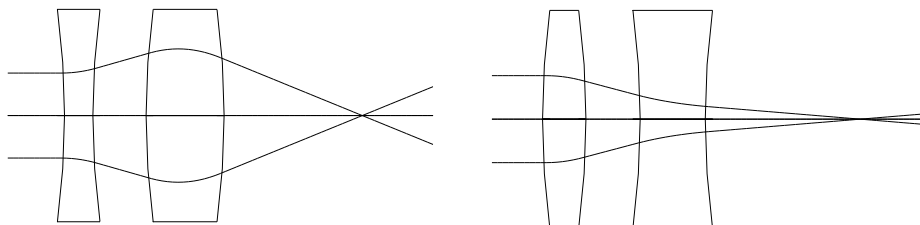


Figure 2-1: Two quadrupole lenses can focus a beam in two directions:  $xz$ -plane (left) and  $yz$ -plane (right).

### 2.1.1 The GPT inputfile

The GPT inputfile needed to describe this simulation is listed in Listing 2-1. Like all inputfiles listed in the tutorial, it can be found at the location indicated in the corresponding caption.

Listing 2-1: GPT inputfile for beam focusing using a quadrupole doublet. Filename: **tutorial/quads/quads.in**

```
1. # GPT Tutorial: Quadrupole focusing
2.
3. # Define beam parameters
4. gamma = 100 ;
5. radius= 6e-3 ;
6.
7. # Start initial beam
8. setparticles("beam",100,me,qe,0.0) ;
9. setrxydist("beam","u",radius/2, radius) ;
10. setphidist("beam","u",0,2*pi) ;
11. setGdist("beam","u",gamma,0) ;
12.
13. # Position the quadrupole lenses
14. quadrupole( "wcs","z",0.2, 0.1, 3.90 ) ;
15. quadrupole( "wcs","z",0.5, 0.2,-3.25 ) ;
16.
17. # Specify output times
18. snapshot(0,4e-9,0.05e-9) ;
```

This sample GPT inputfile is described below line-by-line. The very first line in the sample GPT inputfile is ignored by the parser because it starts with a hash mark **#** indicating that the rest of the line is a comment. Comment-lines can appear anywhere in the GPT inputfile.

1. **# GPT Tutorial: Quadrupole focusing**

The first actual section in the GPT inputfile defines various parameters for later use.

```
3. # Define beam parameters
4. gamma = 100 ;
5. radius= 6e-3 ;
```

Line 4 defines the variable **gamma** to be equal to 100 and line 5 sets the **radius** to 6 mm. At this point, these variables don't have any special meaning; they are just for user convenience. In lines 11 and 9, they are used to define the Lorentz factor of the beam and set the beam radius. User-defined variables can have any name, but can not start with a digit.

The second section starts the initial beam.



```

7. # Start initial beam
8. setparticles("beam",100,me,qe,0.0) ;
9. setrxydist("beam","u",radius/2, radius) ;
10. setphidist("beam","u",0,2*pi) ;
11. setGdist("beam","u",gamma,0) ;

```

The **setparticles** keyword, see section 4.2.1.1, is used to start 100 electrons in a particle set named **beam**. The predefined constants **me** and **qe** are set to the charge and mass of an electron. For other built-in constants we refer to Table 4-B on page 121. Because we will not include space charge in this simulation, the last parameter of **setparticles**, defining total charge, can be zero.

After the particles are created, they are all positioned at the origin with zero velocity. The **setrxydist** keyword, see section 4.2.2.6, modifies the x-coordinates of the particles according to a specific distribution: Uniform ("u") with center **radius/2** and width **radius**. The **setphidist** keyword, see section 4.2.2.7, sets a uniform angular distribution in the xy-plane over all angles. The combined effect of these two keywords is a disk-like beam, uniformly filled with particles in the xy-plane. Please note that the distribution of the x-coordinates as generated by **setrxydist** is far from uniform: It is linearly increasing with x such that after redistribution over all angles in the xy-plane the resulting beam is uniform. To produce an actual uniform distribution in x, the **setxdist** keyword can be used.

The **setGdist** keyword, see section 4.2.3.8, gives all particles a Lorentz factor of **gamma**, previously defined as 100.

The third section positions the two quadrupole lenses.

```

13. # Position the quadrupole lenses
14. quadrupole( "wcs","z",0.2, 0.1, 3.90 ) ;
15. quadrupole( "wcs","z",0.5, 0.2,-3.25 ) ;

```

The first parameter of the **quadrupole** element, see section 4.6.10, is the ECS, the Element Coordinate System. The default coordinate system of a **quadrupole** positions the lens around the origin, oriented in the z-direction. The ECS lists the new 3D position and 3D orientation of the **quadrupole**, relative to its default. The ECS specification "**wcs**", "**z**", **0.2**, instructs GPT to position the **quadrupole** relative to the Word Coordinate System (WCS), the default coordinate system, but moved 0.2 m downstream. The second **quadrupole** is moved 0.5 m downstream. Only the positions are affected, the orientation remains unchanged. For the simulation of complex experiments, it can be useful to define custom coordinate systems and position elements relative to those. We refer to section 1.4 for details about custom coordinate systems and element coordinate transformations.

The following two parameters of the **quadrupole** lens are length and strength. The first quadrupole has a length of 0.1 m and a positive strength. The second lens needs to work opposite to the first lens to focus the beam in two planes. This could have been achieved by rotating the element 90° around its axis using the ECS, but specifying a negative strength has the same result and is much easier.

The fourth section defines when to write output.

```

17. # Specify output times
18. snapshot(0,4e-9,0.05e-9)

```

The **snapshot** keyword, see section 4.3.11, is used to specify the times when output needs to be generated. The parameters are **from**, **to** and **step**, all measured in seconds. Output is written every 50 ps, between 0 and 4 ns.

## 2.1.2 The GPT batch file

Every GPT simulation contains not only a GPT run, but also includes subsequent data analysis. To automate this process, GPT simulations are typically run as a batch file containing various commands.

Listing 2-2: GPT batch file for beam focusing using a quadrupole doublet. Filename: **tutorial/quads/quads.bat**

```

1. gpt -o result.gdf quads.in
2. gdftrans -o traj.gdf result.gdf time x y z
3. gdfa -o std.gdf result.gdf time stdx stdy avgz
4. gdf2a -o std.txt std.gdf

```

Listing 2-2 shows a sample batch file that could be used to run the quadrupole focusing example. It is briefly explained below as a short introduction to some of the capabilities of GPT. We refer to section 2.2 for a

description how to actually run this example using GPTwin. Chapter 3 lists all possible data analysis and pre- and post-processing tools available in the GPT package. Linux users can run GPT and subsequent data-analysis tools using any command processor of their choice. Note that the GPT line needs a **GPTLICENSE=xxx** specification for GPT to run properly.

1. **gpt -o result.gdf quads.in [GPTlicense=xxx]**

This line commands the actual GPT simulation. The set-up, simulation parameters and output method as described in the inputfile **quads.in** are now executed. The result is written to the file **result.gdf** as specified with the **-o** option. The outputfile contains all particle coordinates at the requested times or positions and can directly be plotted using GPTwin, see Figure 2-2. Using GPTwin, one can cycle through the plots to and inspect the results. As explained in the complete GPT syntax in section 1.2, an additional **-v** option is useful to track the progress of lengthy simulations.

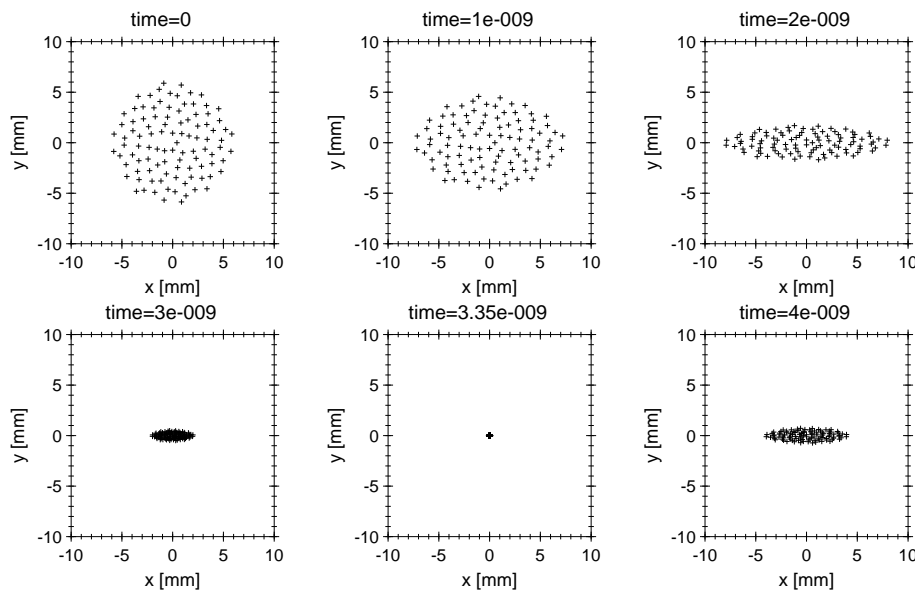


Figure 2-2: Sample raw GPT output: Particle coordinates as function of simulation time.

5. **gdftrans -o traj.gdf result.gdf time x y z**

The GDFTRANS program converts the raw GPT output from **result.gdf** to trajectory output written in the file **traj.gdf**. Again, the **-o** option is used to specify the name of the outputfile. This file contains a list of particle trajectories, as shown in Figure 2-3. The trajectories are plotted as function of **time**, and to reduce the size of the file, only the **x**, **y** and **z** coordinates of the trajectories are stored. When a parameter is scanned using the MR program, the trajectories can also be plotted as function of the scanned parameter. See section 3.17 for more information about the use of GDFTRANS.

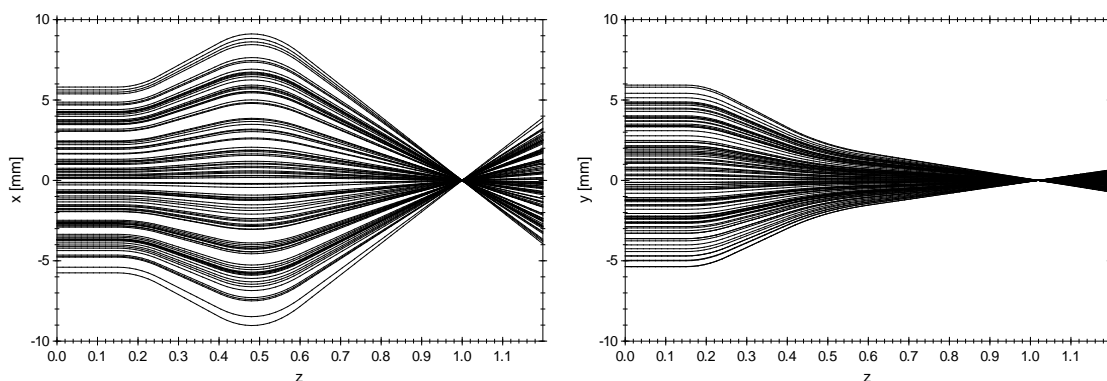


Figure 2-3: GDFTRANS trajectory output.

6. **gdffa -o std.gdf result.gdf time stdx stdy avgz**

The raw GPT output and the trajectory output are typically studied to verify that the inputfile describing the simulation is correct. After this step, one may be interested in overall quantities like bunch-length, beam size and emittance. The GDFFA program reads the GPT output from the file **result.gdf** and writes a new file named **std.gdf** containing various macroscopic quantities. In this case, the file **std.gdf** contains only the

standard x- and y-deviations and the average longitudinal position all as a function of time, see Figure 2-4. As described in reference section 3.12, a very large number of data-analysis routines can be specified. It is even possible to create custom GDFA programs, as explained in the GPT Custom Elements documentation.

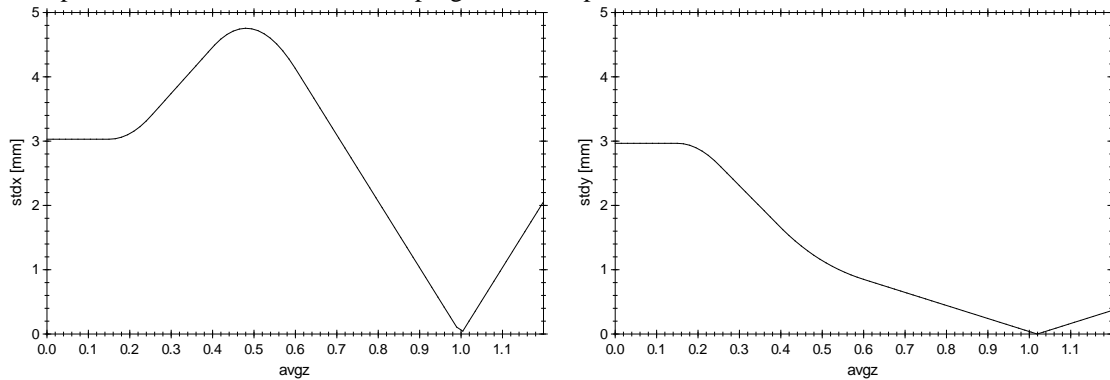


Figure 2-4: GDFA output: Standard deviation of x- and y-size as function of average longitudinal position.

#### 4. `gdf2a -o std.txt std.gdf`

The last line in our batch file converts the file `std.gdf` to the ASCII file `std.txt` using the GDF2A program, see section 3.6. Because GDF files are written in a special binary format, only GPTwin and the GDF utility programs can open them. To be able to export GPT results to other programs, GDF files can be converted to ASCII using the GDF2A program. Part of the result is shown in Figure 2-5.

	<code>stdx</code>	<code>stdy</code>	<code>avgz</code>	<code>time</code>
1.	3.030e-003	2.966e-003	0.000e+000	0.000e+000
2.	3.030e-003	2.966e-003	1.499e-002	5.000e-011
3.	3.030e-003	2.966e-003	2.998e-002	1.000e-010
4.	3.030e-003	2.966e-003	4.497e-002	1.500e-010
5.	3.030e-003	2.966e-003	5.996e-002	2.000e-010
6.	3.030e-003	2.966e-003	7.494e-002	2.500e-010
7.	3.030e-003	2.966e-003	8.993e-002	3.000e-010
8.	3.030e-003	2.966e-003	1.049e-001	3.500e-010
9.	3.030e-003	2.966e-003	1.199e-001	4.000e-010
10.	3.030e-003	2.966e-003	1.349e-001	4.500e-010
11.	3.030e-003	2.966e-003	1.499e-001	5.000e-010
12.	3.030e-003	2.966e-003	1.499e-001	5.000e-010

Figure 2-5: Selected GDF2A output.

## 2.2 The GPTwin user interface

GPTwin is the MS-Windows user interface for the GPT package: An easy-to-use environment that covers all aspects of a GPT simulation:

- It provides an editor for the development of inputfiles and custom elements with on-line help.
- It executes GPT and data-analysis tools, while logging diagnostic messages.
- It plots and prints the simulation results in a variety of formats ranging from scatter to color-density-plots.
- It fully automates the development of custom elements.

After installation, the GPTwin executable can be started using:

**Start/Programs/General Particle Tracer/General Particle Tracer**

GPT infiles can be opened by dragging and dropping the file into GPTwin or by selecting the Open command from the File menu. Please use any of these methods to open the files **quads.in** and **quads.bat** in the **tutorial** folder. The **tutorial** folder is typically located in a subfolder of **c:\program files\general particle tracer**, but this may have been modified during installation.

After performing the above steps, the GPTwin user interface should look similar to Figure 2-6. The toolbar (with the buttons below the menu), element bar (shown on the left) and the status bar (below) can all be switched on or off using the View menu. You can use a pointing device or the Window menu to arrange the documents within GPTwin.

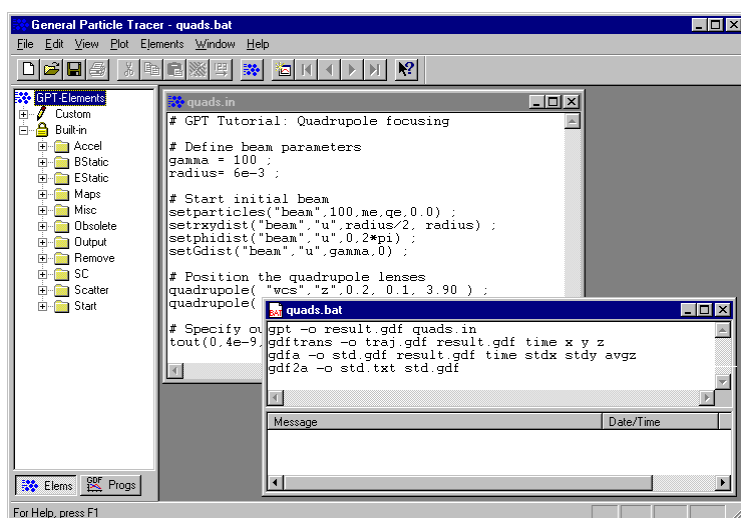


Figure 2-6: The GPTwin user interface with the files **quads.in** and **quads.bat**.

### 2.2.1 On-line help

On-line help can always be obtained by pressing the F1 key or selecting the Help menu. For example, when the cursor is located on a line containing the keyword **quadrupole** while F1 is pressed, a help screen as shown in Figure 2-7 is displayed. The buttons on the Help toolbar allow you to switch quickly between various help topics.

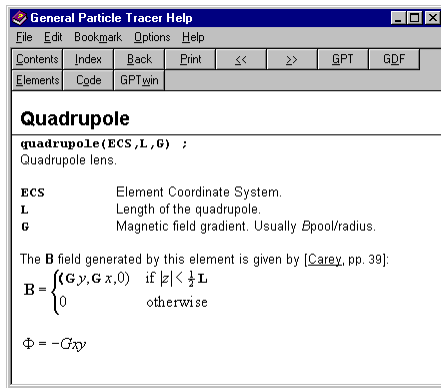



Figure 2-7: On-line help for a quadrupole lens.

### 2.2.2 Running the quadrupole example using GPTwin

The **quads.bat** batch file containing all commands to run the GPT simulation can be executed by selecting the file and clicking the  button on the toolbar. Alternatively, File/Run can be specified on the menu or the CTRL+R key-combination can be pressed. After the run command is specified, simulation messages are shown in the bottom part of the **quads.bat** window, as shown in Figure 2-8. The simulation is completed when the Finished message appears.

More or less space can be reserved for the simulation messages by moving the splitter. When no messages are shown at all, you can still move the splitter, which is in this case located at the bottom of the window. Every diagnostic message is followed by its date and time for your convenience.

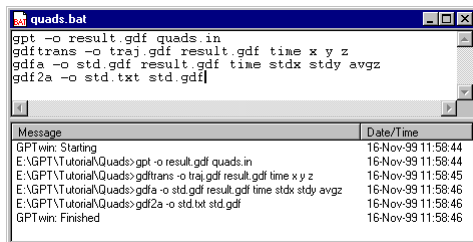



Figure 2-8: Run window with messages.

In this case, because there are no errors, only the commands themselves are shown. Otherwise, an error message will appear with the following format:



**filename.in(linenumber): ErrorMessage**

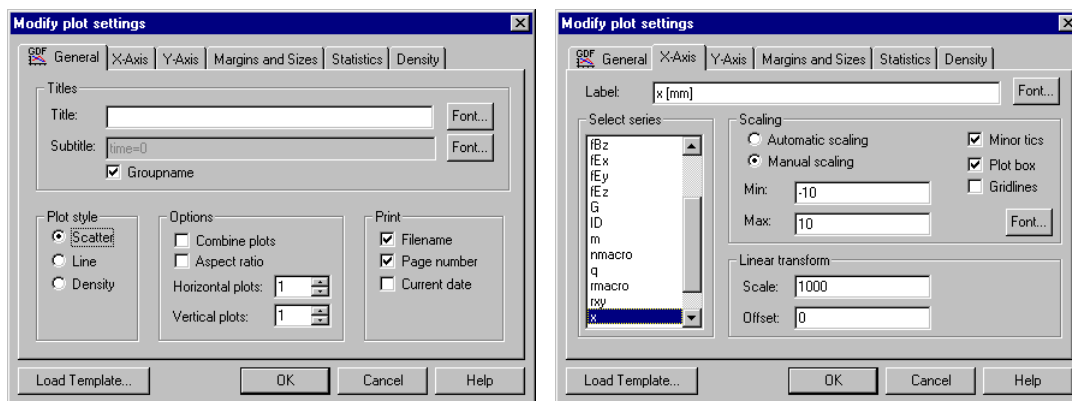
Double-clicking such an error opens the correct file and positions the cursor at the beginning of the line containing the error. Correct any errors and try again. Right-clicking in the messages section shows a pop-up menu with additional commands. It is for example possible to save all messages to an ASCII file for further analysis.

The  button can be clicked to stop any running simulation. Using this feature may result in a corrupted and unusable outputfile.

### 2.2.3 Scatterplots

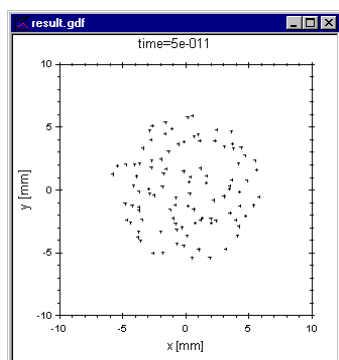
The raw output of GPT consists of all particle coordinates at the requested output times or positions. To inspect the simulation results using GPTwin, you can do the following:

- Open the outputfile **quads.gdf** either by double-clicking on it, by dragging it into GPTwin or by using the Open command from the File menu and selecting **.gdf** files types.
- You will now get a dialog-box asking you what you would like to see. To display xy-scatterplots at the various output times, select to plot variable **x** along the X-axis and **y** along the Y-axis. Press OK.
- You can now cycle through the plots using the cursor keys (← and →) or using the previous and next plot buttons ( and ) on the toolbar. The output times are listed in the subtitle of all plots.


Figure 2-9: Plot settings for **quads.gdf**

Because all plots are autoscaled individually, you can not see the beam going through a waist, except by studying the range of the axes. Furthermore, the units would be more convenient when given in [mm]. To solve these shortcomings, set the scaling to manual and change the units, as shown in Figure 2-9.

- To produce this settings dialog-box, double-click anywhere in the plot window or select the Settings command from the Plot menu.
- Go to the sheet specifying the X-axis. The values plotted along the axis are  $\text{scale} \cdot x + \text{offset}$ . Set the scale to 1000 to convert from [m] to [mm]. When the axis scaling is changed, it is recommended to also change the axis label. Repeat for the Y-axis.
- Select Manual scaling. Now you can enter the values for the minimum and the maximum. We suggest using -10 and 10. Repeat for the Y-axis.

Figure 2-10: **Result.gdf** plotted in GPTwin. “Aspect ratio” is selected to plot a cylindrical-symmetric beam as a circle instead of an ellipse.

Now all plots have the same scale, as shown in Figure 2-10. When you cycle through the plots, you will clearly see the beamsize changing and going through a waist.

If you decide to rerun GPT with different inputfile parameters, you can update the selected plots either by pressing the Update button  on the Toolbar, by pressing F5 or by selecting the Update command from the Plot menu. The plots shown are then based on the new data.

## 2.2.4 Statistics

For detailed data analysis, the GDFA program can be used as explained in section 3.12. However, sometimes it is more convenient to calculate simple statistics directly from the raw GPT data. Figure 2-11 shows the statistics dialog, obtained by double-clicking on the plot, calculating the average z-position of all particles. The result can be plotted in the window and is automatically updated.

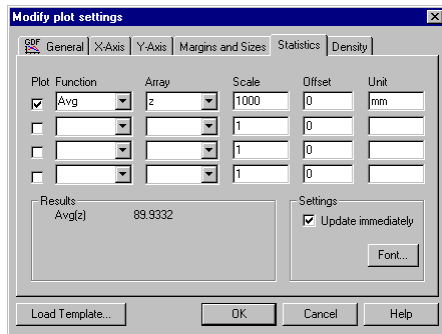


Figure 2-11: Statistics dialog calculating and plotting the average z-position of all particles.

The Plot check box must be checked to plot the selected statistic in the window after the dialog is closed. The scale and offset parameters are identical to those on the x- and y-axis dialogs. Selectable statistical functions are listed in Table 2-A. Statistics are always calculated over the complete data set. Therefore, cropping a plotted axis by selecting manual scaling does not affect the results.

Table 2-A: GPTwin statistics functions


Function	Description
<b>Min</b>	Minimum
<b>Max</b>	Maximum
<b>Max-Min</b>	Maximum-Minimum
<b>Avg</b>	Average
<b>Std</b>	Standard deviation
<b>Sum</b>	Sum
<b>N</b>	Number of particles

## 2.2.5 Trajectory output

Trajectory output is calculated in the batch file **quads.bat** from the raw GPT output by the GDFTRANS program:

```
gdftrans -o traj.gdf result.gdf time x y z
```

To display the results open the file **traj.gdf**, select z horizontally, x vertically and check the lineplot option on the General property page. Now the individual particle trajectories are shown one by one when cycling through the plots. Alternatively, you can check the combine plot option, also on the General page, to plot all trajectories in the same window.

Instead of plotting the x-coordinate along the y-axis, it is also possible to select the y-coordinate along the y-axis. Use the New Window command in the Window menu to open a new window and plot a different projection. The result is shown in Figure 2-12. When the combine plot option is selected in neither of the plots, cycling through the individual trajectories in one plot will automatically show the corresponding trajectory in the other projection. When the GPT inputfile is modified and rerun, updating the plots with the Update button  on the Toolbar will automatically update both windows.

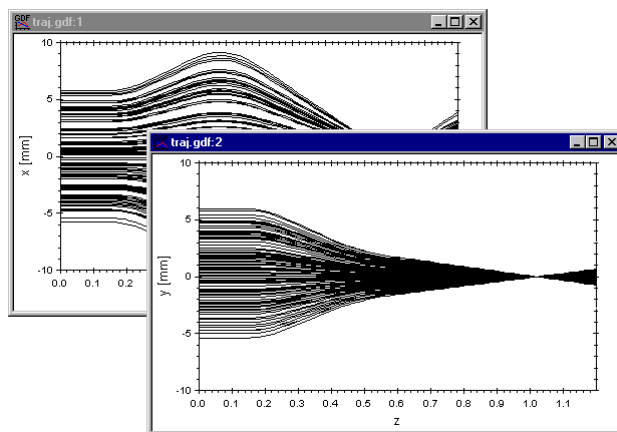


Figure 2-12: Two different projections of all particle trajectories.

### 2.2.6 Extracting beam parameters

Most data analysis is done by the GDFA program, capable of calculating a large number of different beam parameters from the raw GPT output. In this section, we will create plots of the transverse standard deviations as function of longitudinal position

```
gdfa -o std.gdf quads.gdf time stdx stdy avgz
```

The parameters **stdx**, **stdy** and **avgz** are standard programs of GDFA calculating the following beam properties:

<b>stdx</b>	Standard x-deviation of the particles: A measure for the beam size in the x direction.
<b>stdy</b>	Standard y-deviation of the particles: A measure for the beam size in the y direction.
<b>avgz</b>	Average z-coordinate of the particles: Beam position.

The variable **time** instructs GDFA to produce output so that the output contains the requested beam parameters at different times. The output is written to the file **std.gdf**, specified with the **-o** option. For a complete description of GDFA and the built-in programs, we refer to section 3.12.

To view **std.gdf** using GPTwin, you can do the following:

- Open **std.gdf**.
- Select Line plot, **avgz** on the horizontal axis and **stdx** on the vertical axis. Press OK.
- To also see a plot of **stdy**, select the New window command from the Window menu.
- Now select Line plot, **avgz** on the horizontal axis and **stdy** on the vertical axis. Press OK.

You will now see two windows showing different results from the same file, as shown in Figure 2-13.

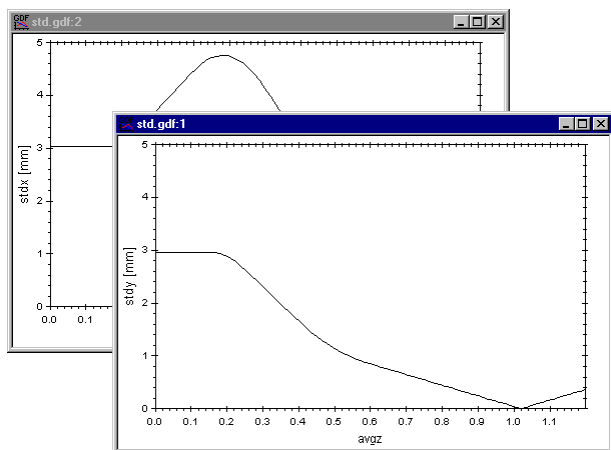


Figure 2-13: Beam size as function of z. The waist in the x-direction is much more position dependent than the waist in the y-direction.

### 2.2.7 Templates

Having to set all plot options can be time consuming. As a convenience it is possible to save and load all plot settings using a template file. Template files always have extension **.gdt**. For example, when the file **traj.gdf** is first opened, loading the template **traj\_y\_z.gdt** immediately sets all options for a trajectory plot of y as function of z. In all tutorial sections, template files are present having a name in this format **filename\_yaxis\_xaxis.gdt**. When **filename.gdf** is opened with such a template, a **yaxis** as function of **xaxis** plot is immediately shown. The most convenient way to open a template is clicking the Load Template button in the lower-left corner of the plot-settings dialog box. Alternatively, the Load Template command in the Plot Menu can be used.

The plot settings of an existing plot can be saved with the Save template command in the Plot menu. A dialog box appears asking what settings to store. To (re)load plot settings from a template file, the (Re)Load template command in the Plot menu can be used. A dialog box appears asking what plot settings to overwrite. Using this mechanism, it is possible to create templates for the x-axis only, or restore only the x-axis from a complete template.



## 2.2.8 Printing and exporting graphics

Everything shown in a GPTwin window can be printed with the Print command in the File menu. The appropriate printer and paper size can be selected using Print setup in the File menu.

When many plots are present, we recommend increasing the number of horizontal and vertical plots in the General dialog of the plot settings. To see if the results are as expected you can use the print preview command in the File menu. This allows you to cycle through the various pages and zoom in and out.

Various important plot settings for printing graphics can be found in the Margins and Sizes property page of the plot settings, shown in Figure 2-14.

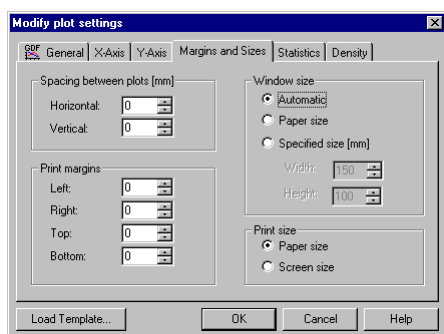


Figure 2-14: Various plot settings

Both text and graphics can be copied to the clipboard using the Copy command in the Edit menu.

It is also possible to save a plot in a Windows Metafile or Enhanced Metafile format using Save As in the File menu. Such metafiles can be included by a variety of other programs like AutoCAD and TeX.

## 2.3 Scanning the beam energy

This section continues with the example of the first section. Here the effect of the initial beam energy on the spot size at  $z=1$  m is examined. The inputfile needed to examine this effect is shown in Listing 2-3 and can be found in the `tutorial/quadscan` folder. The corresponding batch file containing all the necessary commands, `quadscan.bat`, is explained below.

Listing 2-3: GPT inputfile to examine the effect of beam energy on spotsize:

`tutorial/quadscan/quadscan.in`

```
1. # GPT Tutorial: Scanning beam energy
2.
3. # Start initial beam
4. setparticles("beam",100,me,qe,0.0) ;
5. setrxydist("beam","u",radius/2, radius) ;
6. setphidist("beam","u",0,2*pi) ;
7. setGdist("beam","u",gamma,0) ;
8.
9. # Position the quadrupole lenses
10. quadrupole( "wcs","z",0.2, 0.1, 3.90 ) ;
11. quadrupole( "wcs","z",0.5, 0.2,-3.25 ) ;
12.
13. # Specify output screen
14. screen( "wcs","I", 1.0 ) ;
```

The two differences with the previous inputfile are:

- A The beam parameters `gamma=100` and `radius=6e-3` statements are removed. This is needed because they are defined in a separate file, as we will see later in this section.
- B The `snapshot` statement is replaced with a `screen` statement. A screen interpolates the particle coordinates at a fixed plane in 3D space. Here the screen is positioned at  $z=1$  m. For the reference of `screen`, see section 4.3.10.

Now that we have the inputfile, the next step is to scan the beam energy. To accomplish this, various values for gamma and radius could be specified on the GPT commandline as follows:

```
gpt -o res100.gdf quadbeam.in gamma=100 radius=6e-3
gpt -o res110.gdf quadbeam.in gamma=110 radius=6e-3
etc.
```

Although this works, having to analyze all the outputfiles is tedious. Therefore, it is recommended to use Multiple Run (MR) to perform the same job. It runs GPT with one or more varying or fixed parameters, just like the commandline approach, but it collects all output in one structured GDF file. For a complete description of MR we refer to section 3.18.

MR reads which parameter to set or scan from an additional file. For example to scan `gamma` over the range from 50 to 150 in steps of 5, and set the beam radius fixed at 6 mm we typically create a file named `scan.mr` containing the following lines:

```
1. gamma 50 150 5
2. radius 6e-3
```

The command to run GPT with `gamma` varying from 50 to 150 then is:

```
mr -v -o result.gdf scan.mr gpt quadbeam.in
```

After running the MR command, all the output is contained in the file `result.gdf`. We can use GDFA again to calculate the beam's standard  $x$ - and standard  $y$ -deviation:

```
gdfa -o std.gdf result.gdf gamma stdx stdy
```

This time the `group_by` variable is `gamma`. This is because we want to make a plot where every point is calculated for a different `gamma`. As a rule of thumb, the `group_by` variable is usually the scanned parameter, `time` or `position`. The complete batch file is listed in Listing 2-4, where ASCII output of the result is generated using the GDF2A program.

Listing 2-4: Batch file for scanning the beam energy. Filename: **tutorial/quadscan/quadscan.bat**

1. **mr -v -o result.gdf scan.mr gpt quadscan.in**
2. **gdffa -o std.gdf result.gdf gamma stdx stdy**
3. **gdf2a -o std.txt std.gdf**

The result is shown in Figure 2-15. To reproduce these plots, open **std.gdf** in GPTwin with template **std\_xgamma.gdt**, select New Window and open again with template **std\_ygamma.gdt**.

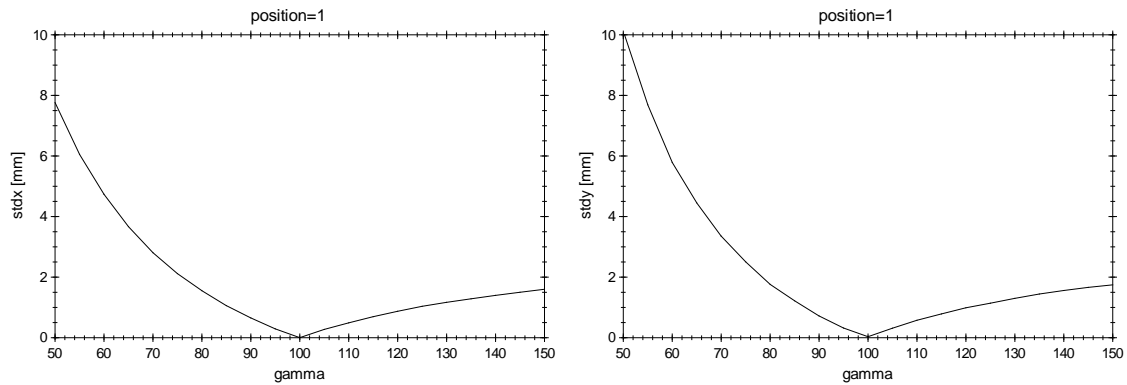


Figure 2-15: Spot size as function of beam energy.

The result shows that the effect of different beam energy on spot size is approximately equal in both planes.

In order to use the same GPT inputfile with and without MR, default values for variables can be defined in the GPT inputfile as shown below:

**if( !defined(gamma) ) gamma=100 ;** If not defined gamma, then set gamma to 100.

## 2.4 Automatic solving

There are two programs that can be used to instruct GPT to automatically find a set of variables for given objectives and constraints: GDFSOLVE and GDFMGO.

GDFMGO optimizes several conflicting objectives, without a-priori making a decision about the relative relevance. For example, in a beamline where total charge and pulse-duration are conflicting objectives, GDFMGO can make a scatterplot where the result is the trade-off between those objectives, and where each point is fully optimized in all variables. This is ideal for decision making and a great aid in understanding complex systems. The underlying genetic algorithm is extremely robust, but CPU intensive.

GDFSOLVE solves for multi-dimensional roots or one-dimensional objectives using more mathematical tools. It is the more analytic program that uses an estimated Hessian matrix for optimization problems, and the Jacobian for root-finding. It is therefore much faster than GDFMGO, but because it works with derivatives of the objective functions it also is more sensitive to numerical noise.

In this section an electron beam is sent through two quadrupole lenses and needs to be focused at  $z=1$  m. Unlike the previous sections, the beam starts with a finite emittance to be able to make use of the Courant-Snyder GDFA routines. Furthermore, both time and position output is requested to simplify reproduction of the results shown below. Finally the tracking accuracy is increased to ensure stable results if small changes are made to the quadrupole strengths. The complete inputfile is shown in Listing 2-5 where the beam energy **gamma** and the strengths of the two quadrupoles **Q1** and **Q2** still need to be specified. All files can be found in the **tutorial/gdfsolve** folder.

Listing 2-5: GPT inputfile describing a beam through two quadrupole lenses with strengths Q1 and Q2. Both time and position output are requested. Filename: tutorial/gdfsolve/quads.in

```

1. # GPT Tutorial: GDFSolve
2.
3. # A slightly higher accuracy is needed
4. accuracy(5)
5.
6. # Real space of initial beam
7. radius = 6e-3 ;
8. setparticles("beam",100,me,qe,0.0) ;
9. setrxydist("beam","u",radius/2, radius) ;
10. setphidist("beam","u",0,2*pi) ;
11.
12. # Phase space of initial beam
13. GBr = 10e-3 ;
14. setGBrxydist("beam","u",GBr/2,GBr) ;
15. setGBphidist("beam","u",0,2*pi) ;
16. setGdist("beam","u",gamma,0) ;
17.
18. # Position the quadrupole lenses
19. quadrupole( "wcs","z",0.2, 0.1, Q1 ) ;
20. quadrupole( "wcs","z",0.5, 0.2, Q2 ) ;
21.
22. # Specify output screen
23. snapshot(0,4e-9,0.05e-9) ;
24. screen( "wcs","I", 1.0 ) ;

```

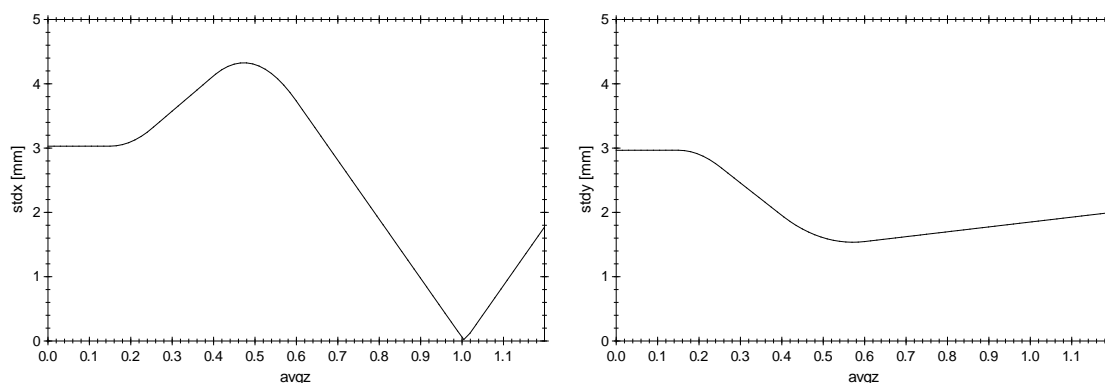


Figure 2-16: Standard deviation of x- and y-size as function of longitudinal position for **gamma**=100. The initial guess for the quadrupole settings, **Q1**=3 and **Q2**=-3 [T/m], does not produce a minimum in both planes at  $z=1$  m.

Figure 2-16 shows the results for **gamma**=100 with an estimated **Q1**=3 and **Q2**=-3 [T/m]. The plots can be reproduced with the following commands and subsequently plotting the file **result.gdf**.

```
gpt -o quads.gdf quads.in gamma=100 Q1=3 Q2=-3
gdfa -o result.gdf quads.gdf time avgz stdx stdy
```

Clearly the beam is not sent through a minimum in the y-plane at  $z=1$  m. The following sections describe how GDFSOLVE can be used to automatically adapt **Q1** and **Q2** such that a minimum is obtained in both planes.

### 2.4.1 Finding a minimum using GDFSolve

The GDFSOLVE program tries to satisfy multi-dimensional constraints and optimizes beam parameters by varying any number of GPT inputfile variables. This section demonstrates the use of GDFSolve by automatically finding the quadrupole settings of the previous sections. A description of the internal algorithms of GDFSOLVE can be found in sections 1.12.1 to 1.12.2 and more practical information can be found in reference section 3.14.

With some patience and a structured approach, it is possible to find quadrupole settings that produce a minimum in both planes at  $z=1$  m. GDFSolve can do this automatically. The required inputfile for GDFSolve describing the free variables and beam parameters to minimize is shown in Listing 2-6.

Listing 2-6: Inputfile for GDFSolve requesting a minimum in x and y at  $z=1$  m by varying **Q1** and **Q2**. Filename:

```
opti.sol
1. [VARIABLES]
2. Q1 = +3 ; # Initial value
3. Q1.absdelta = 0.01 ; # Absolute stepsize
4. Q1.min = 0 ; # Q1 must be positive
5.
6. Q2 = -3 ; # Initial value
7. Q2.absdelta = 0.01 ; # Absolute stepsize
8. Q2.max = 0 ; # Q2 must be negative
9.
10. [OPTIMIZE]
11. stdx = 0 ; # Approximate minimum in stdx
12. stdx.position = 1.0 ; # At position z=1 m
13. stdx.abstol = 0.1e-3 ; # Absolute tolerance
14.
15. stdy = 0 ; # Approximate minimum in stdy
16. stdy.position = 1.0 ; # At position z=1 m
17. stdy.abstol = 0.1e-3 ; # Absolute tolerance
```

The variables **Q1** and **Q2** are defined in the **[VARIABLES]** section and start from 3 and -3 respectively. Both **Q1** and **Q2** have an absolute initial stepsize of 0.01 specified using **absdelta**. This stepsize is very important. A too small step immediately leads to a local minimum caused by simulation noise. A too large step prevents the algorithm from getting started at all because all steps seem to deviate further from the minimum. When GDFSolve does not work as expected the initial stepsize is the first thing to check. To guarantee that **Q1** and **Q2** have the correct sign, **min** and **max** statements are used.

The **[OPTIMIZE]** section describes one or more GDFA analysis routines to optimize. Both standard x and y deviation, **stdx** and **stdy**, must be as small as possible at a **position** of 1 m. A change in beam size below 0.1 mm, specified using **abstol**, is not significant. This tolerance is as important as the **absdelta** specification for a variable. A too high tolerance regards every solution as a minimum, while a too small tolerance instructs GDFsolve to find a minimum in the simulation noise.

Instead of running GPT directly, we now instruct GDFsolve to run GPT repeatedly to find the desired minimum. Because the beam energy **gamma** is not specified in the GPT inputfile, it must also be defined on the commandline. The output of GDFsolve corresponds to the best GPT run found and can, just like any other GPT run, be analyzed by GDFA. The correct instructions to run GDFsolve and analyze the results are shown in Listing 2-7. The plotted output of GDFA immediately shows a minimum in both the horizontal and vertical plane, see Figure 2-17. When compared to manually finding a simultaneous minimum in two variables, GDFsolve saves a lot of tedious work in this example.

Listing 2-7: Batch file to run GDFsolve and analyze the obtained minimum with GDFA. Filename: **opti.bat**.

1. **gdfsolve -v -o quads.gdf opti.sol gpt quads.in gamma=100**
2. **gdffa -o result.gdf quads.gdf time avgz stdx stdy**

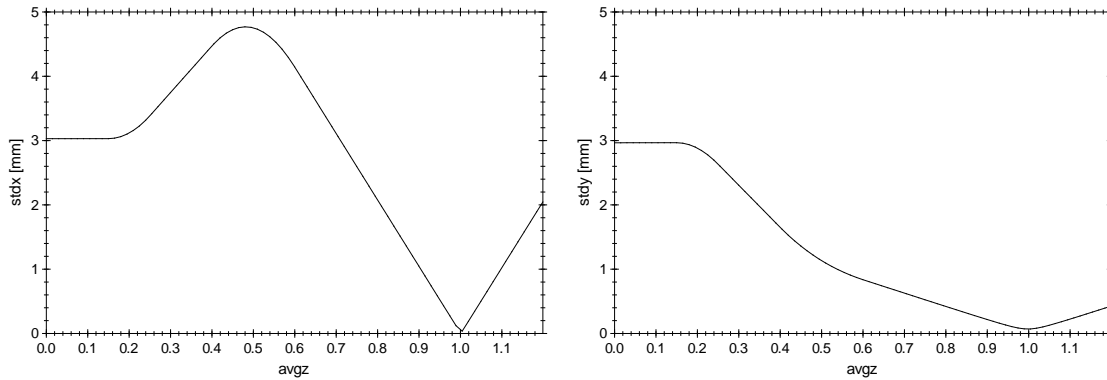


Figure 2-17: Output of GDFsolve used as optimizer, analyzed with GDFA: A minimum in both the horizontal and vertical plane.

Clearly GDFsolve is able to find the requested minimum by varying **Q1** and **Q2**. To know what settings of **Q1** and **Q2** correspond to the final minimum, the outputfile can be inspected using GDF2A. Alternatively, the verbose GDFsolve output can be examined. This output, shown when the **-v** option is specified, shows the progress of GDFsolve after each GPT run as shown in Figure 2-18. The first three columns specify the iteration number **N**, and the current settings for **Q1** and **Q2**. The following two columns specify the resulting **stdx** and **stdy**, where the number between parentheses is the scaled result obtained by dividing by the specified tolerance. The last column is the rms value, the square root of the sum of the squares of the scaled results. This rms column is the value that GDFsolve tries to minimize. As shown in Figure 2-18, GDFsolve works its way in 49 iterations from 3 and -3 for **Q1** and **Q2** to the final solution of 3.92 and -3.25 [T/m].

N	Q1	Q2	stdx	stdy	rms
1	3	-3	5.78e-005 ( 0.6)	0.00185 ( 18.5)	( 19.1)
2	3.01	-3	6.36e-005 ( 0.6)	0.00183 ( 18.3)	( 18.9)
3	3.03	-3	7.3e-005 ( 0.7)	0.00179 ( 17.9)	( 18.7)
4	4.63	-3	0.00107 ( 10.7)	0.00174 ( 17.4)	( 28.1)
5	3.64	-3	0.000445 ( 4.4)	0.000421 ( 4.2)	( 8.7)
6	3.7	-3	0.00048 ( 4.8)	0.000298 ( 3.0)	( 7.8)
7	4.05	-3	0.000706 ( 7.1)	0.000494 ( 4.9)	( 12.0)
8	3.78	-3	0.000535 ( 5.4)	0.000121 ( 1.2)	( 6.6)
9	3.89	-3	0.000596 ( 6.0)	0.000136 ( 1.4)	( 7.3)
10	3.8	-3	0.000545 ( 5.4)	9.12e-005 ( 0.9)	( 6.4)
11	3.82	-3	0.000554 ( 5.5)	7.25e-005 ( 0.7)	( 6.3)
12	3.84	-3	0.00057 ( 5.7)	7.32e-005 ( 0.7)	( 6.4)
13	3.83	-3	0.00056 ( 5.6)	6.74e-005 ( 0.7)	( 6.3)
14	3.82	-2.99	0.00058 ( 5.8)	6.95e-005 ( 0.7)	( 6.5)
.	.	.	.	.	.
.	.	.	.	.	.
43	3.92	-3.25	1.74e-005 ( 0.2)	6.97e-005 ( 0.7)	( 0.9)

```

44      3.94      -3.25  2.55e-005(  0.3)  8.26e-005(  0.8) (  1.1)
45      3.92      -3.24  3.68e-005(  0.4)  7.01e-005(  0.7) (  1.1)
46      3.92      -3.27  3.33e-005(  0.3)  7.12e-005(  0.7) (  1.0)
47      3.93      -3.25  2.28e-005(  0.2)  7.61e-005(  0.8) (  1.0)
48      3.91      -3.25  1.47e-005(  0.1)  7.86e-005(  0.8) (  0.9)
49      3.92      -3.25  1.74e-005(  0.2)  6.97e-005(  0.7) (  0.9)

```

Figure 2-18: GDFsolve verbose output showing the progress from 3 and -3 for **Q1** and **Q2** respectively to the final solution of 3.92 and -3.25 [T/m].

## 2.4.2 Solving for a waist

GDFsolve used as optimizer is a great tool, but 49 iterations for a relatively simple minimization could be a problem. Especially when we realize that when more variables are included the number of iterations often scales with  $N^2$ . Your patience will be severely tested when each GPT run contains a non-trivial design including 3D spacecharge calculations. The solution is straightforward: Don't use the optimizer unless you absolutely have to. In the above case, there is a very good alternative: The waist is not only defined by a minimum in **stdx** and **stdy**, but also as a zero in the Courant-Snyder  $\alpha$  parameter. Minimizing **stdx** and **stdy** is equivalent to finding a zero in **CSalphax** and **CSalphay**. Such a root-finding procedure is typically much faster and often more reliable than minimizing a function. The required inputfile for GDFsolve is shown in Listing 2-8.

Listing 2-8: Inputfile for GDFsolve finding a simultaneous zero in **CSalphax** and **CSalphay** by varying **Q1** and **Q2**.

Filename: **root.sol**

```

1. [VARIABLES]
2. Q1 = +4 ;      # Initial value
3. Q1.absdelta = 0.01 ;      # Absolute stepsize
4. Q1.min = 0 ; # Q1 must be positive
5.
6. Q2 = -3 ;      # Initial value
7. Q2.absdelta = 0.01 ;      # Absolute stepsize
8. Q2.max = 0 ; # Q2 must be negative
9.
10. [CONSTRAINTS]
11. CSalphax = 0 ;      # CSalphax must be zero
12. CSalphax.position = 1 ;      # At position z=1 m
13. CSalphax.abstol = 1 ;      # Absolute tolerance
14.
15. CSalphay = 0 ;      # CSalphay must be zero
16. CSalphay.position = 1 ;      # At position z=1 m
17. CSalphay.abstol = 1 ;      # Absolute tolerance

```

The **[VARIABLES]** section is identical to Listing 2-6, specifying to vary **Q1** and **Q2**. The initial step used to calculate the derivative is specified with an **absdelta** of 0.01 and the correct sign is enforced using the **min** and **max** statements. To use GDFsolve as root finder, the **[OPTIMIZE]** section is replaced by a **[CONSTRAINTS]** section: **CSalphax** and **CSalphay** must both be zero at  $z=1$  m. A solution is found when **CSalphax** and **CSalphay** are within **abstol**, in the rms sense, of the target value of zero. For a tolerance of unity, this reduces to a termination criterion of  $\sqrt{\text{CSalphax}^2 + \text{CSalphay}^2} < 1$ . As shown in Listing 2-9 and Figure 2-19 running GDFsolve and the produced results are almost identical to the minimization case described in section 2.4.1.

Listing 2-9: Batch file to run GDFsolve and analyze the obtained minimum with GDFA. Filename: **root.bat**.

```

1. gdfsolve -v -o quads.gdf root.sol gpt quads.in gamma=100
2. gdfa -o result.gdf quads.gdf time avgz stdx stdy

```

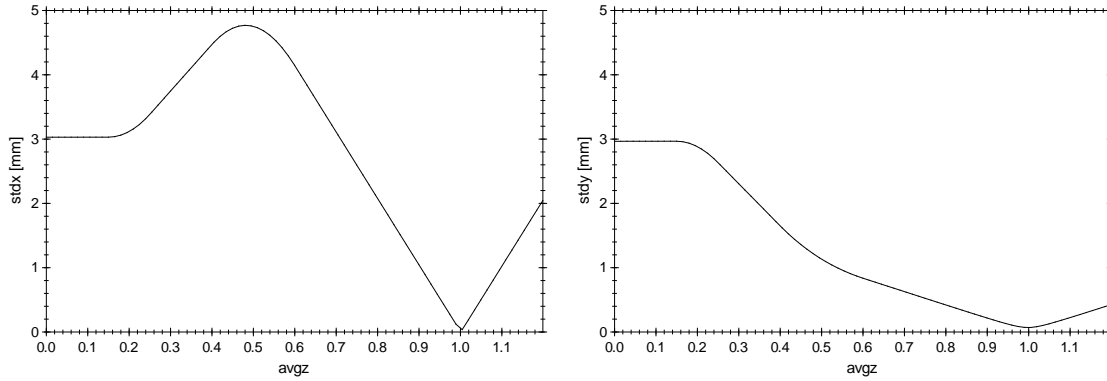


Figure 2-19: Output of GDFSolve used as root-finder, analyzed with GDFA: A minimum in both the horizontal and vertical plane.

The length of the verbose output shown in Figure 2-20 shows the big advantage of the root-finder approach. It takes only 5, compared to 49, attempts to get **Q1** and **Q2** to 3.93 and  $-3.26$ . This is plus or minus the specified **absdelta**, with about an order of magnitude improvement in CPU time. The reason for this improvement is a completely different algorithm for the root finder. The first function evaluation is identical, but then the Jacobian matrix is estimated by varying each variable an amount of **absdelta**. These lines are indicated by a **J**, and only the difference with the previous run is shown. After the first three runs, a matrix-inversion in GDFSolve yields the first new attempt shown in run number four. A small correction to the Jacobian is then applied and the fifth estimate is already on target.

N	Q1	Q2	CSalphax	CSalphay	rms
1	4	-3	40.5 ( 40.5)	-7.22 ( -7.2) (	41.2)
2J	0.01		0.364 ( 0.4)	-0.502 ( -0.5)	
3J		0.01	1.41 ( 1.4)	-0.198 ( -0.2)	
4	3.97	-3.28	-2.22 ( -2.2)	-1.32 ( -1.3) (	2.6)
5	3.93	-3.26	0.444 ( 0.4)	-0.442 ( -0.4) (	0.6)

Figure 2-20: GDFSolve verbose output showing the progress from 4 and  $-3$  for **Q1** and **Q2** respectively to the final solution of 3.93 and  $-3.26$  [T/m].

Is it really that simple to change from minimization to root-finding? Unfortunately, no. Root-finding is fundamentally different from optimization, and typically new (undesired) solutions are introduced. With good initial estimates this provides no problem, but when we start **Q1** and **Q2** for example from  $+2$  and  $-2$  the results as shown in Figure 2-21 are produced: A collimated beam in the y-plane also produces a zero **CSalphay**, but this was not what we were looking for.

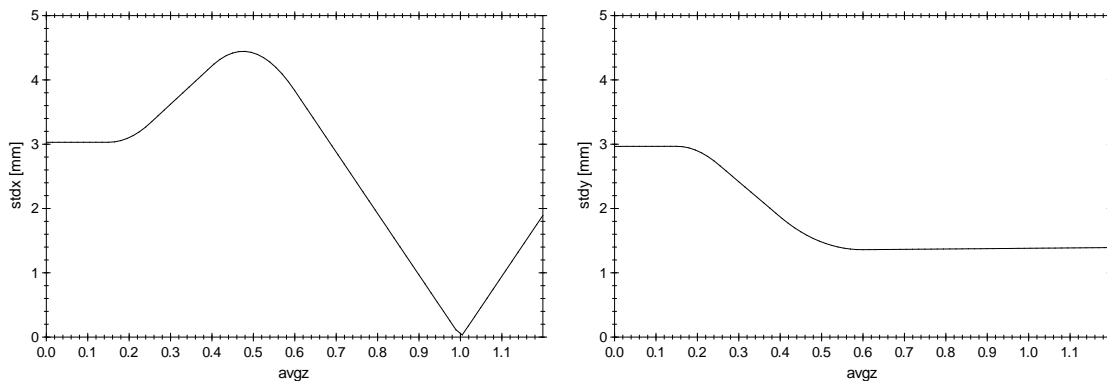


Figure 2-21: Undesired solution for **Q1** and **Q2** starting from an initial estimate of  $+2$  and  $-2$  respectively.

### 2.4.3 Scanning GDFSOLVE using MR

Scanning a GDFSolve command using MR allows you to calculate optimal variable values as function of any other variable. It is not the typical thing to do as a novice GPT user. To explain the procedure, the previous example of section 2.4.2 is continued while scanning the beam energy **gamma** using MR.



Listing 2-10: While MR scans the beam energy **gamma**, GDFsolve is used to find the optimal settings for **Q1** and **Q2**.

Filename: **scan.bat**

```
1. mr -v -o quads.gdf gamma.mr gdfsolve root.sol gpt quads.in
2. gdffa -o result.gdf quads.gdf time avgz stdx stdy
3. gdffa -o Q12.gdf quads.gdf gamma Q1 Q2
```

where the file **gamma.mr** contains the following line:

```
1. gamma 90 110 5
```

As shown in Listing 2-10 the first line of the batch file runs MR with **gamma** varying from 90 to 110 as described in the file **gamma.mr**. Instead of directly running GPT with the **quads.in** file, GDFsolve is used to find the corresponding waist described in the **root.sol** file with identical constraints as described in section 2.4.2. The output of all this, **quads.gdf**, contains the best results for every **gamma**. Here we go one step further: Plotting the optimal **Q1** and **Q2** as function of **gamma**. The values for **Q1** and **Q2** are written in the outputfile which can be inspected using GDF2A:

```
gdf2a -o result.txt result.gdf
```

In order to plot the results using GPTwin, two short custom GDFA programs need to be written:

```
int Q1_func( double *result ) { return( gdfmgetval( "Q1", result ) ) ; }
int Q2_func( double *result ) { return( gdfmgetval( "Q2", result ) ) ; }
```

The procedure how to add these functions is explained in the GPT Custom Elements documentation. After these programs have been added, the last GDFA line calculates **Q1** and **Q2** as function of **gamma** in the file **Q12.gdf**. The result is a perfectly linear correspondence, as shown in Figure 2-22.

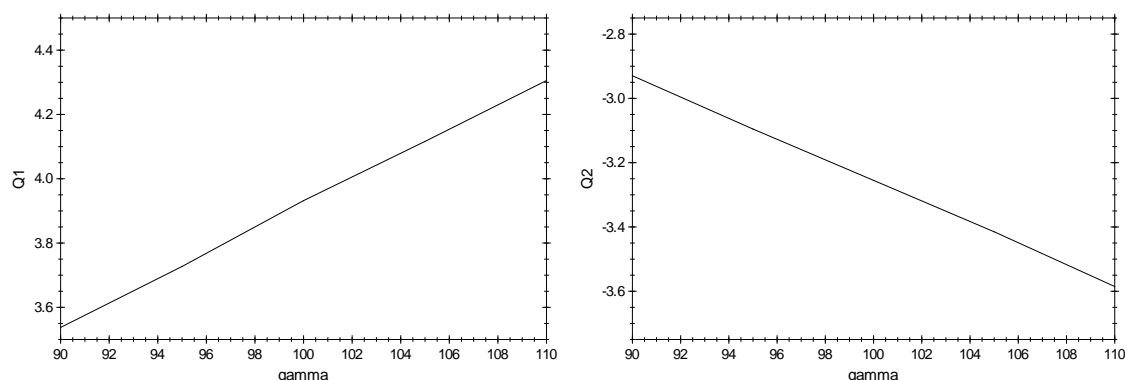


Figure 2-22: Optimum values for **Q1** and **Q2** as function of **gamma**.

## 2.4.4 Multi-objective: GDFMGO

We continue here with the same example of focusing a beam with two quadrupoles, but now as a multi-objective problem. Our two objectives are to minimize **stdx** *and* **stdy**, in order to see how one depends on the other. In other words, we want to know how much bigger **stdy** becomes if we try to further reduce **stdx**. Such multi-objective optimization is the realm of GDFMGO, and the inputfile to accomplish this is given in Listing 2-11.

Listing 2-11: Inputfile for GDFMGO to optimize for both **stdx** and **stdy**. Filename: **opti.mgo**

```

1. [OPTIONS]
2. populationsize=200 ;           # To make nice plots, not really needed
3.
4. [VARIABLES]
5. Q1.min = 0 ;                  # Q1 must be between
6. Q1.max = 10 ;                  # 0 and 10
7.
8. Q2.min = -10 ;                 # Q2 must be between
9. Q2.max = 0 ; # -10 and 0
10.
11. [OPTIMIZE]
12. stdx.position = 1.0 ;         # We look at z=1 m
13. stdx.max = 0.002 ;            # Beam must be smaller than 2 mm
14.
15. stdy.position = 1.0 ;         # Idem for stdy
16. stdy.max = 0.002 ;           #

```

When using GDFMGO it is not needed, or even possible, to specify deltas and tolerances for the variables and objectives. Here the population size is overwritten to 200 to make nicer plots. The default values work pretty well in most cases. Furthermore, to make the example more interesting, we changed the initial zero energy spread and created **quads.mgo.in**:

```

16. setGdist("beam","u",gamma,gamma/5) ;

```

Now we are ready to run GPT via GDFMGO to automatically get the trade-off between **stdx** and **stdy**:

```

gdfmgo -v -o quads.gdf opti.mgo gpt -j 1 quads.mgo.in gamma=100

```

The results can be plotted from **quads.gdf** with templates **stdxy.gdt** and **q1q2.gdt**. To illustrate the genetic algorithm, the 1<sup>st</sup>, 5<sup>th</sup>, 10<sup>th</sup> and final generations are shown in Figure 2-23. The code starts by randomly filling variable space for **Q1** and **Q2**, based on the min and max values for the variables **Q1** and **Q2**. The simulation results for **stdx** and **stdy** are subsequently ranked and only the best ones are candidates for further attempts. The ranking is shown as color coding in the plots, ranging from blue (good) to red (worse). The initial attempt seems hopeless, but already after 5 generations significant progress is observable: Quite a few results are below the 2 mm threshold as set in the **mgo** file, and the area in variable space is significantly reduced. At the 10<sup>th</sup> iteration, the Pareto front is already reached with very good approximation, see the dark blue datapoints. The sampling however is rather poor because too many points are still too far out, so the optimizer continues. At the final generation, number 31 in this case, the desired result is reached. It can be seen that above approximately 0.3 mm you can reduce both **stdx** and **stdy**, but if you want to reduce either below that value, you pay a big price in the other dimension.

Note that the large area in variable space for **Q1** and **Q2** has fully collapsed to a parametric line. The meaning of this line is that if you want a small **stdx** and a small **stdy**, you only have to consider combinations of **Q1** and **Q2** that lie on this line. The initial 2D problem has hereby collapsed into a 1D problem. The final dimensionality is always the number of objectives minus one, regardless of the number of variables. This spectacular reduction of dimensionality is an intrinsic feature of the multi-objective approach, and this makes it such a useful tool for decision making.

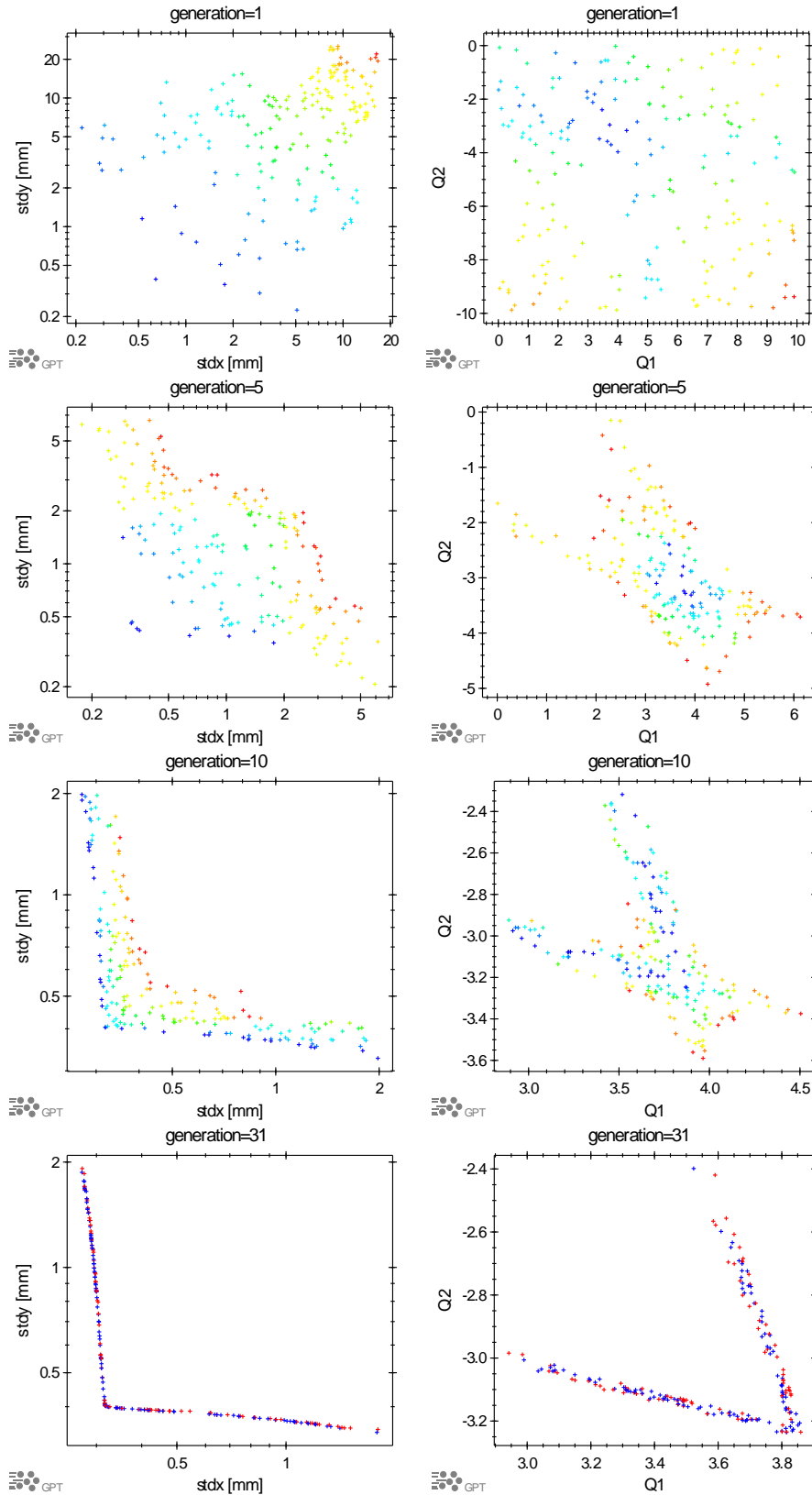


Figure 2-23: Evolution towards minimum values for both **stdx** and **stdy** automatically obtained with GDFMGO.

Especially in the early stages of optimization, GDFMGO might run GPT with parameters very far off realistic settings. This can result in a significant waste of CPU time because unrealistic settings tend to consume relatively large amounts of computational power. It is therefore recommended to always add `setrlimit("CPU",N,M)` to the GPT inputfile, especially when running on large clusters. This instructs GPT to finish the timestep and abort a run softly after N seconds CPU time, while enforcing a hard-limit of M seconds.

## 2.5 Electrostatic accelerator

This GPT simulation contains only one particle that is accelerated in a homogeneous electric field. This particle starts at the origin and is accelerated over 1 meter by a constant electric field of 1 MV/m. It allows us to test the numerical results with analytical expressions. More realistic accelerator models are typically included using the `map2D_E` element, described in section 4.7.5. Parameters of interest are  $z$ ,  $\beta z$  and  $\gamma$ . First we will explain the inputfile and then verify the results quantitatively.

The GPT inputfile located in the `tutorial/accel` folder is shown in Listing 2-12. The batch file `accel.bat` can be used to run the example.

Listing 2-12: GPT inputfile with homogeneous acceleration field: `tutorial/accel/accel.in`

```
1. # GPT Tutorial: Electrostatic accelerator
2.
3. # Homogeneous E-field: 1MV/m
4. erect( "wcs", "z", 0.5, 1, 1, 1, -1e6 ) ;
5.
6. # Position particle at origin with zero velocity
7. setstartpar("beam", 0, 0, 0, 0, 0, 0) ;
8.
9. # Output from 0 to 6 ns every 0.1 ns
10. snapshot( 0, 6e-9, 0.1e-9 ) ;
```

Line 4 positions an `erect`, see section 4.5.4, a uniform homogeneous electric field bounded by a rectangular box. The center of the box is at 0.5 m and all the box dimensions are 1 m. The electric field strength is 1 MV/m. Line 7 starts one particle at the origin with zero velocity using `setstartpar`, see section 4.2.1.13. Line 10 instructs the GPT kernel to generate output every 0.1 ns upto 6 ns.

The instruction to run GPT is:

```
gpt -o result.gdf accel.in
```

The outputfile, `result.gdf`, contains the particle coordinates as function of time, in a format devised for more than one particle to output. We want to plot the  $z$ -,  $\beta$ - and  $\gamma$ -coordinates of the single particle, but this can not be done immediately. As can be verified using `gdf2a result.gdf`, the outputfile has the following structure:

time=0.0 ns	
	particle coordinates
time=0.1 ns	
	particle coordinates
:	
time=6.0 ns	
	particle coordinates

When plotted directly, such a file produces 61 plots containing just one point. What is needed is a GDF file with the following structure:

$z$	$\beta z$	$\gamma$	time
...	...	...	0.0 ns
...	...	...	0.1 ns
:	:	:	:
...	...	...	6.0 ns

Such output can easily be obtained with the GDFTRANS program, but also with GDFA:

```
gdfa -o avg.gdf result.gdf time avgz avgBz avgG
```

Taking the average of just one particle is the same as returning the particle coordinates. Since the programs to calculate averages are standard in GDFA, these can conveniently be used. `avgBz` calculates the average normalized velocity in the  $z$ -direction, `avgG` calculates the average Lorentz factor. The `group_by` variable is `time`, because the points in the plot are all calculated at different times. Whether to use GDFTRANS or

GDFA is a matter of taste, though we prefer GDFA because it allows us to switch between single- and multiple-particle simulations. The results are graphically shown in Figure 2-24.

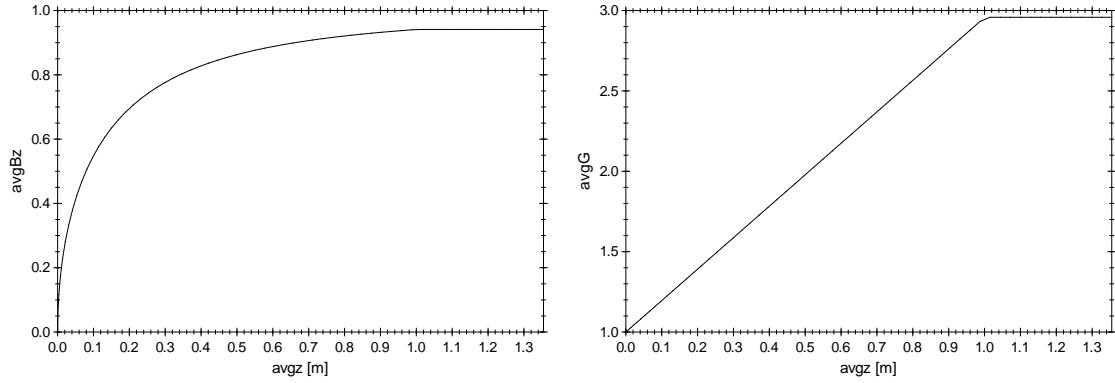


Figure 2-24: Normalized longitudinal velocity (left) and corresponding Lorentz factor (right) for an electron in a uniform acceleration field of 1 MV/m.

As expected the velocity  $\beta z = v_z/c$  increases sharply in the beginning but then flattens asymptotically to 1 as the Lorentz factor  $\gamma = 1/\sqrt{1 - \beta^2}$  starts to differ significantly from unity. The Lorentz factor of the particle increases monotonically, because the acceleration force is constant. At  $z=1$  the particle is at the end of the accelerator, beyond which  $\beta z$  and  $\gamma$  remain constant.

To plot the kinetic energy of an electron, the following relation can be used:

$$\begin{aligned} T[eV] &= (\gamma - 1) mc^2 / |q| \\ T[MeV] &\approx 0.511 \gamma - 0.511 \end{aligned} \quad [2.1]$$

In other words, setting scale to 0.511 and offset to -0.511 converts the Lorentz factor of an electron to kinetic energy in MeV. The result is shown in Figure 2-25.

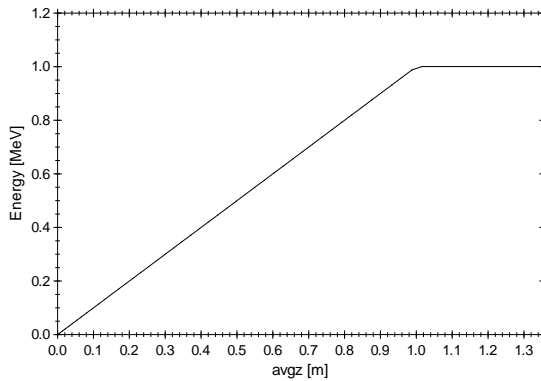


Figure 2-25: Kinetic energy of an electron accelerated in a uniform 1 MV/m electric field.

## 2.6 Accuracy

The quality of the numerical results as produced by GPT depends mainly on the following two factors:

- The number of particles in the simulation
- The specified **accuracy**

Increasing the number of macro-particles in a simulation generally gives a more accurate result, especially for macroscopic quantities. For large numbers of particles the accuracy generally increases with the square root of the number of particles. The needed CPU time however increases at least linear with the number of particles. Therefore using more particles than necessary is not recommended.

Using **accuracy** the number of significant digits in the individual particle coordinates can be specified to the GPT kernel. We refer to section 1.8 for a detailed description of the Runge-Kutta dynamic stepsize algorithm and section 4.3.2 for the **accuracy** reference.

Consider for example the set-up of the previous section: A single particle accelerated over 1 meter in a homogeneous electric field with  $E=1$  MV/m. Listing 2-13 contains the corresponding GPT inputfile where output is generated by a screen at  $z=2$  m. The calculation accuracy is a variable named **acc**.

Listing 2-13: GPT inputfile for electrostatic accelerator producing output  $z=2$  meter with variable accuracy:

**tutorial/accuracy/accuracy.in**

```
1. # GPT Tutorial: Accuracy of the electrostatic accelerator
2.
3. # Accuracy to be used
4. accuracy( acc ) ;
5.
6. # Homogeneous E-field
7. erect( "wcs", "z", 1/2, 1, 1, 1, -1e6 ) ;
8.
9. # Position particle at origin with zero velocity
10. setstartpar("beam", 0, 0, 0, 0, 0, 0 ) ;
11.
12. # Output at z=2 m
13. screen( "wcs", "I", 2 ) ;
```

The analytical expression for  $\gamma$  when  $z>1$  m is:

$$\gamma_{z>1} = 1 + E_{\text{kin}}/E_0 \quad [2.2]$$

where  $E_{\text{kin}}=qE$  and  $E_0=mc^2$ . For 1 MV/m this yields:  $\gamma \approx 2.956935103$ .

An example of using this inputfile, see **acc5.bat**, with an accuracy of 5 is:

```
1. gpt -o acc5.gdf accuracy.in acc=5
2. gdf2a -w 16 acc5.gdf
```

The **-w 16** option specifies a larger column width to print more significant digits. The result is:

$\gamma = 2.956703025$

Using MR a complete scan can be made:

```
1. mr -v -o result.gdf accuracy.mr gpt accuracy.in
2. gdfa -o acc.gdf result.gdf acc avgG tutacc numberivs
```

Where the file **accuracy.mr** contains the following line:

```
1. acc 4 10 0.05
```

This scans the variable **acc** from 4 to 10 in steps of 0.05. The Lorentz factor  $\gamma$  is then grouped by **acc** using GDFA. The number of significant digits and required CPU time as function of **acc** are shown in Figure 2-26. To plot the result with GDFA, we use a custom program to calculate the number of significant digits  $d$ :

$$d = -\log_{10}((\gamma - \gamma_{\text{ref}})/\gamma_{\text{ref}}) \quad [2.3]$$

We refer to the GPT Custom Elements documentation for a description of custom GDFA programs.

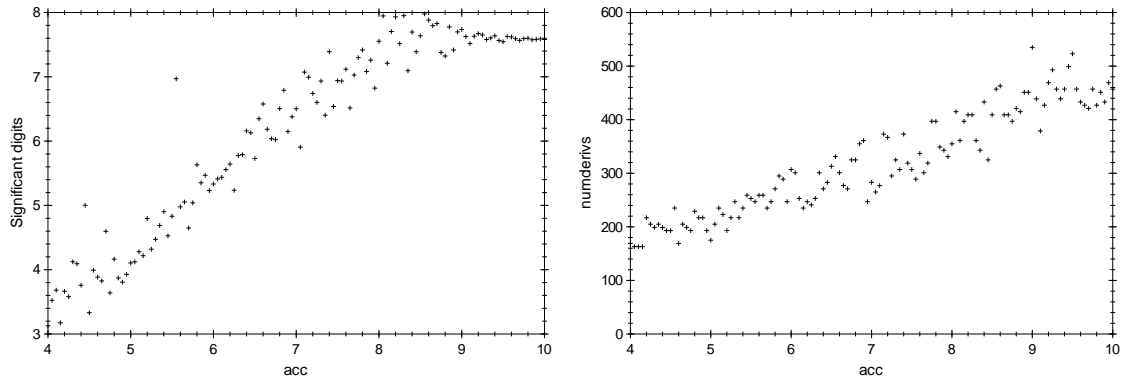


Figure 2-26: Number of significant digits in  $\gamma$  (left) and the number of timesteps in the Runge-Kutta algorithm (right) as function of the specified **accuracy**.

For almost all beamline simulations, the default accuracy setting of GPT of 4 is sufficient. However, high-accuracy, single-particle simulations sometimes require a higher accuracy setting, typically in the range between 6 and 8.

## 2.7 Magnetic mirror

As a demonstration of the high accuracy achievable with GPT a magnetic mirror is simulated. A magnetic field gradient reflects a charged particle gyrating around the magnetic field lines. The following set up is used to demonstrate this effect:

A particle starts at  $z = -1$  m with initial velocity  $\beta=0.01$  making an angle  $\theta$  with the  $z$ -axis in the  $xz$ -plane. The  $y$ -coordinate of the particle is chosen to be the Larmor radius, causing the particle to rotate precisely around the  $z$ -axis. The field gradient is generated by a solenoid located at  $z=0$  with a radius of 20 cm and 100 loops of 100 A.

The loss cone, the angles  $\theta$  for which the particle is not reflected by the gradient, is given by [3]:

$$\sin^2(\theta) < \frac{B_0}{B_m} \quad [2.4]$$

where  $B_0$  and  $B_m$  are the initial and maximum magnetic field strengths respectively. The expression yields  $\theta=4.98^\circ$  in our case. The inputfile used to perform the simulations is given in Listing 2-14.

Listing 2-14: GPT inputfile for a magnetic mirror: `tutorial/magmir/magmir.in`.

```

1. # GPT Tutorial: Magnetic mirror demonstration
2.
3. # Ultra-high accuracy for best results
4. accuracy(8) ;
5.
6. # Define beam parameters
7. GBeta=0.01 ;                # Initial norm. momentum
8. GBetax=GBeta*sin(theta/deg) ; # Norm. Momentum in x-direction
9. GBetaz=GBeta*cos(theta/deg) ; # Norm. Momentum in z-direction
10.
11. Bini=2.36968e-4 ;          # Initial B field (at z=-1)
12. Rl=m*c*GBetax/(q*Bini) ;   # Larmor radius
13.
14. # Start the particle
15. setstartpar( "beam", 0,Rl,-1, GBetax,0,GBetaz ) ;
16.
17. # Position the solenoid
18. solenoid( "wcs", "I", 0.2,10000 ) ;
19.
20. # Time output for trajectories and theta-scan
21. snapshot( 0,0.7e-6,0.5e-9 ) ;
22. # snapshot( 1e-6 ) ;

```

Mathematical functions like `sin`, `cos`, `tan` and `sqrt` can be used in a GPT inputfile like in normal computer code. The operator precedence is similar to C, with the exception of the exponential operator `^`, not present in C, having the highest precedence. For a complete list of operators and built-in functions, we refer to Table 4-A and Table 4-C on page 120.

We will first examine the following two cases:  $\theta=4.75^\circ$  and  $\theta=5.25^\circ$ . In the first case the particle is expected to be lost, in the second case it is expected to be reflected. The results shown in Figure 2-27 were generated by performing the following commands and plotting the trajectory results:

```

gpt -o t475.gdf magmir.in theta=4.75
gdftrans -o traj475.gdf t475.gdf time x y z Bz
gpt -o t525.gdf magmir.in theta=5.25
gdftrans -o traj525.gdf t525.gdf time x y z Bz

```



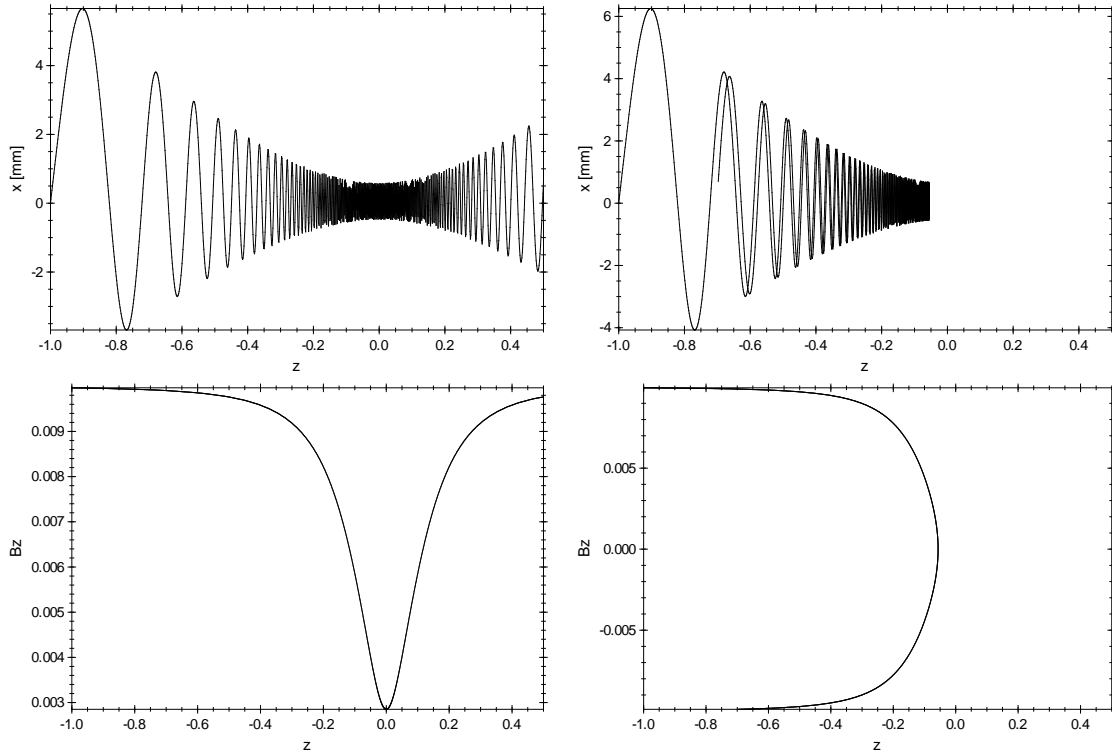


Figure 2-27: Particle trajectory when  $\theta=4.75^\circ$  (left) and  $\theta=5.25^\circ$  (right).

It is clear that in both cases the Larmor radius of the particle decreases because of the increasing magnetic field strength. The particle trajectory remains centered around the  $z$ -axis. When  $\theta=4.75^\circ$  the velocity remains positive and the particle is lost. When  $\theta=5.25^\circ$  the velocity changes sign and the particle is reflected.

Now we will verify **Error! Reference source not found.** by scanning  $\theta$  using MR. The following MR file can be used to scan  $\theta$  from  $0^\circ$  to  $10^\circ$ , using ten times more steps in the interval  $4^\circ < \theta < 6^\circ$ . To reduce the size of the outputfile, only one snapshot at  $1 \mu\text{s}$  is needed.

Listing 2-15: **theta.mr**

```
1. theta 0 3 1
2. theta 4 6 0.1
3. theta 6 10 1
```

To plot the  $z$ -coordinate as function of  $\theta$  the following commands have to be specified. Before running, please make sure that only snapshot output at  $1 \mu\text{s}$  is specified.

```
mr -v -o result.gdf theta.mr gpt magmir.in
gdfa -o magmir.gdf result.gdf theta avgx avgy avgz avgBx avgBy avgBz
```

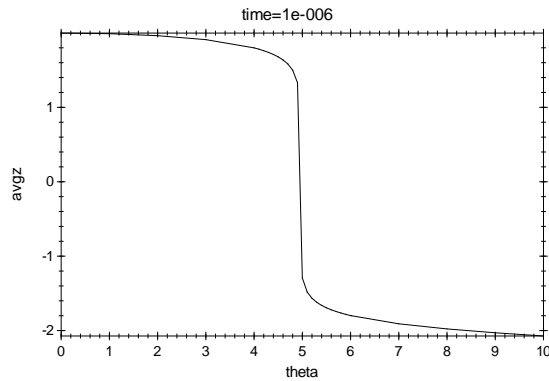


Figure 2-28: Final particle position as function of angle of incidence.

The result, Figure 2-28, indicating for which value of  $\theta$  the particle is lost, is close to the analytical value:  $\theta=4.98^\circ$ . A larger final time or screen output and more points around  $\theta=5^\circ$  can be used to calculate the simulation's loss cone with more accuracy. It yields approximately  $4.96^\circ$  and is left as an exercise.

## 2.8 Element Coordinate System

All GPT elements, both standard and custom, can be positioned anywhere in 3D space with any orientation. This can be very useful when simulating misaligned or rotated beamline components. GPT uses orientation vectors to position elements and their working will be explained in this section. The use of these vectors is the same for all elements.

As an example we will use two current loops placed vertically above and below the beam path, as shown in Figure 2-29. Together these loops produce a vertical field which bends an electron beam in the horizontal plane. To model the current loops we have chosen to use the **solenoid** element because it has its magnetic field defined over all space, not only close the z-axis. For a reference of the element **solenoid** see section 4.6.15.

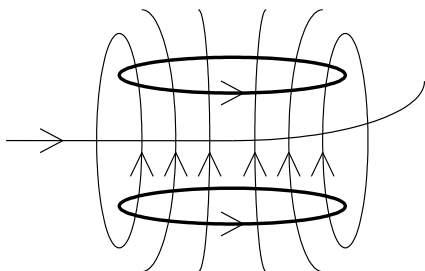


Figure 2-29: Schematic picture of the current loops and the generated field lines.

When using the standard orientation of a solenoid, it is positioned perpendicular to the beam path with the beam going through its center, as shown in Figure 2-30. This is the orientation of a standard focusing coil. As we have seen in previous sections, such a solenoid can be placed using the following syntax:

```
solenoid("wcs","z",1, R, I) ;
```

This places a solenoid at a distance of 1 m from the origin in the z-direction.

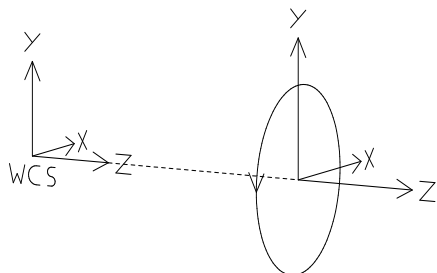


Figure 2-30: Standard orientation of a solenoid.

Because of the 3D capabilities of the GPT kernel, the standard solenoid can still be used to simulate our steering coils. The coils can be positioned off axis and facing a different direction by specifying an element coordinate transform (ECS) in the inputfile. More information about GPT coordinate systems can be found in sections 1.1 and 1.4.3.

First we rotate the solenoid around its origin by specifying its new orientation vectors. The new orientation is shown in Figure 2-31. The solenoid has been rotated 90° around its x-axis.

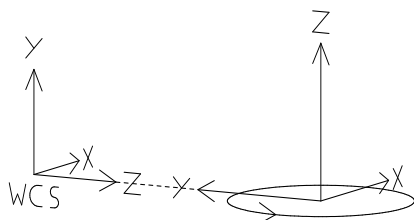


Figure 2-31: Orientation of a solenoid rotated 90° around its x-axis.

The complete syntax line for such a solenoid is:

```
solenoid("wcs", 0,0,1, 1,0,0, 0,0,-1, R, I) ;
```

The first parameter specifies the coordinate system relative to which the subsequent coordinates are given. In our case this is "wcs". Then follow three sets of x-,y-,z-coordinates specifying the position and orientation of the element.

The first coordinate set gives the position of the element in x-, y-, z-coordinates. The specified distances are in meters and relative to the coordinate system specified as the first parameter. In our example the center of the solenoid is placed at a distance of 1 m from the origin of "wcs" in the z-direction. It is not moved in the x- or y-direction. This translation is specified as 0,0,1.

The second coordinate set specifies the direction of the new x-direction using directional cosines. The first parameter determines how much of the new x-vector lies in the direction of the x-axis of the reference coordinate system. The reference coordinate system is specified by the first parameter of the syntax line, in our case it is "wcs". The second parameter determines how much of the new unit x-vector lies in the direction of the y-axis of the reference coordinate system. And the third parameter determines how much of the new unit x-vector lies in the direction of the z-axis of the reference coordinate system. In our case the direction of the x-axis has not changed, because the solenoid has been rotated round its x-axis. Therefore we specify a unity transformation in the x-direction 1,0,0.

The third coordinate set specifies the direction of the new unit y-vector the same way as we did for the new x-direction. The components of the new directions are given relative to the standard unit vectors. In our example the new direction of unit vector y is opposite to the "wcs" z-direction. This is specified as 0,0,-1.

The new z-direction is calculated by the GPT kernel and does not have to be specified:  $\hat{z} = \hat{x} \times \hat{y}$ . The kernel also handles all normalizations.

Finally the reoriented solenoid has to be positioned above the beam path, as shown in Figure 2-32. This means that it has to be moved in the y-direction of the WCS coordinate system. To move the solenoid 5 cm in this direction should be specified as the translation 0,0.05,1.

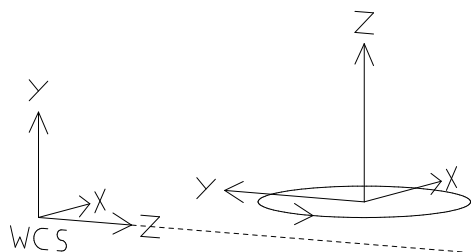


Figure 2-32: Solenoid with a new orientation positioned above the beam path.

The complete syntax line now becomes:

```
solenoid("wcs", 0,0.05,1, 1,0,0, 0,0,-1, R, I) ;
```

A second solenoid is placed 5 cm below the beam path with the same orientation. The corresponding inputfile is shown in Listing 2-16.

Listing 2-16: GPT inputfile demonstrating a non-trivial ECS: **tutorial/ecs/ecs.in**

```

1. # GPT Tutorial: Bending particles using two current loops
2.
3. # Define particle parameters
4. gamma = 10 ;
5. betaz = sqrt(1-gamma^-2) ;
6. vz    = c*betaz ;
7.
8. # Start particles
9. setstartpar( "beam", -.2e-3,0,0, 0,0,gamma*betaz ) ;
10. setstartpar( "beam", .0e-3,0,0, 0,0,gamma*betaz ) ;
11. setstartpar( "beam", +.2e-3,0,0, 0,0,gamma*betaz ) ;
12.
13. # Position the solenoids
14. solenoid( "wcs", 0, 0.05,1, 1,0,0, 0,0,-1, 0.1, 100 ) ;
15. solenoid( "wcs", 0,-0.05,1, 1,0,0, 0,0,-1, 0.1, 100 ) ;
16.
17. # Specify output times
18. snapshot( 0,1.5/vz,0.05/vz ) ;

```

Now the two solenoids are placed above and below the beampath in their new orientation. To view the trajectory of the particle run the batch file: **tutorial/ecs/ecs.bat**. It contains the command to run GPT with inputfile **ecs.in** and outputfile **result.gdf**: Then the trajectories are calculated with the GDFTRANS program and written to **traj.gdf**.

```

gpt -o result.gdf ecs.in
gdftrans -o traj.gdf result.gdf time x y z

```

The particle trajectories can be shown by plotting the z-position horizontally and the x-position vertically, as shown in Figure 2-33.

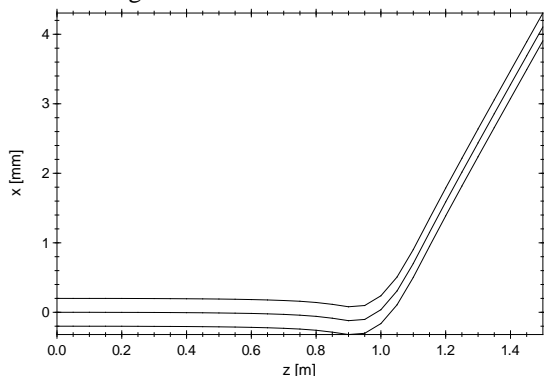


Figure 2-33: Particle trajectories through the steering coils, plotted using GPTwin.

We see in Figure 2-33 that the beam is bent in the positive x-direction due to the solenoid field. Please note that outside the coils there is a small magnetic field with opposite direction, causing a small deflection in the negative x-direction.

For macroscopic beam investigation, we can also use the GDFA program:

```

gdfa -o avg.gdf result.gdf time avgx avgy avgz

```

## 2.9 Initial particle distribution

In this example, we will start a 1 MeV electron beam with a total charge of 100 pC. The position, momentum and energy distributions are all Gaussian, but this can easily be modified to uniform, linear or quadratic distributions when required. Such a beam can be specified in a number of well-defined steps:

Step	Plane(s)	Elements used
Specifying the particle set		<b>setparticles</b>
Specifying the real-space distribution functions	xyz	<b>setzdist</b> , <b>setxdist</b> , <b>setydist</b> , <b>setrxydist</b> , <b>setphidist</b>
Specifying the phase-space distribution functions	$x\beta_x$ , $y\beta_y$	<b>setGBxdist</b> , <b>setGBydist</b>
Scale emittances	$x\beta_x$ , $y\beta_y$	<b>setGBxemittance</b> , <b>setGByemittance</b>
Specifying the energy-distribution function	$\gamma$ (Energy)	<b>setGdist</b>
Specifying divergence angles	$x\beta_x$ , $y\beta_y$	<b>addxdiv</b> , <b>addydiv</b>

The files for this tutorial section are located in the folder **gpt/tutorial/cylbeam**. A **snapshot(0)** statement is used to inspect the initial particle distribution at  $t=0$ . In other words, a **snapshot(0)** statement writes the particle distribution to the outputfile exactly as it starts.

To start the particles in our sample 1 MeV electron beam, we first define a particle set named "beam", containing 1000 particles having a total charge of 100 pC. The **setparticles** element is described in section 4.2.1.1. The built-in constants **me** and **qe** represent the mass and charge of an electron respectively.

```
1. nps = 1000 ;          # Start 1000 particles
2. Qtot = -100e-12 ;    # Total charge 100 pC
3. setparticles( "beam", nps, me, qe, Qtot ) ;
```

To give these particles a Gaussian longitudinal distribution centered around  $z=0$  we use the **setzdist** element, see section 4.2.2.5. The typical length is specified as 4 mm and the distribution is extended to 3 sigma in both directions. In this case the distribution specification is: "g", 0, 4e-3, 3, 3. The resulting longitudinal distribution is shown in Figure 2-34.

```
4. zlen = 0.004 ;       # Bunch length: 4 [mm]
5. radius = 0.002 ;     # Bunch radius: 2 [mm]
6. setzdist( "beam", "g", 0, zlen, 3, 3 ) ;
```

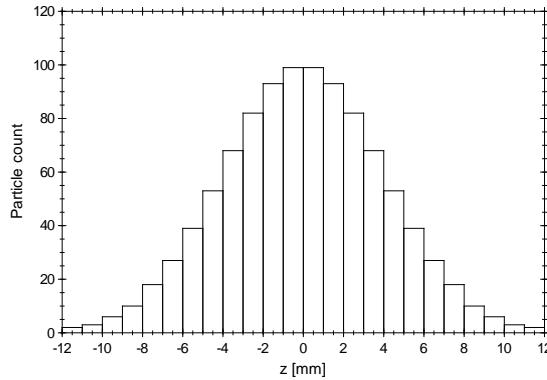


Figure 2-34: Longitudinal particle distribution obtained using GDF2HIS, see section 3.9.

It is quite simple to specify other distributions. For example a uniform distribution centered around  $z=1$  mm could be specified by: "u", 1e-3, 4e-3. Please see section 1.6.1 or Table 1-C on page 19 for a description of all possible distribution specifications.

The elements **setxdist** and **setydist** are used in a similar way as **setzdist**. In this example, the radial distribution of the particles is Gaussian in  $r$  and specified using **setrxydist**, see section 4.2.2.6. For radial distributions it is important to never generate negative radii. Therefore, the left tail of the Gaussian distribution is set to 0 sigma. For a uniform distribution, the distribution parameters of **setrxydist** must always be: "u",  $r_{\max}/2$ ,  $r_{\max}$ .

The **setrxydist** element only modifies the x-coordinates of the particles, assuming a rotational symmetric distribution in the xy-plane. Therefore, **setphidist**, see section 4.2.2.7, must be used to specify a uniform  $\varphi$  distribution over  $2\pi$  in the xy-plane. The resulting distribution is shown in Figure 2-35.

```

7. setrxydist( "beam", "g", 0, radius, 0,3 ) ;
8. setphidist( "beam", "u", 0, 2*pi ) ;

```

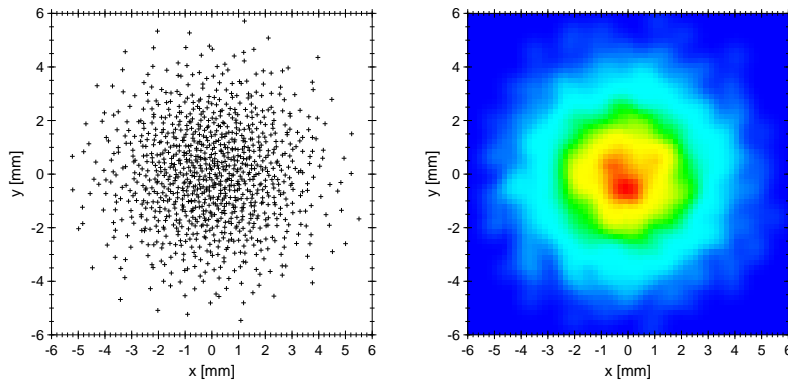


Figure 2-35: Beam distribution in xy-plane scatterplot (left) and density plot (right). The density plot is created with 10 times more particles.

As an alternative to **setrxydist** and **setphidist** the elements **setxdist** and **setydist** can be used to specify the distribution in the xy-plane. Therefore, it is very important to understand the difference between **setrxydist** and **setxdist**. Both elements set the  $x$ -coordinates of the particles to a specified distribution. However, a uniform distribution for **setxdist** sets the  $x$ -coordinates of all particles uniform in the  $x$ -plane only. A uniform distribution for **setrxydist** results in a uniform distribution in the  $xy$ -plane when a uniform **setphidist** is also used. To accomplish this, **setrxydist** adds relatively more particles at larger radii because the amount of ‘space’ on a circle grows linear with  $r$ .

The phase-space distribution is set using **setGBxdist** and **setGBydist**, see section 4.2.3.1 and 4.2.3.3 respectively. We use a Gaussian distribution centered around zero with a standard deviation of  $1e-3$ , cut-off at three sigma. Please note that by specifying these distributions, we implicitly specify the transverse emittances. However, we don’t need to worry about this too much, because the emittances can be fine-tuned later. Also the divergence angles are specified separately. Important in this step is only the type of distribution, e.g. Gaussian or uniform.

```

9. setGBxdist( "beam", "g", 0, 1e-3, 3,3 ) ;
10. setGBydist( "beam", "g", 0, 1e-3, 3,3 ) ;

```

The transverse emittances are set using **setGBxemittance** and **setGByemittance**, see sections 4.2.3.9 and 4.2.3.10 respectively. These elements scale the transverse momentum coordinates linearly till the specified emittance is reached. In this example, the emittance is set to  $5\pi$  mm-mrad. Running the GDFA programs **nemixrms** and **nemiyrms** will result in emittance values of  $5\pi$  mm-mrad, independent on the average beam energy and divergence angles specified later.

```

11. setGBxemittance( "beam", 5e-6 ) ;
12. setGByemittance( "beam", 5e-6 ) ;

```

Now we can specify the beam energy distribution using **setGdist**. In this example, an average energy of 1 MeV and a uniform energy spread of 1% are used. The Lorentz factor is calculated from the average beam energy. The result is shown in Figure 2-36.

```

13. Eo = 1e6 ;           # Average beam energy: 1 [MeV]
14. G  = 1-q*Eo/(m*c*c) ; # Corresponding gamma
15. dG  = (G-1)/100 ;    # 1% Energy spread
16. setGdist( "beam", "u", G, dG ) ;

```

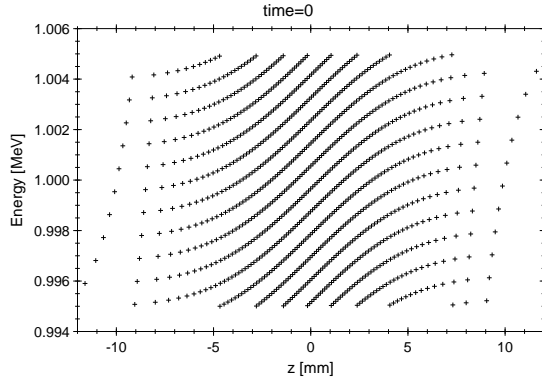


Figure 2-36: Correlation between longitudinal position and beam energy. The interference pattern is an artifact of the Hammersley sequence. The **addzdiv** element rotates this plot.

Optionally, the transverse phase-space divergence angles can be specified using **addxdiv** and **addydiv**, see section 4.2.4.1 and 4.2.4.3 respectively. When written as a separate element, it is not possible to include the beam radius in the divergence calculations because the beam radius is differently defined for a uniform and a Gaussian transverse distribution. Therefore, the divergence must always be specified in [rad/m]. To create a beam with a radius of 2 mm and a divergence angle of 0.1 rad, a divergence of 50 rad/m must be specified. In this example, a divergence of 1 rad/m is used, defocusing in the  $x$ -plane and focusing in the  $y$ -plane. The result is shown in Figure 2-37.

```
17. addxdiv( "beam", 0, 1 ) ;
18. addydiv( "beam", 0, -1 ) ;
```

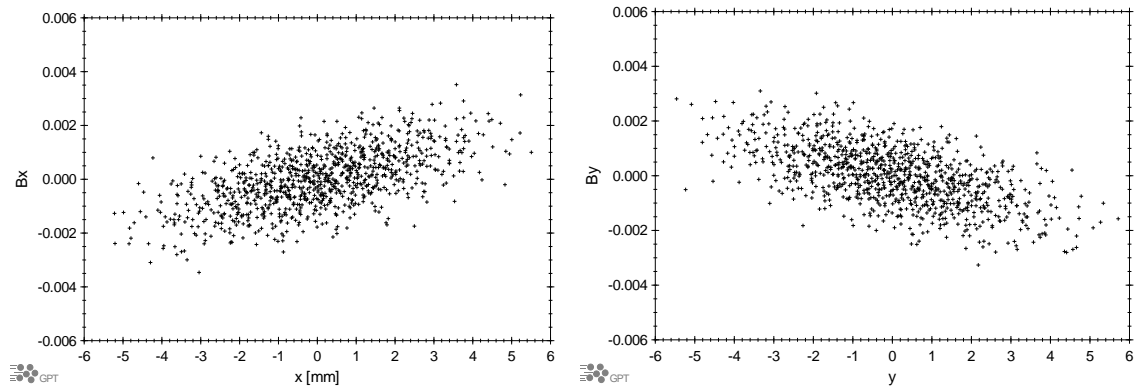


Figure 2-37: Transverse phase-space plots. The vertical axis is the transverse velocity, normalized by the speed of light.

## 2.10 Photo-cathode, starting particles as function of time

This section demonstrates how to start particles as function of time. All files are located in the **tutorial/cathode** folder. The example is a 100 pC electron bunch, emerging from a flat photo-cathode during 100 fs. A typical set-up consists of a copper or semiconductor cathode surface illuminated by a laser pulse. Either an RF cavity or an electrostatic accelerating field must be present to accelerate the electrons away from the cathode. Space-charge effects are not included in this example, but can easily be added with the **spacecharge2Dcircle** element.

To start the electrons emerging from the cathode, we first define a particle set named **"beam"**, containing 1000 particles having a total charge of 100 pC.

```
1. # Photocathode
2. nps = 1000 ;      # Start 1000 particles
3. Qtot = -100e-12 ; # Total charge 100 pC
4. setparticles( "beam", nps, me, qe, Qtot ) ;
```

These particles are to be started uniformly in a 100 fs time interval, having an initial radius of 0.25 mm.

```
7. tlen = 100e-15 ; # Laser pulse length: 100 fs
8. radius = 0.25e-3 ; # Bunch radius: 0.25 mm
```

The radial distribution of the particles is uniform **"u"** in  $r$  and is set using **setrxydist**. The third parameter of **setrxydist** is the center of the radial distribution, half the beam radius. The beam is cylindrical symmetric, specified as a uniform  $\varphi$  distribution over  $2\pi$  using **setphidist**. This will result in a particle distribution as shown in Figure 2-38.

```
5. setrxydist( "beam", "u", radius/2, radius ) ;
6. setphidist( "beam", "u", 0, 2*pi ) ;
```

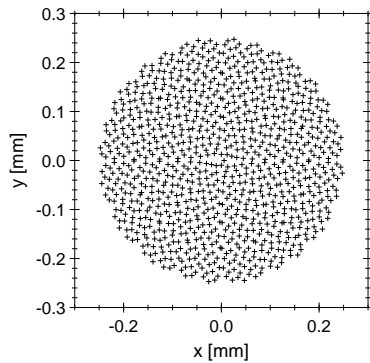


Figure 2-38: Particle distribution in xy-plane.

The following code assumes that all electrons leave the cathode having an energy of precisely 0.4 eV. Initially, **setGBzdist** is used to set the corresponding  $\gamma\beta_z$  of all particles. Then the velocity component is homogeneously distributed over half a sphere using **setGBthetadist**. This element sets a spherical particle distribution in the  $\gamma\beta_z$ - $\gamma\beta_r$ -plane, keeping the angle in the  $\gamma\beta_x$ - $\gamma\beta_y$ -plane constant. **setGBphidist** must be used to enforce cylindrical symmetry. The half-sphere distribution of the particles is shown in Figure 2-39. Please note that these start conditions automatically determine the initial emittance.

```
9. Eo = 0.4 ;      # Start with 0.4 eV
7. G = 1-q*Eo/(m*c*c) ; # Corresponding Gamma
8. GB = sqrt(G^2-1) ; # Corresponding Gamma*Beta
9. setGBzdist( "beam", "u", GB, 0 ) ;
10. setGBthetadist( "beam", "u", pi/4, pi/2 ) ;
11. setGBphidist( "beam", "u", 0, 2*pi ) ;
```



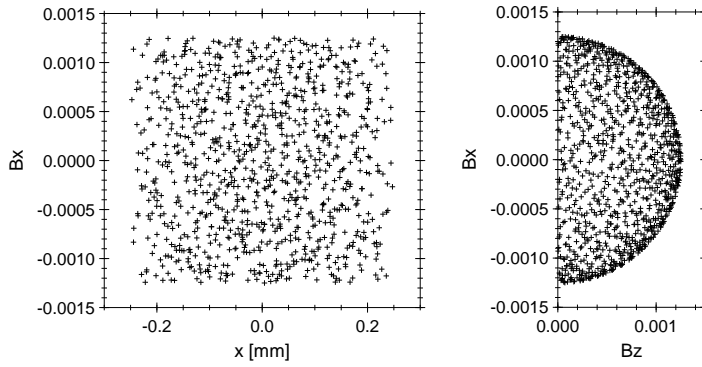


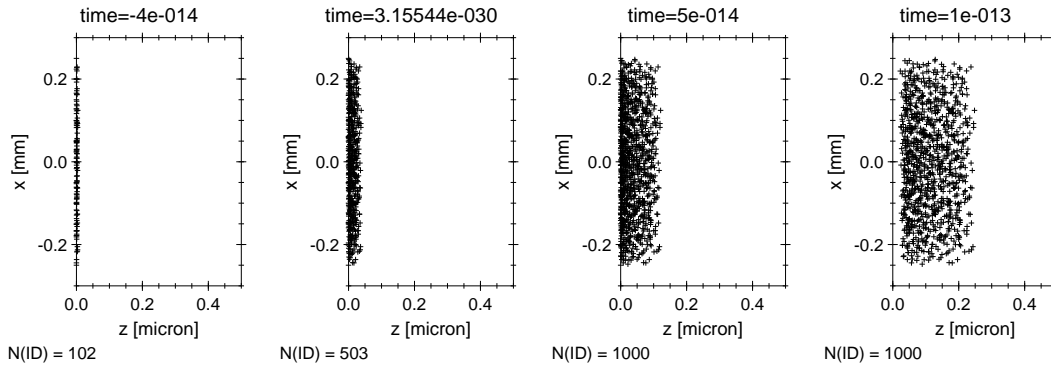
Figure 2-39: Phase space distribution.

Before setting the time-distribution with `settdist`, it is important to check the initial particle distribution. All plots shown before are created with the `snapshot(0)` line and without using `settdist`.

When the simulation is started using the above lines, all particles are emitted from the cathode at  $t=0$ . The `settdist` element sets the time-distribution of the particles. The release-time is independent on all other coordinates, creating the possibility to start any particle anywhere, anytime. To make this tutorial simulation a little more interesting, we add a constant 100 MV/m electric field with the `erect` element to accelerate the electrons away from the cathode surface. In a rf photo-gun simulation it would be appropriate to use the `map25D_TM` element.

```
10. # Start in time
11. erect("wcs","I", 1,1,1, -100e6) ; # Constant electric field 100 MV/m
12. settdist("beam", "u", 0, tlen) ;
13. snapshot(-tlen/2, 1.5*tlen, tlen/10) ;
```

The `settdist` keyword in this example sets a uniform distribution centered around zero having a total width of `tlen`. In other words, it starts all particles uniformly between  $-50$  and  $50$  fs. As a result, the simulation time automatically starts at  $-50$  fs to be able to take all particle trajectories into account. This is observed in the subsequent `snapshot` statement, where the first `snapshot` is requested at  $-tlen/2$ . In this case, this triggers a warning when running this inputfile because no particle starts at the outer left and right points of a distribution. The resulting particle distribution as function of time is shown in Figure 2-40.

Figure 2-40: Particle distribution at various simulation times. The number of particles linearly increases in the interval between  $-50$  and  $50$  fs.

To see the charge and particle emission as function of time, the GDFA program can be used:

```
gdfa -o avgs.gdf cathode.gdf time Q numpar
```

The results are shown in Figure 2-41.

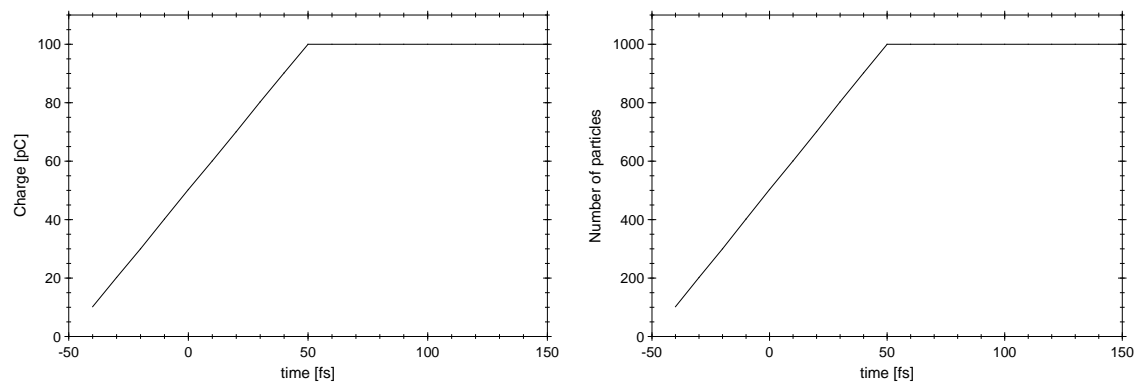


Figure 2-41: Charge (left) and number of particles (right) as function of simulation time.

## 2.11 Collector design

In this section we demonstrate how to use GPT to design a collector. The result is current and power density on the collector plate(s), where space-charge effects and multiple scattering are included. In this example, an artificial 20 mA, 500 eV electron beam is collected in a simple collector, stretched in y-direction, as shown in Figure 2-42. Section 2.11.7 explains how to design a cylindrical-symmetric collector. The potential on the electrode is  $-1$  kV.

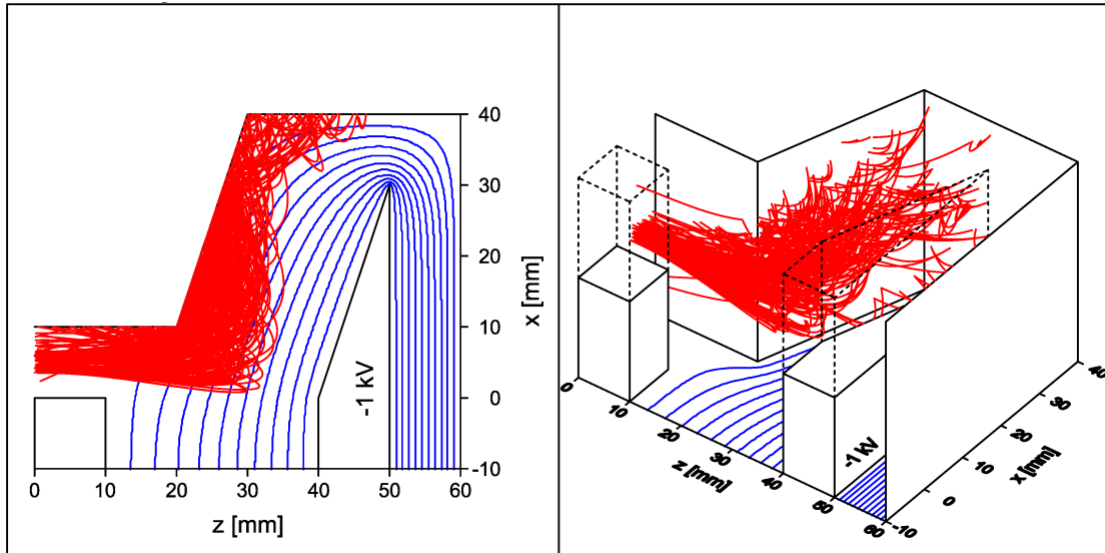


Figure 2-42: Sample collector with particle trajectories. The particle trajectories are imported in a 3D drawing program using the GDF2DXF program.

The files for this tutorial section are located in the folder `gpt/tutorial/collector`.

### 2.11.1 Creating a GPT field-map

In this example, the Poisson code is used to calculate the potential. It is possible to use other field-solvers such as TOSCA or MAFIA. We refer to the ASCI2GDF and RAW2GDF programs for the conversion of the field-output to a GPT field map.

The Poisson-file needed to describe the simple collector is shown in Listing 2-17. Together with all other field-map related files, it can be found in the `fieldmap` subfolder of the collector tutorial files. This folder also includes a batch file named `collector.bat` containing all required commands to run Superfish and convert to the output to GPT format.

The commands to run Poisson are:

```
automesh collector.sf
poisson
```

Listing 2-17: collector.sf: Poisson file to describe the collector shown in Figure 2-42.

```

1. &reg dx=0.1, dy=0.1, conv=1.0, xmin=0,xmax=6, ymin=-1,ymax=4,icylin=0,
2. nbsup=0,nbslo=1,nbsrt=1,nbslf=0,kprob=0,xjfact=0.0 &
3.
4. &po x=0,y=-1 &
5. &po x=6,y=-1 &
6. &po x=6,y=4 &
7. &po x=0,y=4 &
8. &po x=0,y=-1 &
9.
10. &reg mat=0,voltage=0,ibound=-1 &
11. &po x=0,y=1 &
12. &po x=2,y=1 &
13. &po x=3,y=4 &
14. &po x=6,y=4 &
15. &po x=6,y=-1 &
16.
17. &reg mat=0,voltage=0,ibound=-1 &
18. &po x=0,y=0 &
19. &po x=1,y=0 &
20. &po x=1,y=-1 &
21. &po x=0,y=-1 &
22. &po x=0,y=0 &
23.
24. &reg mat=0,voltage=1000.0,ibound=-1 &
25. &po x=4,y=-1 &
26. &po x=4,y=0 &
27. &po x=5,y=3 &
28. &po x=5,y=-1 &
29. &po x=4,y=-1 &

```

The Poisson output cannot be used directly in GPT simulations. It must first be interpolated on a rectangular grid using `sf7`, and then converted to the GDF format with `FISH2GDF`:

```

sf7
fish2gdf -o collector.gdf outsf7.txt

```

The `sf7` program requires an additional file, `collector.in7`, which describes the interpolation parameters as shown in Listing 2-18.

Listing 2-18: collector.in7: interpolation parameters

```

1. rect noscreen
2. 0 -1 6 4
3. 121 101
4. end

```

After the above commands are specified, the `collector.gdf` field-map is ready for use.

### 2.11.2 The GPT boundary file

Before the field-map created in section 2.11.1 can be used, the boundaries must be defined in a separate GPT inputfile. When the field-map is created using Poisson, this step is quite simple:

```

fishfile -g boundaries.in -y 1 collector.sf

```

The file `boundaries.in` now contains a description of all the boundaries in the `collector.sf` file. For a cylindrical-symmetric set-up, the boundaries are defined by `scattercone`, `scattertorus`, `scatterpipe` and other elements. Otherwise, the set-up contains just rectangular `scatterplate` elements.

### 2.11.3 Setting up the simulation

In the file listed in Listing 2-19 a 20 mA, 500 eV rectangular beam is started and send into the collector as described in section 2.11.1. Ofcourse this is not a realistic beam, but serves only as an example.

Listing 2-19: collector.in: Main GPT inputfile for simple collector

```

1. # Basic beam parameters
2. Eo = 500 ; # Energy [eV]
3. G = 1-qe*Eo/(me*c*c) ; # Corresponding Lorentz factor G []
4. Beta = sqrt(1-G^-2) ; # Corresponding Normalized velocity []
5. dE = 0.2 ; # Energy spread [fraction of Eo]
6. I = 0.02 ; # Beam current [A]
7.
8. # Simulation parameters
9. tlen = 1e-9 ; # Gun time [s]
10. nps = 100 ; # Number of particles []
11. Qtot = -I*tlen ; # Total charge in tlen [C]
12. nmac = (Qtot/qe)/nps ; # Initial nmacro
13.
14. # Start a collection of particles (unphysical but simple rectangular beam)
15. setparticles("beam",nps,me,qe,Qtot) ;
16. setxdist("beam","u", 5e-3,3e-3) ;
17. setydist("beam","u", 0e-3,3e-3) ;
18. settldist("beam","u", tlen/2, tlen) ;
19. setGdist("beam","u", G, dE*(G-1) ) ;
20.
21. # Import collector field-map
22. Zcol = 0.0 ;
23. map2Dr_E("wcs","z",Zcol, "fieldmap/fieldmap.gdf","Y","X","Ey","Ex", 1,-Efac ) ;
24. zminmax("wcs","I", -1e-6, 1 ) ;
25.
26. # Define scatter model
27. copperscatter_fix("wcs","z",Zcol, "copper",0.01*nmac,2*nmac) ;
28.
29. # Spacecharge calculations
30. spacecharge3D ;
31.
32. # Output specification
33. accuracy(5) ;
34. outputvalue("tlen",tlen) ; # Used by hierarchical data-analysis
35. snapshot(0,1e-7,1e-10) ; # Trajectory plots
36. # tcontinue(1e-7) ; # Data analysis only

```

The field map of the collector is imported using the **map2Dr\_E** element. For a cylindrical symmetric collector, **map2D\_E** must be used. By convention, the collector is placed at longitudinal position **Zcol**. On the sample disk, the field strength is defined as **Efac** on the GPT command-line to be able to perform a scan in a later stage.

Normally collector simulations need to be performed for (semi) continuous beams. Because GPT is a time-domain code, such a beam is often represented by a much shorter bunch to save CPU time. In the above case, we start a beam with a uniform distribution during the variable **tlen**, equal to 1 ns. For reliable results, only 100 particles are typically insufficient. Because convergence is sometimes much slower, we strongly recommend rerunning the simulation with double the number of particles till the parameters of interest stabilize.

The **copperscatter** element is used to define all the scatter statistics. For a simulation of the primary beam only, the **forwardscatter** element with a probability of 0 can be used instead.

The **snapshot** statement is required for trajectory plotting. Only **tcontinue** is sufficient for power- or current-density analysis.

## 2.11.4 Trajectory output

The multiple-snapshot option must be selected to plot particle trajectories. The following commands can be used to produce the results as shown in Figure 2-43. Using GPTwin you can open the file **traj.gdf**, load template **traj.gdt** and the result should be identical.

```
gpt -o collector.gdf collector.in fieldmap/boundaries.in
```

```
gdftrans -o traj.gdf collector.gdf time x y z G
```

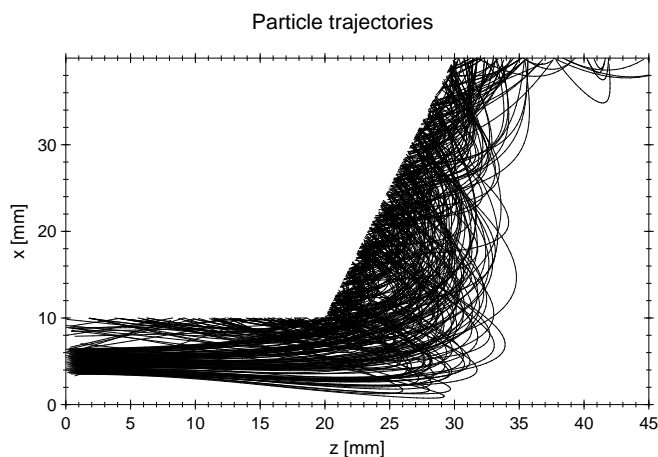


Figure 2-43: Particle trajectories inside the collector. File **traj.gdf** plotted with template **traj.gdt**.

For trajectory results, the combine-plot option must always be selected. As a result, the primary and secondary particles are always potted in the same graph.

### 2.11.5 Unrolled position

For power- and current-density calculations, only the **tcontinue** output statement is required and the **snapshot** keyword can be removed. This stores the 3D scatterstatistics in the outputfile. However, when this file is plotted directly, the results are not much illuminating, see Figure 2-44. For example the trajectory plot indicates that the vertical line at  $x=40$  mm is caused by a  $z$ -dependence, but there simply is no reliable way to tell if the power density is lower or higher in that area from these plots.

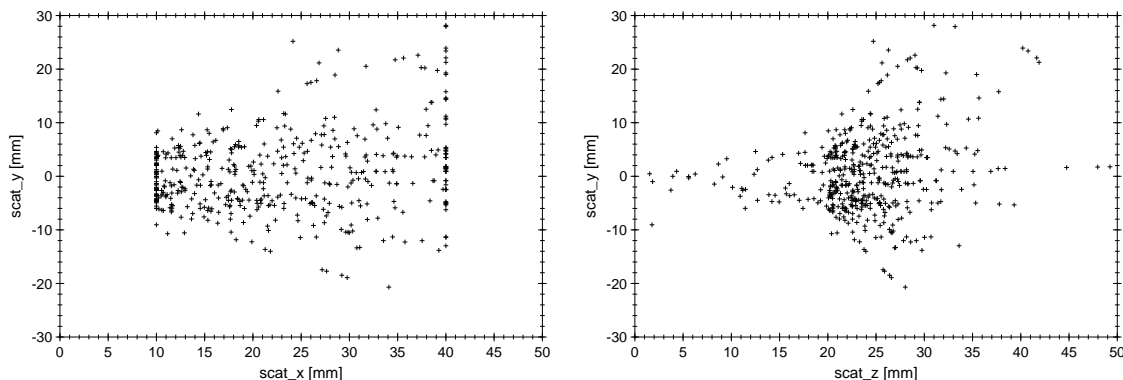


Figure 2-44: Direct output of the scatter elements. File **collector.gdf** with **tcontinue** keyword only.

To overcome these problems, we define a coordinate  $d$  specifying the ‘unrolled’ position. This coordinate  $d$  runs along a collector plate and keeps measuring the distance along the edge. The unrolled coordinate for our single collector plate is listed in Table 2-B. Because  $d$  is monotonically increasing, following the distance of the plate, it is area preserving. As such, it is the most convenient parameter to plot along the horizontal axis for density plots.

Table 2-B: Collector plate coordinates and corresponding unrolled position.

$z$ [mm]	$x$ [mm]	$d$ [mm]
0	10	0
20	10	20
30	40	51
60	40	81

The FISHFILE program can be used again to calculate this ‘unrolled position’ parameter:

```
fishfile -y 1 -o scatter.gdf fieldmap/collector.sf collector.gdf
```

The result of the above command is the file **scatter.gdf**, plotted in Figure 2-45. The vertical lines are completely gone as desired. A new problem is the fact that the scatter elements are able to generate fractions of the incoming particles to keep the statistics correct. In other words, not all dots in the plots represent an

equal amount of particles. Therefore, it is essential to use the density-plot feature of GPTwin using weighted data.

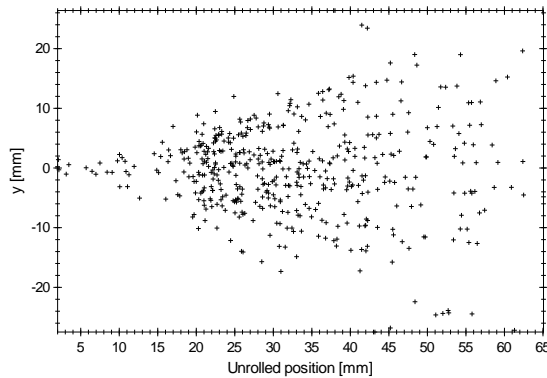


Figure 2-45: Scatter statistics as function of unrolled position. File `scatter.gdf` plotted with template `scatter_d.gdt`.

### 2.11.6 Current- and power-density

Creating a density plot using GPTwin is straightforward: Select the density-plot option. Using this option is scientifically correct however can be a challenge. When not enough data is present, it is tempting to increase the blur, but this in turn makes everything Gaussian, independent on the actual distribution.

The important things to do when creating a density plot of power density are:

- Select `scat_01E` in the `weight_by` box. This array represents the total **E**nergy for the collector plate **01**.
- Weight by bin area
- Set the scaling to manual.
- Set the maximum Energy in the `Max` box. The ratio between energy and power is the simulation time `tlen`. Therefore, in our 1 ns simulation, an energy density of 1 W/m<sup>2</sup> corresponds to a Max energy of 10<sup>-9</sup>.

When properly done, the scaling adapts itself to the number of bins, is independent on the number of particles in the simulation and follows the units along the x- and y-axes in the plot. When these are both mm, the scaling is to W/mm<sup>2</sup>, see Figure 2-46.

The total energy on the collector plate can be calculated using the statistics as `Sum(scat_01E)`. Scaling to power can be done by dividing by `tlen` in the `scale` box.

Current density is completely analogous to power density, except that the `scat_01Q` array must be used. It represents the total charge **Q** for collector plate **01**.

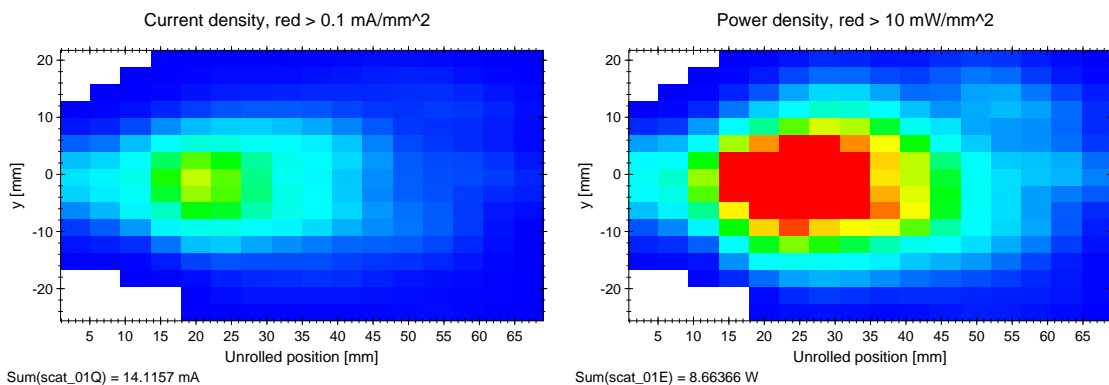


Figure 2-46: Current and power density as function of position on collector plate. File `scatter.gdf` plotted with templates `scatter_Q.gdt` and `scatter_P.gdt` respectively.

### 2.11.7 A Cylindrical symmetric collector

The GPT simulation of a cylindrical-symmetric cavity is analogous to the previous case. All required modifications are shown in Table 2-C. For a detailed explanation of the FISHFILE output, please see section 3.5.

Table 2-C: Modifications required for a cylindrical-symmetric cavity.

	Rectangular	Cylindrical	Description
GPT Fieldmap	<b>map2D_Er</b>	<b>map2D_E</b>	Cylindrical field map.
FISHFILE options	<b>-y height</b>		Don't specify the height.
Plot arrays (x,y)	<b>scat_nnd,</b> <b>scat_nny</b>	<b>scat_nnd,</b> <b>scat_nnphi</b>	The angle in the xy-plane is typically plotted.
Density scaling	<b>scat_nnE,</b> <b>scat_nnQ</b>	<b>scat_nnEor,</b> <b>scat_nnQor</b>	For correct scaling, E/r and Q/r must be used.

### 2.11.8 Scanning a parameter

Practically any parameter can be scanned with the MR program. The typical use is running GDFA on the output of the FISHFILE program to directly obtain total current and power statistics per collector plate as function of the scanned parameter. The **scatterInn** and **scatterPnn** programs can be used to calculate plot total current and power for the first ten collector plates. For example, the following commands calculate current and power on the first collector plate as function of potential. The results are shown in Figure 2-47.

```
mr -v -o collector.gdf Efac.mr gpt collector.in fieldmap/boundaries.in
fishfile -y 1 -o scatter.gdf fieldmap/collector.sf collector.gdf
gdfa -o stats.gdf scatter.gdf Efac scatterI01 scatterP01
```

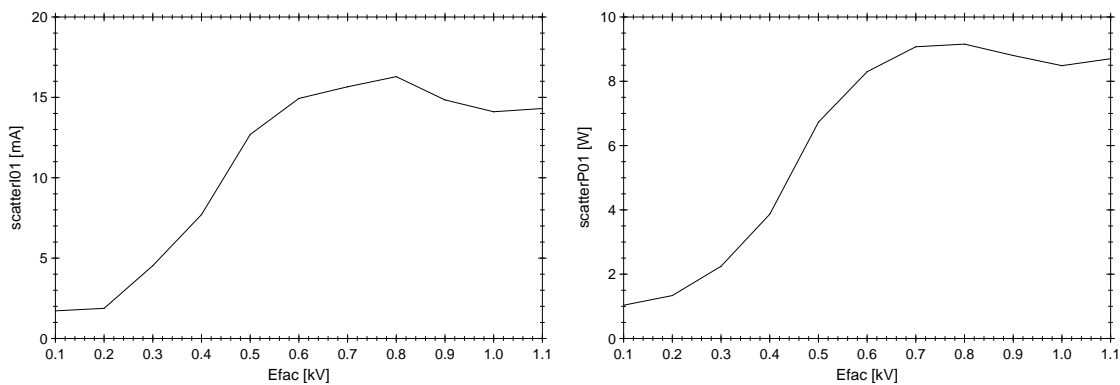


Figure 2-47: Total current and power on first collector plate as function of potential. File **avgs.gdf** plotted with templates **avgs\_Q.gdt** and **avgs\_P.gdt** respectively.



# 3 GDF

GPT Datafile Format, GDF, is a file format developed for programs producing large amounts of numerical data. It is the native output format of the General Particle Tracer, GPT, allowing it to automatically scan parameters and perform efficient data processing and visualization. GDF-files are machine independent and can be transferred between PC's and Linux machines.

This chapter describes the basics of a GDF file and the following utility programs:

ASCII2GDF	Converts an ASCII file to a GDF file.
ASTRA2GDF	Convert output from the ASTRA program to input for GPT.
FISH2GDF	Converts SUPERFISH output to a GDF file.
FISHFILE	Calculates “unrolled” scatter statistics or creates a GPT inputfile based on a Superfish file.
GDF2A	Writes the contents of a GDF file in ASCII to the terminal or a file. The file can be processed by an ASCII-based editor or imported into a spreadsheet program.
GDFFLATTEN	Removes one level from the hierarchical structure of a GDF file by combining the results.
GDF2DXF	Converts a GDF file to a point, line or vector drawing for further customization in a 2D or 3D drawing package.
GDF2GDF	Combines several GDF files into a single file, optionally sorting the top-level group.
GDF2HIS	Calculates histograms from the contents of a GDF file. The output is in GDF format and can be plotted or converted to ASCII.
GDF2SDDS	Converts a GDF file to an SDDS file.
GDF2VTP	Convert a GDF file to ParaView format.
GDFFA	Removes one level of hierarchy in a GDF file by performing user-specified calculations. The calculations typically produce averages and standard deviations of arrays, reducing the total amount of data considerably.
GDFMGO	Multi-objective genetic optimizer for GPT.
GDFSELECT	Select a specific or a range of groups from a GDF file.
GDFSOLVE	Multi-dimensional root finder and optimizer for GPT.
GDFTRANS	Transpose a GDF file to calculate trajectories as function of any parameter.
MR	Scan one or more parameters and concatenate the output in a single hierarchical file
RAW2GDF	Converts a raw binary datafile to a GDF file.

### 3.1 Basics

A GDF file is a file containing binary data in a structured form. Basically, a GDF file consists of a general header followed by one or more data blocks. Every block has a name and contains data. Almost all native C/FORTRAN data types are supported. A simple GDF file is shown schematically in Figure 3-1.

General header	
string	"This is a string"
number	12
value	1234e56
array	{1.1,2.1,3.1,4.1,5.1}

Figure 3-1: Simple GDF file

Such a list of named blocks containing all kinds of data is impractical when the number of blocks becomes excessively large. Therefore the blocks are stored hierarchically.

As an example consider the output of the particle tracer GPT. It needs to store particle coordinates at different simulation times. The particle coordinates are stored as separate arrays containing the coordinates of the individual particles. Because the particle coordinates are calculated at different times, the blocks are grouped together by time. A (simplified) GPT outputfile is shown schematically in Figure 3-2.

General header	
time	1
x	{x1,x2,x3,...}
y	{y1,y2,y3,...}
z	{z1,z2,z3,...}

time	2
x	{x1,x2,x3,...}
y	{y1,y2,y3,...}
z	{z1,z2,z3,...}

Figure 3-2: GDF-output of the particle tracer GPT.

Groups can be nested. Suppose, for example, that the coordinates of the particles are calculated at two times with a different value for the variable **var**. The GDF file can then be represented as shown in Figure 3-3.

General header	
var	4
time	0
	particle coordinates
time	1
	particle coordinates
var	5
time	0
	particle coordinates
time	1
	particle coordinates

Figure 3-3: GDF-file containing nested groups.

The MR program, see section 3.18, is used to create groups based on parameter scans, while the GDFA program, see section 3.12, is used to flatten the hierarchy by one level to ease interpretation of the results.

## 3.2 ASCI2GDF

```
asci2gdf [-hHimv] [-c chars] [-s number] [-t topline] [-o outfile] [-a outfile]
infile [arr1 fac1] ...
```

ASCII file to GDF converter.

<b>-h</b>	Give short help and quit.
<b>-H</b>	Give long help and quit.
<b>-i</b>	Ignore error lines and continue.
<b>-m</b>	Low memory mode reading all columns one at a time.
<b>-v</b>	Verbose mode. Progress and file statistics are shown.
<b>-c chars</b>	Ignore lines starting with any of <b>chars</b> . Default "#;".
<b>-s number</b>	Skip the first <b>number</b> of lines.
<b>-t columns</b>	Lists the names of all <b>columns</b> in a file that contains the data only.
<b>-o outfile</b>	Write output to <b>outfile</b> .
<b>-a outfile</b>	Append output to <b>outfile</b> .
<b>infile</b>	ASCII file to be converted.
<b>arrN facN</b>	Name of the array(s) as listed in <b>infile</b> , directly followed by their multiplication factor.

ASCI2GDF converts a tabulated ASCII file to a GDF file. The resulting GDF file can be read by the field map elements and by all GPT utility programs capable of handling GDF files. ASCI2GDF writes all columns that are present in **infile** in the **outfile**, except for columns with a specified multiplication factor **fac** of 0. Non-zero multiplication factors can be used to convert from non-SI units to SI units. When the original column is already in SI units, neither the name nor its multiplication factor need to be specified on the commandline. All lines starting with a hash mark # and all blank lines are ignored. To test if the resulting file is correct, the GDF2A program can be used.

The ASCII file to be converted must have the following structure:

```
1. # Comment section
2. name1 name2 name3 name4
3. data data data data
4. data data data data
5. ... ... ... ...
```

The following commandline converts the above-listed file **sample.txt** to GDF:

```
asci2gdf -o sample.gdf sample.txt
```

The conversion can be verified with GDF2A. Without the **-o** option the output appears on the screen:

```
gdf2a sample.gdf
```

The following commandline instructs ASCI2GDF to multiply array **name2** by 100 and to omit **name4** in the resulting GDF file. Because **name1** and **name3** are not specified, they are converted to the outputfile with multiplication factor 1.

```
asci2gdf -o sample.gdf sample.txt name2 100 name4 0
```

Files with a non-conforming header, or files without header at all, can in many cases still be imported using the **-s** and **-t** options. The **-s** option skips the specified **number** of lines, whereas the **-t** option can be used to list the names of all the columns. They can be used in combination to overwrite the column names without modifying the file itself. The following example imports the above file importing the columns as **n1...n4** instead of **name1...name4**.

```
asci2gdf -o sample.gdf -s 1 -t "n1 n2 n3 n4" sample.txt
```

### 3.3 ASTRA2GDF

**astra2gdf** [-hHv] [-o outfile] [-a outfile] [-s flag] infile

Convert ASTRA output to GDF format.

<b>-h</b>	Give short help and quit.
<b>-H</b>	Give long help and quit.
<b>-v</b>	Verbose mode. Progress and file statistics are shown.
<b>-s flag</b>	Import particles with given status <b>flag</b> .
<b>-o outfile</b>	Write output to <b>outfile</b> .
<b>-a outfile</b>	Append output to <b>outfile</b> .
<b>infile</b>	ASTRA file to be converted.

ASTRA2GDF converts the 10 column ascii ASTRA output to the binary GDF format. This GDF file can subsequently be read by **setfile** in a GPT inputfile to further track the particles. Only particles with 'flag' is 5 are written to the outfile. All other particles are silently ignored.

The following conversions take place:

- The z-, pz- and time-coordinate of the first line are added to all other lines.
- Time in [ns] is converted to time in [s].
- The momenta px,py and pz in [eV/s] are converted to dimensionless GBx,GBy,GBz where  $GB_i = p_i/mc$ .
- The charge per macroparticle in [nC] is converted to dimensionless number of elementary particles.
- The ASTRA particle 'index' is converted to two columns m [kg] and q [C] containing the mass and charge of the underlying elementary particles. This is implemented for index values 1=electrons, 2=positrons, 3=protons, and 4=hydrogen ions.

The following commandline converts the ASTRA outputfile file **TestRun.0031.001** to GDF:

```
astra2gdf -o TestRun.gdf TestRun.0031.001
```

The file can subsequently be used as initial paticle distribution in a GPT inputfile using:

```
setfile("beam", "TestRun.gdf") ;  
settdist("beam", "u", 0, 0) ;
```

The reason for the last line is that ASTRA confusingly writes both time and position coordinates. Either one can be used, but care should be taken to not use both time and position coordinates simultaneously. If the output is used directly, **setfile** will assume an initial particle distribution with both time and position coordinates varying, and without warning the initial conditions will not correspond to the intended output of ASTRA. Because both GPT and ASTRA are time-domain tracking codes the most natural thing to do is having a varying position coordinate at a fixed time. We therefore use **settdist** to overwrite the time distribution to zero.

Only the ascii output variant of ASTRA is currently supported.

### 3.4 FISH2GDF

**fish2gdf** [-hHv] [-o outfile] [-a outfile] infile  
Converts SUPERFISH output to a GDF file.

**-h** Give short help and quit  
**-H** Give long help and quit  
**-v** Verbose mode  
**-o outfile** Write output to outfile  
**-a outfile** Append output to outfile  
**infile** Name of the SF7 file to convert to GDF

FISH2GDF is the first part of the interface between the SUPERFISH set of codes and GPT. Electrostatic, cylindrical symmetric magnetostatic field profiles and cylindrical symmetric rf cavities can be imported into GPT using FISH2GDF and the GPT elements listed in Table 3-A. The reference for the GPT field-map elements is given in section 4.7 and for a description of the SUPERFISH codes, we refer to [4].

Table 3-A: GPT Field map elements for various SUPERFISH solvers.

Problem	SuperFish Solvers	GPT elements
Electrostatic	POISSON/PANDIRA	<b>map2D_E, map2Dr_E</b>
Magnetostatic	POISSON/PANDIRA	<b>map2D_B</b>
RF Cavity	FISH	<b>map25D_TM</b>

The different SUPERFISH programs output the results in different units. For example electric field strength is calculated in V/cm for electrostatic problems, while MV/m is used for cavity calculations. FISH2GDF converts all units to SI using the conversion factors listed in Table 3-B.

Table 3-B: Conversion factors to SI.

SF unit	New (SI) unit	Conversion factor	Type
Cm	m	$10^{-2}$	All
G	T	$10^{-4}$	Magnetostatic
G-cm	Tm	$10^{-6}$	Magnetostatic
MV/m	V/m	$10^6$	Cavity
A/m	T	$\mu_0 = 1.25664 \cdot 10^{-6}$	Cavity
V/cm	V/m	$10^2$	Electrostatic
V	Volt	1	Electrostatic

Some columns in the SUPERFISH output contain characters in the upper 128 characters of the MS-Linedraw character set. FISH2GDF converts these names to regular ASCII using Table 3-C.

Table 3-C: Conversion from SUPERFISH to ASCII names

SF Name in MS-LineDraw	GDF Name
E	<b>E</b>
B	<b>B</b>
B $\phi$	<b>Bphi</b>
A $\phi$	<b>Aphi</b>

To be able to use FISH2GDF, first a problem-description file for SUPERFISH must be created. After running AUTOMESH and one of the SUPERFISH solvers, the results can be inspected using VGAPLOT. The calculated field profile must then be interpolated to a rectangular grid and converted to the GDF format using SF7 and FISH2GDF. The resulting GDF file can be imported into GPT using one of the corresponding field-map elements. The following batch file automates the whole process:

```
1. automesh infile
2. poisson / pandira / fish
3. vgaplot           (Optional to inspect the results)
4. sfo              (Optional to normalize the fields)
5. sf7
6. fish2gdf -o fieldmap.gdf outsf7
7. gdf2a fieldmap.gdf (Optional to inspect the results)
```

where the file `infile.in7` specifies the interpolation range for either cylindricaly symmetric (left option) or xy (right option) mode of operation.

```
1. rect noscreen          rect noscreen
2. rmin zmin rmax zmax    xmin ymin xmax ymax
3. Nr Nz                  Nx Ny
4. end                    end
```

The following line in the GPT inputfile positions a magentostatic field map at  $z=1\text{m}$ .

```
map2D_B("wcs","z",1,"fieldmap.gdf", "r","z", "Br","Bz", 1.0 ) ;
```

### 3.5 FISHFILE

```
fishfile [-hHvr] [-o outfile] [-t tolerance] [-g GPTfile] [-y height]
          [-z offset] fishfile [scatfile.gdf]
```

Calculates ‘unrolled’ scatter statistics or creates a GPT inputfile based on a Superfish file.

<b>-o outfile</b>	Write output to a file named <b>outfile</b> containing the ‘unrolled’ scatter statistics and other useful information
<b>-h</b>	Give short help and quit.
<b>-H</b>	Give long help and quit.
<b>-v</b>	Verbose output.
<b>-t tolerance</b>	The maximum tolerance [m] between the Superfish geometry and the scattered data. This option is useful when the GPT inputfile doesn’t precisely match the superfish file. The default tolerance is 1 micron.
<b>-g GPTfile</b>	Writes a GPT scatter file based in the Superfish geometry as specified in <b>fishfile</b> .
<b>-y height</b>	Specifies the y-height [m] for a rectangular geometry. When a GPT inputfile is generated the boundary elements range from $y=-\text{height}/2$ to $y=\text{height}/2$ . When not specified, the geometry is assumed to be cylindrical symmetric.
<b>-z offset</b>	Subtract the specified offset [m] from the data before starting the analysis.
<b>fishfile</b>	Superfish file describing the cylindrical symmetric geometry. The first region is assumed to be the boundary and is ignored.
<b>scatfile.gdf</b>	GPT outputfile with scatter statistics to be ‘unrolled’.

The arrays written in **outfile.gdf** are written per plate number **nn**. They are:

<b>scat_nnx</b>	x-coordinate of primary particle [m].
<b>scat_nny</b>	y-coordinate of primary particle [m].
<b>scat_nnz</b>	z-coordinate of primary particle [m].
<b>scat_nnE</b>	Energy of primary particle minus the energy of all scattered particles [J].
<b>scat_nnQ</b>	Charge of primary particle minus the charge of all scattered particles [Q].
<b>scat_nnd</b>	Unrolled position [m].

For cylindrical symmetric geometries, the following arrays are also written:

<b>scat_nnphi</b>	Angle in xy-plane [rad], measured counterclockwise from the x-axis.
<b>scat_nnr</b>	Distance to z-axis [m].
<b>scat_nnEor</b>	Identical to scat_nnE divided by scat_nnr.
<b>scat_nnQor</b>	Identical to scat_nnQ divided by scat_nnr.
<b>scat_nnrphi</b>	Identical to scat_nnr times scat_nnphi.

Fishfile is the main program to analyze the results of a collector simulation using GPT. The raw output of GPT consists of the 3D collision point and the charge and energy of both the primary and the scattered particles, as described in section 1.11.2. Interpreting these results is time-consuming and difficult. The Fishfile program automates most analysis parts using the concept of ‘unrolled’ data. Furthermore, Fishfile is capable of generating a GPT file containing the boundary elements from a Superfish inputfile.

For cylindrical-symmetric geometries, the **x** and **y** coordinates in the Superfish file are converted to **r** and **z** respectively. When the **-y** option is used, the geometry is assumed to be cartesian and the **x** and **y** coordinates are converted to **z** and **x** respectively. In both cases, the units are converted from [cm] to [m].

## 3.6 GDF2A

**gdf2a** [-hHv] [-w width] [-o outfile] infile [arrays...]

Writes a GDF-file in ASCII form to the terminal or to a file.

<b>-h</b>	Give short help and quit.
<b>-H</b>	Give long help and quit.
<b>-v</b>	Verbose mode. Instructs the program to write additional information, such as data type.
<b>-w width</b>	Specify the width (in characters) of each field. Default 10.
<b>-o outfile</b>	Write output to a file named <b>outfile</b> . If not specified, output is written to <b>stdout</b> .
<b>infile</b>	Filename of the GDF file to convert to ASCII. If not specified, the program reads the GDF file from <b>stdin</b> unless <b>arrays</b> are listed. In the latter case, a dash - must be specified to read from <b>stdin</b> .
<b>arrays</b>	The names of the arrays to be written to <b>outfile</b> . If not specified, all arrays are written.

Note: To reduce the size of the outputfile, the default number of digits written is set to single precision. The **-w 16** option can be used to instruct GDF2A to write output in double precision.

Because GDF2A can read from **stdin** and write to **stdout**, it can be piped after any command that writes a GDF file to **stdout**.



### 3.7 GDF2DXF

**gdf2dxf [-hHvlp] [-f scaling] [-o outfile] inputfile x y [z] [fx fy [fz]]**

Converts a GDF file to a point, line or vector drawing for further use in a 2D or 3D drawing package.

<b>-h</b>	Give short help and quit
<b>-H</b>	Give long help and quit
<b>-v</b>	Verbose mode
<b>-l</b>	Output lineplots
<b>-p</b>	Output scatterplots (default)
<b>-o outfile</b>	Write output to outfile
<b>infile</b>	Name of the file to perform the calculations on. When GDF2DXF has to read from <b>stdin</b> , a dash (-) must be specified explicitly for <b>infile</b> .
<b>x</b>	The name of the array specifying the x-coordinates.
<b>y</b>	The name of the array specifying the y-coordinates.
<b>z</b>	Optional name of the array specifying the z-coordinates. If this array is specified, the drawing package must be able to handle 3D data.

For vector plots, the following additional options are available:

<b>-f scaling</b>	Vector plot only: Specify the scaling for the vector length.
<b>fx</b>	Optional name of the array specifying the x-direction for vector plots.
<b>fy</b>	Optional name of the array specifying the y-direction for vector plots.
<b>fz</b>	Optional name of the array specifying the z-direction for vector plots.

GDF2DXF can be used to export GDF data to the DXF format. The latter format is recognized by almost all drawing packages and DTP programs currently available. It allows you for example to plot simulated particle trajectories through a schematic drawing of your set-up. For example to import the zx-plane of a GDF file as a line drawing into AutoCAD, the following commands can be specified:

**GDF2DXF -l -o outfile.dxf infile.gdf z x**

Start AutoCAD

**dxfin outfile.dxf**

### 3.8 GDF2GDF

```
gdf2gdf [-hHvis] [-t group] [-o outfile] [-a outfile]
  infile1 [value1] [infile2 [value2]] ...
```

Combines several GDF files into a single file, optionally sorting the top-level group.

<b>-h</b>	Give short help and quit.
<b>-H</b>	Give long help and quit.
<b>-v</b>	Verbose mode. Progress and file statistics are shown.
<b>-i</b>	Ignore recoverable errors and continue.
<b>-s</b>	Sort top-level group.
<b>-t group</b>	Top-level group.
<b>-o outfile</b>	Write output to <b>outfile</b> .
<b>-a outfile</b>	Append output to <b>outfile</b> .
<b>infile[s]</b>	Names of all the GDF files to be concatenated
<b>value[s]</b>	Optional values for the top-level group.

GDF2GDF combines several GDF files into a single large one. If **file1.gdf**, **file2.gdf** and **file3.gdf** have the exact same hierarchy, they can be combined into **all.gdf** with the following commandline:

```
gdf2gdf -o all.gdf file1.gdf file2.gdf file3.gdf.
```

Things get a little more complicated if the files to be combined do not have the same hierarchy. A typical scenario for this is when a file produced by MR needs to be combined with the result of a single additional run. Suppose that the MR file **var135.gdf** contains the simulation results for the variable **var** being 1, 3 and 5 and that the single run, **single4.gdf**, is created for **var** equal 4. These files can be combined, but only if the top-level group is specified with the **-t** option:

```
gdf2gdf -t var -o all.gdf var135.gdf single4.gdf
```

GDF2GDF will try to extract the value of **var** from **single4.gdf** to rearrange the hierarchy, but this only works if the file has been produced by MR. If the file has been produced by GPT, e.g. **gpt -o single4.gdf inputfile.in var=4**, this will not work. In that case, the value for the top-level group must be given directly after the filename on the commandline as follows:

```
gdf2gdf -t var -o all.gdf var135.gdf single4.gdf 4
```

Even this may not produce the desired result, as the ordering for **var** will become 1, 3, 5, 4. If sorted output is desired, please use the **-s** option to sort the top-level domain ascending order.

```
gdf2gdf -s -t var -o all.gdf var135.gdf single4.gdf 4
```

Technical note: When the inputfiles are huge, GDF2GDF first locks them, and subsequently reads them all storing only the hierarchy. The actual data is not stored but recorded as 64-bit file-offsets into the locked inputfiles. The next step builds the structure of the outputfile in memory by concatenating the hierarchy of the inputfiles. If needed, one level of hierarchy is added for single runs, and optionally the top-level domain is sorted. As a last step, the outputfile is written as one set of consecutive write operations, where each time the data is fetched from the appropriate inputfile at the stored location.

### 3.9 GDF2HIS

**gdf2his [-hHvb1s] [-n weight] [-o outfile] infile array width [offset]**

Calculates histograms of the specified array. For every particle in this array GDF2HIS determines which interval of the histogram it belongs to and raises the count for that bar by one.

<b>-h</b>	Give short help and quit.
<b>-H</b>	Give long help and quit.
<b>-v</b>	Verbose mode. Displays the number of bars in the histogram for every group in the <b>infile</b> .
<b>-b</b>	Write the complete histogram. When this option is selected, the output can be plotted as a lineplot outlining the individual bars of the histogram.
<b>-1</b>	Write the outline of the histogram. When plotted as a lineplot only the outline of the histogram is shown, not the individual bars.
<b>-s</b>	Divide the height of the histograms by the specified <b>width</b> .
<b>-n weight</b>	Count all contributions as specified in the <b>weight</b> array. For GPT simulations, <b>nmacro</b> can be used to count the number of elementary particles.
<b>-o outfile</b>	Write output to a file named <b>outfile</b> . If not specified the output is written to <b>stdout</b> .
<b>infile</b>	Name of the file containing the array to calculate histograms of. When GDF2HIS has to read from <b>stdin</b> , a dash (-) must be specified explicitly for <b>infile</b> .
<b>array</b>	Name of the array used to calculate the histogram. Typical examples are <b>z</b> and <b>G</b> .
<b>width</b>	Width of an interval within the histogram.
<b>offset</b>	The 'left-right' offset of the bars. If not specified, 0 is assumed, indicating one bar to the left side of zero and one to the right.

When GDF2HIS is run, a histogram is calculated for every group in the GDF file containing the specified array. In these groups, the following two arrays are appended:

**array\_his:** Array of the positions of the centers of the intervals.

**array\_cnt:** Array of the number of datapoints within one interval.

The string **array** is replaced by the name of the array specified on the commandline. The range of the histograms is obtained automatically from the minimum and maximum values of the data.

When the **-b** option is selected on the commandline, the arrays **array\_hisbar** and **array\_cntbar** are written in the outfile as well. When these two arrays are plotted as a xy-lineplot, the bars of the histogram are drawn.

When the **-1** option is selected, the arrays **array\_hisline** and **array\_cntline** are also written in the outfile. When these two arrays are plotted as a xy-lineplot, the outline of the histogram is drawn.

Example:

Suppose **infile.gdf** is a file containing all particle coordinates at different times. To calculate a histogram of the energy distribution in steps of 0.01, the following command can be specified:

**gdf2his -b -o outfile.gdf infile.gdf G 0.01**

This produces the file **outfile.gdf** where the arrays **G\_cntbar** and **G\_hisbar** are appended for every GDF group containing the particles. The outfile should be plotted using a line plot, Figure 3-4.

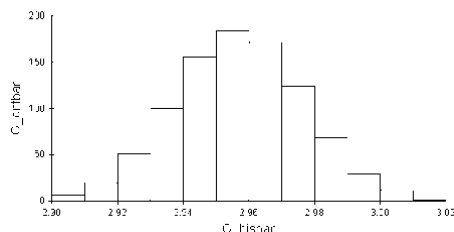


Figure 3-4: Example of GDF2HIS. The gamma's of the particles of a bunch are converted to a histogram to show the energy distribution.

### 3.10 GDF2SDDS

**gdf2sdds** [-hHva] [-o outfile] infile [arrays ...]

Converts a GDF file to the SDDS format.

<b>-h</b>	Give short help and quit.
<b>-H</b>	Give long help and quit.
<b>-v</b>	Verbose mode, instructs the program to write additional information during processing.
<b>-a</b>	Writes an ASCII SDDS file. When not specified, a binary file is written. Before use, please see the note below about precision.
<b>-o outfile</b>	Write output to a file named <b>outfile</b> . If not specified, output is written to <b>stdout</b> .
<b>infile</b>	Filename of the GDF file to convert to ASCII. If not specified, the program reads the GDF file from <b>stdin</b> . To read from <b>stdin</b> when <b>arrays</b> are specified, a dash ('-') must be specified.
<b>arrays</b>	The names of the arrays/parameters to convert. If not specified, all GDF information is converted to the SDDS format.

This program converts a GDF file to a file in the Self Describing Data Set (SDDS) format [5]. The SDDS format is supported by a toolkit consisting of a number of powerful and efficient programs for analyzing, manipulating and plotting SDDS data. The SDDS toolkit can be downloaded free of charge from Argonne National Laboratory.

The GDF2SDDS program writes GDF arrays as column data in SDDS format. Single values in GDF are converted to parameters in SDDS. When one or more **arrays** are specified, only the selected arrays are written to SDDS. GDF group names such as time, position and the values of one or more scanned parameters are always written to SDDS. As dictated by the SDDS column format, all specified arrays must have equal length.

To convert the x-, y- and z-coordinates in the GDF file **test.gdf** to the SDDS file **test.sdds**, the following command can be used:

```
gdf2sdds -o test.sdds test.gdf x y z
```

Because GDF2SDDS writes to **stdout** when no output filename is given, it can be piped before any command that reads an SDDS file from **stdin**. This allows efficient use of the **-pipe=in** option of many of the SDDS toolkit programs, as demonstrated in the following example:

```
gdf2sdds test.gdf | sddsquery -pipe=in
```

Note: The **-a** option writes an ASCII SDDS file. To reduce the size of the outputfile, double-precision floating-point numbers are written with only 8 digits precision. Because this causes loss of precision, it is recommended not to use this option except for diagnostic purposes.

### 3.11 GDF2VTP

```
gdf2vtp [-hHv] [-m] [-i index] [-o outfile] infile [arrays...]
```

Converts a GDF-file to ParaView format

<b>-h</b>	Give short help and quit.
<b>-H</b>	Give long help and quit.
<b>-v</b>	Verbose mode. Instructs the program to write additional information during every stage of the conversion process.
<b>-m</b>	Force multi-page <b>outfile.pvd</b> file to be written, also for single-group input.
<b>-i index</b>	Group the files in <b>outfile.pvd</b> by specified <b>index</b> . Default <b>time</b> .
<b>-o outfile</b>	Write output to a file named <b>outfile.vtr</b> for rectilinear grids, <b>outfile.vtp</b> for point data, and <b>outfile.pvd</b> for group information.
<b>infile</b>	Filename of the GDF-file to convert to ParaView format. A dash ("-") can be specified to read from <b>stdin</b> .
<b>arrays</b>	The names of the arrays to be written to <b>outfile</b> . If not specified, all arrays are written.

This program converts a multi-group GDF-file to a sequence of ParaView files. When **infile** contains a GPT phase-phase distribution, the output will be point-data containing the particle phase-space coordinates. When the input is an axis-aligned grid containing field-information, the output will be a rectilinear grid that can be sliced in ParaView. The program automatically distinguishes between these different modes of operation, and it automatically assigns the correct extension to outfile: **.vtp** for point-data and **.vtr** for rectilinear (field) grids. When the input has multiple GDF-groups, the output is a sequence of files numbered from 1 to **N** and a separate collection file named **outfile.pvd** is written that contains the pointers to the individual files.

Because ParaView format is meant for 3D visualization, *xyz*-data must be present. It is currently not possible to convert for example the output of GDFA. Default all arrays present in the GDF file are converted to ParaView format. This can be limited using the **arrays** option by specifying the list of arrays that need to be stored.

Many GDF-files contain separate groups containing for example multiple time outputs or as a result of a parameter scan. Such multi-group files are converted to a sequence of files named **outfile.N.vtp** for point-data and **outfile.N.vtr** for rectilinear grids. In addition, a separate **outfile.pvd** file is written referencing these individual files and providing collection information to ParaView. Although the numbered files can be opened by ParaView, the typical procedure is to open the **.pvd** file instead because this allows you to conveniently cycle back and forth through the multi-group results.

In a workflow where sometimes single-group and sometimes multi-group output is generated, we strongly advice the use of the **-m** option and always work with the **.pvd** file. This is because when switching from multi-group to single-group output, the old numbered files will not be deleted from disk. Consequently, it is very easy to mistakenly open a file that was produced by a previous or maybe even older simulation. This issue is solved by working with the **.pvd** since it will always contain the correct collection, where sometimes this happens to be a collection of 1. In terms of performance there is no penalty for working with the collection since **.pvd** files are tiny because they do not contain any simulation data.

Vector data in the GDF file is automatically converted to a single array. For example, the magnetic field arrays named **fBx**, **fBy** and **fBz** in the GDF inputfile will be stored as a single vector array named **fB**. If individual arrays are specified using the **array** specification, and if this list does not list all vector components, the conversion to vector form does not take place.

One remaining issue converting multi-group files is that the **.pvd** collection file format only supports “**timestep**” as running variable. This potentially conflicts with the GDF format where it is possible to have scans with some other variable changing from group to group. For a sequence of time-outputs, the **timestep** in the **.pvd** file is set to the GPT simulation **time**. In all other cases, **timestep** in the **.vtp** file is simply set to an integer matching the number of the referenced outfile instead. The latter behavior can be overwritten using the **-i index** option, where you can for example specify that the output of a scan over **phase** should be converted such that **phase** in GPT becomes **timestep** in ParaView. Running with the **-v** option gives hints and suggestions in confusing cases.

Group information is also converted to ParaView format in the form of so-called **<FieldData>**. This information is visible in ParaView alongside the **<PointData>**, and it can be shown in Render View using the **AnnotateAttributeData** filter.

A few examples of how to use GDF2VTP are listed in Table 3-D shown below.

Table 3-D: Example use of GDF2VTP.

Command:	Comments:
<pre>gpt -o outfile.gdf infile.in gdf2vtp -o outfile.vtp outfile.gdf</pre> <p>where <b>infile.in</b> contains:  <b>tout(1e-9);</b></p>	Writes <b>outfile.vtp</b> containing the phase-space coordinates of all particles at $t=10^{-9}$ .
<p>Idem, where <b>infile.in</b> contains:  <b>tout(0,10e-9,1e-9);</b></p>	Writes <b>outfile.1.vtp...outfile.11.vtp</b> containing phase-space coordinates of all particles at the specified times. Also writes the collection file <b>outfile.pvd</b> where <b>timestep</b> lists the correct simulation time.
<p>Idem, where <b>infile.in</b> contains:  <b>screen(10e-3,20e-3,1e-3);</b></p>	Writes <b>outfile.1.vtp...outfile.11.vtp</b> containing phase-space coordinates of all particles at the specified positions. Also writes the collection file <b>outfile.pvd</b> where <b>timestep</b> just runs from 1 to 11.
<pre>gpt -o outfile.gdf infile.in gdf2vtp -i position -o outfile.vtp outfile.gdf</pre> <p>where <b>infile.in</b> contains:  <b>screen(10e-3,20e-3,1e-3);</b></p>	Schizophrenic mode where position in GPT is shown as time in Paraview.
<pre>gpt -o outfile.gdf infile.in gdf2vtp -o outfile.vtp outfile.gdf</pre> <p>where <b>infile.in</b> contains:  <b>setstartxyzgrid(...);</b>  <b>tout(0);</b></p>	Writes <b>outfile.vtr</b> containing a rectilinear grid of field-data. The position and spacing where the fields are sampled is given by the parameters of <b>setstartxyzgrid("set", Lx,dx, Ly,dy, Lz,dz)</b> where <b>L</b> and <b>d</b> specify the length and spacing respectively in the <i>xyz</i> -directions. Not all dimension need to have thickness, and for example a slice in the <i>zx</i> -plane can be specified by setting <b>Ly=dy=0</b> .
<p>Idem, where <b>infile.in</b> contains:  <b>q=0.0;</b>  <b>setstartxyzgrid("set",...);</b>  <b>settransform("wcs","ox,oy,oz",1,0,0,</b>  <b>0,1,0, "set) ;</b>  <b>tout(0,10e-9,1e-9);</b></p>	Here we position stationary particles with zero charge so that the observer grid itself is not being tracked during the multiple-time output. Furthermore, the field-data is centered around the point <b>ox,oy,oz</b> .

## 3.12 GDFA

**gdfa** [-hHv] [-o outfile] [-a outfile] **infile** **group\_by** **prog** ...

Writes a GDF file containing the results of performed calculations.

**-h** Give short help and quit.  
**-H** Give long help and quit.  
**-v** Verbose mode.  
**-s** Silent mode. Don't display informative messages about unsuccessful progs.  
**-o outfile** Write output to a file named **outfile**. If not specified, the output is written to **stdout**.  
**-a outfile** Append output to a file named **outfile**. This option is for internal use only.  
**infile** Name of the file to perform the calculations on. When GDFA has to read from **stdin**, a dash (-) must be specified explicitly for **infile**.  
**group\_by** The name of the variable used to group the data. Use **time** for **snapshot/tout** output and **position** for **screen** output. When **MR** is used, you can also use the name of the scanned parameter.  
**prog ...** The name(s) of one or more programs to run on the **infile**. See the following sections for a complete overview. The GPT programmer's reference describes the procedure how to create custom GDFA programs.

The following GDFA programs are currently available:

3.12.1	Averages.....	98
3.12.2	Standard deviations .....	98
3.12.3	RMS Emittance routines .....	99
3.12.4	90% and 100% Emittance routines .....	100
3.12.5	Courant-Snyder parameters .....	100
3.12.6	Robust estimates: Median and Range .....	101
3.12.7	Miscellaneous routines .....	102
3.12.8	Scatter statistics .....	102
3.12.9	Obsolete functions .....	102

To explain GDFA we continue with the example of Figure 3-3. For convenience, we now represent this GDF file in the form shown in Figure 3-5.

	time=0	time=1
var=4	Particle coordinates	Particle coordinates
var=5	Particle coordinates	Particle coordinates

Figure 3-5: GDFA representation of a GDF-file containing two nested groups.

Firstly, GDFA runs the specified **progs** on the data of the **infile**. A **prog** is a function of the data and returns a scalar. **stdz** for example returns the standard deviation of the array of the z-coordinates. After the first pass, the data can be represented as shown in Figure 3-6. For a complete list of the **progs** currently available we refer to the following sections.

	time=0	time=1
var=4	stdz	stdz
var=5	stdz	stdz

Figure 3-6: GDFA representation of a GDF-file containing two nested groups.

Secondly, GDFA eliminates the **group\_by** group by making arrays of the results returned by the **progs**. Continuing with our example, we have two possible **group\_by** variables: **time** and **var**. The results when grouped by time and var are both shown in Figure 3-7.

When **time** is chosen, the **var** hierarchy is maintained and the result is shown schematically in Figure 3-7. When **var** is chosen, the **time** hierarchy is maintained and the result is shown schematically in Figure 3-7.

General header		
var	4	
	stdz	{.,.}
	time	{0,1}

General header		
time	0	
	stdz	{.,.}
	var	{4,5}

var	5		time	1	
	stdz	{.,.}		stdz	{.,.}
	time	{0,1}		var	{4,5}

Figure 3-7: Grouped by **time** (left) and grouped by **var** (right).

The **group\_by** variable itself is always included as an array. If more than one **prog** is specified, GDFA makes separate arrays for the results of all the **progs**. If one **prog** fails to calculate its result, the results of all the other **progs** are ignored too.

Custom GDFA programs can be created similar to custom GPT elements. The procedure is described in the separate GPT programmer's reference.

We would like to thank Dr A. Büchner for providing us with the initial versions of the emittance and Courant-Snyder routines and allowing us to share them with other GPT users.

### 3.12.1 Averages

The average is a good estimate for the center of a distribution without outliers. For an alternative robust estimate insensitive to outliers, please see Median in section 3.12.6. All averages are weighted by the number of elementary particles each macro-particle represents. The following GDFA routines are implemented:

Name	Equation	Description
<b>avgx</b>	$\bar{x} = \frac{\sum n_i x_i}{\sum n_i}$	Average $x$ -coordinate [m].
<b>avgy</b>	$\bar{y}$	Average $y$ -coordinate [m].
<b>avgz</b>	$\bar{z}$	Average $z$ -coordinate [m].
<b>avgr</b>	$\sum n_i \sqrt{(x_i - \bar{x})^2 + (y_i - \bar{y})^2} / \sum n_i$	Average $r$ -coordinate [m].
<b>avgBx</b>	$\bar{\beta}_x$	Average $\beta_x$ -coordinate
<b>avgBy</b>	$\bar{\beta}_y$	Average $\beta_y$ -coordinate
<b>avgBz</b>	$\bar{\beta}_z$	Average $\beta_z$ -coordinate
<b>avgG</b>	$\bar{\gamma}$	Average $\gamma$
<b>avgt</b>	$\bar{t}$	Average time [s] useful for position output.
<b>avgfEx</b>	$\bar{E}_x$	Average $E_x$ -field [V/m].
<b>avgfEy</b>	$\bar{E}_y$	Average $E_y$ -field [V/m].
<b>avgfEz</b>	$\bar{E}_z$	Average $E_z$ -field [V/m].
<b>avgfBx</b>	$\bar{B}_x$	Average $B_x$ -field [T].
<b>avgfBy</b>	$\bar{B}_y$	Average $B_y$ -field [T].
<b>avgfBz</b>	$\bar{B}_z$	Average $B_z$ -field [T].
<b>avgp</b>	$\frac{\beta_0}{(1-\beta_0^2)^{1/2}} \frac{mc}{ e }$ with $\beta_0 = \frac{\bar{\gamma}\bar{\beta}}{\bar{\gamma}}$	Mean beam momentum [eV-s/m].

### 3.12.2 Standard deviations

The standard deviation, also known as rms value, is a good estimate for the width of a distribution without outliers. For an alternative robust estimate insensitive to outliers, please see the 50% ranges in section 3.12.6. All standard deviations are weighted by the number of elementary particles each macro-particle represents. The following GDFA routines are implemented:

Name	Equation	Description
<b>stdx</b>	$\text{std}(x) = \sqrt{\frac{\sum n_i (x_i - \bar{x})^2}{\sum n_i}}$	Standard $x$ -deviation [m].
<b>stdy</b>	$\text{std}(y)$	Standard $y$ -deviation [m].
<b>stdz</b>	$\text{std}(z)$	Standard $z$ -deviation [m].
<b>stdBx</b>	$\text{std}(\beta_x)$	Standard $\beta_x$ -deviation
<b>stdBy</b>	$\text{std}(\beta_y)$	Standard $\beta_y$ -deviation
<b>stdBz</b>	$\text{std}(\beta_z)$	Standard $\beta_z$ -deviation
<b>stdG</b>	$\text{std}(\gamma)$	Standard $\gamma$ -deviation
<b>stdt</b>	$\text{std}(t)$	Standard time deviation [s].



### 3.12.3 RMS Emittance routines

In our opinion, the normalized transverse emittance can best be calculated as the area in position and transverse momentum coordinates:  $x$  and  $\gamma\beta_x$ . However, to remain compatible with other codes, the emittance in the following GDFA programs is calculated in velocity space,  $x$  and  $\beta_x$ . This value is multiplied by the average of the Lorentz factor  $\gamma$  for normalization. Without energy spread, these results are identical. However, when there is a relatively large energy spread, or when the phase space is far from elliptical, the results can be significantly different. See the GPT programmer's reference to adapt the routines to your own taste.

In all routines, the emittance is defined as the phase-space area divided by  $\pi$ . Therefore, the units of emittance are often presented as [ $\pi$  mm-mrad]. The factor  $\pi$  in the dimension is included to assure the reader that  $\pi$  has been factored out of the phase-space area.

The SI units for transverse and longitudinal emittance are [m-rad] and [J-s] respectively. The transverse emittance routines **nemixrms**, **nemiyrms**, **nemirrms**, **nemix90**, **nemiy90**, **nemix100** and **nemiy100** calculate their results in [m-rad]. The longitudinal emittance is calculated in [eV-s] by **nemizrms**, **nemiz90** and **nemiz100** for convenience. To convert **nemixrms** from its SI result to [ $\pi$  mm-mrad] one should multiply by 1,000,000: One time by 1000 to convert from [m] to [mm] and one time by 1000 to convert from [rad] to [mrad].

To calculate the normalized RMS-emittances, first  $x_c$ ,  $y_c$ ,  $x'_c$  and  $y'_c$  are calculated by GDFA using:

$$\begin{aligned} x_c &= x - \bar{x} & y_c &= y - \bar{y} \\ x'_c &= \beta_x - \bar{\beta}_x & y'_c &= \beta_y - \bar{\beta}_y \end{aligned} \quad [3.1]$$

The quantities  $x'$  and  $y'$  are directly multiplied by  $\gamma$  to provide correct normalization for beams with high energy spread and high divergence angles. All parameters are centered around zero.

The RMS emittance for the  $x$ - $x'$  and  $y$ - $y'$  phase spaces are defined by:

$$\begin{aligned} \text{nemixrms} &= \bar{\gamma} \sqrt{x_c^2 \cdot \overline{x'^2_c} - \overline{x_c x'^c}^2} \\ \text{nemiyrms} &= \bar{\gamma} \sqrt{y_c^2 \cdot \overline{y'^2_c} - \overline{y_c y'^c}^2} \end{aligned} \quad [3.2]$$

When a cylindrical symmetric beam rotates around the  $z$ -axis, such as in a solenoidal field, strong  $x$ - $y'$  and  $x'-y$  correlations result in very large values for the rms  $x$ - and  $y$ -emittances. This does not signal phase-space dilution or loss of beam quality in any way. It is just an artifact of the numerical method used to calculate the emittance. The emittance decreases again when the solenoidal field vanishes. This effect can be reduced by calculating the  $r$ -emittance, using the hypervolume in  $x$ - $x'$ - $y$ - $y'$  subspace, to calculate the emittance using:

$$\text{nemirrms} = \bar{\gamma} \sqrt{\varepsilon_{x,rms} \cdot \varepsilon_{y,rms} - |\overline{x_c y_c} \cdot \overline{x'_c y'^c} - \overline{x_c y'^c} \cdot \overline{x'_c y_c}|} \quad [3.3]$$

The units of **nemixrms**, **nemiyrms** and **nemirrms** are emittances in [m-rad]. However, the values are typically multiplied by 1,000,000 and quoted as [ $\pi$  mm-mrad]. Also please note that the results will be a factor of 4 less than the results produced by the now-obsolete **nemix** and **nemiy** programs.

The longitudinal emittance is calculated by:

$$\begin{aligned} t_c &= t - \bar{t} \\ \gamma_c &= \gamma - \bar{\gamma} \\ \text{nemizrms} &= \frac{mc^2}{|q_e|} \sqrt{t_c^2 \cdot \overline{\gamma_c^2} - \overline{t_c \gamma_c}^2} \end{aligned} \quad [3.4]$$

The factor  $mc^2/q_e$  is used to convert the units to [eV-s].

When time output is used, all particle coordinates have the same time coordinate. In this case, the time coordinate is obtained by extrapolating the centered position using  $t_i = -(z_i - \bar{z})/c\beta_{z,i}$ .

### 3.12.4 90% and 100% Emittance routines

As an alternative to the RMS emittance, one can define ‘per-particle’ emittance values: Every particle is at the boundary of an ellipse with the same orientation and shape as the ‘average ellipse’, but with a different size. The area/ $\pi$  of this ellipse is the emittance of the particle.

The calculations are estimates, based on the overall ellipse parameters calculated by the Courant-Snyder parameters. As such, they do not necessarily produce the smallest possible ellipse enclosing 90% or 100% of the particles. When distributions are far from elliptical in phase space, these routines can not be used.

First the following parameters are calculated using all particles:

$$\begin{aligned} a_x &= -\overline{x_c x'_c} & b_x &= \overline{x_c^2} & c_x &= \overline{x'^2_c} & e_x &= \sqrt{b_x c_x - a_x^2} \\ a_y &= -\overline{y_c y'_c} & b_y &= \overline{y_c^2} & c_y &= \overline{y'^2_c} & e_y &= \sqrt{b_y c_y - a_y^2} \\ a_z &= -\overline{t_c \gamma_c} & b_z &= \overline{t_c^2} & c_z &= \overline{\gamma_c^2} & e_z &= \sqrt{b_z c_z - a_z^2} \end{aligned} \quad [3.5]$$

The  $a, b, c$  parameters are very similar to the Courant-Snyder parameters  $\alpha, \beta, \gamma$ . The ‘per-particle’ emittance is then given by:

$$\begin{aligned} \varepsilon_{x,i} &= (c_x(x_i - \bar{x})^2 + 2a_x(x_i - \bar{x})(x'_i - \bar{x}') + b_x(x'_i - \bar{x}')^2)/e_x \\ \varepsilon_{y,i} &= (c_y(y_i - \bar{y})^2 + 2a_y(y_i - \bar{y})(y'_i - \bar{y}') + b_y(y'_i - \bar{y}')^2)/e_y \\ \varepsilon_{z,i} &= (c_z(t_i - \bar{t})^2 + 2a_z(t_i - \bar{t})(\gamma_i - \bar{\gamma}) + b_z(\gamma_i - \bar{\gamma})^2) \frac{mc^2}{|q_e|e_z} \end{aligned} \quad [3.6]$$

The **nemi\*100** programs calculate the emittance of the worst offender, equal to the area/ $\pi$  of the ellipse enclosing all particles:

$$\begin{aligned} \mathbf{nemix100} &= \max(\varepsilon_x) \\ \mathbf{nemiy100} &= \max(\varepsilon_y) \\ \mathbf{nemiz100} &= \max(\varepsilon_z) \end{aligned} \quad [3.7]$$

The **nemi\*90** programs calculate the area/ $\pi$  of the smallest ellipse enclosing 90% of the particles. It provides more stable results than the 100% values, but it should be noted that all particles are used in the determination of the phase-space ellipse dimensions and orientation.

$$\begin{aligned} \mathbf{nemix90} &= \varepsilon_{x,i} \mid 90\% \text{ of particles } j \text{ have } \varepsilon_{x,j} \leq \varepsilon_{x,i} \\ \mathbf{nemiy90} &= \varepsilon_{y,i} \mid 90\% \text{ of particles } j \text{ have } \varepsilon_{y,j} \leq \varepsilon_{y,i} \\ \mathbf{nemiz90} &= \varepsilon_{z,i} \mid 90\% \text{ of particles } j \text{ have } \varepsilon_{z,j} \leq \varepsilon_{z,i} \end{aligned} \quad [3.8]$$

### 3.12.5 Courant-Snyder parameters

The **CSalpha\***, **CSbeta\*** and **CSgamma\*** routines calculate the Courant-Snyder parameters named  $\alpha, \beta$  and  $\gamma$ . All Courant-Snyder parameters satisfy the equation:  $\gamma\beta - \alpha^2 = 1$ .

To avoid confusion, the symbols  $\beta$  and  $\gamma$  are always used for the normalized velocity and the Lorentz factor respectively when not specified otherwise. To obtain the Courant-Snyder parameters, first the following quantities are calculated:

$$\begin{aligned} x_c &= x - \bar{x} & x'_c &= \beta_x - \bar{\beta}_x & \varepsilon_x &= \sqrt{\overline{x_c^2} \cdot \overline{x'^2_c} - \overline{x_c x'_c}^2} \\ y_c &= y - \bar{y} & y'_c &= \beta_y - \bar{\beta}_y & \varepsilon_y &= \sqrt{\overline{y_c^2} \cdot \overline{y'^2_c} - \overline{y_c y'_c}^2} \\ t_c &= t - \bar{t} & \gamma_c &= \gamma - \bar{\gamma} & \varepsilon_z &= \sqrt{\overline{t_c^2} \cdot \overline{\gamma_c^2} - \overline{t_c \gamma_c}^2} \end{aligned} \quad [3.9]$$

Please note that the emittance values are not normalized. Furthermore, the quantities  $\beta_x$  and  $\beta_y$  are not divided by  $\beta_z$ , similar to the **nemixrms** and **nemiyrms** equations.

The Courant-Snyder parameters are then calculated by:

$$\begin{aligned}
\mathbf{CSalpha}_x &= -\overline{x_c x'_c} / \varepsilon_x & \mathbf{CSbeta}_x &= \overline{\beta_z} \cdot \overline{x'_c} / \varepsilon_x & \mathbf{CSgamma}_x &= \overline{x'^2_c} / (\varepsilon_x \cdot \overline{\beta_z}) \\
\mathbf{CSalpha}_y &= -\overline{y_c y'_c} / \varepsilon_y & \mathbf{CSbeta}_y &= \overline{\beta_z} \cdot \overline{y'_c} / \varepsilon_y & \mathbf{CSgamma}_y &= \overline{y'^2_c} / (\varepsilon_y \cdot \overline{\beta_z}) \\
\mathbf{CSalpha}_z &= -\overline{t_c \gamma_c} / \varepsilon_z & \mathbf{CSbeta}_z &= \frac{|q_e|}{mc^2} \cdot \frac{\overline{t_c^2}}{\varepsilon_z} & \mathbf{CSgamma}_z &= \frac{mc^2}{|q_e|} \cdot \frac{\overline{\gamma_c^2}}{\varepsilon_z}
\end{aligned} \tag{3.10}$$

The average of  $\beta_z$  is a correction factor applied to remain consistent with other codes. The units of **CSalpha** are dimensionless. The units of **CSbeta<sub>x</sub>** and **CSbeta<sub>y</sub>** are [m/rad] and the units of **CSgamma<sub>x</sub>** and **CSgamma<sub>y</sub>** are [rad/m]. The units of **CSbeta<sub>z</sub>** and **CSgamma<sub>z</sub>** are [s/eV] and [eV/s] respectively.

### 3.12.6 Robust estimates: Median and Range

Data analysis based on averages, standard deviations or rms emittances is very sensitive to outliers. This is typically of little concern when analyzing GPT results obtained with a mesh-based space-charge model, but it can be disastrous with point-to-point Coulomb interactions. The reason for this is that these point-to-point interactions cause non-Gaussian heating, leading to a Holtsmark distribution in phase-space. This distribution has incredibly long tails with divergent rms values. Consequently, calculating the average value of a limited number of sample particles gives an extremely inaccurate estimate for the center of the distribution. Using the standard deviation as a measure for the width of the distribution doesn't work either, and even increasing the amount of particles to be tracked in the hope to improve things doesn't help. Clearly it is *not* wise to calculate averages, or any statistic that is sensitive to outliers, when outliers are expected to be present. In such cases, use robust estimates such as the median instead of the average, and for example a 50% range instead of the standard deviation. Just as with most actual experiments, these quantities essentially ignore a few outliers, regardless of where these outliers happen to be.

Name	Equation	Description
<b>medianx</b>	$\text{sort}(\mathbf{x})[\frac{1}{2}N]$	Median of the $x$ -coordinates [m]
<b>mediany</b>	$\text{sort}(\mathbf{y})[\frac{1}{2}N]$	Median of the $y$ -coordinates [m]
<b>medianz</b>	$\text{sort}(\mathbf{z})[\frac{1}{2}N]$	Median of the $z$ -coordinates [m]
<b>mediant</b>	$\text{sort}(\mathbf{t})[\frac{1}{2}N]$	Median of the time-coordinates [s]
<b>medianBx</b>	$\text{sort}(\mathbf{Bx})[\frac{1}{2}N]$	Median of the $\beta_x$ -coordinates []
<b>medianBy</b>	$\text{sort}(\mathbf{By})[\frac{1}{2}N]$	Median of the $\beta_y$ -coordinates []
<b>medianBz</b>	$\text{sort}(\mathbf{Bz})[\frac{1}{2}N]$	Median of the $\beta_z$ -coordinates []

where the notation  $\text{sort}(\mathbf{x})[\frac{1}{2}N]$  indicates the center element of the sorted array of  $x$ -coordinates. When  $N$  is even, a linear interpolation is used between the middle two elements.

Name	Equation	Description
<b>Dx_50</b>	$\text{sort}(\mathbf{x})[\frac{3}{4}N] - \text{sort}(\mathbf{x})[\frac{1}{4}N]$	50% range of the $x$ -coordinates [m]
<b>Dy_50</b>	$\text{sort}(\mathbf{y})[\frac{3}{4}N] - \text{sort}(\mathbf{y})[\frac{1}{4}N]$	50% range of the $y$ -coordinates [m]
<b>Dz_50</b>	$\text{sort}(\mathbf{z})[\frac{3}{4}N] - \text{sort}(\mathbf{z})[\frac{1}{4}N]$	50% range of the $z$ -coordinates [m]
<b>Dt_50</b>	$\text{sort}(\mathbf{t})[\frac{3}{4}N] - \text{sort}(\mathbf{t})[\frac{1}{4}N]$	50% range of the time-coordinates [s]
<b>dBx_50</b>	$\text{sort}(\mathbf{Bx})[\frac{3}{4}N] - \text{sort}(\mathbf{Bx})[\frac{1}{4}N]$	50% range of the $\beta_x$ -coordinates []
<b>dBy_50</b>	$\text{sort}(\mathbf{By})[\frac{3}{4}N] - \text{sort}(\mathbf{By})[\frac{1}{4}N]$	50% range of the $\beta_y$ -coordinates []
<b>dBz_50</b>	$\text{sort}(\mathbf{Bz})[\frac{3}{4}N] - \text{sort}(\mathbf{Bz})[\frac{1}{4}N]$	50% range of the $\beta_z$ -coordinates []

The above robust analysis routines are primarily used for the analysis of point-to-point interactions results where each particle in the simulation represents exactly one elementary particle. Nevertheless, all routines properly take into account the amount of elementary particles that each macro particle represents. In other words, if some particle represents for example two elementary particles, the code handles this case as if this particle appears twice in the list to be sorted and  $N$  is adjusted accordingly. The implementation properly handles cases where the number of elementary particles represented by a macro particle in the simulation is non-integer or extremely large.

### 3.12.7 Miscellaneous routines

Name	Equation	Description
<b>cputime</b>	cputime	Total CPU time used by the simulation [s]. On a multi-core machine this is the combined time of all the individual cores.
<b>rmax</b>	$\max(\sqrt{x^2 + y^2})$	Maximum of radius [m].
<b>numpar</b>	length(x)	Number of particles ‘alive’.
<b>Q</b>	$\sum_i N_i q_i$	Total charge [Q].

### 3.12.8 Scatter statistics

The following functions work in combination with the FISHFILE program, described in section 3.5, to obtain total current and power for each collector plate. Each **nn** must be replaced by 01, 02, ..., 10 indicating the plate number. The programs convert total charge and energy to current and power respectively by dividing by the variable **tlen**. This variable must be present in the GPT outputfile, written using **outputvalue**, and must indicate the width of the uniform time distribution of the initial particles. An example is shown in tutorial section 2.11.8.

Name	Equation	Description
<b>scatterInn</b>	$\frac{\sum \text{scat\_nnQ}}{\text{tlen}}$	Total current on collector plate number <b>nn</b> .
<b>ScatterPnn</b>	$\frac{\sum \text{scat\_nnE}}{\text{tlen}}$	Total power on collector plate number <b>nn</b> .

### 3.12.9 Obsolete functions

The following functions are maintained for backward compatibility only. Please use the given alternatives instead.

Name	Equation	Alternative	Description
<b>nemix</b>	See below	<b>nemirrms</b>	Normalized rms emittance in $(x, \beta_x)$ subspace
<b>nemiy</b>	See below	<b>nemirrms</b>	Normalized rms emittance for $(y, \beta_y)$ subspace

The **nemix** and **nemiy** routines start by calculating

$$\begin{aligned} x_c &= x - \bar{x} & y_c &= y - \bar{y} \\ x'_c &= \beta_x - \bar{\beta}_x & y'_c &= \beta_y - \bar{\beta}_y \end{aligned} \quad [3.11]$$

Then the average rotation around the  $z$ -axis is subtracted:

$$\begin{aligned} \bar{\omega}/c &= \frac{\sum_i \beta_{y,i} x_i - \beta_{x,i} y_i}{\sum_i x_i^2 + y_i^2} \\ \beta_{x,i} &= \beta_{x,i} + \bar{\omega} y_i / c \\ \beta_{y,i} &= \beta_{y,i} - \bar{\omega} x_i / c \end{aligned} \quad [3.12]$$

The emittance for the  $x$ - $x'$  and  $y$ - $y'$  phase spaces are then defined by:

$$\begin{aligned} \text{nemix} &= 4\bar{y} \sqrt{\overline{x_c^2} \cdot \overline{x'^2_c} - \overline{x_c x'^2_c}} \\ \text{nemiy} &= 4\bar{y} \sqrt{\overline{y_c^2} \cdot \overline{y'^2_c} - \overline{y_c y'^2_c}} \end{aligned} \quad [3.13]$$

It is important to note that the **nemix** and **nemiy** routines always produce a factor 4 higher emittance values. Furthermore, they do not calculate weighted averages.

### 3.13 GDFFLATTEN

**gdfflatten** [-hHg] [-o **outfile**] **group\_by** **infile.gdf**

Removes one level from the hierarchical structure of a GDF file by combining the results.

<b>-o outfile</b>	Write output to a file named <b>outfile</b>
<b>-a outfile</b>	Append output to a file named <b>outfile</b>
<b>-h</b>	Give short help and quit.
<b>-H</b>	Give long help and quit.
<b>-g</b>	Write group information as separate column.
<b>-v</b>	Verbose mode. Display iteration output containing all variables and constraints.
<b>group_by</b>	Group to be removed during flattening.
<b>infile.gdf</b>	File to be flattened

GDFFLATTEN changes the hierarchical structure of a GDF file by concatenating data from several groups. The data itself is hereby not changed. GDFFLATTEN eliminates the **group\_by** group of the inputfile while maintaining the rest of the hierarchical structure. This is done by rearranging the data such that all data is grouped together without taking into account the **group\_by** level in the hierarchy.

When the **-g** option is specified, GDFFLATTEN runs in lossless mode by writing the **group\_by** variable as a separate column to the outputfile.

One possible use of GDFFLATTEN is to obtain better statistics by combining the results of several GPT runs where each run is launched with a different seed for the random number generator. In that case, the MR program is used to launch N different runs, with N different seeds. Although this works great with the MPI version of MR on a cluster with N nodes, the resulting outputfile is difficult to analyze because it contains “seed” as outermost group in the hierarchy. Flattening on “seed” solves this issue because it will produce a file as if N times more particles had been tracked. Such a file is much easier to post-process with the standard tools such as GDFA.

### 3.14 GDFMGO

```
gdfmgo [-hHvk] -j nCPU [-o outfile] infile.sol program [parameters]
or
mpirun [options] gdfmgo [-hHvk] -o [outfile] infile.sol program [-j 1]
[parameters]
```

Multi-objective genetic global optimizer for the specified program.

<b>-o outfile</b>	Write output to a file named <b>outfile</b>
<b>-a outfile</b>	Append output to a file named <b>outfile</b>
<b>-h</b>	Give short help and quit.
<b>-H</b>	Give long help and quit.
<b>-v</b>	Verbose mode. Display iteration output containing all variables and constraints.
<b>-j nCPU</b>	Run simultaneously over <b>nCPU</b> processors in a multi-processor system. When not specified, all cores in the system are used. The MPI version uses the [options] of <b>mpiexec</b> to allocate computational resources and the <b>-j</b> option is ignored.
<b>-s initial</b>	Read the initial population from the file <b>initial</b> instead of generating a random distribution. This file can be the output of a previous GDFMGO run.
<b>-k</b>	Keep all datapoints in the initial distribution, even if the population size is smaller.
<b>-r</b>	Do not delete raw outputfiles.
<b>-f path</b>	Store raw simulation results in <b>path</b> .
<b>-g executable</b>	Use the given <b>executable</b> for data analysis. Default G DFA.
<b>infile.sol</b>	Name of the file containing information about the parameters that are to be varied and the constraints to be met. See Table 3-I for specific sections in this file.
<b>mpiexec [options]</b>	Use <b>mpiexec</b> to launch multiple instances of <b>program</b> in parallel.
<b>program [parameters]</b>	Command line of a program that creates a GDF file and recognizes the <b>-o</b> option, for example <b>GPT</b> .

GDFMGO is a multi-objective genetic global optimizer that is applicable to a wide range of optimization problems. Its main use is to estimate the optimal trade-off between conflicting objectives, such as large current and low emittance, while adjusting all free variables. It approximates this optimal trade-off, better known as the pareto front, by genetically optimizing a population of samples across all their variables. This is a CPU intensive method, but very stable and relatively insensitive to simulation noise. An MPI version is available to run GDFMGO on clusters and supercomputers. Information about the internal algorithms of GDFMGO can be found in section 1.12.3. One dimensional optimization problems are sometimes better suited for GDFSOLVE, described in section 0.

GDFMGO is a load-balanced optimizer: Different runs can use a different amount of CPU time to complete without degrading performance. However care should be taken that the program to run does not spawn new threads in an attempt to increase calculation speed. This will work counter-productively in almost all cases because the coarse-grain multithreading by GDFMGO will typically outperform fine-grain multithreading of the program. We have seen cases where the performance dropped by over a factor of 10. Consequently, when GDFMGO is used in combination with MR and/or GPT we strongly recommend including **-j 1** in the commandline options for these programs. This yields:

```
gdfmgo -o output.gdf infile.sol mr -j 1 scan.mr gpt -j 1 input.in
or the same with mpirun [options] prepended for the MPI version.
```

It is possible to continue the optimization of a previous GDFMGO run, or start with a custom dataset, using the **-s** option. This option is rather forgiving in terms of the amount of data provided: Neither the columns nor the length of the dataset is critical. This makes it possible to continue a previous run, but with one or more variables added. In that case, the initial population is based on the provided data with the newly added variables randomly initialized. If the initial dataset is larger than the population size, the dataset is truncated based on the values in the column mgorank. The **-k** option can be used to force the first generation to use the entire dataset, even if it is larger than the population size. A smaller dataset than population size is appended with random points. The GDFSELECT program can be used to start from a specific generation of a previous run.

The variables and objectives for GDFMGO are read from `infile.sol` file, or any other filename you provide on the command line. It is an ASCII file that must contain all section listed in Table 3-E. A sample `.mgo` file is shown in Listing 3-2.

Table 3-E: Sections in the `.mgo` file and a GDFMGO output description

Section	Section	Description
[OPTIONS]	3.14.1	Sets various options and constants directly related to the algorithm.
[VARIABLES]	3.14.2	Defines the variables to be varied.
[OPTIMIZE]	3.14.3	Defines the constraints to be minimized or maximized.
	3.14.4	Output description of GDFMGO

Listing 3-1: Sample `.mgo` file for GDFMGO.

```

1. # Minimize stdx and maximize stdG by varying Isol1 and Isol2.
2.
3. [OPTIONS]
4. populationsize = 50 ;      # Increase default population size to 50
5. generations = 50 ;        # Decrease default maximum number of generations to 50
6. ignoreerrors = 1 ;        # Interpret errors as bad objectives
7.
8. [VARIABLES]
9. Isol.min = 0 ;            # Variable Isol must be positive
10. Isol.max = 1000 ;         # with max value 1 kA
11.
12. Isol2.min = 0 ;           # Same for Isol2
13. Isol2.max = 1000 ;        #
14. Isol2.startmin = 500 ;    # But we start in the range [500-1000]
15.
16. [OPTIMIZE]
17. stdx.position = 1 ;       # Minimize stdx at z=1 m, requires screen at z=1 m
18. stdx.log = 1 ;            # where log(stdx) is what matters
19.
20. stdG.weight = -1 ;        # Maximize stdG
21. stdG.position = 1 ;       # also at z=1 m

```

### 3.14.1 Options

In the [OPTIONS] section, the following options can be set. The syntax is shown in Table 3-F.

Table 3-F: Options syntax.

Syntax	Required	Default	Description
[OPTIONS]	No		Start of options section.
ignoreerrors	No	0	If set to 1, all error codes are equivalent to an infinitely bad simulation result. The optimization continues and in most cases this works surprisingly well.
populationsize	No	Calculated	Total size of the population
generations	No	100	Maximum number of generations
minfronts	No	2	Minimum number of fronts
minviolatoins	No		Stop when all candidate solutions have less than the given number of constraint violations.
scalefactor	No	0.6	See description in section 1.12.3.1
mutationrate	No	0.9	See description in section 1.12.3.1
dynamicminmax	No	1	See description in section 1.12.3.3 and 3.14.3. Value 1 turns dynamicminmax on.
defaulttime	No		Default time for all objectives
defaultposition	No		Default position for all objectives
printGDFAwarnings	No	1	Print warnings for unsuccessful GDFA progs.

The optimization process is terminated when either the maximum number of generations or the minimum number of fronts is reached.

If not specified, the population size is calculated as  $10 \cdot N_v \cdot (1 + N_o)$ , with  $N_v$  the number of variables and  $N_o$  the number of objectives. In many cases this is a rather safe setting and the same solution can be reached more efficiently by reducing the population size.

This **minviolations** option can be used to bootstrap the optimisation with quick-and-dirty simulations that focus on getting all variables into the correct range. It is particularly effective when many of the initial runs give very poor results or don't run to completion at all. The rationale using this option is that in most cases the initial variables are so far off that the first runs are not an optimisation, but elimination of variable space. As long as not all constraints are met almost all evolutionary pressure is applied into the direction of getting all variables into acceptable range. This process does not require very precise simulations: It makes no sense to calculate one run with very high precision when it is internally compared to a run that fails to be within any of the constraints. This option allows elimination of variable space using less-precise simulations (no space charge, few hundred particles, low accuracy), optionally with a rather large population size in order to not miss any of the solutions. The final population can be fed into a subsequent highprecision run using the **-s** option of the optimiser. As a generalisation it is possible to specify a value different from 1. In that case the optimisation process stops when all candidate solutions have less than  $N$  constraint violations.

### 3.14.2 Variables

The [VARIABLES] section defines all variables to be varied. The syntax is shown in Table 3-G. In case an estimate for the optimal values is already known, these can be specified with **startmin** and **startmax** separately from the obligatory **min** and **max** values.

Table 3-G: Variable syntax.

Syntax	Required	Description
[VARIABLES]	Yes	Start of variables section.
<b>var.min = min ;</b>	Yes	Set the lower bound for variable <b>var</b> to <b>min</b> .
<b>var.max = max ;</b>	Yes	Set the upper bound for variable <b>var</b> to <b>max</b> .
<b>var.startmin = min ;</b>	No	Set the lower bound of the initial population to <b>min</b> .
<b>var.startmax = max ;</b>	No	Set the upper bound of the initial population to <b>max</b> .
<b>var.log = 1 ;</b>	No	A value of <b>1</b> indicates that the initial sampling of this variable is linear on a logarithmic scale. A value of <b>-1</b> must be used when all values, i.e. min and max, are negative.
<b>var.cyclic = 1</b>	No	Informs the optimizer that the given <b>var</b> is cyclic.

The usual Differential Evolution (DE) algorithm does not work well for cyclic variables such as rf-phases because candidate solutions near the outer edges of the variable range cannot be successfully combined with the usual equations. The reason is as follows: If we omit crossover from the discussion, a new candidate  $x$  is formed from  $u$ ,  $v$  and  $w$  using:  $x = w + s (u - v)$  where  $s$  is a scale factor to enforce convergence. If  $u$  and  $v$  are at the outer edges of the min-max range, the actual difference is almost zero when cyclicity is taken into account. However, with the above equation it is the full-range multiplied by  $s$  that is added to  $w$ , instead of almost zero. This results in two sub-populations being formed near the min and max values of the variable range. Setting **cyclic** switches the internal algorithm to modulo (max-min) mathematics solving the problem.

Example: Add a variable **phi** that is cyclic in  $[0, 2\pi]$ .

```
[VARIABLES]
phi.min = 0 ;
phi.max = 6.28318530718 ;
phi.cyclic = 1 ;
```

### 3.14.3 Optimize

The [OPTIMIZE] section defines the objective(s) to be minimized/maximized and their boundaries. The syntax is shown in table Table 3-H. All objectives must hold either at a specific **position** or **time**, and this must correspond to a matching **screen** or **tout** line in the GPT inputfile. The sign of the **weight** determines if the objective must be minimized (default) or maximized. Objectives can have **min** and **max** values, and this takes precedence in the ranking procedure. Effectively this means that the optimizer will first try to find settings where all objectives are within their min/max values, and only then will it start the actual multi-objective optimization process.



Table 3-H: Optimize syntax.

Syntax	Required	Description
<b>[OPTIMIZE]</b>	Yes	Start of optimize section.
<b>opt.time = t ;</b> <b>opt.position = p ;</b>	One of these	Specify the time <b>t</b> when function <b>opt</b> must be minimized. Specify the position <b>p</b> where constraint <b>opt</b> must be minimized.
<b>opt.weight = m ;</b>	No	A weight of <b>1</b> instructs the optimizer to minimize this objective while a weight of <b>-1</b> maximizes this objective. Objectives with zero weight are ignored by the optimizer, but the value is written in the outpufile.
<b>opt.log = 1 ;</b>	No	A value of <b>1</b> indicates that the optimal sampling of this objective along the pareto front is equidistant on a logarithmic scale. A value of <b>-1</b> must be used when all values are negative.
<b>opt.min = min ;</b> <b>opt.max = max ;</b>	No No	Objective must be larger than <b>min</b> . Objective must be smaller than <b>max</b> .

Setting **weight=0** makes the objective irrelevant for the final ranking, but **min/max** values for the same objective can be used to filter out unwanted solutions. Furthermore, the constraint will be written in the outpufile for further analysis.

It is possible to have a variable also as objective. For example, if we want to know the tradeoff between the current through a small focusing solenoid and the achievable spotsize, than the current through the solenoid is both a variable (in the GPT inputfile) and an objective (lower current is better). To accomplish this, it is sufficient to repeat the name of the variable in the constraints section with the proper **weight** setting (**1** to minimize, **-1** to maximize). In that case the **min/max** values of the objective are automatically transferred to the variable.

The **min** and **max** constraints have priority in the ranking procedure to get the most selective pressure in the direction of satisfied constraints. Typically this yields an entire population within all constraints in the first few generations. However, priority ranking of the constraints can backfire if the entire population is outside the min/max boundaries in only one of the objectives. In that case, there is a lot of pressure to get all *other* objectives inside their min/max boundaries, but the objective that is the furthest off is virtually ignored. To compensate for this undesired side-effect, the **min/max** boundaries are in that case temporarily adjusted to span at least 25% of the population. This yields balanced selective pressure for all constraints, even if none of the population is within the constraints. This temporary adjustment of the boundaries can be switched off by setting **dynamicminmax=0** in the **[OPTIONS]** part of the inputfile.

If neither **time** or **position** is specified, the **defaulttime** or **defaultposition** is used instead. These can be set in the **[OPTIONS]** section of the inputfile.

### 3.14.4 Output

GDFMGO writes all variables and all objectives of the entire population to the outpufile in separate groups for each generation. The one group that is not labeled with a generation number is the final result, and this is the group that is plotted in GPTwin when opening the outpufile.

The rank of each member of the population and the number of constraint violations are written to the outpufile in the columns **mgorank** and **mgoviolations** respectively. All points closest to the Pareto front have rank zero, the adjacent points have rank one, and so on. It is instructive to make scatterplots color-coded on **mgorank** and/or **mgoviolations** to visually inspect the progress of the optimizer.

### 3.14.5 Technical notes

Not all runs of GDFMGO produce the exact same result, on the contrary. Even when starting from the exact same distribution, spawning different runs on different threads and/or CPUs results in an unpredictable ordering of the results coming in. This slightly randomizes the entire optimization process, potentially producing very different results after many generations. However, each GDFMGO will converge towards a uniformly sampled Pareto front.

It is often expected that with the **-s** option the results of the first generation are an exact copy of the initial data provided. However, because GDFMGO is a load-balanced optimizer, this is hardly ever the case for the following reason: When a few function evaluations, i.e. GPT runs, take a long time to complete, the first

generation is reached before all datapoints in the initial dataset are evaluated. The first generation therefore contains the fastest to calculate variables in the initial dataset combined with a few newly created samples. If the initial dataset is a relatively good initial condition, this shows as a first generation that is very good except for a few strange outliers. The outliers disappear because the remaining datapoints of the initial set will be mixed in with the second, or maybe even later generations.

For performance reasons the constraints could also be read from file when the `-s` option is used to continue from a previous run. This however, is *not* done: The initial variables are read, but the objectives are always newly recalculated. The reason for this is that reading the results from file will be disastrous when in the meantime the GPT inputfile, MR setting or fieldmaps have been modified. Since reading the results from file saves the recalculation of just one generation we decided this is not worth the risk.

It is recommended to add `setrlimit("CPU",N,M) ;` to the GPT inputfile when running the optimizer on large clusters. The reason is that in practice there are always a few GPT runs in an unfortunate parameter regime that take forever to complete, if at all. These runs can be automatically cut with `setrlimit`, saving valuable resources. The above line instructs GPT to attempt not start a new timestep after `N` seconds of CPU time, whereas after `M` seconds the program is hard-terminated by the underlying operating system no matter what.

On large clusters it is sometimes difficult to set path environment variables. One of the approaches is to copy all executables into the same directory as the inputfiles, and use `./gpt` on the command line in combination with `-g ./gdfa`. For us it solved a problem, although we realize that there are much more elegant solutions available.

### 3.15 GDFSELECT

**gdfselect** [-hHvkr] [-o outfile] infile.gdf groupname [value | begin end]

Select a specific group by fixed value or with a range of values from another GDF file.

<b>-o outfile</b>	Write output to a file named <b>outfile</b>
<b>-a outfile</b>	Append output to a file named <b>outfile</b>
<b>-h</b>	Give short help and quit.
<b>-H</b>	Give long help and quit.
<b>-v</b>	Verbose mode.
<b>-k</b>	Do not collapse hierarchy on single-value selection.
<b>-r</b>	Reverse selection criteria.
<b>groupname</b>	Name of the group to be selected.
<b>value</b>	Select a single value.
<b>begin end</b>	Select a range of values.

GDFselect can be used to create a GDF file containing a subset of the groups present in another GDF file. It can for example be used to select a subset of a GDF file for further processing, reduce file size by removing unneeded information, or prepare initial conditions for GDFMGO by selecting which generation of a previous run to start from. Selection is based on **groupname** that must either have the specified **value** or a value that falls in the **begin end** range, endpoints included. For example, to convert time output at 1 ns from a GPT simulation to ASCII, the following commands can be given (assuming GPT produces output at 1 ns by a **tout(1e-9)** line):

```
gdfselect -o output_1ns.gdf gpt_output.gdf time 1e-9
gdf2a -o output_1ns.txt output_1ns.gdf
```

Selecting a range between 1 and 5 ns is also possible:

```
gdfselect -o ouput_1to5ns.gdf gpt_output.gdf 1e-9 5e-9
```

Despite its name, **gdfselect** actually removes information when anywhere in the hierarchy the specified **groupname** is present with a value or range outside the given criteria. You essentially specify what to remove, not what to keep. This implies that all information remains where the given groupname is not present all. Consequently, specifying a range for time output, such as **time -1e100 +1e100** will *not* remove the position output from a GPT simulation result that contains both time and position output. However, specifying a bogus value for the position output will remove all position output while keeping all time output:

```
gdfselect -o time_output.gdf combined_output.gdf position -1e100
```

It is possible to run **gdfselect** iteratively on the output of **gdfselect**. This is useful when dealing with more complicated hierarchies created by the **mx** program, but also when selecting a subset of the time output from a simulation result that contains both time and position output.

When only a single **value** is specified, the entire group is removed from the hierarchy unless the **-k** option is specified. The selection criteria can be reversed using the **-r** option.

### 3.16 GDFSOLVE

**gdfsolve** [-hHv] [-o outfile] infile.sol program [parameters]

Multidimensional solver for the specified program

**-o outfile** Write output to a file named **outfile**  
**-a outfile** Append output to a file named **outfile**  
**-h** Give short help and quit.  
**-H** Give long help and quit.  
**-v** Verbose mode. Display iteration output containing all variables and constraints.  
**infile.sol** Name of the file containing information about the parameters that are to be varied and the constraints to be met. See Table 3-I for specific sections in this file.  
**program [parameters]** Command line of a program that creates a GDF file and recognizes the **-o** option, for example GPT.

GDFSolve can be used to polish off a solution, based on a good initial estimate. The primary method used is based on multidimensional Newton-Raphson, providing quadratic convergence in the vicinity of a solution. GDFSolve can also be used as multidimensional optimizer, but this feature is less useful as it is far less efficient and sensitive to local minima and simulation noise.

Table 3-I: Sections in the .sol file and a GDFSolve output description

Section	Section	Description
[OPTIONS]	3.16.1	Sets various options and constants directly related to the algorithm.
[VARIABLES]	3.16.2	Defines the variables to be varied.
[CONSTRAINTS]	3.16.3	Defines the constraints to be met.
[OPTIMIZE]	3.16.4	Defines the constraints to be minimized or maximized.
	3.16.5	Output description of GDFSolve

Information about the internal algorithms of GDFSolve can be found in sections 1.12.1 to 1.12.2. A sample .sol file without an optimize section is shown in Listing 3-2.

Listing 3-2: Sample .sol for GDFSolve: Find Isol resulting in an avgr of 1 mm.

```
22. # Solve average beam radius (avgr) = 1 mm by varying Isol.
23.
24. [OPTIONS]
25. backtracking = 0 ;
26.
27. [VARIABLES]
28. Isol = 1000 ;           # Define variable to vary, starting value is 1000
29. Isol.reldelta = 0.01 ;  # Use 1% difference to obtain derivative information
30. Isol.min = 0 ;         # Isol must be positive
31.
32. [CONSTRAINTS]
33. avgr = 1.0e-3 ;        # avgr must be 1 mm
34. avgr.pos = 1 ;         # at z=1 m
35. avgr.abstol = 0.1e-3 ;  # with a tolerance of +/- 0.1 mm
```

### 3.16.1 Options

In the [OPTIONS] sections, the following options can be set. The syntax is shown in Table 3-J.

Table 3-J: Options syntax.

Syntax	Required	Default	Description
[OPTIONS]	No		Start of options section.
<b>forcejacobian = 1 ;</b>	No	Depends	Forces a full Jacobian matrix to be calculated after each successful step. When not specified, Broydens' update method is used when the number of variables is less or equal than the number of constraints, see section 1.12.1.5.
<b>SVDtolerance = tol ;</b>	No	0.001	Ratio between the largest and smallest Singular Value. When the ratio is smaller than <b>tol</b> , the corresponding direction is dropped.
<b>minconvergence = a ;</b>	No	0.01	Every step must bring the scaled constraints (1- <b>a</b> ) closer to the solution. When this criterion can not be met, GDFSolve terminates with an error.
<b>backtracking = 0 ;</b>	No	1	Disable the backtracking algorithm and terminate with an error when <b> F </b> increases.
<b>keepgoing = 1 ;</b>	No	0	Disable all termination criteria and keep running until the executable is forced to stop externally. Using this option is not recommended for inexperienced users.
<b>optimizetolerance = tol ;</b>	No	0.05	The optimizer stops iterating when the target scaled rms value does not change more than <b>tol</b> .
<b>ignoreerrors = 1 ;</b>	No	0	Assume all error codes from GPT and GDFA to be a very bad simulation result. Please use with care.

### 3.16.2 Variables

The [VARIABLES] section defines all variables to be varied. The syntax is shown in Table 3-K.

Table 3-K: Variable syntax.

Syntax	Required	Description
[VARIABLES]	Yes	Start of variables section.
<b>var = x ;</b>	Yes	Defines a new variable named <b>var</b> , with initial estimate <b>x</b> .
<b>var.absdelta = abs ;</b> <b>var.reldelta = rel ;</b>	At least one	The absolute scaling of variable <b>var</b> is <b>abs</b> . The relative scaling of variable <b>var</b> is <b>rel</b> . The total scaling is defined as: $dx = \pm\sqrt{abs^2 + x^2 \cdot rel^2}$ .
<b>var.min = lb ;</b>	No	Variable lower bound for variable <b>var</b> is <b>lb</b> .
<b>var.max = ub ;</b>	No	Variable upper bound for variable <b>var</b> is <b>ub</b> .

The scaling **delta** is important for the internal algorithms of GDFSolve because the derivative of all constraints is approximated by taking steps larger or equal to **delta**. As a result, a too small **delta** is very sensitive to simulation noise caused by a too low accuracy setting or insufficient particles in the simulation. On the other hand, a too large **delta** could send the derivative approximation into the non-linear regime. Before GDFSolve is used, we recommended first making a scan over a number of **delta**'s and plotting every constraint.

### 3.16.3 Constraints

The [CONSTRAINTS] section defines all constraints to be met simultaneously. The syntax is shown in Table 3-L.

Table 3-L: Constraints syntax

Syntax	Required	Description
[CONSTRAINTS]	No	Start of constraints section.
<b>con</b> = <b>ft</b> ;	Yes	Define a new constraint named <b>con</b> to have target value <b>ft</b> .
<b>con.time</b> = <b>t</b> ; <b>con.position</b> = <b>p</b> ;	One of these	Specify the time <b>t</b> when constraint <b>con</b> must be met. Specify the position <b>p</b> where constraint <b>con</b> must be met.
<b>con.abstol</b> = <b>abs</b> ; <b>con.reltol</b> = <b>rel</b> ;	At least one	The absolute tolerance of constraint <b>con</b> is <b>abs</b> . The relative tolerance of constraint <b>con</b> is <b>rel</b> . The total tolerance is defined as: $df = \sqrt{abs^2 + ft^2 \cdot rel^2}$ .

The geometric length of all scaled constraints  $|\mathbf{F}|$  is given by:

$$|\mathbf{F}| = \sqrt{\sum \left( \frac{\mathbf{con} - \mathbf{ft}}{df} \right)^2} \quad [3.14]$$

A solution is found when  $|\mathbf{F}| \leq 1$ . Apart from the termination criterion, the tolerance is also used in the internal algorithms of GDFSolve as the inverse weight of the constraints.

When an identical constraint must be used at different times or locations, the **con** name can be prepended with **group**: notation. For example, the following section makes the average beam radius 3 mm at z=1 m and 2 mm at z=2 m. The tolerance is set to 0.1 mm in both cases.

```
[CONSTRAINTS]
a:avgr = 3.0e-3 ;
a:avgr.position = 1.0 ;
a:avgr.abstol = 0.1e-3 ;
```

```
b:avgr = 2.0e-3 ;
b:avgr.position = 2.0 ;
b:avgr.abstol = 0.1e-3 ;
```

### 3.16.4 Optimize

The [OPTIMIZE] section defines the function(s) to be minimized. The syntax is shown in Table 3-M.

Table 3-M: Optimize syntax.

Syntax	Required	Description
[OPTIMIZE]	No	Start of optimize section.
<b>opt</b> = <b>ft</b> ;	Yes	Define a new function named <b>opt</b> with approximate minimum <b>ft</b> .
<b>opt.time</b> = <b>t</b> ; <b>opt.position</b> = <b>p</b> ;	One of these	Specify the time <b>t</b> when function <b>opt</b> must be minimized. Specify the position <b>p</b> where constraint <b>opt</b> must be minimized.
<b>opt.abstol</b> = <b>abs</b> ; <b>opt.reltol</b> = <b>rel</b> ;	At least one	The absolute tolerance of function <b>opt</b> is <b>abs</b> . The relative tolerance of function <b>opt</b> is <b>rel</b> . The total tolerance is defined as: $df = \pm \sqrt{abs^2 + ft^2 \cdot rel^2}$ .
<b>opt.weight</b> = <b>m</b> ;	No	Defines the weight of the constraint. When not specified 1 is assumed. A negative value must be specified to maximize a function.

When more than one function and/or additional constraints are specified, GDFSolve tries to minimize:

$$f = |\mathbf{F}| + \sum m \frac{opt}{df} \quad [3.15]$$

A negative weight parameter can be used to maximize a function.

### 3.16.5 Output

GDFSolve writes output when all constraints are met and/or when a minimum has been found. Without a solution, there is no output. The outputfile itself contains the settings of all variables and the values of the corresponding constraints, followed by the complete output of the successful GPT run. All variables and constraints can be inspected using GDF2A.

The output of GDFSolve can also be analyzed with GDFA like the output of a normal GPT run. Furthermore, the MR utility can be used in combination with GDFSolve. This solves for identical constraints as function

of a scanned parameter. This construction builds an outputfile of all successful GPT runs as function of the scanned parameter. GDFA can be used to analyze these results.

When the **-v** option is specified, GDFSolve writes iteration output to the messages window. It consists of the following columns:

<b>N</b>	The iteration number.
<b>varN</b>	Value of the N'th variable.
<b>conN</b>	Value of the N'th constraint to be solved. This value is followed by the scaled F value, the number of tolerances off the target, between parentheses. When for example <b>con1</b> has a value of 10, a target of 4 and a delta of 1, the display will be 10(6) indicating that the constraint is 6 tolerances off its desired value.
<b>optN</b>	Value of the N'th function to minimize. This value is followed by the scaled result, the number of tolerances off the estimated minimum times the weight, between parentheses. When for example <b>opt1</b> has a value of 10, an estimated minimum of 4 and a delta of 1, the display will be 10(6) indicating that the value is expected to drop 6 tolerances.
<b>rms</b>	When GDFSolve is used as root finder, the rms value is the vector length of F, the scaled distance from a solution. When GDFSolve is used as optimizer, the scaled results of the functions to minimize are added to this value.

Only the differences in variables and constraints are displayed when the root finder is calculating the Jacobian as indicated by a J following the iteration number.

### 3.17 GDFTRANS

**gdftrans** [-hHv] [-s **array**] [-o **outfile**] [-a **outfile**] **infile** **group\_by** **arrays** ...

Transpose a GDF file to calculate trajectories as function of any parameter.

<b>-h</b>	Give short help and quit.
<b>-H</b>	Give long help and quit.
<b>-v</b>	Verbose mode.
<b>-s array</b>	Sort by <b>array</b> . Default set to array "ID".
<b>-o outfile</b>	Write output to outfile.
<b>-a outfile</b>	Append output to outfile.
<b>infile</b>	Name of the file to perform the calculations on. When GDFTRANS has to read from <b>stdin</b> , a dash (-) must be specified explicitly for infile.
<b>group_by</b>	The name of the variable used to group the data.
<b>arrays ...</b>	The name(s) of one or more arrays to convert. Typically these are <b>x y z Bx By Bz</b> and <b>G</b> .

GDFTRANS can be used to obtain particle trajectories by transposing a GDF file. For example to obtain the arrays of the x- and z-coordinates for all individual particles as function of time, the following command can be specified:

```
GDFTRANS -o outfile.gdf infile.gdf time x z
```

By default the arrays are sorted by an additional array named ID, containing the actual numbering. GPT writes the particle number in array ID to allow trajectory plots to be created. An alternative array can be specified using the **-s** option and the array index is used when the ID array is not present.

Apart from the **group\_by** variable, the hierarchy in the GDF File is preserved by GDFTRANS.



### 3.18 MR

```
mr [-hHvn] [-j nCPU] [-o outfile] [-a outfile] mrfile gpt [-j 1] [options]
```

or

```
mpirun [options] mr [-hHvn] [-o outfile] [-a outfile] mrfile program [options]
```

Scan one or more parameters and concatenate the output in a single hierarchical file.

```
-o outfile    Write output to a file named outfile.
-a outfile    Append output to a file named outfile.
-h           Give short help and quit.
-H          Give long help and quit.
-j nCPU      Run simultaneously over nCPU cores. If not specified, all cores in the system are used.
-v          Verbose mode. Echo the commands to the terminal as they are run.
-n          Display commands but do not actually run them.
mrfile       Name of the file containing information about the parameter(s) that are to be set or varied.
              It must be an ASCII-file with one or more lines each with the following syntax:
              param value
              or
              param from to step
              Lines beginning with # are ignored.
program [options]  Command line of a program to be run that creates a GDF file.
```

When the effect of one parameter in a simulation is to be studied, MR can be used to automate this process. The steps needed to use MR are:

- Give the parameter of interest a symbolic name in the inputfile instead of a value. For example the phase of a prebuncher could be named **phi**.
- Create a MR file containing information about the varying parameter. It consists of lines with the name of the varying parameter followed by either a **value** or a **from to step** specification. For example the following columns are equivalent and they can all be used to scan **phi** in the range from 0.4 to 0.7.

<b>phi</b> 0.4 <b>phi</b> 0.5 <b>phi</b> 0.6 <b>phi</b> 0.7	<b>phi</b> 0.4 0.7 0.1	<b>phi</b> 0.4 0.6 0.1 <b>phi</b> 0.7
--	------------------------	--

- Run MR using the syntax specified above. For example:  

```
mr -o result.gdf phi.mr gpt inputfile.in
```

 runs GPT with varying **phi**, where **phi.mr** is one of the files above and **inputfile.in** is a valid simulation inputfile containing **phi**.

MR can be used to efficiently group all parameters of interest into a single file. If, for example, not only **phi** is a parameter of interest, but also **len**, **amp** and **theta**, the following **scan.mr** file sets these additional parameters for varying **phi**.

```
1. # MR file for varying phi
2. phi 0.4 0.7 0.1
3.
4. # Fixed len, amp and theta
5. len 10
6. amp 1
7. theta 5
```

Multidimensional scans are easily created by specifying a range of values for two (or more) parameters. To run the above scan for three different values of **len**, the following **scan.mr** file will start the required 12 runs.

```

1. # MR file for varying phi and len
2. phi 0.4 0.7 0.1
3. len 10
4. len 12
5. len 15
6.
7. # Fixed amp and theta
8. amp 1
9. theta 5

```

In the case of multidimensional scans, the **group\_by** parameter of the GDFA program can be used to create plots with any varying parameter along the horizontal (or vertical) axis. For example:

```

1. mr -o result.gdf scan.mr gpt infile.in
2. gdfa -o avgs_as_function_of_phi.gdf result.gdf phi ...
3. gdfa -o avgs_as_function_of_len.gdf result.gdf len ...

```

### 3.18.1 Multi-core / MPI usage

On a single system, MR runs as many parallel jobs as there are cores on the system. The MPI version of MR launches runs on different physical machines using **mpirun**. In both cases, the output of all jobs is stored in temporary files and subsequently concatenated into **outfile** in the correct order. Load balancing is achieved by initially feeding all cores/nodes one job and assigning new jobs when the previous run is finished. This allows different runs to use a different amount of CPU time to complete without degrading performance. However care should be taken that the running program does not spawn new threads in an attempt to increase calculation speed. This will work counter-productively in almost all cases because the course-grain multithreading by MR will typically outperform fine-grain multithreading of the running program. Consequently, when MR is used to run GPT and when the total number of MR runs far exceeds the number of cores/nodes we strongly recommend including **-j 1** in the GPT commandline. For example:

```
[mpirun -n N] mr -o result.gdf huge_scan.mr gpt -j 1 file.in
```

The MPI version of MR reserves the first node for communication, spawning new processes and concatenating the temporary outputfiles. As these tasks consume virtually no CPU time, one usually also wants to also run an extra simulation job on the first machine. For example, to run on **apple**, **pear** and **berry**, where each machine runs six copies of GPT in parallel, the following command may be used:

```
mpirun -hosts 3 apple 7 pear 6 berry 6 mr -o result.gdf scan.mr gpt -j 1
file.in
```

To be able to use the MPI version of MR all executables must be in the search path of all machines. On large clusters we found that this is often a nightmare with PATH environment variables. As a simple alternative, specifying full pathnames seems to work almost everywhere.

### 3.19 RAW2GDF

**raw2gdf** [-hHved] [-o outfile] [-a outfile] **infile** **arr1** **fac1** [**arr2** **fac2**] ...

Raw binary file to GDF converter.

<b>-h</b>	Give short help and quit.
<b>-H</b>	Give long help and quit.
<b>-v</b>	Verbose mode. Progress and file statistics are shown.
<b>-e</b>	Convert endian format. This is typically needed when RAW2GDF is run on a non-intel Linux machine and <b>infile</b> was generated on a PC, or vice versa.
<b>-d</b>	Specify when data is given in double-precision numbers.
<b>-o outfile</b>	Write output to <b>outfile</b> .
<b>-a outfile</b>	Append output to <b>outfile</b> .
<b>infile</b>	Name of the binary file to be converted.
<b>arr1</b>	Name of the array as it is to be specified in the outputfile.
<b>fac1</b>	Multiplication factor for <b>arr1</b> .
<b>...</b>	Specify all arrays present in <b>infile</b> with their conversion factor.

RAW2GDF converts a binary file to a GDF file. The resulting GDF file can be read by the field map elements and all GPT utility programs capable of handling GDF files. For example, to test if the resulting file is correct GDF2A can be used.

RAW2GDF writes the columns in the outputfile specified by the **arr** parameters. These column names should be specified in all subsequent handling of the GDF file. To allow conversion to SI units, the arrays are multiplied by their corresponding multiplication factors: **fac**. A **fac** of **1** must be specified if the array is already in SI units. When **fac** is specified to be **0**, the corresponding column is not written in the outputfile.

When a raw data file is generated on a PC, but converted using RAW2GDF on a big-endian (typically a non-intel Linux) machine, the **-e** option must be specified. This is also the case when a raw data file generated on a big-endian machine must be converted on a PC. Because GDF files are machine independent, a GDF file from any Linux machine can be used without conversion on a PC and vice versa (if transferred in binary format).

Note: All arrays present in the binary file must be specified on the RAW2GDF commandline, whether they are relevant or not.



## 4 GPT Reference

This chapter serves as a reference of the simulation variables, keywords and elements. It is not recommended for first reading. The inputfile syntax, operator precedence and predefined constants are provided in section 4.1.

4.1	Inputfile syntax.....	120
4.2	Initial particle distribution .....	123
4.3	Timestep and output control.....	139
4.4	Accelerating structures .....	147
4.5	Static electric fields .....	155
4.6	Static magnetic fields .....	159
4.7	Field maps .....	174
4.8	Spacecharge.....	188
4.9	Scattering.....	203
4.10	Remove particles .....	210
4.11	Miscellaneous.....	212
4.12	Free Electron Laser (FEL), Wakefields, and CSR .....	216
4.13	Obsolete elements.....	223

If necessary, you can also write your own element or modify an existing one. How this is done is explained in the GPT Programmer's Reference.

## 4.1 Inputfile syntax

A GPT inputfile is an ASCII file describing the set up that is to be simulated. This section is a reference for the inputfile language. For information on how to write your own GPT inputfiles, we refer to the tutorial (chapter 2).

A YACC generated parser is used to handle the expressions, if-statements, functions and variables that can be used in the GPT inputfile. YACC uses a specified grammar and operator precedence and generates code to parse the inputfile accordingly. The grammar is chosen to be very close to the standard C expression language with the addition of string concatenation using the + operator. Tables of built-in constants, operator precedence and built-in functions are given at the end of this section.

A GPT inputfile is defined as follows:

<b>inputfile</b>	An ASCII file containing a <b>statementlist</b> . All blanks, tabs, new lines and everything following the character # till the end of the line are ignored.
<b>statementlist</b>	One or more <b>statements</b> .
<b>statement</b>	One of the following: <b>variable = value ;</b> <b>variable = string ;</b> <b>keyword( parameters ) ;</b> <b>if(condition) statement [else statement]</b> <b>{ statementlist }</b>
<b>variable</b>	Sequence of letters and digits, not starting with a digit. Built-in and previously assigned constants can be set to a new value. This is generally not advisable and a warning is printed.
<b>value</b>	A floating point number, a built-in constant or a formula in standard notation. The formula may contain floating point numbers, built-in constants, user-defined variables and functions.
<b>keyword</b>	Any of the keywords listed in chapter 3.
<b>parameters</b>	One or more <b>values</b> or <b>strings</b> separated by commas.
<b>string</b>	Anything enclosed by double quotation marks.

Table 4-A: Operators in decreasing order of precedence. Their associativity indicates in what order operators of equal precedence in an expression are applied.

Symbol	Description	Associativity
()	Parenthesis (grouping)	Left-to-right
!	Factorial	Right-to-left
+, -	Unary plus, minus	
^	Exponential, right associative	Right-to-left
*, /	Multiplication, division	Left-to-right
+, -	Value: Addition, subtraction	Left-to-right
<, <=	Relational less than/less than or equal to	Left-to-right
>, >=	Relational greater than/greater than or equal to	Left-to-right
!=, ==	Relational is not equal to/is equal to	Left-to-right
and, &&	Logical AND	Left-to-right
or,	Logical OR	Left-to-right
? :	Ternary conditional	Right-to-left
=	Assignment	Right-to-left

Table 4-B: Built-in constants.

Name	Value	Description
<b>c</b>	299792458	Speed of light
<b>deg</b>	$180/\pi$	Conversion factor from radians to degrees
<b>e</b>	2.71828182845904523536	e
<b>eps0</b>	$1/\mu_0 c^2$	Permittivity of vacuum: $\epsilon_0$
<b>m</b>	Default: <b>me</b>	Mass of an elementary particle
<b>ma</b>	$1.66057 \cdot 10^{-27}$	Unified mass constant
<b>me</b>	$9.10953 \cdot 10^{-31}$	Mass of an electron
<b>mp</b>	$1.67265 \cdot 10^{-27}$	Mass of a proton
<b>mu0</b>	$4\pi \cdot 10^{-7}$	Permeability of vacuum: $\mu_0$
<b>pi</b>	3.14159265358979323846	$\pi$
<b>q</b>	Default: <b>qe</b>	Charge of an elementary particle
<b>qe</b>	$-1.6021892 \cdot 10^{-19}$	Charge of an electron

Table 4-C: Built-in functions.

Name	Description
<b>defined(x)</b>	TRUE if <b>x</b> is defined, FALSE otherwise
<b>sin(x)</b>	sine of <b>x</b>
<b>cos(x)</b>	cosine of <b>x</b>
<b>tan(x)</b>	tangent of <b>x</b>
<b>asin(x)</b>	$\sin^{-1}(\mathbf{x})$ in range $[-\pi/2, \pi/2]$ , $\mathbf{x} \in [-1, 1]$
<b>acos(x)</b>	$\cos^{-1}(\mathbf{x})$ in range $[0, \pi]$ , $\mathbf{x} \in [-1, 1]$
<b>atan(x)</b>	$\tan^{-1}(\mathbf{x})$ in range $[-\pi/2, \pi/2]$
<b>sinh(x)</b>	hyperbolic sine of <b>x</b>
<b>cosh(x)</b>	hyperbolic cosine of <b>x</b>
<b>tanh(x)</b>	hyperbolic tangent of <b>x</b>
<b>asinh(x)</b>	Area (inverse) hyperbolic sine of <b>x</b>
<b>acosh(x)</b>	Area (inverse) hyperbolic cosine of <b>x</b>
<b>atanh(x)</b>	Area (inverse) hyperbolic tangent of <b>x</b>
<b>log(x)</b>	Natural (base-e) logarithm of <b>x</b> .
<b>log10(x)</b>	Common (base 10) logarithm of <b>x</b> .
<b>log2(x)</b>	Binary (base-2) logarithm of <b>x</b>
<b>log1p(x)</b>	High precision version of <b>log(1+x)</b> for small <b>x</b>
<b>exp(x)</b>	Base-e exponential of <b>x</b>
<b>exp2(x)</b>	Base-2 exponential of <b>x</b>
<b>expm1(x)</b>	High precision version of <b>exp(x) - 1</b> for small <b>x</b>
<b>sqrt(x)</b>	$\sqrt{\mathbf{x}}$ , $\mathbf{x} \geq 0$
<b>cbrt(x)</b>	$\mathbf{x}^{1/3}$
<b>abs(x)</b> , <b> x </b>	$ \mathbf{x} $
<b>ceil(x)</b>	Smallest integer <sup>2</sup> not less than <b>x</b>
<b>floor(x)</b>	Largest integer <sup>2</sup> not greater than <b>x</b>
<b>round(x)</b>	Integer nearest to <b>x</b>
<b>trunc(x)</b>	Round <b>x</b> towards zero
<b>erf(x)</b>	Error function $\frac{1}{\sqrt{\pi}} \int_0^x e^{-t^2} dt$
<b>erfc(x)</b>	Complimentary error function <b>1-erf(x)</b>
<b>gamma(x)</b>	Gamma function of <b>x</b>
<b>lgamma(x)</b>	Natural logarithm of the absolute value of the Gamma function of <b>x</b>
<b>random(...)</b>	Pseudorandom number number with parameters given in Table 1-C.

Pseudorandom number support is provided through the **random** function, where available parameters are given in the 1D column of Table 1-C on page 19. For example **random("u", 0, 1)** creates a pseudorandom number from a uniform distribution centered around 0 having a total width of 1.

<sup>2</sup> Please note that **ceil(-pi)=-3** and **floor(-pi)=-4**

The GPT inputfile parser has limited support for string operations. The table below gives the basic functionality.

Table 4-D: String functions

Name	Description
<b>getenv(s)</b>	Returns the environment variable <b>s</b> as a string. An error is printed when environment variable <b>s</b> does not exist.
<b>(a + b)</b>	Concatenate string <b>a</b> and <b>b</b>
<b>string(n)</b>	Returns number <b>n</b> as a string.
<b>string(n, f)</b>	Returns number <b>n</b> as a string in specified format <b>f</b> . The format is interpreted as C-style printf notation, for example "%.15e" will return a number in exponential notation with 15 digits precision.
<b>number(s)</b>	Convert string <b>s</b> to a number. An error is printed when <b>s</b> is not a number.



## 4.2 Initial particle distribution

The following elements can be used to specify the initial particle distribution. More information can be found in the corresponding tutorial sections 2.9 and 2.10.

4.2.1	Set manipulation.....	123
4.2.1.1	SetParticles.....	123
4.2.1.2	SetFile .....	124
4.2.1.3	SetScale .....	125
4.2.1.4	SetTransform.....	125
4.2.1.5	SetExtrapolate .....	125
4.2.1.6	SetMove .....	126
4.2.1.7	SetCopy .....	126
4.2.1.8	SetCurvature.....	126
4.2.1.9	SetTCopy .....	127
4.2.1.10	SetShuffle.....	128
4.2.1.11	SetReduce.....	128
4.2.1.12	SetRmacrodist .....	129
4.2.1.13	SetStartPar.....	129
4.2.1.14	SetStartLine.....	129
4.2.1.15	SetStartxyzGrid.....	130
4.2.2	X, Y and Z manipulators .....	130
4.2.2.1	AddZoscillation.....	130
4.2.2.2	SetXdist .....	131
4.2.2.3	SetXYdistbmp .....	131
4.2.2.4	SetYdist .....	132
4.2.2.5	SetZdist .....	133
4.2.2.6	SetRxydist (2D).....	133
4.2.2.7	SetPhidist .....	133
4.2.2.8	SetEllipse .....	133
4.2.3	GBx, GBy and GBz manipulators .....	133
4.2.3.1	AddGoscillation .....	133
4.2.3.2	SetGBxdist .....	134
4.2.3.3	SetGBydist .....	134
4.2.3.4	SetGBzdist .....	134
4.2.3.5	SetGBrxydist (2D) .....	134
4.2.3.6	SetGBphidist .....	135
4.2.3.7	SetGBthetadist (2D spherical) .....	135
4.2.3.8	SetGdist .....	135
4.2.3.9	SetGBxemittance .....	135
4.2.3.10	SetGByemittance .....	136
4.2.4	X-GBx, Y-GBy and Z-G manipulators .....	136
4.2.4.1	AddGzoscillation .....	136
4.2.4.2	AddXDiv .....	137
4.2.4.3	AddYDiv .....	137
4.2.4.4	AddZDiv .....	137
4.2.5	Time-dependent particle distributions.....	138
4.2.5.1	SetTdist .....	138

### 4.2.1 Set manipulation

The following keywords perform an action on an entire particle set.

#### 4.2.1.1 SetParticles

**setparticles (set, N, m, q, Qtot) ;**

Create a particle set with a specified number of particles.

<b>set</b>	Name of particle set to create.
<b>N</b>	Number of particles in this set.
<b>m</b>	Mass of elementary particle in this set [kg].
<b>q</b>	Charge of elementary particle in this set [C].
<b>Qtot</b>	Total charge of all particles in this set [C].

The total charge  $Q_{tot}$  is uniformly distributed among the particles: The number of elementary particles every macro-particle represents is given by:

$$n = \frac{Q_{tot}}{Nq}$$

One of the space-charge elements as described in section 4.8 must be used to include space-charge calculations. Otherwise, the  $Q_{tot}$  parameter is ignored.

#### 4.2.1.2 SetFile

**setfile(set, filename) ;**

Read a complete particle distribution from a GDF file.

**set**                      Name of particle set to generate.  
**filename**                Name of the GDF file containing the particle coordinates.

This element reads a macro-particle distribution from **filename** into the specified particle **set**. All particles are set relative to 'wcs'. The file can be created using **ascii2gdf** or an outputfile of a previous GPT run can be specified. The GDF File must contain at least the following arrays:

**x**                        Particle  $x$ -coordinates [m]  
**y**                        Particle  $y$ -coordinates [m]  
**z**                        Particle  $z$ -coordinates [m]  
**GBx**                    Particle normalized  $x$ -momentum:  $p_x/mc$ .  
**GBy**                    Particle normalized  $y$ -momentum:  $p_y/mc$ .  
**GBz**                    Particle normalized  $z$ -momentum:  $p_z/mc$ .

Instead of the momentum coordinates, it is also possible to specify the velocity components:

**Bx**                        Particle normalized  $x$ -velocity:  $v_x/c$ .  
**By**                        Particle normalized  $y$ -velocity:  $v_y/c$ .  
**Bz**                        Particle normalized  $z$ -velocity:  $v_z/c$ .

Optionally, the following arrays can be present:

**t**                        Release time of the particle [s]. Use this column to set the initial temporal distribution. If this column is not present, all particles start at  $t=0$ .  
**G**                        Particle Lorentz factor. If not specified, the Lorentz factor is calculated from:  

$$G = 1/\sqrt{1 - (Bx^2 + By^2 + Bz^2)}$$
. Explicitly specifying **G** slightly improves the numerical accuracy of the calculations, but this effect is only noticeable when  $G > 10^6$ .  
**m**                        Mass of the elementary particles this macro-particle represents. Default: See below.  
**q**                        Charge of the elementary particles this macro-particle represents. Default: See below.  
**nmacro**                Number of elementary particles this macro-particle represents. Default: 0.  
**rmacro**                Typical radius of this macro-particle. See the space-charge elements for a detailed description of this parameter. Default: 0.

The mass and charge of the elementary particles can be specified as separate arrays. When these are not present, the user-defined variables **m** and **q** are read from the inputfile. When also these are not specified, the mass and charge of an electron are used. To start protons, without specifying their mass and charge in **m** and **q** columns, the following lines could be used:

```
1. m = mp ;
2. q = -qe ;
3. setfile("protons", "file.gdf") ;
```

If the file is a GPT outputfile created with a **tout(t) ;** statement, this group must be specified by a **time=t ;** statement above **setfile**. Outputfiles created by MR can also be used. Either use MR again with exactly the same parameter sweep or specify **var=value** above **setfile** to specify which group has to be used. Listing 4-3 and Listing 4-2 show an example how to start particles from a previous GPT run.

Listing 4-1: **file1.in**: First inputfile writing output at  $t=1$  ns to **file1.gdf**

```
1. setparticles("beam",1000,10*me,10*qe,Qtot) ;
2. setrxydist("beam","u",1,2) ;
3. setphidist("beam","u",0,2*pi) ;
4. ...
5. tout(1e-9) ;
```

Listing 4-2: **file2.in**: Second inputfile, reading the particle coordinates from **file1.gdf**

```
1. time=1e-9 ;
2. setfile("beam", "file1.gdf" ) ;
3. ...
4. tout(2e-9) ;
```

#### 4.2.1.3 SetScale

**setscale(set,x,y,z,GBx,GBy,GBz,[t,[nmacro,rmacro]]) ;**  
Multiplies all initial particle coordinates by a specified constant

<b>set</b>	Particle set
<b>x</b>	Scale factor for the $x$ -coordinates
<b>y</b>	Scale factor for the $y$ -coordinates
<b>z</b>	Scale factor for the $z$ -coordinates
<b>GBx</b>	Scale factor for the $\gamma\beta_x$ -coordinates
<b>GBy</b>	Scale factor for the $\gamma\beta_y$ -coordinates
<b>GBz</b>	Scale factor for the $\gamma\beta_z$ -coordinates
<b>t</b>	Optional scale factor for the release times
<b>nmacro</b>	Optional scale factor for the number of elementary particles
<b>rmacro</b>	Optional scale factor for the macro particle radius

This element multiplies all initial particle coordinates in a set by a specified constant. It is particularly useful to scale the initial coordinates read from an external file with **setfile**.

Example: If, for example, the file **particles.gdf** has  $x$ ,  $y$  and  $z$ -coordinates in [mm], they can be converted to [m] as follows:

```
1. mm=1e-3 ;
2. setfile("beam","particles.gdf") ;
3. setscale("beam",mm,mm,mm,1,1,1) ;
```

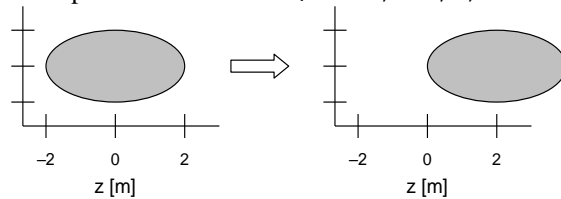
#### 4.2.1.4 SetTransform

**settransform(ecs,set) ;**  
Apply a coordinate transform on the particles in a set.

<b>ECS</b>	Transform specification.
<b>set</b>	Name of particle set.

The particle coordinates are modified according to the specified **ECS**. When the **ECS** specification transform does not start with "**wcs**", all particles are moved to the specified **CCS**. In that case only local and global elements specified relative to the same **CCS** will affect the particle trajectories.

Example: **settransform("wcs","z",2, "set") ;**



#### 4.2.1.5 SetExtrapolate

**setextrapolate(set,time) ;**  
Linearly extrapolate the initial particle distribution to a given time

**set**                      Name of the particle set  
**time**                    Desired time [s]

This element modifies the position coordinate of all particles in the specified **set** by linearly extrapolating them to the specified **time**. The equations applied are:

$$\mathbf{r}_{\text{new}} = \mathbf{r}_{\text{old}} + (\mathbf{time} - t) \mathbf{v}$$

$$t = \mathbf{time}$$

where  $\mathbf{v}$  is the velocity of the particle. This element does not affect the momentum coordinates.

#### 4.2.1.6 SetMove

**setmove(setfrom, setto) ;**

Move all particles in a set to a different set.

**setfrom**                Original particle set.  
**setto**                    Set to add particles to.

All particles in **setfrom** will be moved to the particles in **setto**.

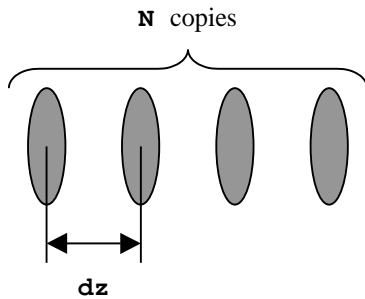
#### 4.2.1.7 SetCopy

**setcopy(set, N, dz) ;**

Multi-Copy a particle set in the z-direction

**set**                      Particle set.  
**N**                        Number of copies (including original).  
**dz**                      Distance between copies in z-direction [m], may be negative.

The **setcopy** element makes **N** duplicates of all particles in a specific set in the z-direction. The spacing between the different bunches is **dz**, as shown below.



To copy a particle set in time domain, please use **settcopy**.

#### 4.2.1.8 SetCurvature

**setcurvature(set, Ra, Rc, Lc) ;**

Model photo-emission from a curved cathode.

**set**                      Particle set.  
**Ra**                      Aperture [m].  
**Rc**                      Cathode curvature radius [m]. Specify zero for a flat surface.  
**Lc**                      Laser curvature radius [m]. Specify zero for a flat laser front.

This element changes the position and release time coordinates of all particles in the specified set to model photo-emission from a curved cathode.

As illustrated in Figure 4-24, a hollow cathode is simulated with a negative value for **Rc**. This moves all initial particle coordinates in the negative z-direction; the ones nearest to the axis the most. Combined with a flat laser front, a hollow cathode releases particles furthest away from the axis first.

A curved laser front is simulated with a non-zero value for  $\mathbf{Lc}$ . The sign of  $\mathbf{Lc}$  is chosen identical to the sign of  $\mathbf{Rc}$ . Combined with a flat cathode surface,  $\mathbf{Rc}=0$ , a negative value for  $\mathbf{Lc}$  releases particles near the axis first. When  $\mathbf{Lc}$  is equal to  $\mathbf{Rc}$  (with identical sign), the release time of the particles is not affected.

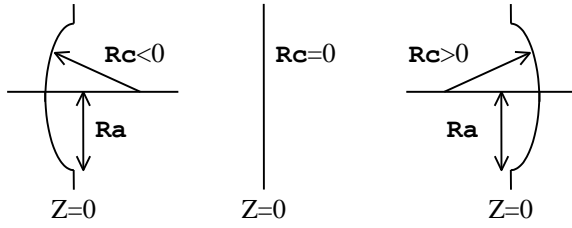


Figure 4-1: Spherical cathode for negative, zero and positive  $\mathbf{Rc}$ .

All particles  $i$  with  $r_i > \mathbf{Ra}$  or  $r_i > \mathbf{Lc}$  are removed and a warning is printed.

The initial position coordinates are changed as function of particle radius  $r_i$ , cathode aperture  $\mathbf{Ra}$  and cathode curvature  $\mathbf{Rc}$ :

$$\Delta z_i = \begin{cases} -\left(\sqrt{\mathbf{Rc}^2 - r_i^2} - \sqrt{\mathbf{Rc}^2 - \mathbf{Ra}^2}\right) & \text{if } \mathbf{Rc} < 0 \\ 0 & \text{if } \mathbf{Rc} = 0 \\ +\left(\sqrt{\mathbf{Rc}^2 - r_i^2} - \sqrt{\mathbf{Rc}^2 - \mathbf{Ra}^2}\right) & \text{if } \mathbf{Rc} > 0 \end{cases}$$

The release time coordinates are changed as function of particle radius  $r_i$ , the initial position offset  $\Delta z_i$  and the laser curvature  $\mathbf{Lc}$ .

$$\Delta t_i = \begin{cases} -\left(\sqrt{\mathbf{Lc}^2 - r_i^2} - \sqrt{\mathbf{Lc}^2 - L_a^2}\right) / c - \Delta z_i / c & \text{if } \mathbf{Lc} < 0 \\ -\Delta z_i / c & \text{if } \mathbf{Lc} = 0 \\ -\left(\sqrt{\mathbf{Lc}^2 - r_i^2} - \sqrt{\mathbf{Lc}^2 - L_a^2}\right) / c - \Delta z_i / c & \text{if } \mathbf{Lc} > 0 \end{cases}$$

where  $L_a$  is the minimum of  $\mathbf{Ra}$  and  $|\mathbf{Lc}|$ .

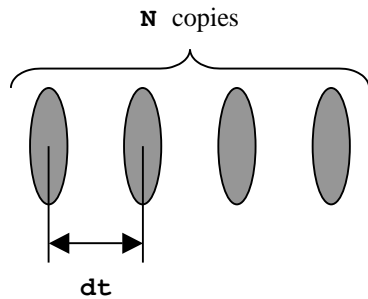
#### 4.2.1.9 SetTCopy

**settcopy**(**set**,**N**,**dt**) ;

Multi-Copy a particle set in time domain.

**set** Particle set.  
**N** Number of copies (including original).  
**dt** Distance between copies [s], may be negative.

The **settcopy** element makes **N** duplicates of all particles in a set, equidistantly spaced in time domain. The spacing between the different bunches is **dt**, as shown below.



**settcopy** is typically used to start a number of identical bunches as function of time. The example below starts five identical 1 ps bunches with 5 ps separation. Divergence was added to better show the effect of the element.

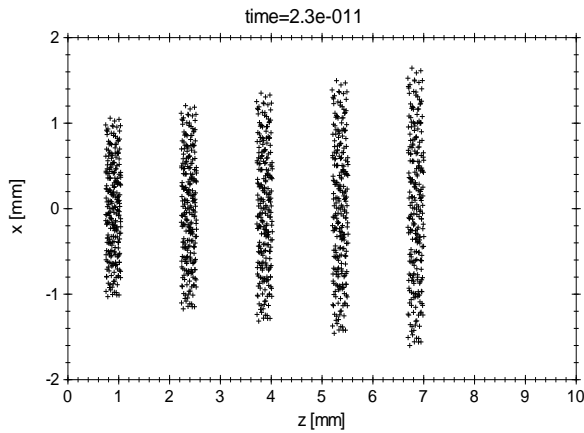


Figure: Five identical 1 ps bunches, started one after the other with, 5 ps separation. The plot shows a snapshot at  $t=23$  ps.

```

1. # Bunch Parameters
2. G = 10 ; # Lorentz factor Gamma=10
3. len = 1e-12 ; # Bunch length 1 [ps]
4. R = 1e-3 ; # Initial bunch radius 1 [mm]
5. div = 1e+3 ; # Divergence of 100 [rad/m]
6.
7. # Multi-bunch parameters
8. dt = 5e-12 ; # Bunch spacing 5 [ns] ;
9. Nb = 5 ; # 5 Bunches total
10.
11. # Create initial cylindrical bunch
12. setparticles("beam",250,me,qe,0.0) ;
13. settddist("beam","u",0,len) ;
14. setrxydist("beam","u",R/2,R) ;
15. setphidist("beam","u",0,2*pi) ;
16. setGdist("beam","u",G,0) ;
17. addxdiv("beam",0,div) ;
18. addydiv("beam",0,div) ;
19.
20. # Copy particle set
21. settcopy("beam",Nb,dt) ;
22.
23. # Output from 0 to 30 [ps]
24. tout(0,30e-12,1e-12) ;

```

#### 4.2.1.10 SetShuffle

**setshuffle(set) ;**

Randomize the order of all particles in the set.

The location of the particles in the specified **set** is randomized. Because this will not affect the actual particle coordinates, none of the distributions is affected.

#### 4.2.1.11 SetReduce

**setreduce(set,N) ;**

Reduce the number of particles in a set.

**set**                      Selected particle set

**N**                        Final number of particles in the set.

This element randomly removes all but **N** particles in the specified set. As shown in Figure 4-2, this operation affects the smoothness and accuracy of the original distribution considerably. Therefore it should never be used without a verification that the resulting particle set is as desired.

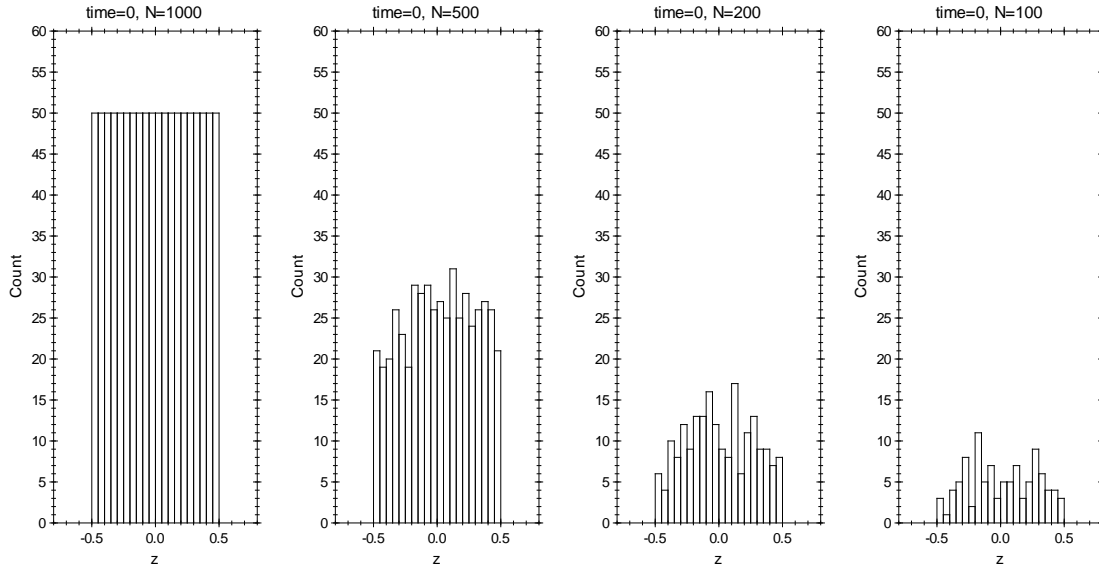


Figure 4-2: Uniform distribution containing 1000 particles (top left), reduced to 500, 200 and 100 particles.

#### 4.2.1.12 SetRmacrodist

**setmacrodist(set,distribution);**  
Sets the distribution for the particle radii.

The radius of all particles in the **set** is modified according to the specified **distribution**. The distribution is interpreted as a 1D distribution.

This element can be used to specify the radius of the particles in a set. This radius is used by **spacecharge3D**, **spacecharge2Dline** and related elements to assign a volume to the individual macro-particles. **spacecharge2Dcircle** ignores **setmacrodist** due to the complexity of the equations.

Example: The following line sets the radius of all particles in set "beam" to R:

```
setmacrodist("beam","u",R,0);
```

#### 4.2.1.13 SetStartPar

**setstartpar(set,x,y,z,GBx,GBy,GBz,[m,q,n])**  
Add one macro-particle to a particle set.

<b>set</b>	Name of particle set.
<b>x</b>	Particle x-coordinate [m].
<b>y</b>	Particle y-coordinate [m].
<b>z</b>	Particle z-coordinate [m].
<b>GBx</b>	Particle normalized x-momentum: $\gamma v_x/c$ .
<b>GBy</b>	Particle normalized y-momentum: $\gamma v_y/c$ .
<b>GBz</b>	Particle normalized z-momentum: $\gamma v_z/c$ .
<b>m</b>	Mass [kg] of the elementary particles this macro-particle represents, typically <b>me</b> .
<b>q</b>	Charge [C] of the elementary particles this macro-particle represents, typically <b>qe</b> .
<b>n</b>	Number of elementary particles this macro-particle represents.

Use this function to start one particle with a specified position and momentum. The mass and charge parameters are optional. When not specified, the inputfile variables **m** and **q** are used. An empty particle set is created before the particle is added if the specified **set** does not exist.

#### 4.2.1.14 SetStartLine

**setstartline(set,N,x1,y1,z1,x2,y2,z2,[GBx,GBy,GBz,[m,q,n]])**  
Start a number of particles on a line.

**set** Name of particle set.

<b>N</b>	Number of particles to generate, minimum 2.
<b>x1</b>	Start $x$ -position of line [m].
<b>y1</b>	Start $y$ -position of line [m].
<b>z1</b>	Start $z$ -position of line [m].
<b>x2</b>	End $x$ -position of line [m].
<b>y2</b>	End $y$ -position of line [m].
<b>z2</b>	End $z$ -position of line [m].
<b>GBx</b>	Particle normalized $x$ -momentum: $\gamma v_x/c$ .
<b>GBy</b>	Particle normalized $y$ -momentum: $\gamma v_y/c$ .
<b>GBz</b>	Particle normalized $z$ -momentum: $\gamma v_z/c$ .
<b>m</b>	Mass [kg] of the elementary particles this macro-particle represents, typically <b>me</b> .
<b>q</b>	Charge [C] of the elementary particles this macro-particle represents, typically <b>qe</b> .
<b>n</b>	Number of elementary particles this macro-particle represents.

Use this function to start **N** particles equidistantly spaced on a straight line, optionally with a specified momentum. The endpoints are always included.

The mass and charge parameters are optional, but can only be specified when the momentum is given. When not specified, the inputfile variables **m** and **q** are used. An empty particle set is created before the particle is added if the specified **set** does not exist.

Example: Start 101 particles between 0 and 10 m on the  $z$ -axis.

```
1. setstartline("beam",101, 0,0,0, 0,0,10 ) ;
```

#### 4.2.1.15 SetStartxyzGrid

```
setstartxyzgrid(set,Lx,dx,Ly,dy,Lz,dz,[GBx,GBy,GBz]) ;
```

Starts the macro-particles in a rectangular grid with equal velocity.

<b>set</b>	Name of particle set.
<b>Lx</b>	Length of array in $x$ -direction. This length may be zero.
<b>dx</b>	Spacing in $x$ -direction.
<b>Ly</b>	Length of array in $y$ -direction. This length may be zero.
<b>dy</b>	Spacing in $y$ -direction.
<b>Lz</b>	Length of array in $z$ -direction. This length may be zero.
<b>dz</b>	Spacing in $z$ -direction.
<b>GBx</b>	Particle normalized $x$ -momentum: $\gamma v_x/c$ .
<b>GBy</b>	Particle normalized $y$ -momentum: $\gamma v_y/c$ .
<b>GBz</b>	Particle normalized $z$ -momentum: $\gamma v_z/c$ .

The particles start in a rectangular grid centered around the origin. The grid extends from  $-L_x/2, -L_y/2, -L_z/2$  to  $L_x/2, L_y/2, L_z/2$  with spacing **dx,dy,dz**.

It is simple to instruct GPT to initialize billions of particles using this keyword. Since GPT has no built-in limit for the number of particles, it must rely on the operating system to indicate an ‘out of memory’ condition. On some virtual-memory machines, this error message may come too late, causing either GPT or the complete system to crash.

## 4.2.2 X, Y and Z manipulators

The following keywords modify the  $x$ -,  $y$ - and  $z$ -coordinates of the particles. The distribution syntax is listed in section 1.6.1.

### 4.2.2.1 AddZoscillation

```
addzoscillation(set,alpha,kz) ;
```

Add a periodic longitudinal density modulation

<b>set</b>	Name of the particle set
<b>alpha</b>	Amplitude of the oscillation []
<b>kz</b>	Wavenumber [ $m^{-1}$ ]



This element modifies the longitudinal coordinate of all particles in the specified **set** according the following equation:

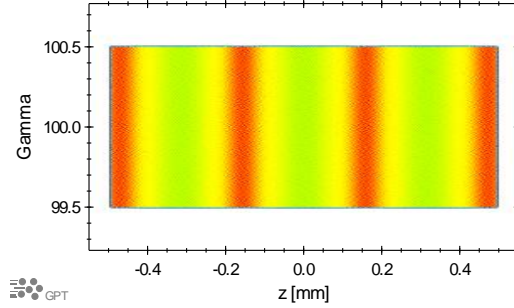
$$z_{\text{new}} = z_{\text{old}} + \frac{\alpha}{kz} \sin(kz z_{\text{old}})$$

Example: Add a modulation in  $z$ .

25.

```
1. setparticles("beam",1e6,me,qe,0) ;
2. setzdist("beam","u",0,1e-3) ;
3. setGdist("beam","u",100,1) ;
4. addzoscillation("beam",0.2,20000) ;
5. tout(0) ;
```

26.



The amplitude of an oscillation is often expressed in terms of the bunching factor  $b(k)$  defined as:

$$b(k) = \frac{1}{N} \sum_i \cos(k z_i)$$

After running **addzoscillation**, the new distribution has a bunching factor of:

$$\begin{aligned} b(k) &= \frac{1}{N} \sum_i \cos(k z_{i,\text{new}}) \\ &= \frac{1}{N} \sum_i \cos(k z_{i,\text{old}} + \alpha \sin(k z_{i,\text{old}})) \\ &\approx \frac{1}{N} \sum_i \cos(k z_{i,\text{old}}) \cos(\alpha \sin(k z_{i,\text{old}})) - \sin(\alpha \sin(k z_{i,\text{old}})) \sin(k z_{i,\text{old}}) \quad \text{if } \alpha \ll 1 \\ &\approx \frac{1}{N} \sum_i \cos(k z_{i,\text{old}}) - \alpha \sin^2(k z_{i,\text{old}}) \\ &\approx b_{\text{old}}(k) + \frac{\alpha}{2} \end{aligned}$$

#### 4.2.2.2 SetXdist

**setxdist(set,distribution) ;**  
Set  $x$  coordinate distribution.

Modifies  $x$  [m] such that  $x_i = \text{distribution}_i$

The  $x$ -coordinate of all particles in the **set** is modified according to the specified **distribution**. The distribution is interpreted as a 1D distribution. To specify a uniform distribution between  $-1$  and  $1$  centered around zero, the following line can be used:

```
setxdist("beam","u",0,2) ;
```

#### 4.2.2.3 SetXYdistbmp

**setxydistbmp(set,filename,[xres,yres]) ;**

Sets the  $xy$ -projection of the initial particle distribution based on a grayscale bitmap image

<b>set</b>	Particle set.
<b>filename</b>	Name of the grayscale bitmap file.
<b>xres</b>	Horizontal resolution [pixels/meter].
<b>yres</b>	Vertical resolution [pixels/meter].

This element sets the  $xy$ -projection of the initial particle distribution according to the specified grayscale bitmap image. Each pixel of the image is treated as a rectangular surface area with a uniformly distributed chance of emitting particles, given by the pixel color. Black pixels have zero chance of emitting particles,

white pixels have maximum chance and grayscale values are linearly interpolated in between. This element is very convenient for the simulation of photoemission in for example an rf-photogun, where an actual image of the laser focus on the cathode plane can be used to set the initial particle distribution.

The **filename** must be a grayscale, 8-bit per pixel, uncompressed MS-Windows bitmap file, typically having extension bmp or dib. Reverse row order is supported, but RLE compression is not. A variety of other image formats such as TIFF can easily be converted to grayscale MS-Windows bitmaps with image processing software such as Adobe® Photoshop®.

The pixel size, as stored in the bitmap file, can be overruled with the **xres** and **yres** parameters. The bitmap is placed with its center in the origin. The horizontal and vertical axes of the image are aligned with the *x*- and *y*-axis respectively. To move the center and/or change the alignment, please use the **settransform** element after **setxydistbmp**.

#### Example:

We used Adobe® Photoshop® to create a 1000x1000 test bitmap of an elliptical hard-edge bunch with checkerboard modulation, as shown in the left plot of Figure 4-3: The following GPT inputfile sets the *xy*-projection of the initial particle distribution with 100k electrons based on this bitmap.

```
4. setparticles("beam",100000,me,qe,0) ;
5. setxydistbmp("beam","test.bmp") ;
6. tout(0) ;
```

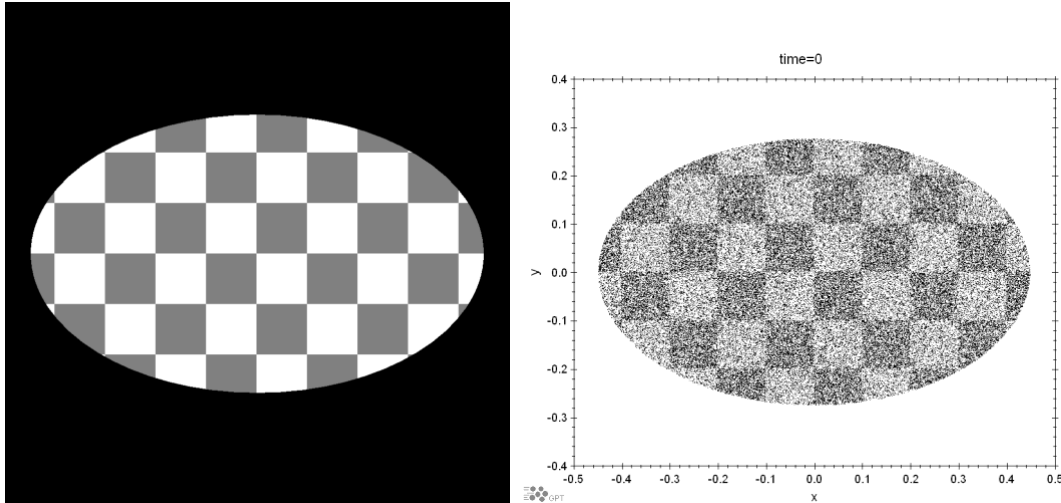


Figure 4-3: Left: Original test.bmp grayscale bitmap of an elliptical bunch with checkerboard modulation. Right: Corresponding GPTwin plot of the initial particle distribution with 100k particles. Because white pixels emit most particles while particles are shown in black in the right plot, the plots look like color-reversed versions of each other.

#### Technical notes:

Grayscale bitmap files are essentially indexed-color images with 256 or less grayscale color entries. **setxydistbmp** does not use the 8-bit color-index to determine the particle density, but actually looks up the corresponding RGB pixel color from the color table. This ensures correct results even in case the color table is not filled with 256 monotonically increasing grayscale colors. An error message is produced if the red, green and blue values of any pixel in the image are not identical.

The newer V4 and V5 BITMAPINFOHEADER structures are recognized, but the added functionality is ignored because this only concerns color information.

#### 4.2.2.4 SetYdist

```
setydist(set,distribution) ;
```

Set *y*-coordinate distribution.

Modifies *y* [m] such that  $y_i = \text{distribution}_i$

The  $y$ -coordinate of all particles in the **set** is modified according to the specified **distribution**. The distribution is interpreted as a 1D distribution.

#### 4.2.2.5 SetZdist

**setzdist(set,distribution) ;**

Set longitudinal particle distribution.

Modifies  $z$  [m] such that  $z_i = \text{distribution}_i$

The  $z$ -coordinate of all particles in the **set** is modified according to the specified **distribution**. The distribution is interpreted as a 1D distribution.

#### 4.2.2.6 SetRxydist (2D)

**setrxydist(set,distribution) ;**

Set radial distribution in  $x$ -coordinate.

Modifies  $x$  [m] such that  $x_i = \text{distribution}_i \mid 2D$

The  $x$ -coordinate of all particles in the **set** is modified according to the specified **distribution**. The distribution is interpreted as a 2D distribution. This keyword is typically followed by:

**setphidist(set,"u",0,2\*pi) ;**

#### 4.2.2.7 SetPhidist

**setphidist(set,distribution) ;**

Set phi distribution.

Modifies:  $x$  and,  $y$  such that:

$$rxy_i = \sqrt{x_i^2 + y_i^2}$$

$$x_i = rxy_i \cos(\text{distribution}_i)$$

$$y_i = rxy_i \sin(\text{distribution}_i)$$

The angle in the  $xy$ -plane of all particles in the **set** is modified according to the specified distribution. The distribution is interpreted as a 1D distribution. The  $z$ -distribution of the particles will not be affected.

#### 4.2.2.8 SetEllipse

**setellipse(set,a,b,c) ;**

Set the  $xyz$  distribution as a uniformly filled ellipsoid.

<b>set</b>	Name of particle set.
<b>a</b>	Size in $x$ -dimension [m].
<b>b</b>	Size in $y$ -dimension [m].
<b>c</b>	Size in $z$ -dimension [m].

The ellipsoid is aligned with the primary axes where **a**, **b** and **c** specify the maximum  $x$ ,  $y$  and  $z$  coordinate respectively.

### 4.2.3 GBx, GBy and GBz manipulators

The following keywords modify the  $\gamma\beta_x$ ,  $\gamma\beta_y$ - and  $\gamma\beta_z$ -coordinates of the particles. In many cases, the Lorentz factor  $\gamma$  is modified simultaneously. The distribution syntax is listed in section 1.6.1.

#### 4.2.3.1 AddGoscillation

**addGoscillation(set,alpha,kz) ;**

Add a periodic density modulation in energy

<b>set</b>	Name of the particle set
<b>alpha</b>	Amplitude of the oscillation []

**kG** Wavenumber []

This element modifies the longitudinal momentum coordinates of all particles in the specified **set** according the following equation:

$$\gamma_{\text{old}} = \sqrt{1 + (\gamma\beta)^2}$$

$$\gamma_{\text{new}} = \gamma_{\text{old}} + \frac{\alpha}{\mathbf{kG}} \sin(\mathbf{kG} \gamma_{\text{old}})$$

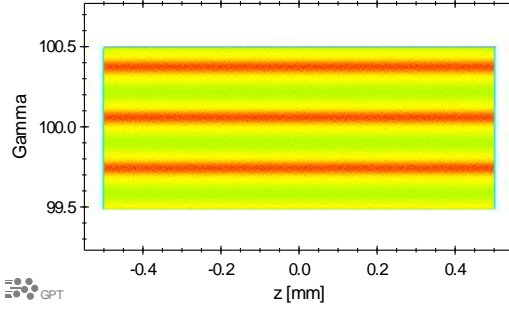
$$\gamma\beta_z = \sqrt{\gamma_{\text{new}}^2 - \gamma^2\beta_x^2 - \gamma^2\beta_y^2 - 1}$$

Example: Add a modulation in energy

27.

```
1. setparticles("beam",1e6,me,qe,0) ;
2. setzdist("beam","u",0,1e-3) ;
3. setGdist("beam","u",100,1) ;
4. addGoscillation_fix("beam",0.2,20) ;
5. tout(0) ;
```

28.



#### 4.2.3.2 SetGBxdist

**setGBxdist(set,distribution) ;**

Sets the momentum distribution in  $x$ -direction.

Modifies:  $\gamma\beta x$  such that  $\gamma\beta x_i = \mathbf{distribution}_i$

The  $\gamma\beta x$ -coordinates of the particles in the **set** are modified according to the specified distribution. The distribution is interpreted as a 1D distribution.

#### 4.2.3.3 SetGBydist

**setGBydist(set,distribution) ;**

Sets the momentum distribution in  $y$ -direction.

Modifies  $\gamma\beta y$  such that  $\gamma\beta y_i = \mathbf{distribution}_i$

The  $\gamma\beta y$ -coordinates of the particles in the **set** are modified according to the specified distribution. The distribution is interpreted as a 1D distribution.

#### 4.2.3.4 SetGBzdist

**setGBzdist(set,distribution) ;**

Sets the momentum distribution in  $z$ -direction.

Modifies  $\gamma\beta z$  such that  $\gamma\beta z_i = \mathbf{distribution}_i$

The  $\gamma\beta z$ -coordinates of the particles in the **set** are modified according to the specified distribution. The distribution is interpreted as a 1D distribution.

#### 4.2.3.5 SetGBrxydist (2D)

**setGBrxydist(set,distribution) ;**

Sets radial distribution in  $\gamma\beta x$ -coordinate.

Modifies  $\gamma\beta x$  such that  $\gamma\beta x_i = \mathbf{distribution}_i | 2D$

The  $\gamma\beta x$ -coordinate of all particles in the **set** is modified according to the specified **distribution**. Although the distribution is interpreted as a 2D distribution, the  $\gamma\beta x$  coordinate is left unchanged. This keyword is therefore typically followed by:

```
setGBphidist(set,"u",0,2*pi) ;
```

#### 4.2.3.6 SetGBphidist

```
setGBphidist(set,distribution) ;
```

Set  $\gamma\beta$ phi distribution.

Modifies  $\gamma\beta x$  and  $\gamma\beta y$  such that:

$$\begin{aligned}\gamma\beta r_{xy_i} &= \sqrt{\gamma^2 \beta_{x_i}^2 + \gamma^2 \beta_{y_i}^2} \\ \gamma\beta x_i &= \gamma\beta r_{xy_i} \cos(\text{distribution}_i) \\ \gamma\beta y_i &= \gamma\beta r_{xy_i} \sin(\text{distribution}_i)\end{aligned}$$

The angle in the  $\gamma\beta x\gamma\beta y$ -plane of all particles in the **set** is modified according to the specified distribution. The distribution is interpreted as a 1D distribution. The theta distribution of the particles will not be affected.

#### 4.2.3.7 SetGBthetadist (2D spherical)

```
setGBthetadist(set,distribution) ;
```

Set the  $\gamma\beta$ - $\theta$  distribution.

Modifies  $\gamma\beta x$ ,  $\gamma\beta y$  and  $\gamma\beta z$  such that:

$$\begin{aligned}\gamma\beta r_{xy_i} &= \sqrt{\gamma^2 \beta_{x_i}^2 + \gamma^2 \beta_{y_i}^2} \\ \gamma\beta r_{xyz_i} &= \sqrt{\gamma^2 \beta_{x_i}^2 + \gamma^2 \beta_{y_i}^2 + \gamma^2 \beta_{z_i}^2} \\ \gamma\beta x_i &= \gamma\beta r_{xyz_i} \sin(\text{distribution}_i) \gamma\beta x_i / \gamma\beta r_{xy_i} \\ \gamma\beta y_i &= \gamma\beta r_{xyz_i} \sin(\text{distribution}_i) \gamma\beta y_i / \gamma\beta r_{xy_i} \\ \gamma\beta z_i &= \gamma\beta r_{xyz_i} \cos(\text{distribution}_i)\end{aligned}$$

The  $\gamma\beta x$ -,  $\gamma\beta y$ - and  $\gamma\beta z$ -coordinates of the particles in the **set** are modified to create the specified  $\gamma\beta$ - $\theta$  distribution. The distribution is interpreted as a 2D spherical distribution. The  $\gamma$ - and  $\gamma\beta$ - $\phi$  distribution of the particles will not be affected. When  $\gamma\beta x$  and  $\gamma\beta y$  are both zero, a phi angle of zero is assumed.

#### 4.2.3.8 SetGdist

```
setGdist(set,distribution) ;
```

Set the  $\gamma$  distribution.

Modifies  $\gamma\beta z$  such that:

$$\begin{aligned}\gamma &= \text{distribution} \\ \gamma\beta z &= \sqrt{\gamma^2 - \gamma^2 \beta_x^2 - \gamma^2 \beta_y^2 - 1}\end{aligned}$$

The  $\gamma\beta z$ -coordinates of the particles in the **set** are modified to create the specified  $\gamma$ -distribution. The distribution is interpreted as a 1D distribution.

Useful equations:

$$\begin{aligned}\text{Lorentz factor} \quad \gamma &= 1/\sqrt{1-\beta^2} \\ \text{Kinetic energy} \quad E [eV] &= (\gamma-1) mc^2 / |q_e|\end{aligned}$$

#### 4.2.3.9 SetGBxemittance

```
setGBxemittance(set,emittance) ;
```

Sets the emittance in  $x\beta x$ -space. Modifies:  $\gamma\beta x$ .

**set**                      Selected particle set

**emittance** Requested emittance in  $x\beta x$ -space in [m-rad]

This element sets the emittance in  $x\beta x$ -space by scaling all  $\gamma\beta x$ -coordinates linearly using:

$$x_c = x - \bar{x} \quad x'_c = \gamma(\beta_x - \bar{\beta}_x)$$

$$\gamma\beta x = \gamma\beta x \frac{\text{emittance}}{\sqrt{x_c^2 \cdot x'^2_c - x_c x'^2_c}}$$

Because this element modifies the  $\gamma\beta x$ -coordinates, it should not be used after **setGdist**. A warning is printed when over one order of magnitude or more needs to be scaled.

This element sets the emittance in transverse position and momentum space. Therefore, the results can be slightly different from the results calculated by the **nemixrms** routines, especially in the presence of a large energy spread.

The element assumes all particles in the set to represent an equal amount of elementary particles.

#### 4.2.3.10 SetGByemittance

**setGByemittance(set, emittance) ;**

Sets the emittance in  $y\beta y$ -space. Modifies:  $\gamma\beta y$ .

**set** Selected particle set

**emittance** Requested emittance in  $y\beta y$ -space in [m-rad]

This element sets the emittance in  $y\beta y$ -space by scaling all  $\gamma\beta y$ -coordinates linearly using:

$$y_c = y - \bar{y} \quad y'_c = \gamma(\beta_y - \bar{\beta}_y)$$

$$\gamma\beta y = \gamma\beta y \frac{\text{emittance}}{\sqrt{y_c^2 \cdot y'^2_c - y_c y'^2_c}}$$

Because this element modifies the  $\gamma\beta y$ -coordinates, it should not be used after **setGdist**. A warning is printed when over one order of magnitude or more needs to be scaled.

This element sets the emittance in transverse position and momentum space. Therefore, the results can be slightly different from the results calculated by the **nemixrms** routines, especially in the presence of a large energy spread.

The element assumes all particles in the set to represent an equal amount of elementary particles.

### 4.2.4 X-GBx, Y-GBy and Z-G manipulators

The following keywords skew the phase-space areas. They will not affect the transverse or longitudinal emittance, nor will they affect the  $x$ -,  $y$ - and  $z$ -distributions. The distribution syntax is listed in section 1.6.1.

#### 4.2.4.1 AddGzoscillation

**addGzoscillation(set, alpha, kz) ;**

Add a periodic energy modulation correlated with the  $z$ -coordinate

**set** Name of the particle set

**alpha** Amplitude of the oscillation []

**kz** Wavenumber [ $\text{m}^{-1}$ ]

This element modifies the longitudinal momentum coordinates of all particles in the specified **set** by adding an oscillatory energy modulation with respect to the  $z$ -coordinate. The equations applied are:

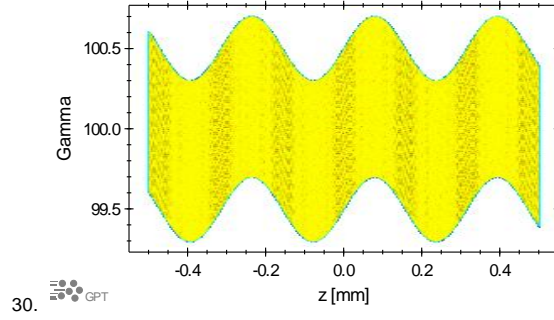
$$\gamma_{\text{old}} = \sqrt{1 + (\gamma\beta)^2}$$

$$\gamma_{\text{new}} = \gamma_{\text{old}} + \alpha \sin(\mathbf{kz} \, z)$$

$$\gamma\beta_z = \sqrt{\gamma_{\text{new}}^2 - \gamma^2 \beta_x^2 - \gamma^2 \beta_y^2 - 1}$$

Example: Add a modulation in energy 29.  
correlated with  $z$ .

```
1. setparticles("beam",1e6,me,qe,0) ;
2. setzdist("beam","u",0,1e-3) ;
3. setGdist("beam","u",100,1) ;
4. addGzoscillation("beam",0.2,20000)
5. tout(0) ;
```



#### 4.2.4.2 AddXDiv

```
addxdiv(set,xc,div) ;
```

Add divergence in the  $x$ - $\beta_x$  plane.

**set** Selected particle set.  
**xc** Center of  $x$ -distribution [m], typically 0.  
**div** Divergence, see equations below.

The  $\gamma\beta_x$ -coordinate is modified by:

$$\gamma\beta_x = \gamma\beta_x + \mathbf{div} \cdot (x - \mathbf{xc})$$

$$\gamma\beta_z = \sqrt{\gamma^2 - \gamma^2\beta_x^2 - \gamma^2\beta_y^2 - 1}$$

A linear  $x$ - $\gamma\beta_x$ -dependence is added, keeping the transverse emittance constant. To keep the particle energy and the longitudinal emittance constant, the  $\gamma\beta_z$ -coordinate is modified accordingly.

Please note that although a bunch is typically characterized by a radius  $R$  and a divergence angle  $\theta$ , this element does not have  $\theta$  as its divergence parameter. The reason for that is that it would give unintuitive results for hard-edges beams.

#### 4.2.4.3 AddYDiv

```
addydiv(set,yc,div) ;
```

Add divergence in the  $y$ - $\beta_y$ -plane

**set** Selected particle set.  
**yc** Center of  $y$ -distribution [m], typically 0.  
**div** Divergence, see equations below.

The  $\gamma\beta_y$ -coordinate is modified by:

$$\gamma\beta_y = \gamma\beta_y + \mathbf{div} \cdot (y - \mathbf{yc})$$

$$\gamma\beta_z = \sqrt{\gamma^2 - \gamma^2\beta_x^2 - \gamma^2\beta_y^2 - 1}$$

A linear  $y$ - $\gamma\beta_y$  dependence is added, keeping the transverse emittance constant. To keep the particle energy and the longitudinal emittance constant, the  $\gamma\beta_z$ -coordinate is modified accordingly.

#### 4.2.4.4 AddZDiv

```
addzdiv(set,zc, div1, [div2, [div3, [...]]]) ;
```

Add divergence in the  $z$ - $\gamma$ -plane.

**set** Selected particle set.  
**zc** Center of  $z$ -distribution [m].  
**div1** Divergence in [eV/m].  
**div2** Second order term in [eV/m<sup>2</sup>].

**div3** Third order term in [eV/m<sup>3</sup>].

The  $\gamma\beta z$ -coordinate is modified by:

$$\gamma_{new} = \gamma_{old} + \frac{|q_e|}{mc^2} \cdot (\mathbf{div1} \cdot (z - \mathbf{zc}) + \mathbf{div2} \cdot (z - \mathbf{zc})^2 + \mathbf{div3} \cdot (z - \mathbf{zc})^3 + \dots)$$

$$\gamma\beta_z = \sqrt{\gamma_{new}^2 - \gamma^2\beta_x^2 - \gamma^2\beta_y^2 - 1}$$

A  $z$ - $\gamma$ -dependance is added to the initial particle distribution. When only a linear term is added, the longitudinal emittance remains constant. This element has no effect on the transverse emittance or transverse particle distribution.

## 4.2.5 Time-dependent particle distributions

Default, all particles are emitted at once at  $t=0$  in the simulation. This can be changed using the elements presented in this section to start particles at any time in the simulation.

### 4.2.5.1 SetTdist

**settdist(set,distribution);**  
Set particle-release time distribution.

Modifies **t** [s] such that  $t_i = \mathbf{distribution}_i$

The release time of the particles in the **set** is modified according to the specified **distribution**. The distribution is interpreted as a 1D distribution. To specify a uniform distribution between  $-1$  ns and  $1$  ns centered around zero, the following line can be used:

**settdist("beam","u",0,2e-9) ;**



## 4.3 Timestep and output control

This section contains the elements controlling the Runge-Kutta solver and output generation. Using **accuracy**, the calculation accuracy can be specified. The **tout** and **screen** keywords specify the time and position when output is written. The other elements can be used to have more control over the timestep mechanism or provide additional or diagnostic output.

4.3.1	Acceptance .....	139
4.3.2	Accuracy.....	140
4.3.3	dtmax.....	141
4.3.4	dtmaxt.....	141
4.3.5	dtmin.....	141
4.3.6	dtstart.....	141
4.3.7	Outputvalue .....	141
4.3.8	Pp.....	141
4.3.9	safety .....	142
4.3.10	Screen .....	142
4.3.11	Snapshot .....	142
4.3.12	Tcontinue.....	143
4.3.13	time.....	143
4.3.14	tmax .....	143
4.3.15	Tout .....	144
4.3.16	Writeelegant .....	144
4.3.17	Writefloorplan .....	144
4.3.18	Writesteps.....	145

### 4.3.1 Acceptance

**acceptance (ECS) ;**

Write acceptance information to the GPT outputfile.

**ECS**                      All output is written relative to the Element Coordinate System specified here.

When beam-pipes and other obstacles are introduced in a GPT simulation not all particles necessarily make it through. To investigate which part of the initial phase space is (not) removed downstream the **acceptance** keyword can be used. Furthermore, this element can be very helpful in debugging GPT inputfiles when particles are lost by an unknown element. The following arrays are written to the GPT outputfile.

Particles that make it through:

<b>OK_x_start</b>	$x$ -position [m] where the particle is started
<b>OK_y_start</b>	$y$ -position [m] where the particle is started
<b>OK_z_start</b>	$z$ -position [m] where the particle is started
<b>OK_Bx_start</b>	$x$ -velocity/ $c$ when the particle is started
<b>OK_By_start</b>	$y$ -velocity/ $c$ when the particle is started
<b>OK_Bz_start</b>	$z$ -velocity/ $c$ when the particle is started
<b>OK_G_start</b>	Lorentz factor when the particle is started
<b>OK_t_start</b>	Simulation time [s] when the particle is started

Particles that are removed from the simulation:

<b>NOK_x_start</b>	$x$ -position [m] where the particle is started
<b>NOK_y_start</b>	$y$ -position [m] where the particle is started
<b>NOK_z_start</b>	$z$ -position [m] where the particle is started
<b>NOK_Bx_start</b>	$x$ -velocity/ $c$ when the particle is started
<b>NOK_By_start</b>	$y$ -velocity/ $c$ when the particle is started
<b>NOK_Bz_start</b>	$z$ -velocity/ $c$ when the particle is started
<b>NOK_G_start</b>	Lorentz factor when the particle is started
<b>NOK_t_start</b>	Simulation time [s] when the particle is started

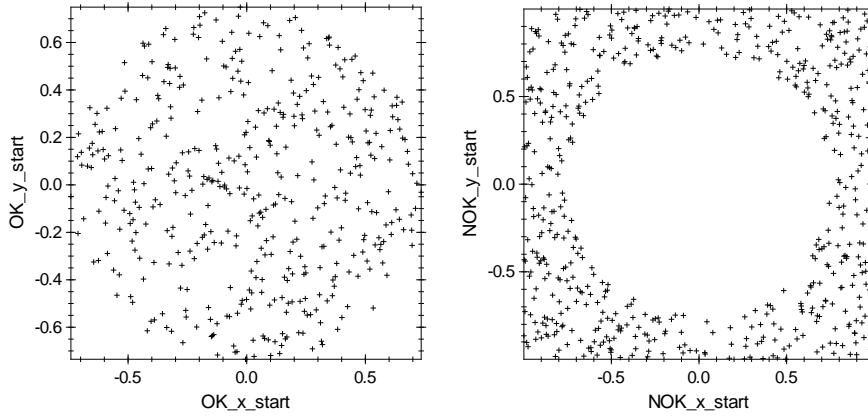
<b>NOK_x_end</b>	$x$ -position [m] where the particle is removed
------------------	---

**NOK\_y\_end**      y-position [m] where the particle is removed  
**NOK\_z\_end**      z-position [m] where the particle is removed  
**NOK\_Bx\_end**     x-velocity/c when the particle is removed  
**NOK\_By\_end**     y-velocity/c when the particle is removed  
**NOK\_Bz\_end**     z-velocity/c when the particle is removed  
**NOK\_G\_end**      Lorentz factor when the particle is removed  
**NOK\_t\_end**      Simulation time [s] when the particle is removed

A simple example is shown below: A rectangular beam is sent into a pipe.

```

1. # Start 1000 particles, square distribution in xy-space
2. setparticles("beam",1000,me,qe,0.0) ;
3. setxdist("beam","u",0,2) ;
4. setydist("beam","u",0,2) ;
5. setGdist("beam","u",200,0) ;
6.
7. # Beam pipe with R=0.75 m, between z=1 and z=2 m
8. rmax("wcs","z",1.5, 0.75,1 ) ;
9.
10. # Acceptance output
11. acceptance("wcs","I") ;
12. tcontinue(4/c) ;
  
```



The accepted (left) and not accepted (right) part of the initial beam.

### 4.3.2 Accuracy

**accuracy(GBacc,[xacc]) ;**  
 Specifies the calculation accuracy.

**GBacc**            Negative base 10 logarithm of the simulation accuracy for  $\gamma\beta$ . If not specified, 4 is assumed.  
**xacc**             Negative base 10 logarithm for the simulation accuracy for position. If not specified, 6 is assumed. It is rarely needed to change this value. Increasing **GBacc** usually increases the accuracy for the position simultaneously.

The simulation accuracy is calculated as follows:

$$\gamma\beta_{\max} = 10^{-\text{GBacc}}$$

$$x_{\max} = 10^{-\text{xacc}}$$

The requested accuracy is the minimal accuracy per step. For very long runs with over  $10^4$  steps, the final accuracy should be checked by increasing the accuracy and verifying that the result does not change significantly.

For more information about accuracy and timesteps see section 1.8.

### 4.3.3 dtmax

**dtmax=expression ;**

Specifies the maximum timestep size.

**expression** Maximum timestep. If the automatic timestep mechanism suggests a timestep larger than **dtmax**, **dtmax** is used. **dtmax** can be used to avoid particles ‘jumping over’ small global elements. Default  $\infty$ .

### 4.3.4 dtmaxt

**dtmaxt(tstart,tend,dtmax) ;**

Enforce a maximum timestep within a specified interval.

**tstart** Start time.

**tend** End time.

**dtmax** Maximum timestep when **tstart** < *t* < **tend**

Forces the timesteps to remain less than **dtmax** when the simulation time is within **tstart** and **tend**. This element should only be used when the adaptive stepsize control mechanism doesn’t perform satisfactory.

Example: 100 timesteps are enforced between 85 and 95 ns.

1. **startpar( "wcs","I", 0,0,0, 0,0,0.5 ) ;**
2. **tout( 0, 100e-9, 20e-9 ) ;**
3. **dtmaxt( 85e-9, 95e-9, 0.1e-9 ) ;**

### 4.3.5 dtmin

**dtmin=expression ;**

Specifies the minimum timestep size.

**expression** Minimum timestep. If the automatic timestep mechanism suggests a timestep smaller than **dtmin**, **dtmin** is used. Please note that in this case the required accuracy cannot be guaranteed. Before using **dtmin** consider lowering your **accuracy**. Default 0.

### 4.3.6 dtstart

**dtstart=expression ;**

Specifies the initial timestep.

**expression** This is the initial value for *h* as described in section 1.8. Subsequent values for *h* are calculated automatically. Default: Twice the separation between the initial two particles, or  $\frac{1}{1000c}$  if all particles are started simultaneously.

### 4.3.7 Outputvalue

**outputvalue(name,expr) ;**

Writes a value in the outputfile.

**name** Name of the value as it will be written in the outputfile.

**expr** Value to be written in the outputfile. Any expression can be entered.

Example:

1. **w = 240e6 ;**
2. **outputvalue("freq", 2\*pi\*w) ;**

### 4.3.8 Pp

**pp(param1,param2,...) ;**

Print parameters for diagnostic purposes.

This line instructs GPT to print the values of the parameters to **stderr**. Checking the results of intermediate calculations in an inputfile is a useful debug aid.

### 4.3.9 safety

**safety=expression** ;

Specifies the safety parameter.

**expression** The safety parameter  $S$  as described in section 1.8. Default 0.85.

Reducing the safety parameter can save a small amount of CPU time when tracking particle trajectories through fast changing fields.

### 4.3.10 Screen

**screen(ECS,at,[CCSname])** ;

**screen(ECS,from,to,step,[CCSname])** ;

Writes particle coordinates when the particles pass through a nondestructive screen to the outputfile.

**ECS** Element Coordinate System of the screen. Using the ECS, the screen(s) can be located anywhere in space with any orientation.

**at** The screen is positioned at  $z=\text{at}$  with respect to the specified **ECS**.

**from,to,step** The screens are positioned at  $z=\text{from}+N\text{step}$  if  $\text{from} \leq t \leq \text{to}$ , where  $N \in [0,1,2,\dots]$ .

**CCSname** The name of the CCS relative to which the coordinates of the particles will be written. If not specified, the screens ECS is used.

The typical use to position a screen at for example the  $z=5$  meter plane is:

**screen("wcs", "I", 5)** ;

For every screen a separate group in the GPT outputfile, named **position** with value **at** is created. The coordinates written in the outputfile are listed in Table 4-E. When positioning multiple screens in combination with GDFA, you can group by **position** to create useful plots. Particles in rings can 'hit' the same screen several times. In that case multiple recordings of the same particle, with different  $t$ , will be present in the outputfile.

Table 4-E: Coordinates in the **position** group written by the **screen** element.

<b>ID</b>	Particle identification numbers.
<b>x,y,z</b>	Positions of the particles.
<b>rx,ry</b>	Particle distances from the $z$ -axis.
<b>Bx,By,Bz</b>	Velocities of the particles normalized to the speed of light.
<b>G</b>	Lorentz factors of the particles.
<b>t</b>	Time when the particles pass the screen.

The equation for the screen is:

$$\mathbf{M}_{EW}^{-1}(\mathbf{r}_{WCS} - \mathbf{o}) \cdot \hat{\mathbf{z}} = 0$$

where

$$\mathbf{o} = \mathbf{o}_{EW} + \text{at} \mathbf{M}_{CW} \cdot \hat{\mathbf{z}}$$

For information about the used notation and coordinate systems in general, see section 1.4.

The coordinates are calculated via 'perfect' interpolation between two consecutive timesteps, where the interpolation error is always below or equal to the tracking error. Screens need to buffer particle coordinates and involve complex interpolations. They are slower and consume more resources compared to snapshots.

### 4.3.11 Snapshot

**snapshot(time,[CCSname])** ;

**snapshot(from,to,step,[CCSname])** ;

Writes the coordinates of the particles at the given simulation time to the outputfile.

**time** Simulation time when the coordinates of the particles are to be written in the outputfile.

**from,to,step** The coordinates of the particles are to be written in the outputfile at  $t=\text{from}+N\text{step}$  if  $\text{from} \leq t \leq \text{to}$ , where  $N \in [0,1,2,\dots]$ .

**CCSname** The name of the CCS relative to which the coordinates of the particles are to be written. If not specified, WCS is assumed.

The coordinates of the particles are written in the outputfile when the simulation time is the specified **time**. When **from to step** is specified, output is written periodically.

For every time output a separate group in the outputfile, named **time** with value **time**, is created containing the following coordinates:

Table 4-F: Coordinates in the **time** group written by the **tout** element.

<b>ID</b>	Particle identification numbers.
<b>x,y,z</b>	Positions of the particles.
<b>rx,y</b>	Particle distances from the z-axis.
<b>Bx,By,Bz</b>	Velocities of the particles normalized to the speed of light.
<b>G</b>	Lorentz factors of the particles.

The automatic timestep algorithm is not affected by the snapshots. This allows the ODE solver to take the largest possible step, given the current accuracy setting, making snapshots the fastest output mechanism. Please see the **tout** keyword when the electromagnetic fields output is required.

#### 4.3.12 Tcontinue

**tcontinue(t) ;**

Continue the simulation till the specified time

**t** Minimum simulation time [s].

Normally, GPT stops execution after the last **tout** or **screen**. To overrule this behavior, the **tcontinue** element forces GPT to continue until the specified time **t**. This element is useful when solving additional differential equations with custom output routines. When scattering statistics are to be obtained it is typically used with all **tout** statements removed.

Stopping GPT takes precedence over **tcontinue**. In other words, when an element actively signals to stop GPT, the simulation will always be stopped.

#### 4.3.13 time

**time=expression ;**

Specifies the simulation starting time.

**expression** Starting time of the simulation. Default: Release time of first particles to be started.

Usually used to continue a simulation using a different inputfile. See **setfile** for more documentation.

#### 4.3.14 tmax

**tmax=expression ;**

Forces the simulation to stop at the specified simulation time.

**expression** Maximum simulation time [s]. Default:  $\infty$ .

A GPT simulation typically continues to run until all particles pass all screens. However, when particles go back due to for example a decelerating rf-phase, they never hit the last screen. This potentially results in a simulation that continues to run forever. Ideally this situation is prevented by removing all backstreaming particles with for example **zminmax** and **rmax**. A very effective alternative is setting a maximum simulation time with **tmax**.

Please note that **tmax** does not set the maximum CPU time.

### 4.3.15 Tout

```
tout(time,[CCSname]) ;
tout(from,to,step,[CCSname]) ;
```

Writes the electromagnetic fields at the position of all particle coordinates at the given simulation time to the GPT outputfile.

**time** Simulation time when the coordinates of the particles are to be written in the outputfile.  
**from,to,step** The coordinates of the particles are to be written in the outputfile at  $t=\text{from}+N\text{step}$  if  $\text{from} \leq t \leq \text{to}$ , where  $N \in [0,1,2,\dots]$ .  
**CCSname** The name of the CCS relative to which the coordinates of the particles are to be written. If not specified, WCS is assumed.

The coordinates of the particles are written in the outputfile when the simulation time is the specified **time**. When **from to step** is specified, output is written periodically.

For every time output a separate group in the outputfile, named **time** with value **time**, is created containing the following coordinates:

Table 4-G: Coordinates in the **time** group written by the **tout** element.

<b>ID</b>	Particle identification numbers.
<b>x,y,z</b>	Positions of the particles.
<b>rx,y</b>	Particle distances from the z-axis.
<b>Bx,By,Bz</b>	Velocities of the particles normalized to the speed of light.
<b>G</b>	Lorentz factors of the particles.
<b>fEx,fEy,fEz</b>	Electric fields at particle positions.
<b>fBx,fBy,fBz</b>	Magnetic fields at particle positions.

To obtain field information, the automatic timestep algorithm generates its timesteps in such a way that the particle coordinates are calculated at exactly the requested **time**. This slows down the ODE solver. If electromagnetic field information is not required, please use the snapshot keyword.

e relative to maximum acceleration.

### 4.3.16 Writeelegant

```
writeelegant() ;
```

Adds additional information to GPT screen output such that it can be used 1:1 as an Elegant inputfile

Adding this line to the GPT inputfile instructs GPT to write additional information to the GPT outputfile for all screens. More specifically, the following data is written:

**xp** Vector given by **GBx/GBz**  
**yp** Vector given by **GBy/GBz**  
**p** Vector given by  $\sqrt{G^2-1}$   
**Particles** Number of particles  
**pCentral** Average of **p**  
**Charge** Total charge

where **GBx**, **GBy**, **GBz** and **G** are the normalized momenta and the Lorentz factor respectively.

To use the written GDF output as Elegant inputfile, it still has to be converted to SDDS format using the GDF2SDDS program using:

```
gdf2sdds -o output.sdds output.gdf
```

### 4.3.17 Writefloorplan

```
writefloorplan(filename) ;
```

Writes all center coordinates and orientations of all beamline components to a file.

**filename** Name of the file to write information to [gdf].

This element writes positional information of all coordinate systems and all beamline components defined in the GPT inputfile to the specified **filename**. Both the center coordinates and the orientation are transformed back to World Coordinate System (WCS) to ease comparison with CAD programs and other simulations codes. Despite the name **writetoorplan**, the element does *not* project 3D information onto a 2D plane.

The specified **filename** is written in **gdf** format and has the following structure:

For the built-in WCS and for each CCS a separate group is created with the name of the Coordinate System. Each group contains the positional information of the Coordinate System itself, the positional information of all local elements and the positional information of all global elements. The encoding is as follows:

<b>type</b>	Flag to indicate the type of information:
0:	CCS definition
1:	Local element
2:	Global element
<b>xcenter, ycenter, zcenter</b>	Center position, measured in WCS [m,m,m]
<b>xx, xy, xz</b>	Normalized direction of the x-axis, measured in WCS []
<b>yx, yy, yz</b>	Normalized Direction of the y-axis, measured in WCS []
<b>zx, zy, zz</b>	Normalized Direction of the z-axis, measured in WCS []

Modeling large accelerator facilities with many bend magnets is possible in GPT using Custom Coordinate Systems. These additional coordinate systems ease the positioning of downstream beamline components, while simultaneously providing a performance increase. However, especially when many coordinate systems are all defined relative to each other, it can be challenging to figure out where beamline components are positioned relative to World Coordinate System (WCS). This **writetoorplan** element can be used to debug such situations by cross-checking the WCS coordinates with CAD drawings or other simulations codes.

If desired, the output of **writetoorplan** can be converted to ASCII using the GDF2A program

```
GDF2A -w 16 -o filename.txt filename.gdf
```

### 4.3.18 Writesteps

```
writesteps([filename.gdf])
```

Write timestep information to the outputfile for performance debugging

**filename.gdf** Optional external filename for output

The **writesteps** command stores all timestep information of the entire simulation to either the usual GPT outputfile or in the specified **outputfile.gdf**. The following information is recorded:

<b>t</b>	Simulation time [s].
<b>dt</b>	Timestep taken [s].
<b>fail</b>	Number of failed steps at t.
<b>avgx</b>	Average x-coordinate [m] of all particles at t.
<b>avgy</b>	Average y-coordinate [m] of all particles at t.
<b>avgz</b>	Average z-coordinate [m] of all particles at t.

The automatic stepsize algorithm in GPT does not aim for the highest possible accuracy. It aims for the largest allowed stepsize. The algorithm that dynamically adjusts the stepsizes for each beamline component is written such that once in a while a timestep fails. This is by design because recovering from a few failures once in a while gives far better overall performance than ‘playing it safe’. After a timestep fails the dynamic timestep algorithm estimates the best size of a smaller timestep based on the assumption that the fields are differentiable to 5<sup>th</sup> order. And this is where performance can suffer dramatically. Even small discontinuities in the fields, such as a beamline component with a fringe-field that is cut too soon can cause many failed steps.

To show where CPU time is spent during the simulation, one can make various plots of the output of **writesteps**. A good starting point is observing if the fail rate is at or below about 4 everywhere. This value is a arguably arbitrary, but in our experience discontinuous fields give very high fail rates and are easily detectable. Plotting avgx,avgy,avgz at high fail counts gives an immediate indication where performance can

be improved. Often it is simple changes, such as extending the fringes a bit further, that make dramatic differences in performance.



## 4.4 Accelerating structures

This section contains the build-in accelerating structures with time-varying electromagnetic fields. Please note that only the **TE110gauss** and **TMx10gauss** elements have proper transverse fringe fields for the entrance and exit fields. If these models can not be applied, and if transverse fringes are required, please see the fieldmaps section 4.7.

4.4.1	TE011cylcavity .....	147
4.4.2	TE011gauss .....	147
4.4.3	TE110gauss .....	148
4.4.4	TErectcavity .....	148
4.4.5	TM010cylcavity .....	149
4.4.6	TM110gauss .....	149
4.4.7	TM110cylcavity .....	149
4.4.8	TM010gauss .....	150
4.4.9	TMrectcavity .....	151
4.4.10	Trwcell.....	151
4.4.11	Trwlinac.....	152
4.4.12	Trwlinbm .....	153

### 4.4.1 TE011cylcavity

**TE011cylcavity** (ECS, L, R, A, phi) ;

Cylindrically symmetric pillbox cavity in TE<sub>011</sub> mode.

<b>ECS</b>	Element coordinate system.
<b>L</b>	Total cavity length in z direction [m].
<b>R</b>	Radius of the cavity [m].
<b>A</b>	Multiplication factor for all fields [T].
<b>phi</b>	Phase factor: $\varphi$ in radians.

The fields are calculated by [6]:

$$B_z = \mathbf{A} J_0 \left( x_{11} \frac{r}{\mathbf{R}} \right) \cos \left( \frac{\pi z}{\mathbf{L}} \right) \sin(\omega_{011} \cdot t + \varphi)$$

$$B_r = \mathbf{A} \frac{\pi R}{x_{11} \mathbf{L}} J_1 \left( x_{11} \frac{r}{\mathbf{R}} \right) \sin \left( \frac{\pi z}{\mathbf{L}} \right) \sin(\omega_{011} \cdot t + \varphi)$$

$$E_\varphi = \mathbf{A} \frac{R \omega_{011}}{x_{11}} J_1 \left( x_{11} \frac{r}{\mathbf{R}} \right) \cos \left( \frac{\pi z}{\mathbf{L}} \right) \sin(\omega_{011} \cdot t + \varphi)$$

where  $-\mathbf{L}/2 < z < \mathbf{L}$  and where  $x_{11} \approx 3.8317$  is the first zero of  $J_1$ . The resonance frequency is given by:

$$\omega_{011} = c \sqrt{\frac{\pi^2}{\mathbf{L}^2} + \frac{x_{11}^2}{\mathbf{R}^2}}$$

where  $c$  is the speed of light. Please note that this element does not model fringe fields. To model a cavity with fringe fields, please use the **TE011gauss** element.

### 4.4.2 TE011gauss

**TE110gauss** (ECS, A, sigma, phi, omega) ;

Cylindrically symmetric rf cavity in TE<sub>011</sub> mode with Gaussian on-axis  $B_z$  field profile.

<b>ECS</b>	Element coordinate system.
<b>A</b>	Maximum amplitude [T]
<b>sigma</b>	Width of the Gaussian profile [m]
<b>phi</b>	Phase offset [rad]
<b>omega</b>	Angular frequency [rad/s]

This element models a standing wave rf cavity in TE<sub>011</sub> mode. The on-axis longitudinal magnetic profile is assumed to be Gaussian with maximum amplitude **A** and width **sigma**:

$$B_z(z) = A \exp\left(-\frac{z^2}{2\sigma^2}\right) \cos(\omega t + \varphi)$$

The off-axis fields are derived from a 5<sup>th</sup> order expansion. Consequently, this element can only be used for particles relatively close to the  $z$ -axis.

#### 4.4.3 TE110gauss

**TE110gauss** (**ECS**, **A**, **sigma**, **phi**, **omega**) ;

Cylindrically symmetric rf cavity in TE<sub>110</sub> mode with Gaussian on-axis  $E_x$  field profile.

<b>ECS</b>	Element coordinate system.
<b>A</b>	Maximum amplitude [V/m]
<b>sigma</b>	Width of the Gaussian profile [m]
<b>phi</b>	Phase offset [rad]
<b>omega</b>	Angular frequency [rad/s]

This element models a standing wave rf cavity in TE<sub>110</sub> mode. The on-axis deflection profile is assumed to be Gaussian with maximum amplitude **A** and width **sigma**:

$$E_x(z) = A \exp\left(-\frac{z^2}{2\sigma^2}\right) \cos(\omega t + \varphi)$$

The off-axis fields are derived from a 5<sup>th</sup> order expansion. Consequently, this element can only be used for particles relatively close to the  $z$ -axis.

#### 4.4.4 Terecavity

**Terecavity** (**ECS**, **a**, **b**, **L**, **m**, **n**, **p**, **const**, **phi**) ;

Rectangular TE<sub>mnp</sub> mode resonant cavity.

<b>ECS</b>	Element coordinate system.
<b>a</b>	Total cavity length in x-direction [m].
<b>b</b>	Total cavity length in y-direction [m].
<b>L</b>	Total cavity length in z-direction [m].
<b>m</b>	Mode index in x-direction.
<b>n</b>	Mode index in y-direction.
<b>p</b>	Mode index in z-direction.
<b>Bo</b>	Multiplication factor for all fields.
<b>phi</b>	Phase factor: $\varphi$ in radians.

The fields generated by this element are given by [6]:

$$\mathbf{B} = B_0 \begin{pmatrix} -\frac{1}{k_c^2} \frac{p\pi m\pi}{d a} \sin\left(\frac{m\pi x}{a}\right) \cos\left(\frac{n\pi y}{b}\right) \cos\left(\frac{p\pi z}{d}\right) \\ -\frac{1}{k_c^2} \frac{p\pi n\pi}{d b} \cos\left(\frac{m\pi x}{a}\right) \sin\left(\frac{n\pi y}{b}\right) \cos\left(\frac{p\pi z}{d}\right) \\ \cos\left(\frac{m\pi x}{a}\right) \cos\left(\frac{n\pi y}{b}\right) \sin\left(\frac{p\pi z}{d}\right) \end{pmatrix} \sin(\omega t + \varphi)$$

$$\mathbf{E} = B_0 \frac{\omega}{k_c^2} \begin{pmatrix} \frac{n\pi}{b} \cos\left(\frac{m\pi x}{a}\right) \sin\left(\frac{n\pi y}{b}\right) \sin\left(\frac{p\pi z}{d}\right) \\ -\frac{m\pi}{a} \sin\left(\frac{m\pi x}{a}\right) \cos\left(\frac{n\pi y}{b}\right) \sin\left(\frac{p\pi z}{d}\right) \\ 0 \end{pmatrix} \cos(\omega t + \varphi)$$

where

$$k_c^2 = \left(\frac{m\pi}{a}\right)^2 + \left(\frac{n\pi}{b}\right)^2$$

$$\beta = \left[ \left(\frac{2\pi}{\lambda}\right)^2 - k_c^2 \right]^{\frac{1}{2}} = \frac{p\pi}{d}$$

$$k = \frac{2\pi}{\lambda} = \left[ \left(\frac{m\pi}{a}\right)^2 + \left(\frac{n\pi}{b}\right)^2 + \left(\frac{p\pi}{d}\right)^2 \right]^{\frac{1}{2}} = \frac{\omega}{c}$$

#### 4.4.5 TM010cylcavity

**TM010cylcavity** (**ECS**, **L**, **R**, **A**, **phi**) ;

Cylindrically symmetric pillbox cavity in TM<sub>010</sub> mode.

<b>ECS</b>	Element coordinate system.
<b>L</b>	Total cavity length in z direction [m].
<b>R</b>	Radius of the cavity.
<b>A</b>	Multiplication factor for all fields [V/m].
<b>phi</b>	Phase factor: $\varphi$ in radians.

The fields are calculated by [6]:

$$E_z = \mathbf{A} J_0 \left( x_{01} \frac{r}{\mathbf{R}} \right) \sin(\omega_{010} \cdot t + \varphi)$$

$$B_\varphi = \mathbf{A} J_1 \left( x_{01} \frac{r}{\mathbf{R}} \right) \cos(\omega_{010} \cdot t + \varphi) / c$$

where  $c$  is the speed of light,  $x_{01} \approx 2.4048$  is the first zero of  $J_0$  and the resonance frequency is

$$\omega_{010} = k c = \frac{p_{01}}{\mathbf{R}} c$$

The resonant wavelength is given by:

$$\lambda = \frac{2\pi}{k} = 2.61\mathbf{R}$$

Please note that this element does not model fringe fields and consequently can only be used to study longitudinal dynamics. To model a cavity with fringe fields, please use **TM010gauss** or for example **map1D\_TM** or **map25D\_TM**.

#### 4.4.6 TM110gauss

**TM110gauss** (**ECS**, **A**, **sigma**, **phi**, **omega**) ;

Cylindrically symmetric rf cavity in TM<sub>010</sub> mode with Gaussian on-axis field profile.

<b>ECS</b>	Element coordinate system.
<b>A</b>	Maximum amplitude [T]
<b>sigma</b>	Width of the Gaussian profile [m]
<b>phi</b>	Phase offset [rad]
<b>omega</b>	Angular frequency [rad/s]

This element models a standing wave rf cavity in TM<sub>110</sub> mode. The on-axis acceleration profile is assumed to be Gaussian with maximum amplitude **A** and width **sigma**:

$$B_y(z) = A \exp\left(-\frac{z^2}{2\sigma^2}\right) \cos(\omega t + \varphi)$$

The off-axis fields are derived from a 5<sup>th</sup> order expansion. Consequently, this element can only be used for particles relatively close to the  $z$ -axis.

#### 4.4.7 TM110cylcavity

**TM110cylcavity** (**ECS**, **L**, **R**, **A**, **phi**) ;

Cylindrically symmetric pillbox cavity in TM<sub>110</sub> mode.

<b>ECS</b>	Element Coordinate System.
<b>L</b>	Total cavity length in z direction [m].
<b>R</b>	Outer radius of the cavity.
<b>A</b>	Multiplcations factor for all fields.
<b>phi</b>	Phase factor in radians.

The electromagnetic fields of this element are in cylindrical coordinates given by:

$$E_z = J_1\left(\frac{x_{110} r}{R}\right) \cos(\varphi) \sin(\omega_{110} t + \mathbf{phi})$$

$$B_r = -\frac{J_1\left(\frac{x_{110} r}{R}\right)}{\omega_{110} r} \sin(\varphi) \cos(\omega_{110} t + \mathbf{phi})$$

$$B_\varphi = -\frac{x_{110} J_0\left(\frac{x_{110} r}{R}\right)/R - J_1\left(\frac{x_{110} r}{R}\right)/r}{\omega_{110}} \cos(\varphi) \sin(\omega_{110} t + \mathbf{phi})$$

where  $x_{110} \approx 3.8317$  is the first zero of  $J_1$  and  $\omega_{110} = c \cdot x_{110}/R$  with  $c$  the speed of light. To avoid the singularities at  $r=0$ , the following Taylor expansion of the fields is used for all  $r < 10^{-6}$ :

$$E_z = \frac{x'}{2} \sin(\omega_{110} t + \mathbf{phi})$$

$$B_x = -\frac{x' y'}{8 c} \cos(\omega_{110} t + \mathbf{phi})$$

$$B_y = -\frac{x'^2 (y'^2 - 12) - 4(y'^2 - 8)}{64 c} \cos(\omega_{110} t + \mathbf{phi})$$

where  $x' = x_{110} x/R$  and  $y' = x_{110} y/R$  are the dimensionless position variables.

Example: Idealized cylindrically symmetric 1 mT, 5 cm, 3 Ghz TM<sub>110</sub> cavity at  $z=10$  cm.

```
1. freq=2998e6 ;          # European 3 GHz
2. x110=3.8317 ;          # First zero of J1
3. R =c*x110 / (2*pi*freq) ;          # Calculate Radius based on frequency
4. Bmax=1e-3 ; # Maximum field: 1 mT
5. TM110cylcavity("wcs", "z", 0.1, 0.05, R, 2*c*Bmax, phi) ;
```

#### 4.4.8 TM010gauss

**TM010gauss (ECS, A, sigma, phi, omega) ;**

Standing wave cylindrically symmetric TM010 cavity with Gaussian acceleration profile

<b>ECS</b>	Element coordinate system
<b>A</b>	Maximum amplitude [V/m]
<b>sigma</b>	Width of the Gaussian profile [m]
<b>phi</b>	Phase offset [rad]
<b>omega</b>	Angular frequency [rad/s]

This element models a standing wave rf cavity in TM010 mode. The on-axis acceleration profile is assumed to be Gaussian with maximum amplitude **A** and width **sigma**:

$$E_z(z) = A \exp\left(-\frac{z^2}{2\sigma^2}\right) \cos(\omega t + \varphi)$$

The off-axis fields are derived from a 5<sup>th</sup> order expansion. Consequently, this element can only be used for particles relatively close to the  $z$ -axis.

A particle entering this cavity, such that its  $z=0$  position corresponds to  $t=0$ , encounters an integrated field  $\Delta V$  given by:

$$\Delta V = \int_{-\infty}^{\infty} A \exp\left(-\frac{z^2}{2\sigma^2}\right) \cos\left(\omega \frac{z}{v} + \varphi\right) dz = A \sigma \sqrt{2\pi} \exp\left(-\frac{\omega^2 \sigma^2}{2v^2}\right) \cos(\varphi)$$

where it is assumed that the cavity does not introduce significant velocity differences. Under that condition, a given energy gain/loss  $\Delta V$  corresponds to an  $A$  to use for gaussTM010 given by:

$$A = \frac{\Delta V}{\sigma \sqrt{2\pi} \exp\left(-\frac{\omega^2 \sigma^2}{2v^2}\right) \cos(\varphi)}$$

where  $\varphi$  specifies the phase relative to maximum acceleration.

#### 4.4.9 TMrectcavity

**TMrectcavity** (**ECS**, **a**, **b**, **L**, **m**, **n**, **p**, **const**, **phi**) ;

Rectangular TM<sub>mnp</sub> mode resonant cavity.

<b>ECS</b>	Element coordinate system.
<b>a</b>	Total cavity length in x-direction [m].
<b>b</b>	Total cavity length in y-direction [m].
<b>L</b>	Total cavity length in z-direction [m].
<b>m</b>	Mode index in x-direction.
<b>n</b>	Mode index in y-direction.
<b>p</b>	Mode index in z-direction.
<b>Eo</b>	Multiplication factor for all fields.
<b>phi</b>	Phase factor: $\varphi$ in radians.

The fields generated by this element are given by [6]:

$$\mathbf{E} = E_0 \begin{pmatrix} -\frac{1}{k_c^2} \frac{p\pi m\pi}{d a} \cos\left(\frac{m\pi x}{a}\right) \sin\left(\frac{n\pi y}{b}\right) \sin\left(\frac{p\pi z}{d}\right) \\ -\frac{1}{k_c^2} \frac{p\pi n\pi}{d b} \sin\left(\frac{m\pi x}{a}\right) \cos\left(\frac{n\pi y}{b}\right) \sin\left(\frac{p\pi z}{d}\right) \\ \sin\left(\frac{m\pi x}{a}\right) \sin\left(\frac{n\pi y}{b}\right) \cos\left(\frac{p\pi z}{d}\right) \end{pmatrix} \sin(\omega t + \varphi)$$

$$\mathbf{B} = E_0 \frac{\omega}{k_c^2 c^2} \begin{pmatrix} \frac{n\pi}{b} \sin\left(\frac{m\pi x}{a}\right) \cos\left(\frac{n\pi y}{b}\right) \cos\left(\frac{p\pi z}{d}\right) \\ -\frac{m\pi}{a} \cos\left(\frac{m\pi x}{a}\right) \sin\left(\frac{n\pi y}{b}\right) \cos\left(\frac{p\pi z}{d}\right) \\ 0 \end{pmatrix} \cos(\omega t + \varphi)$$

where

$$k_c^2 = \left(\frac{m\pi}{a}\right)^2 + \left(\frac{n\pi}{b}\right)^2$$

$$\beta = \left[ \left(\frac{2\pi}{\lambda}\right)^2 - k_c^2 \right]^{\frac{1}{2}} = \frac{p\pi}{d}$$

$$k = \frac{2\pi}{\lambda} = \left[ \left(\frac{m\pi}{a}\right)^2 + \left(\frac{n\pi}{b}\right)^2 + \left(\frac{p\pi}{d}\right)^2 \right]^{\frac{1}{2}} = \frac{\omega}{c}$$

#### 4.4.10 Trwcell

**trwcell** (**ECS**, **Ezef**, **phi**, **w**, **L**) ;

Resonant cavity of a  $\frac{2}{3}\pi$  traveling wave buncher or linac.

<b>ECS</b>	Element Coordinate System.
<b>Ezef</b>	Effective <b>E</b> field [V/m].
<b>phi</b>	Phase factor: $\phi$ in radians.
<b>w</b>	Angular frequency: $\omega$ in [s <sup>-1</sup> ].
<b>L</b>	Cell length [m].

The fields generated by this element are given in cylindrical coordinates by:

$$E_z = M \sin(\omega t + \phi - k_z z) I_0(k_t r)$$

$$E_r = M \cos(\omega t + \phi - k_z z) I_1(k_t r) \frac{k_z}{k_t}$$

$$B_\phi = E_r / c$$

where the following definitions are used:

$$k_z = \frac{2}{3} \pi / L$$

$$k_t = \sqrt{k_z^2 - \omega^2 / c^2}$$

$$M = \frac{3\sqrt{3}}{2\pi} E_{\text{zef}}$$

The factor in front of **Ezef** is the average of a sine in range  $\frac{1}{6} \pi - \frac{5}{6} \pi$ . It converts peak field to average field and is introduced for compatibility.

The formulas are proposed by G. Saxon [7].

#### 4.4.11 Trwlinac

**trwlinac(ECS,ao,Rs,Po,P,Go,thetao,phi,w,L) ;**

Constant gradient  $\frac{2}{3} \pi$  traveling wave buncher or linac without beamloading.

<b>ECS</b>	Element Coordinate System.
<b>ao</b>	Initial attenuation constant: $\alpha_0$ .
<b>Rs</b>	Shunt impedance: $R_s$ .
<b>Po</b>	Input power, design value: $P_0$ [W].
<b>P</b>	Input power, actual power used: $P$ [W].
<b>Go</b>	Design gamma at entrance: $\gamma_0$ .
<b>thetao</b>	Bunch phase with respect to wave, design value: $\theta_0$ .
<b>phi</b>	RF phase offset: $\phi$ .
<b>w</b>	Angular frequency: $\omega$ in $[s^{-1}]$ .
<b>L</b>	Length of the structure: $L$ [m].

An rf-wave with constant amplitude travels through the structure. The phase velocity of the wave increases along the structure in such a way that an electron entering the linac with initial energy  $\gamma_0 mc^2$  is accelerated but remains in the same position relative to the wave. For this to take place, the linac needs to be operated at its design power  $P_0$  and the particle must be input at the design phase  $\theta_0$  with respect to the ‘crest’ of the wave. It is possible however to operate the linac at a different power than the design power and the particles can enter at any phase.

According to the design values the amplitude and phase of the field that accelerates the particles is:

$$E_0 = \sqrt{2\alpha_0 R_s P_0} \cos(\theta_0)$$

$$\phi = \omega t - \int_0^z k_z(z') dz' + \theta_0$$

where  $z$  is the longitudinal position of the particle relative to the beginning of the structure.

To calculate the integral, we first calculate the particle velocity using the linear increase in energy from  $\gamma_0 mc^2$  to  $\gamma_0 mc^2 + E_0 q_e z$ :

$$\beta(z)^2 = 1 - \frac{1}{(\gamma_0 + Fz)^2}$$

where  $F$  is the normalized design acceleration:

$$F = -\frac{E_0 q_e}{m_e c^2}$$

The longitudinal and transverse wavenumbers are given by:

$$k_z = \frac{k_0}{\beta(z)}, \quad k_t = \sqrt{k_z^2 - k_0^2}$$

$$\text{where } k_0 = \frac{\omega}{c}$$

Yielding:

$$\int_0^z k_z(z') dz' = \frac{k_0}{F} \left[ \sqrt{(Fz + \gamma_0)^2 - 1} - \sqrt{\gamma_0^2 - 1} \right]$$

The amplitude and phase of the actual accelerating field are due to the rf input power  $P$  and the rf phase  $\varphi$ . They are given by:

$$E_1 = \sqrt{2\alpha_0 R_s P}$$

$$\theta = \omega t - \int_0^z k_z(z') dz' + \varphi$$

$P$  may differ from  $P_0$  and  $\varphi$  does not need to be chosen such that the particles enter the linac at phase  $\theta_0$ .

The fields produced in cylindrical coordinates are:

$$E_z = E_1 \sin(\theta) I_0(k_t r)$$

$$E_r = E_1 \cos(\theta) I_1(k_t r) \frac{k_z}{k_t}$$

$$B_\varphi = \frac{E_r}{c}$$

This element is shaped using an erf function at the entrance and exit of the structure. The characteristic length is 1 mm. The shaping does not affect the numerical results but improves the simulation speed considerably because it reduces the sudden turn on and off of the fields.

#### 4.4.12 Trwlinbm

**trwlinbm**(ECS,ao,Rs,Po,P,Ib,Go,thetao,phi,w,L) ;

Constant gradient  $\frac{2}{3}\pi$  traveling wave buncher or linac with selfconsistent beamloading.

<b>ECS</b>	Element Coordinate System.
<b>ao</b>	Initial attenuation constant: $\alpha_0$ .
<b>Rs</b>	Shunt impedance: $R_s$ .
<b>Po</b>	Input power, design value: $P_0$ [W].
<b>P</b>	Input power, actual power used: $P$ [W].
<b>Ib</b>	Beam current: $I_b$ .
<b>Go</b>	Design gamma at entrance: $\gamma_0$ .
<b>thetao</b>	Bunch phase with respect to wave, design value: $\theta_0$ .
<b>phi</b>	RF phase offset: $\varphi$ .
<b>w</b>	Angular frequency: $\omega$ .in [s <sup>-1</sup> ].
<b>L</b>	Length of the structure: $L$ [m].

The electromagnetic fields generated by this element are separated into two independent waves:

- The accelerating rf-wave.
- The beam induced beamloading wave.

The accelerating wave is calculated in precisely the same way as in trwlinac, described in section 4.4.11. The beamloading wave has the same structure, i.e. the same wavenumbers, but different amplitude and phase. When the linac is run at its design values, the beamloading field opposes the accelerating field and the field's amplitude increases along the structure. When the linac is used far off its nominal settings, analytical expressions or correct approximations for the beamloading wave can not be derived. To allow this model to be used for all input settings, differential equations for the beamloading amplitude and phase are solved while tracing the particles.

The accelerating rf-wave has amplitude  $E_1$  and  $\varphi$  as defined in section 4.4.11. The beamloading wave has amplitude  $E_b$  and phase  $\varphi + \varphi_b$ . Because the structure of both waves is similar, the total fields are:

$$\begin{aligned}
E_z &= (E_1 \sin(\theta) + E_b \sin(\theta + \theta_b)) I_0(k_t r) \\
E_r &= (E_1 \cos(\theta) + E_b \cos(\theta + \theta_b)) I_1(k_t r) \frac{k_z}{k_t} \\
B_\phi &= \frac{E_r}{c}
\end{aligned}$$

Both the amplitude and phase of the beamloading wave are calculated from the particle trajectories. However, an amplitude and phase representation is not very efficient computationally. Therefore the beamloading wave is internally characterized by the amplitudes  $u$  and  $v$  of two independent waves,  $90^\circ$  out of phase.

$$\begin{cases} u = A \cos(\varphi_b) \\ v = A \sin(\varphi_b) \end{cases} \Rightarrow \begin{cases} A \sin(\theta + \varphi_b) \rightarrow u \sin(\theta) + v \cos(\theta) \\ A \cos(\theta + \varphi_b) \rightarrow u \cos(\theta) - v \sin(\theta) \end{cases}$$

The differential equations for  $u$  and  $v$  to be solved are then given by:

$$\begin{aligned}
\frac{du}{dt} &= \frac{du}{dz} \frac{dz}{dt} = \frac{\alpha_0 I_b R_s}{1 - 2\alpha_0 z} \frac{v_z}{N} \sin(\theta) \\
\frac{dv}{dt} &= \frac{dv}{dz} \frac{dz}{dt} = \frac{\alpha_0 I_b R_s}{1 - 2\alpha_0 z} \frac{v_z}{N} \cos(\theta)
\end{aligned}$$

with boundary condition

$$u_{t=0} = v_{t=0} = 0$$

The  $u$  and  $v$  representation is transformed back using:

$$\begin{aligned}
E_b &= \sqrt{u^2 + v^2} \\
\varphi_b &= \arctan\left(\frac{v}{u}\right)
\end{aligned}$$

The amplitude and the phase of the beamloading wave are written in the outputfile as **Eb** and **phib**.



## 4.5 Static electric fields

This section contains the elements generating static electric fields.

4.5.1	Circlecharge.....	155
4.5.2	Ecyl.....	155
4.5.3	Ehole.....	156
4.5.4	Erect.....	157
4.5.5	Linecharge .....	157
4.5.6	Platecharge .....	157
4.5.7	Pointcharge.....	157
4.5.8	pointchargeset.....	158

### 4.5.1 Circlecharge

**circlecharge (ECS, R, lambda) ;**

Circle with homogeneous charge density.

**ECS**                      Element Coordinate System.  
**R**                              Radius of the ring [m].  
**lambda**                      Charge density [C/m].

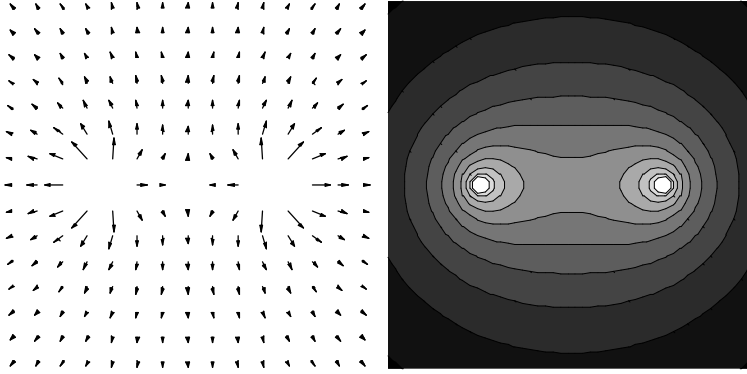


Figure 4-4: Electric field in the xz-plane and corresponding potential.

The circle with radius **R** having a homogeneous charge density **lambda** in [C/m] is located in the xy-plane centered around the origin. The potential of the electric field is given in spherical coordinates by:

$$V(r, \theta) = \frac{\lambda R}{4\pi\epsilon_0} \int_0^{2\pi} \frac{1}{\sqrt{R^2 + r^2 - 2Rr \sin(\theta) \cos(\phi)}} d\phi$$

The electric field is calculated from  $\mathbf{E} = -\nabla V$ . The integral and gradient are calculated analytically.

### 4.5.2 Ecyl

**ecyl (ECS, R, L, E) ;**

Constant **E** field bounded by cylinder.

**ECS**                      Element Coordinate System.  
**R**                              Radius of the cylinder [m].  
**L**                              Cylinder length [m].  
**E**                              Electric field strength [V/m].

The **E** field generated by this element is given by:

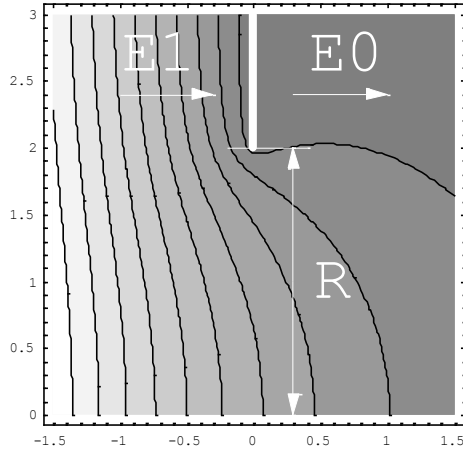
$$\mathbf{E} = \begin{cases} \mathbf{E}\hat{z} & \text{if } x^2 + y^2 < R^2 \text{ and } |z| < \frac{1}{2}L \\ 0 & \text{otherwise} \end{cases}$$

### 4.5.3 Ehole

**ehole**(ECS,R,E1,E0) ;

Two regions with uniform electric field, separated by a conducting plate with circular hole.

**ECS**            Element Coordinate System.  
**R**                Radius of the hole.  
**E1**               Uniform field strength at negative  $z$ .  
**E0**               Uniform field strength at positive  $z$ .



This element models two regions of uniform electric field in the  $z$ -direction, separated by an infinitely thin conducting plate with a circular hole. The electromagnetic field is fully analytic, where the effect of the hole is given by [8]:

$$V(z,r) = \frac{(E0 - E1)R}{\pi} \left( \sqrt{\frac{\rho - \lambda}{2}} - \frac{|z|}{R} \arctan \left( \sqrt{\frac{2}{\rho + \lambda}} \right) \right)$$

with  $\lambda = (z^2 + r^2)/R^2 - 1$  and  $\rho = \sqrt{\lambda^2 + 4z^2/R^2}$ . In case  $R$  is specified as zero, this element reduces to two regions of uniform electric field in the  $z$ -direction.

To remove particles crossing the plate, **ehole** can be combined with **scatteriris** as shown below:

```
; Plate at z=1 m, with 1 mm hole.
zplate = 1 ;
radius = 1e-3 ;
ehole("wcs","z",zplate, radius, E1, E0) ;
; Remove particles crossing the plate
forwardscatter("wcs","I","remove", 0) ;
scatteriris("wcs","z",zplate, radius,1) scatter="remove" ;
```

#### Example: Einzel lens

The **ehole** element is not particularly useful itself, as it stretches from  $-\infty$  to  $+\infty$ . However, it can be used as building block to construct all kinds of electrostatic focusing systems. For example an Einzel lens can easily be constructed by combining three **ehole** elements:

```
zcenter = 1 ;
separation = 0.1 ;
radius = 10e-3
ehole("wcs","z",zcenter-separation, radius, -Efield/2, Efield/2) ;
ehole("wcs","z",zcenter, radius, Efield, -Efield) ;
ehole("wcs","z",zcenter+separation, radius, -Efield/2, Efield/2) ;
rmax("wcs","z",zcenter, radius,2*separation) ;
```

Note: The above summation of three **ehole** elements is only correct if **radius** is much smaller than **separation**. If this assumption is violated an external Poisson solver, such as present in the Superfish set

of codes, must be used to obtain the electrostatic fields. The resulting field can subsequently be imported into GPT with the **map2D\_E** element.

#### 4.5.4 Erect

**erect(ECS,a,b,L,E) ;**

Constant **E** field bounded by a rectangular box.

<b>ECS</b>	Element Coordinate System.
<b>a</b>	Total box length in x-direction [m].
<b>b</b>	Total box length in y-direction [m].
<b>L</b>	Total box length in z-direction [m].
<b>E</b>	Electric field strength [V/m].

The **E** field generated by this element is given by:

$$\mathbf{E} = \begin{cases} \mathbf{E}\hat{z} & \text{if } |x| < \frac{1}{2}\mathbf{a}, |y| < \frac{1}{2}\mathbf{b}, |z| < \frac{1}{2}\mathbf{L} \\ 0 & \text{otherwise} \end{cases}$$

#### 4.5.5 Linecharge

**linecharge(ECS,L,lambda) ;**

Line with homogeneous charge density.

<b>ECS</b>	Element Coordinate System.
<b>L</b>	Total line length [m].
<b>lambda</b>	Line charge density [C/m].

The equation for the line is:  $x = y = 0, |z| < \frac{1}{2}\mathbf{L}$

The electric field generated by this element is given by:

$$\mathbf{E} = -\text{grad} \left( \frac{\lambda}{4\pi\epsilon_0} \int_{-L/2}^{L/2} \frac{1}{\sqrt{x^2 + y^2 + (z-z')^2}} dz' \right)$$

where the integral and gradient are calculated analytically.

#### 4.5.6 Platecharge

**platecharge(ECS,a,b,sigma) ;**

Rectangular plate with homogeneous charge density.

<b>ECS</b>	Element Coordinate System.
<b>a</b>	Total plate length in x-direction [m].
<b>b</b>	Total plate length in y-direction [m].
<b>sigma</b>	Surface charge density [C/m <sup>2</sup> ].

The equation for the plate is:  $z = 0, |x| < \frac{1}{2}\mathbf{a}, |y| < \frac{1}{2}\mathbf{b}$

The electric field generated by this element is given by:

$$\mathbf{E} = -\text{grad} \left( \frac{\sigma}{4\pi\epsilon_0} \int_{-a/2}^{a/2} \int_{-b/2}^{b/2} \frac{1}{\sqrt{(x-x')^2 + (y-y')^2 + z^2}} dy' dx' \right)$$

where the integral and gradient are calculated analytically.

#### 4.5.7 Pointcharge

**pointcharge(ECS,Q) ;**

Pointcharge at the origin.

<b>ECS</b>	Element Coordinate System.
<b>Q</b>	Charge in Coulomb.

The electric field generated by this element in spherical coordinates is given by:

$$\mathbf{E} = \frac{Q}{4\pi\epsilon_0} \frac{\mathbf{r}}{|\mathbf{r}|^3}$$

#### 4.5.8 pointchargeset

**pointchargeset(set, theta) ;**

Electrostatic field of a point charge distribution, calculated with the Barnes-Hut tree algorithm [9,10].

<b>set</b>	Particle set
<b>theta</b>	Overall accuracy parameter. The typical range is from 0.3 (publication quality) to 1.0 (quick and dirty).

The main use of **pointchargeset** is to specify a fixed particle set, such as an ion background while tracking electrons. All particles in the specified set are removed from the tracking and internally stored as a fixed electrostatic field.

For efficiency reasons, the Barnes&Hut hierarchical tree method is used to calculate the combined field. This method allows a tradeoff between speed and accuracy, governed by the **theta** parameter. Please see the analogous element **spacecharge3Dtree** in section 4.8.2 for a more detailed description.

To avoid singularities, it is important to set the smoothing length **R** of the particles. The current implementation only allows identical radii:

**setmacrodist(set, "u", R, 0)**

## 4.6 Static magnetic fields

This section contains elements that model static magnetic fields.

4.6.1	Barmagnet .....	159
4.6.2	Bmultipole .....	160
4.6.3	Bzsolenoid .....	162
4.6.4	Isectormagnet .....	162
4.6.5	Linecurrent .....	164
4.6.6	Magline.....	165
4.6.7	Magplate.....	165
4.6.8	Magdipole.....	165
4.6.9	Magpoint .....	166
4.6.10	Quadrupole .....	166
4.6.11	Rectcoil.....	167
4.6.12	Rectmagnet.....	168
4.6.13	Sectormagnet.....	168
4.6.14	Sextupole .....	171
4.6.15	Solenoid.....	172

The elements **magpoint**, **magline** and **magplate** calculate a **B** field as if magnetic charge were present. They can be convenient in a simulation, but should be used with caution because magnetic charge does not exist. The **B** field generated by a monopole is assumed to be [11]:

$$\mathbf{B} = \frac{\mu_0 P}{4\pi} \frac{\mathbf{r}}{|\mathbf{r}|^3}$$

with  $P$  the magnetic pole strength. The fields of the magnetic line charge  $\lambda_m$  and surface charge  $\sigma_m$  are derived analogue to the electrical case.

The magnetic scalar potential  $\Phi$  is defined such that  $\mathbf{B} = -\text{grad}(\Phi)$  analogous to the electrical case.

### 4.6.1 Barmagnet

**barmagnet** (**ECS**, **a**, **b**, **L**, **B**) ;

Rectangular magnet modeled as two plates with opposite magnetic charge density.

<b>ECS</b>	Element Coordinate System.
<b>a</b>	Magnet length in x-direction [m].
<b>b</b>	Magnet length in y-direction [m].
<b>L</b>	Magnet length in z-direction [m].
<b>B</b>	Nominal magnetic field [T].

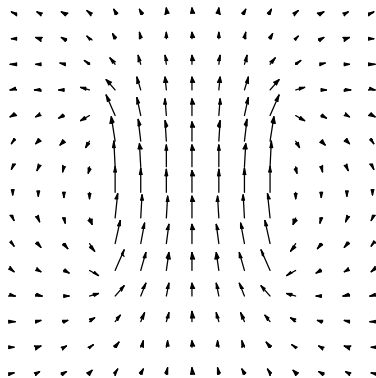


Figure 4-5: Typical **B** field in the x-z- and y-z-plane.

The **B** field generated by this element can be written as the field of two identical plates with opposite magnetic surface charge density. The plates are located at:

$$|x| < \frac{1}{2} \mathbf{a}, |y| < \frac{1}{2} \mathbf{b}, z = \pm \frac{1}{2} \mathbf{L}.$$

with corresponding surface charge density:

$$\sigma_m = \pm \frac{\mathbf{B}}{\mu_0}$$

Within the magnet  $\{0,0,\mathbf{B}\}$  is added to the magnetic field to convert the  $\mathbf{H}$  field to a  $\mathbf{B}$  field.

For the magnetic field generated by a rectangular plate with homogeneous magnetic surface charge density see **magplate**, section 4.6.7.

#### 4.6.2 Bmultipole

**Bmultipole**(**ECS**,**zlen**, **Bdipole**,**Bdl**,**Bb1**, **Gquadrupole**,**Gdl**,**Gbl**,  
**Hsextupole**,**Hdl**,**Hb1**, **Ooctupole**,**Odl**,**Ob1**) ;  
Generic magnetic multipole with fringe fields

<b>ECS</b>	Element Coordinate System
<b>zlen</b>	Length of element
<b>Bdipole</b>	Nominal dipole field [T]. Normally this is $\pm mc\gamma\beta/qR$ .
<b>Bdl</b>	Dipole fringe field offset for the entry and exit planes [m] to change the effective length.
<b>Bb1</b>	First coefficient of the dipole fringe Enge function [m <sup>-1</sup> ]. Must be nonzero.
<b>Gquadrupole</b>	Nominal quadrupole gradient [T/m].
<b>Gdl</b>	Quadrupole fringe field offset for the entry and exit planes [m].
<b>Gbl</b>	First coefficient of the quadrupole fringe Enge function [m <sup>-1</sup> ].
<b>Hsextupole</b>	Nominal sextupole gradient [T/m <sup>2</sup> ].
<b>Hdl</b>	Sextupole fringe field offset for the entry and exit planes [m].
<b>Hb1</b>	First coefficient of the sextupole fringe Enge function [m <sup>-1</sup> ].
<b>Ooctupole</b>	Nominal octupole gradient [T/m <sup>3</sup> ].
<b>Odl</b>	Sextupole fringe field offset for the entry and exit planes [m].
<b>Ob1</b>	First coefficient of the sextupole fringe Enge function [m <sup>-1</sup> ].

This element models a generic magnetic multipole based on 7<sup>th</sup> order expansion around the z-axis, including fringe fields. The field-profile on-axis for each of the multipole-components is assumed to be a first-order Enge function as function of  $z$  of the form:

$$f(z; L, A, dl, bl) = A \left( \frac{1}{1 + e^{bl(-z - (\frac{1}{2}L + dl))}} + \frac{1}{1 + e^{bl(+z - (\frac{1}{2}L + dl))}} - 1 \right)$$

where  $A$  is the overall amplitude,  $L$  the length of the element,  $dl$  a correction tem for the length and  $bl$  a measure for the inverse steepness of the fringes. The amplitude, length correction and steepness can be individually specified for each multipole-component, as documented in the parameter list. For example, the quadrupole component has an on-axis gradient in [T/m] given by  $f(z, \mathbf{L}, \mathbf{Gquadrupole}, \mathbf{Gdl}, \mathbf{gbl})$ .

Implemented is a 7<sup>th</sup> order expansion for the magnetic potential  $V$  given by:

$$V(z) = \sum_{n=1}^7 \sum_{m=1}^7 c_{nm}(z) \frac{r^m}{m} \sin(n\theta)$$

where

$$r = \sqrt{x^2 + y^2}$$

$$\theta = \arctan(x, y)$$

and where  $\mathbf{B} = \nabla V$ .

Maxwell equation requiring  $\nabla^2 B = O(r^6)$  and the given parameters are used to uniquely construct the  $c_{nm}(z)$  coefficients. This yields:

$$c_{11}(z) = f(z, \mathbf{L}; \mathbf{Bdipole}, \mathbf{Bd1}, \mathbf{Bb1})$$

$$c_{22}(z) = f(z, \mathbf{L}; \mathbf{Gquadrupole}, \mathbf{Gd1}, \mathbf{Gb1})$$

$$c_{33}(z) = f(z, \mathbf{L}; \mathbf{Hsextupole}, \mathbf{Hd1}, \mathbf{Hb1})$$

$$c_{44}(z) = f(z, \mathbf{L}; \mathbf{Ooctupole}, \mathbf{Od1}, \mathbf{Ob1})$$

$$c_{13}(z) = -\frac{3}{8} c_{11}''(z) \quad c_{35}(z) = -\frac{5}{48} c_{33}''(z) \quad c_{17}(z) = -\frac{7}{9216} c_{11}^{(6)}(z)$$

$$c_{24}(z) = -\frac{1}{6} c_{22}''(z) \quad c_{26}(z) = +\frac{1}{128} c_{22}^{(4)}(z) \quad c_{37}(z) = +\frac{7}{1920} c_{33}^{(4)}(z)$$

$$c_{15}(z) = +\frac{5}{192} c_{11}^{(4)}(z) \quad c_{46}(z) = -\frac{3}{40} c_{44}''(z) \quad c_{57}(z) = -\frac{7}{120} c_{55}''(z) = 0$$

A graphical representation of the fields, in the fringe region at  $z=L/2$ , is shown in the figures below. The color-scale ranges from blue, via green and yellow, to red. This scale is set individually for each plot, so the plots cannot be compared in absolute value.

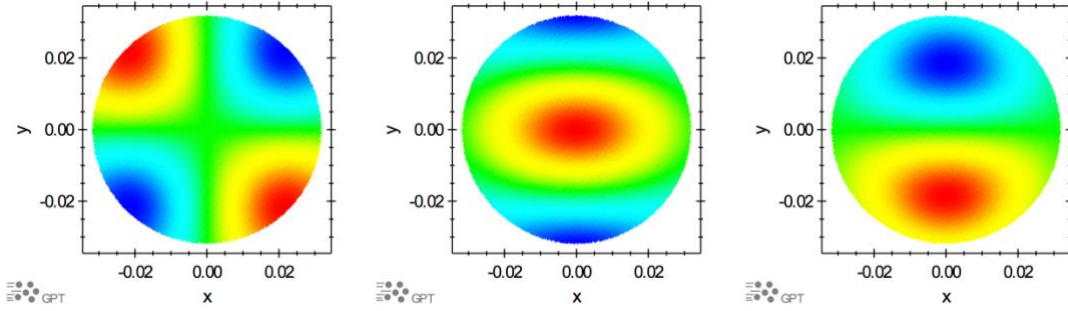


Figure 4-6: Dipole fields for the  $B_x$ ,  $B_y$  and  $B_z$  components respectively in the fringe region.

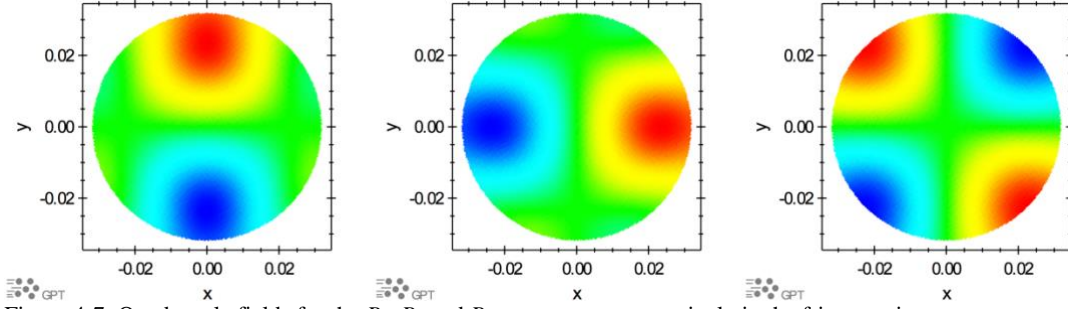


Figure 4-7: Quadrupole fields for the  $B_x$ ,  $B_y$  and  $B_z$  components respectively in the fringe region.

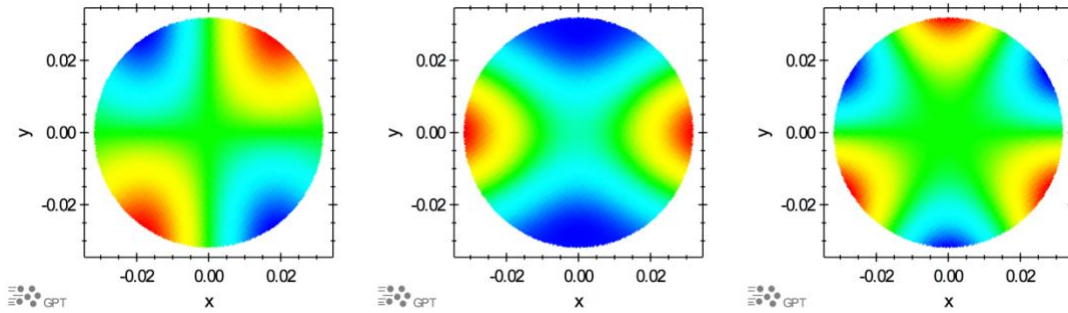


Figure 4-8: Sextupole fields for the  $B_x$ ,  $B_y$  and  $B_z$  components respectively in the fringe region.

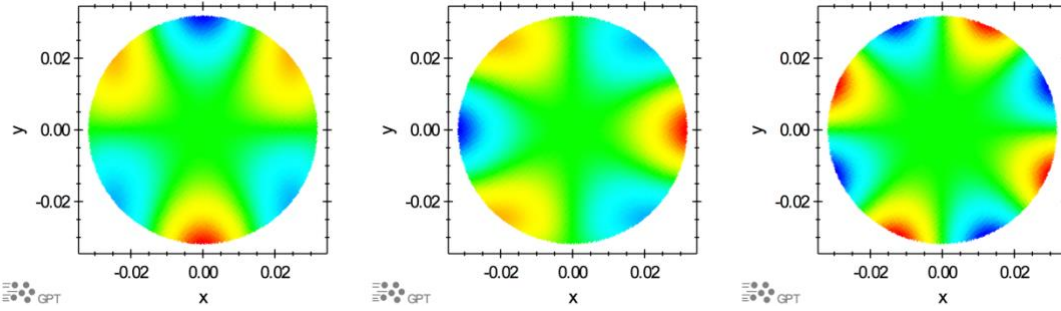


Figure 4-9: Octupole fields for the  $B_x$ ,  $B_y$  and  $B_z$  components respectively in the fringe region.

#### 4.6.3 Bzsolonoid

**bzsolenoid**(**ECS**,**R**,**L**,**nI**) ;

A homogeneous solenoid without thickness approximated as circular current sheet.

<b>ECS</b>	Element Coordinate System.
<b>R</b>	Radius of the solenoid [m].
<b>L</b>	Solenoid length [m].
<b>nI</b>	Ampere turns per meter [A].

The fields generated by this element in cylindrical coordinates are:

$$B_z = \frac{1}{2} \mu_0 \left[ \frac{z + \frac{1}{2} L}{\left\{ \left( z + \frac{1}{2} L \right)^2 + R^2 \right\}^{\frac{1}{2}}} - \frac{z - \frac{1}{2} L}{\left\{ \left( z - \frac{1}{2} L \right)^2 + R^2 \right\}^{\frac{1}{2}}} \right] nI$$

$$B_r = -\frac{r}{4} \mu_0 \left[ \frac{1}{\left\{ \left( z + \frac{1}{2} L \right)^2 + R^2 \right\}^{\frac{3}{2}}} - \frac{1}{\left\{ \left( z - \frac{1}{2} L \right)^2 + R^2 \right\}^{\frac{3}{2}}} \right] nI R^2$$

$$B_\phi = 0$$

The fields generated are only correct near the **z**-axis of the element.

#### 4.6.4 Isectormagnet

**isectormagnet**(**fromCCS**,**toCCS**,**[finalCCS]**,**R**,**Bfield**,**Bd1**,**Bb1**,**Gquadrupole**,**Gd1**,**Gb1**,**Hsextupole**,**Hd1**,**Hb1**) ;

A sectormagnet with optional quadrupole and sextupole components, including fringe fields.

<b>fromCCS</b>	Name of the CCS the particles start on.
<b>toCCS</b>	Name of the CCS the particles are bended to.
<b>finalCCS</b>	Optional name of the CCS where to position the magnet.
<b>R</b>	Radius of the bend [m].
<b>Bfield</b>	Nominal dipole field [T]. Normally this is $\pm mc\gamma\beta/qR$ .
<b>Bd1</b>	Dipole fringe field offset for the entry and exit planes [m] to change the effective length.
<b>Bb1</b>	First coefficient of the dipole fringe Enge function [m <sup>-1</sup> ]. Must be nonzero.
<b>Gquadrupole</b>	Nominal quadrupole gradient [T/m].
<b>Gd1</b>	Quadrupole fringe field offset for the entry and exit planes [m].
<b>Gb1</b>	First coefficient of the quadrupole fringe Enge function [m <sup>-1</sup> ].
<b>Hsextupole</b>	Nominal sextupole gradient [T/m <sup>2</sup> ].
<b>Hd1</b>	Sextupole fringe field offset for the entry and exit planes [m].
<b>Hb1</b>	First coefficient of the sextupole fringe Enge function [m <sup>-1</sup> ].

This element models a sectormagnet based on 7<sup>th</sup> order multipole expansion along a curved trajectory. The position of the magnet is given by the intersection of **fromCCS** and **toCCS**, fully analogous to a normal **sectormagnet** element. The radius of curvature for the nominal **Bfield** is assumed to be **R**. The inverse steepness of the fringe fields can be adjusted with the **Bb1** parameter, and an offset of the entry and exit planes can be specified using **Bd1**. Independent on the dipole component, a quadrupole and sextupole



component can be specified using **Gquadrupole**, **Gb1** and **Gd1** for the quadrupole and **Hsextupole**, **Hb1** and **Hd1** for the sextupole component.

To describe the fields of this element, a toroidal coordinate system is used where a circle in the  $xz$ -plane, represented as  $(r, \theta)$  is centered at offset  $R$  and rotated around the  $z$ -axis over toroidal angle  $\varphi$ . Consequently:

$$\begin{aligned} r &= \sqrt{\left(\sqrt{x^2 + y^2} - R\right)^2 + z^2} \\ \theta &= \arctan(\sqrt{x^2 + y^2} - R, z) \\ \varphi &= \arctan(x, y) \end{aligned}$$

This specific coordinate system is chosen because it can be positioned in 3D space such that particles travelling through a curved trajectory with radius  $R$  will always have very small  $r$  coordinates. This allows a multipole expansion in  $r$  to approximate off-axis fields.

The field-profile on-axis for the dipole, quadrupole and sextupole components of this element is assumed to be a first-order Enge function as function of  $\varphi$  of the form:

$$f(\varphi; L, A, dl, bl) = A \left( \frac{1}{1 + e^{\frac{R bl}{L} (-\varphi - (\frac{1}{2}L + dl/R))}} + \frac{1}{1 + e^{\frac{R bl}{L} (\varphi - (\frac{1}{2}L + dl/R))}} - 1 \right)$$

where  $A$  is the overall amplitude,  $L$  the length of the element in radians,  $dl$  a correction term for the length and  $bl$  a measure for the inverse steepness of the fringes. The amplitude, length correction and steepness can be individually specified for each multipole-component, as documented in the parameter list. For example for the quadrupole component has an on-axis gradient in [T/m] given by  $f(\varphi, L, \mathbf{Gquadrupole}, \mathbf{Gd1}, \mathbf{gb1})$ .

The fields are implemented as a 7<sup>th</sup> order expansion for the magnetic potential  $V$  given by:

$$V(\varphi) = \sum_{n=1}^7 \sum_{m=1}^7 c_{nm}(\varphi) \frac{r^m}{m} \sin(n\theta)$$

where

$$B = \nabla V = \sum_{n=1}^7 \sum_{m=1}^7 \frac{r^{m-1}}{m \rho} \begin{pmatrix} c_{nm}(\varphi) \rho (m \cos(\theta) \sin(n\theta) - n \sin(\theta) \cos(n\theta)) \cos(\varphi) - c_{nm}'(\varphi) r \sin(\varphi) \sin(n\theta) \\ c_{nm}(\varphi) \rho (m \cos(\theta) \sin(n\theta) - n \sin(\theta) \cos(n\theta)) \sin(\varphi) + c_{nm}'(\varphi) r \cos(\varphi) \sin(n\theta) \\ c_{nm}(\varphi) \rho^2 (m \sin(\theta) \sin(n\theta) + n \cos(\theta) \cos(n\theta)) \sin(\varphi) \end{pmatrix}$$

and  $\rho = R + r \cos(\theta)$ .

The dipole, quadrupole and sextupole components,  $c_{11}$ ,  $c_{22}$  and  $c_{33}$  respectively, are defined by the following expressions as function of toroidal angle  $\varphi$ :

$$c_{11}(\varphi) = f(z, L; \mathbf{Bdipole}, \mathbf{Bd1}, \mathbf{Bb1})$$

$$c_{22}(\varphi) = f(z, L; \mathbf{Gquadrupole}, \mathbf{Gd1}, \mathbf{Gb1})$$

$$c_{33}(\varphi) = f(z, L; \mathbf{Hsextupole}, \mathbf{Hd1}, \mathbf{Hb1})$$

These expressions are identical the on-axis fringe fields of a normal sectormagnet, and also identical to the on-axis gradient of a quadrupole with analytical fringes. The other multipole components along the curved trajectory are uniquely defined up to  $n^{\text{th}}$  order by requiring that the Laplacian of the magnetic potential is zero up to  $n^{\text{th}}$  order in  $r$ . Consequently:

$$\nabla^2 B = \sum_{n=1}^7 \sum_{m=1}^7 -\frac{r^{m-2}}{2m \rho^2} \left( 2c_{nm}(\varphi) \rho (nr \cos(n\theta) \sin(\theta) - (\rho(m^2 - n^2 + m) - mR) \sin(n\theta)) - 2c_{nm}''(\varphi) r^2 \sin(n\theta) \right)$$

must vanish up-to  $n^{\text{th}}$  order for all  $\theta$ . This yields:

$$c_{13}(\varphi) = \frac{-3}{8R^2} (Rc_{22}(\varphi) + c_{11}''(\varphi))$$

$$c_{24}(\varphi) = \frac{1}{24R^3} (5Rc_{22}(\varphi) - 8R^2c_{33}(\varphi) + 9c_{11}''(\varphi) - 4Rc_{22}''(\varphi))$$

$$c_{15}(\varphi) = \frac{5}{768R^4} (-15Rc_{22}(\varphi) + 24R^2c_{33}(\varphi) - 35c_{11}''(\varphi) + 24Rc_{22}''(\varphi) + 4c_{11}^{(4)}(\varphi))$$

$$c_{35}(\varphi) = \frac{5}{1536R^4} (-35Rc_{22}(\varphi) + 56R^2c_{33}(\varphi) - 87c_{11}''(\varphi) + 52Rc_{22}''(\varphi) - 32R^2c_{33}''(\varphi))$$

$$c_{26}(\varphi) = \frac{1}{1024R^5} (105Rc_{22}(\varphi) - 168R^2c_{33}(\varphi) + 301c_{11}''(\varphi) - 232Rc_{22}''(\varphi) + 96R^2c_{33}''(\varphi) - 44c_{11}^{(4)}(\varphi) + 8Rc_{22}^{(4)}(\varphi))$$

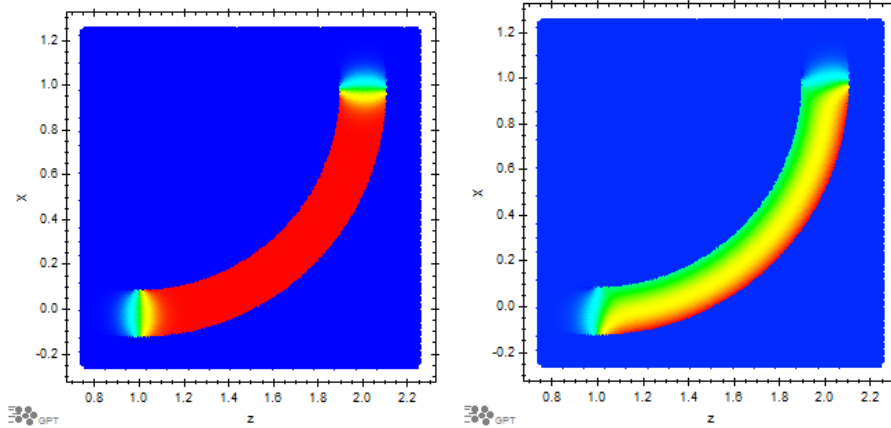
The remaining  $c_{46}$ ,  $c_{17}$ ,  $c_{37}$  and  $c_{77}$  coefficients are not particularly illuminating apart from the fact that derivatives of increasing order are used, that  $n < m$  and that  $n+m$  is always even.

Particles are removed from the simulations when they are far outside the convergence range of the power series. This happens when  $r b I > \pi$ .

#### 4.6.4.1 Example

The following example visualizes a 90° indexed sectormagnet with and without field-index:

```
1. Rbend = 1 ;
2. beta = 0.99 ;
3. gamma = 1/sqrt(1-beta^2) ;
4. Bfield = -me*c*gamma*beta/(qe*Rbend) ;
5.
6. angle = pi/2 ;
7. ccs("wcs",0,0,2, cos(angle),0,-sin(angle),0,1,0, "ccs") ;
8. sectormagnet_indexed("wcs","ccs","wcs",Rbend, Bfield,0.0,30, .05,0,30, 0,0,0) ;
9.
10. setparticles("beam",100000,me,qe,0) ;
11. setxdist("beam","u",0.5,1.5) ;
12. setzdist("beam","u",1.5,1.5) ;
13. tout(0) ;
```



$B_y$  component of the field, without (left) and with (right) field-index.

#### 4.6.5 Linecurrent

```
linecurrent(ECS, x1,y1,z1, x2,y2,z2, I) ;
```

Straight line segment.

<b>ECS</b>	Element Coordinate System.
<b>x1,y1,z1</b>	Start position of the line [m].
<b>x2,y2,z2</b>	End position of the line [m].
<b>I</b>	Current through the line [A].

The line runs from  $(x_1, y_1, z_1)$  to  $(x_2, y_2, z_2)$ . The current flows from the starting point of the line to the endpoint.

The field of this element is calculated in a frame in which the  $\mathbf{z}$ -direction is parallel to the line segment and the origin is chosen to be the center point of the line. In this new coordinate system, the magnetic field generated by this element is given by:

$$\mathbf{B} = \nabla \times \frac{\mu_0 \mathbf{I}}{4\pi} \left( 0, 0, \int_{z-L/2}^{z+L/2} \frac{1}{\sqrt{x^2 + y^2 + z'^2}} dz' \right)$$

$$L = \sqrt{(x_2 - x_1)^2 + (y_2 - y_1)^2 + (z_2 - z_1)^2}$$

where the integral and curl are calculated analytically.

#### 4.6.6 Magline

**magline**(ECS, L, lambda) ;

Line with homogeneous magnetic charge density.

**ECS**                      Element Coordinate System.  
**L**                         Total line length [m].  
**lambda**                  Magnetic line charge density [A].

The equation for the line is:  $x = y = 0$ ,  $|z| < \frac{1}{2} L$

The magnetic field generated by this element is given by:

$$\mathbf{B} = -\text{grad} \left( \frac{\mu_0 \lambda}{4\pi} \int_{-L/2}^{L/2} \frac{1}{\sqrt{x^2 + y^2 + (z - z')^2}} dz' \right)$$

where the integral and gradient are calculated analytically.

#### 4.6.7 Magplate

**magplate**(ECS, a, b, sigma) ;

Rectangular plate with homogeneous magnetic charge density.

**ECS**                      Element Coordinate System.  
**a**                         Total plate length in x-direction [m].  
**b**                         Total plate length in y-direction [m].  
**sigma**                    Magnetic surface charge density [A/m].

The equation for the plate is:  $z = 0$ ,  $|x| < \frac{1}{2} a$ ,  $|y| < \frac{1}{2} b$

The magnetic field generated by this element is given by:

$$\mathbf{B} = -\text{grad} \left( \frac{\mu_0 \sigma}{4\pi} \int_{-a/2}^{a/2} \int_{-b/2}^{b/2} \frac{1}{\sqrt{(x - x')^2 + (y - y')^2 + z^2}} dy' dx' \right)$$

where the integrals and gradient are calculated analytically.

#### 4.6.8 Magdipole

**magdipole**(ECS, m) ;

Magnetic mathematical dipole.

**ECS**                      Element Coordinate System.  
**m**                         Magnetic dipole moment [A m<sup>2</sup>].

This element models a mathematical magnetic dipole, located at the origin and aligned with the z-axis. The magnetostatic field is given by:

$$\mathbf{B} = \left( \frac{\mu_0 \mathbf{m}}{4\pi r^3} \right) \{3(\hat{\mathbf{m}} \cdot \hat{\mathbf{r}})\hat{\mathbf{r}} - \hat{\mathbf{m}}\}$$

#### 4.6.9 Magpoint

**magpoint(ECS, P)** ;

Magnetic pointcharge at the origin.

**ECS** Element Coordinate System

**P** Magnetic charge [Am].

The magnetic field generated by this element in spherical coordinates is given by:

$$\mathbf{B} = \frac{\mu_0 \mathbf{P} \mathbf{r}}{4\pi |\mathbf{r}|^3}$$

#### 4.6.10 Quadrupole

**quadrupole(ECS, L, Go, [b1])** ;

Magnetostatic quadrupole with optional 3D fringe fields

**ECS** Element coordinate system.

**L** Effective length of the quadrupole [m].

**Go** Nominal magnetic field gradient [T/m].

**b1** First coefficient of the fringe fields Enge function [1/m], roughly  $\pi/r_{\text{bore}}$ .

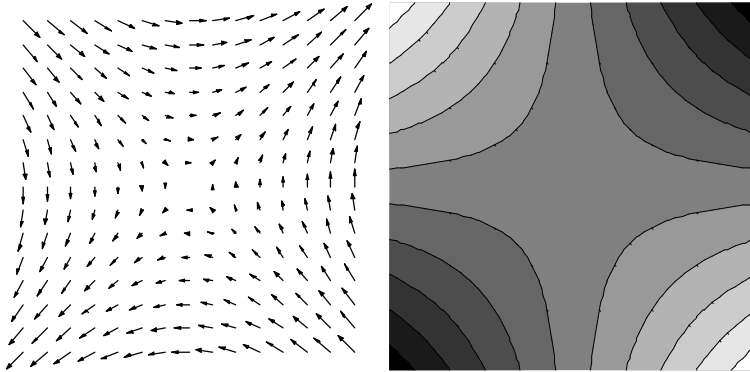


Figure 4-10: Magnetic field in the xy-plane and corresponding scalar potential.

This element models a magnetostatic quadrupole with effective length **L**, gradient **Go**, and a transverse size of approximately  $\pi/b1$ . The field equations are fully 3D and Maxwell compatible, as described by Bruno Muratori and coworkers 12. Because the fields are continuously differentiable they allow for much faster tracking compared to a hard-edged approximation.

The fields close to the axis are a normal quadrupole field:

$$\mathbf{B} = \begin{pmatrix} G(z) y \\ G(z) x \\ 0 \end{pmatrix}$$

where the gradient  $G(z)$  is given by the superposition of two Enge functions:

$$\begin{aligned} G(z) &= \mathbf{Go} \left( \frac{1}{1 + e^{b1(-z - \frac{1}{2}L)}} + \frac{1}{1 + e^{b1(+z - \frac{1}{2}L)}} - 1 \right) \\ &= \frac{\mathbf{Go}}{2} (\tanh(\frac{1}{2}b1(\frac{1}{2}L - z)) + \tanh(\frac{1}{2}b1(\frac{1}{2}L + z))) \end{aligned}$$

The shape of  $G(z)$  is a flat-top distribution in the range  $-\frac{1}{2}L < z < \frac{1}{2}L$  with amplitude **Go**, smoothed by convolution such that a) the effective length remains the same, b) the fields drops exponentially to zero outside the magnet and c) the final 3D expressions for the fields can be implemented efficiently. The

steepness of the edges is defined by the **b1** parameter, in units of [1/m]. The larger **b1**, the smaller the transverse size of the magnet and the steeper the edges.

The best way to obtain **b1** is by fitting the above equation to measured or simulated field data. However, from the 3D-case described below it will be seen that there is a field-singularity at the entrance and at the exit of the magnet at  $r=\pi/\mathbf{b1}$ . This corresponds to the physical size of the magnet and a good approximation for **b1** is therefore  $\mathbf{b1} \approx \pi/r_{\text{bore}}$  with  $r_{\text{bore}}$  the inner size of the magnet. If a level of precision is required that makes it impossible to select an appropriate **b1** we recommend switching to the **map3D\_B** element.

Particles further off-axis than  $\pi/\mathbf{b1}$  are removed from the simulation to prevent numerical problems near the field singularities. This should not pose any problems because this is within the physical magnet and particles should not be there. Furthermore, we choose to implement the equations such that the field-singularity is as far off-axis as theoretically possible given the chosen shape of  $G(z)$ .

A quadrupole with a transverse size larger than its longitudinal length can also be simulated: All equations remain the same, but the gradient just never reaches **Go**. Nevertheless, the focusing strength remains the same because

$$\int_{-\infty}^{\infty} G(z) dz = L \cdot Go$$

regardless of the choice of **L** and **b1**. This is not surprising once we realize that  $G(z)$  can be written as the convolution of a flat-top distribution and hyperbolic-secant-like distribution with unit area:

$$G(z) = \mathbf{Go} \left( H\left(\frac{1}{2}\mathbf{L} - z\right) H\left(\frac{1}{2}\mathbf{L} + z\right) \right) \otimes \frac{\mathbf{b1}}{2 + 2 \cosh(\mathbf{b1} z)}$$

where  $H(z)$  is the Heaviside step function and the area of the smoothening function

$$\int_{-\infty}^{\infty} \frac{\mathbf{b1}}{2 + 2 \cosh(\mathbf{b1} z)} dz = 1$$

The full 3D Maxwell compatible field of **quad\_fringe** are given by:

$$\begin{pmatrix} B_x \\ B_y \\ B_z \end{pmatrix} = -\frac{\mathbf{Go}}{\mathbf{b1}} \cdot \begin{pmatrix} B_{\text{fringe},x}(\mathbf{b1} x, \mathbf{b1} y, \mathbf{b1} (z - \frac{1}{2}L)) + B_{\text{fringe},x}(\mathbf{b1} x, \mathbf{b1} y, \mathbf{b1} (-z - \frac{1}{2}L)) \\ B_{\text{fringe},y}(\mathbf{b1} x, \mathbf{b1} y, \mathbf{b1} (z - \frac{1}{2}L)) + B_{\text{fringe},y}(\mathbf{b1} x, \mathbf{b1} y, \mathbf{b1} (-z - \frac{1}{2}L)) \\ B_{\text{fringe},z}(\mathbf{b1} x, \mathbf{b1} y, \mathbf{b1} (z - \frac{1}{2}L)) - B_{\text{fringe},z}(\mathbf{b1} x, \mathbf{b1} y, \mathbf{b1} (-z - \frac{1}{2}L)) \end{pmatrix}$$

where:

$$\mathbf{B}_{\text{fringe}}(x, y, z) = \frac{1}{4} \begin{pmatrix} -y - 2 \arctan\left(-\frac{\sin(y)}{e^{-z} + \cos(y)}\right) + \frac{y \sinh(z)}{\cos(x) + \cosh(z)} \\ -x - 2 \arctan\left(-\frac{\sin(x)}{e^{-z} + \cos(x)}\right) + \frac{x \sinh(z)}{\cos(y) + \cosh(z)} \\ \frac{y \sin(x)}{\cos(x) + \cosh(z)} + \frac{x \sin(y)}{\cos(y) + \cosh(z)} \end{pmatrix}$$

To maintain backward compatibility with GPT version 3.2 it is possible to omit the **b1** parameter. In that case an unrealistic hard-edged quadrupole is created with fields given by:

$$B = \begin{cases} (\mathbf{Go} y, \mathbf{Go} x, 0) & \text{if } |z| < \frac{1}{2}L \\ 0 & \text{otherwise} \end{cases}$$

Despite the fact that these fields might look much easier to calculate, they are not: The discontinuous fields stall the 5<sup>th</sup> order Runge Kutta solver of GPT resulting in much longer tracking times. For simulations where a high accuracy is required the difference can easily exceed an order of magnitude.

#### 4.6.11 Rectcoil

**rectcoil**(**ECS**, **r1**, **r2**, **L**, **I**) ;

Homogeneous solenoid with length and thickness.

<b>ECS</b>	Element Coordinate System.
<b>r1</b>	Inner radius of the coil [m].
<b>r2</b>	Outer radius of the coil [m].
<b>L</b>	Length of the coil [m].

**I** Total current through the coil [A].

To calculate the field on-axis the field of a single current loop is integrated in both the  $z$ - and  $r$ -direction:

$$B(z, r) = \int_{z1}^{z2} \int_{r1}^{r2} \frac{\mu_0 I r^2}{2(r^2 + z^2)^{3/2}} dz dr$$

where  $a = L/2$ .

The field off-axis is approximated using a 4<sup>th</sup>-order power series expansion [13].

$$B_z(z, r) = B(z) - \frac{1}{4} B''(z) r^2 + \frac{1}{64} B''''(z) r^4$$

$$B_r(z, r) = -\frac{1}{2} B'(z) r + \frac{1}{16} B'''(z) r^3$$

The fields are only correct near the  $z$ -axis of the element.

#### 4.6.12 Rectmagnet

**rectmagnet** (**ECS**, **a**, **b**, **Bfield**, **d1**, **b1**, **b2**) ;

Rectangular magnet with fringe fields.

<b>ECS</b>	Element Coordinate System
<b>a</b>	Length of the magnet in $x$ -direction [m].
<b>b</b>	Length of the magnet in $z$ -direction [m].
<b>Bfield</b>	Maximum magnetic field [T].
<b>d1</b>	Fringe field offset for the magnet's entry and exit planes [m] to change the effective length.
<b>b1</b>	First coefficient of the fringe fields Enge function [ $m^{-1}$ ]. A value of 0 disables fringe fields.
<b>b2</b>	Second order coefficient of the fringe fields Enge function [ $m^{-2}$ ]. Typically 0.

This element models a rectangular magnet with a magnetic field-component **Bfield** in the  $y$ -direction in the region  $-1/2a < x < 1/2a$  and  $-1/2b < z < 1/2b$ , see Figure 4-11.

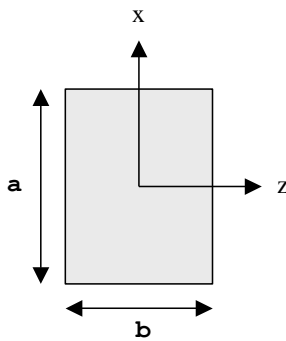


Figure 4-11: Geometry of rectmagnet.

The entrance and exit sides, assuming the  $z$ -direction as propagation direction of the particles, have fringe fields analogous to the fringe fields of the **sectormagnet** element. A reasonable estimate for **b1** is  $2/gap$ , and we recommend a zero value for both **d1** and **b2**. Please see the documentation of the **sectormagnet** element for a detailed description of the fringe fields.

#### 4.6.13 Sectormagnet

**sectormagnet** (**fromCCS**, [**finalCCS**], **toCCS**, **R**, **Bfield**, [**phiin**, **phiout**, **d1**, **b1**, **b2**]) ;

Sector magnet with options for rotated pole faces and fringe fields.

<b>fromCCS</b>	Name of the CCS the particles start on.
<b>finalCCS</b>	Name of the CCS where to position the magnet.
<b>toCCS</b>	Name of the CCS the particles are bended to.
<b>R</b>	Radius of the bend [m].
<b>Bfield</b>	Maximum magnetic field [T] in the negative $y$ -direction. Normally this is $\pm mc\gamma\beta/qR$ .

<b>phiin</b>	Angle of incident pole face [rad]. Specify 0 for normal incidence.
<b>phiout</b>	Angle of exit pole face [rad]. Specify 0 for normal incidence.
<b>d1</b>	Fringe field offset for the magnet's entry and exit planes [m] to change the effective length.
<b>b1</b>	First coefficient of the fringe fields Enge function [ $\text{m}^{-1}$ ]. A value of 0 disables fringe fields.
<b>b2</b>	Second order coefficient of the fringe fields Enge function [ $\text{m}^{-2}$ ]. Typically 0.

This element models a bending magnet with a **B** field perpendicular to the **z**-directions of both the **fromCCS** and **toCCS** coordinate systems. The geometry is that of a wedge with the two straight sides perpendicular to the **z**-directions of the specified coordinate systems. When the **z**-axes do not intersect, or when they are parallel, this element can not be used. Please use the **isectorbent** element to model an indexed sectorbend, i.e. a sectorbend with a quadrupole component.

The optional **phiin** and **phiout** parameters can be used to specify the angle (with respect to normal incidence) of the input and output pole faces in the bending plane. A positive angle means that the total angle of the 'wedge' will decrease. This is shown schematically in Figure 4-12.

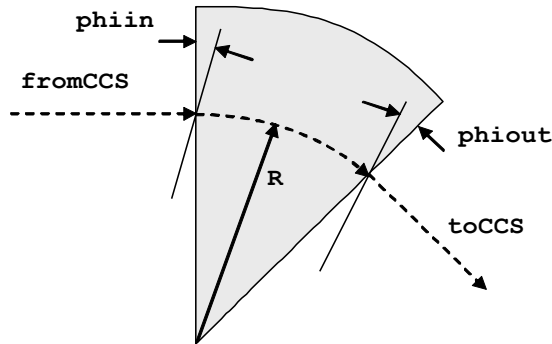


Figure 4-12: Geometry of the sectormagnet, with positive values for **phiin** and **phiout**.

The fringe fields are modeled as a second order Enge function, given on-axis by [14]

$$B_y(z, y=0) = \frac{1}{1 + \exp(\mathbf{b}_1(z - \mathbf{d1}) + \mathbf{b}_2(z - \mathbf{d1})^2)}$$

in the coordinate system shown in Figure 4-13. The parameter **d1** changes the effective length of the magnet, while **b1** affects the steepness of the drop-off of the magnetic field. The second order correction, given by parameter **b2**, is implemented but should be used with care as it can reverse the field drop-off at a distance far away from the magnet.

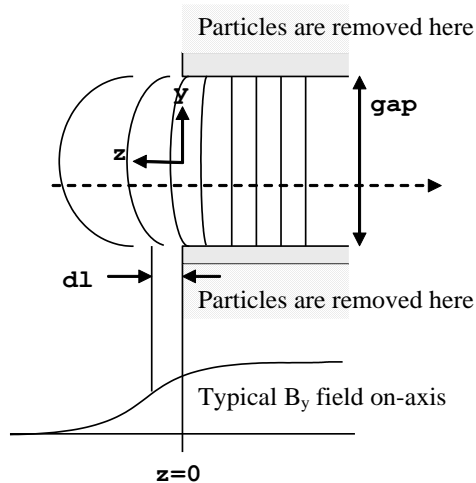


Figure 4-13: Fringe fields of the sectormagnet.

GPT removes all particles outside the gap region from the simulation. This is at a distance  $|y| \geq \pi / \mathbf{b}_1$ .

There are a number of ways to obtain the parameters **d1**, **b1** and **b2**. Arguably the best method is to fit equation (1) to a measured field-profile of the magnet to be simulated. Second best is to use the 'field integral' FINT, such as used in MAD, and given by:

$$\frac{1}{\mathbf{b}_1} = g \cdot \text{FINT} = \int \frac{B_y(s)(B_0 - B_y(s))}{B_0^2} ds$$

where  $B_0$  is the nominal field inside the magnet in [T] and  $g$  the gap of the dipole in [m]. If everything else fails, a reasonable average value for  $\mathbf{b}_1$  is  $2/\text{gap}$ . As mentioned before, we recommend a zero value for  $\mathbf{b}_2$ .

The normal use of the **sectormagnet** element is that the specified **radius** of the bend is the ‘effective radius’, based on the magnetic properties of the magnet. In that case, the **d1** parameter is (almost) zero and in any case far smaller than the size of the gap. To ease interpretation of the simulation results, **d1** can be used to fine-tune the magnet such that the particles exist the magnet exactly on-axis.

If on the other hand the **radius** parameter is based on the physical dimensions of the magnet, than the **d1** parameter should be used to specify how far the fringe fields extend out of the magnet. This is typically in the order of the size of the gap. In that case, the correct value for **d1** is approximated by:

$$\mathbf{d1} = \int \frac{B_y(s)}{B_0} - H(s) ds$$

where  $H(s)$  is the Heaviside unit step function.

To disable fringe-field calculations, both **b** parameters must be specified as 0. This is not recommended, as it slows down simulation speed considerably due to the resulting discontinuous field, especially in combination with space-charge calculations.

The full expression for the magnetic field used in this element are given by [15].

$$B_y = \frac{-B(1 + e^f \cos(h))}{1 + 2e^f \cos(h) + e^{2f}}$$

$$B_z = \frac{B(e^f \sin(h))}{1 + 2e^f \cos(h) + e^{2f}}$$

with  $f = \mathbf{b}_1 z + \mathbf{b}_2(z^2 - y^2)$  and  $h = y(\mathbf{b}_1 + 2\mathbf{b}_2 z)$ .

We realize that fringe fields exist in all kinds of shapes and forms, and that these expressions model only a limited number of actual fields. On the other hand, it is our experience that the exact shape of the fringe fields does in many cases not affect the overall simulation results significantly. If needed, accurate modeling of all different shapes is possible with the **map3D\_B** element in combination with an external field solver. In that case, the **ccsflip** element might be needed to ‘manually’ move the particles from one coordinate system to the other.

#### 4.6.13.1 Coordinate systems

Apart from position and momentum coordinates, particles in a GPT simulations also hold a reference to a coordinate system. By default this starts at “**wcs**”, the so-called World Coordinate System. Only beamline components specified relative to the particle’s coordinate system are visible to the particles and all other beamline components are ignored. Only two elements can transfer particles from one coordinate system to another coordinate system: **sectormagnet** and **ccsflip**. Usually the built-in coordinate system transfer of a **sectormagnet** is exactly what is desired, but there are use-cases where it is conceptually easier to run the whole simulations in **wcs**. In that case **finalCCS** is an elegant way to accomplish this.

If **finalCCS** is not specified, half a bending magnet is constructed on the **fromCCS** and the other half on the **toCCS**. When a particle leaves one half of the bending magnet it is placed on the other coordinate system to go through the remaining part of the bend. Both half magnets are local elements and are not allowed to overlap other local elements.

In case **finalCCS** is specified, the fields remain the same but the entire magnet is positioned in the given coordinate system, typically “**wcs**”.

#### 4.6.13.2 Example

An example inputfile **sector.in** with two sectormagnets in a half-chicane configuration is given below. Particles start in the origin of the “**wcs**” coordinate system. They are subsequently bent in the  $zx$ -plane onto the “**bend**” coordinate system using the first sectormagnet. The downstream second sectormagnet bends the particles in the opposite direction onto coordinate system “**straight**”, causing a total offset  $d=0.1$  m. It is



crucial to get the sign of the B-field correct, as otherwise particles are -without warning- deflected in the wrong direction.

This example does not contain any additional elements, but these can easily be placed with respect to the "wcs", "bend" or "straight" coordinate systems. Spacecharge effects can be added using the spacecharge3Dmesh element. Output is provided as snapshots, 20 ns apart in this case, and such output works well for plotting trajectories. In a later stage it is more useful to work with screen output, and the last line shows this as an example. Output is written when particles pass the  $z=1$  m plane, as measured in the "straight" coordinate system. Without the last parameter, output is written relative to the default "wcs" coordinate system. This implies that the center of the bunch would be at  $x=0.1$  m. Although technically correct, in most cases this is not desired. The extra "straight" as last parameter forces GPT to write output relative to the coordinate system after the last bend, having an average  $x$  of zero.

```

1. # GPT example inputfile for a half chicane
2.
3. # --beam parameters--
4.   N=100 ;                # Number of particles
5.   zlen=0.5e-3 ;          # bunch length [m]
6.   R=1.0e-3 ;             # Bunch radius [m]
7.   gamma=30 ;             # Bunch energy []
8.
9. # --position particles using particle sets--
10.  setparticles( "beam", N, me, qe, 0 ) ;
11.  setzdist( "beam", "g", 0, zlen, 3, 3 ) ;          # Gaussian longitudinal distribution
12.  setxydist( "beam", "u", R/2, R ) ;                # Uniform radial distribution
13.  setphidist( "beam", "u", 0, 2*pi ) ;              # Fill xy phase space
14.  setGdist( "beam", "g", gamma, 0, 3, 3 ) ;        # Fixed energy, no energy spread
15.
16. # --sectormagnet parameters--
17.  Bfield=0.085 ;          # Magnetic field [T]
18.  angle=17 ;              # Bend angle [degrees]
19.  d=0.1 ;                 # Parallel translation [m]
20.  phiin=4.3 ;             # Entrance pole face [degrees]
21.  phiout=4.34 ;           # Exit pole face [degrees]
22.  dl=-0.7e-3 ;           # Field extends
23.  b1=44 ;                 # b1=2/gap, gap=45 mm
24.  b2=0 ;                  # No second order effects
25.
26. # --half chicane consisting of 2 sectormagnets--
27.  beta = sqrt(gamma*gamma-1)/gamma ;
28.  Rbend = -me*c*gamma*beta/(qe*Bfield) ; # Mind the SIGN!
29.  Lbend = d/sin(angle/deg) ;
30.
31.  ccs("wcs" , 0,0,1,      cos(angle/deg),0,-sin(angle/deg), 0,1,0, "bend") ;
32.  ccs("bend", 0,0,Lbend, cos(angle/deg),0, sin(angle/deg), 0,1,0, "straight") ;
33.  sectormagnet("wcs" ,"bend" , Rbend, Bfield, phiin/deg,phiout/deg, dl, b1, b2) ;
34.  sectormagnet("bend","straight", Rbend, Bfield, phiin/deg,phiout/deg, dl, b1, b2) ;
35.
36. # --output--
37.  accuracy(6) ;
38.  ns = 1e-9 ;
39.  tout( 0*ns,20*ns,0.05*ns ) ;
40. # screen("straight","I", 1, "straight") ;

```

Typical lines to run the above example are:

```

1. gpt -o sector.gdf sector.in
2. gdffa -o avgs.gdf sector.gdf time avgx avgy avgz avgG stdx stdy stdz stdG avgfBy
3. gdftrans -o traj.gdf sector.gdf time x y z

```

## 4.6.14 Sextupole

sextupole(ECS,L,G) ;

Hard edged sextupole lens.

<b>ECS</b>	Element Coordinate System.
<b>L</b>	Length of the sextupole [m].
<b>G</b>	Magnetic field gradient in [T/m <sup>2</sup> ]. Please see the field-equations carefully, as our definition gives magnetic fields a factor of 2 stronger compared to other codes and analytical theory <sup>3</sup> .

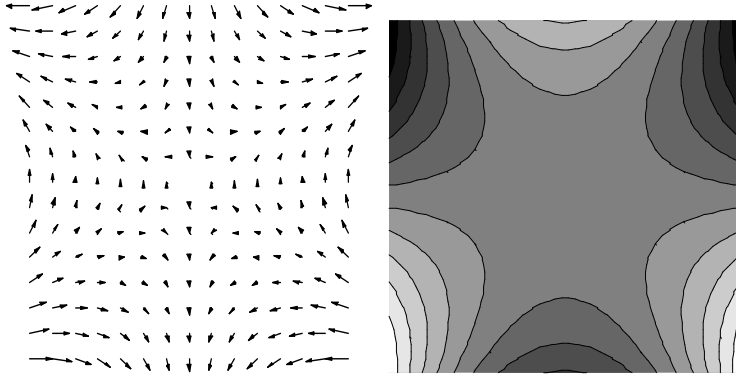


Figure 4-14: Magnetic field in the xy-plane and corresponding scalar potential.

The **B** field and scalar potential generated by this element are given:

$$\mathbf{B} = \begin{cases} \mathbf{G} \begin{pmatrix} 2xy \\ x^2 - y^2 \\ 0 \end{pmatrix} & \text{if } |z| < \frac{1}{2}L \\ \mathbf{0} & \text{otherwise} \end{cases}$$

$$\Phi = \frac{G}{3}(y^3 - 3x^2y)$$

#### 4.6.15 Solenoid

**solenoid(ECS, R, I) ;**  
Single turn solenoid.

<b>ECS</b>	Element Coordinate System.
<b>R</b>	Radius of the solenoid [m]
<b>I</b>	Current through the solenoid [A].

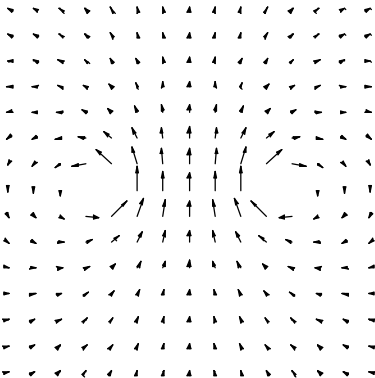


Figure 4-15: Magnetic field in the xz-plane.

The solenoid is modeled as a circle centered around the origin in the xy-plane with radius **R** carrying a current **I**. The resulting magnetic field is directed in the positive z-direction, within the current loop. The vector potential of the magnetic field is given in spherical coordinates by [16, pp. 117]:

$$A_\phi(r, \theta) = \frac{\mu_0 I R}{4\pi} \int_0^{2\pi} \frac{\cos(\phi)}{\sqrt{R^2 + r^2 - 2Rr \sin(\theta) \cos(\phi)}} d\phi$$

<sup>3</sup> As was brought to our attention by Dr. D. Dowell. For reasons of backward compatibility we can not change this element, but we advice to specify the gradient in the GPT inputfile as 0.5\*Gsextupole to emphase the missing prefactor. We apologise for the inconvenience.

The magnetic field is calculated from  $\mathbf{B} = \nabla \times \mathbf{A}$ . The integral and rotation are calculated analytically.

As the field is defined everywhere and no approximations are made, this element is very useful to study aberrations in solenoid lens systems.

## 4.7 Field maps

This section describes the built-in elements capable of handling external field maps created by external software. The 1D models use 2<sup>nd</sup> order splines, all other elements use 1<sup>st</sup> order interpolation and require a rectangular grid aligned with the axes. Before use, the output of the external software must be converted to GDF format using the utility programs ASCI2GDF and RAW2GDF, see sections 3.2 and 3.19 respectively. Output created by one of the SUPERFISH [4] set of codes can be converted using FISH2GDF, see section 3.4.

4.7.1	map1D_B.....	175
4.7.2	map1D_E.....	176
4.7.3	map1D_TM.....	176
4.7.4	Map2D_B.....	177
4.7.5	Map2D_E.....	177
4.7.6	Map2D_Et.....	178
4.7.7	Map2Dr_E.....	179
4.7.8	Map2D_V.....	179
4.7.9	Map25D_E.....	180
4.7.10	Map25D_B.....	180
4.7.11	map25D_TM.....	181
4.7.12	Map3D_E.....	181
4.7.13	Map3D_TM.....	182
4.7.14	Map3D_Ecomplex.....	183
4.7.15	Map3D_Hcomplex.....	185
4.7.16	Map3D_V.....	185
4.7.17	Map3D_B.....	186
4.7.18	Map3D_remove.....	187

The zero position for  $z$  in the GDF file containing the field map is always placed at the ECS specified in the field map element syntax. Therefore, `map3D_E("wcs","z",position, ...)` sets the  $z=0$  position in the field map at  $z=\text{position}$  in GPT.

If a binary file named `outbin` consists of four arrays, the  $r$ - and  $z$ - coordinates and the radial and longitudinal electric field, and is located in the current directory then

```
raw2gdf -o outbin.gdf outbin r 1 z 1 Er 1 Ez 1
```

converts the file to the GDF format. Because GPT uses SI units, any non-SI parameter must be converted using the multiplication factors. For example, if the coordinates are specified in cm and the electric field is in V/cm, the following line can be used to convert all units to SI:

```
raw2gdf -o outbin.gdf outbin r 0.01 z 0.01 Er 100 Ez 100
```

Analogously, an ASCII file named `outfile.txt` can be converted using:

```
asci2gdf -o outbin.gdf outfile.txt r 0.01 z 0.01 Er 100 Ez 100
```

A file created by SF7 of the SUPERFISH codes can be directly converted using:

```
fish2gdf -o outbin.gdf outsf7
```

Once the file has been converted, the field map can be used in a GPT inputfile as demonstrated in the following example:

```

1. # GPT Inputfile demonstrating the use of map2D_E
2.
3. # Start a particle at 0,0,0 with v=0.5 c
4. startpar( "wcs", "I", 0,0,0, 0,0,0.5) ;
5.
6. position = 1 ;
7.
8. map2D_E("wcs","z",position, # Position field map around z=1
9.         "outbin.gdf", # Read data from file outbin.gdf
10.        "r","z", # r and z coordinates
11.        "Er","Ez",1 # Er and Ez are multiplied by 1
12.        ) ;
13.
14. tout(0,4/c,0.1/c) ; # Output every 0.1/c till t=4/c

```

#### 4.7.1 map1D\_B

**map1D\_B(ECS, filename, z, Bz, Bfac) ;**

Reads a 1D table of Bz samples on-axis from the specified GDF file and extrapolates these to a cylindrical symmetric field map for the magnetic field.

<b>ECS</b>	Element Coordinate System.
<b>filename</b>	Filename of GDF file containing the Bz-samples along the z-axis.
<b>z</b>	Name of array in the file specifying the z-coordinates.
<b>Bz</b>	Name of array in the file specifying the longitudinal magnetic field on-axis.
<b>Bfac</b>	Multiplication factor for the magnetic field.

The fields generated by this element are derived from [13]:

$$B_r(r, z) = -\frac{1}{2} r B_z'(z)$$

$$B_z(r, z) = B_z(z) - \frac{1}{4} r^2 B_z''(z)$$

These fields are only correct near the **z**-axis of the element. The map25D\_B and map3D\_B elements can be used to specify off-axis field information.

A so-called ‘natural cubic spline’ is calculated from the given (**z**,**Bz**) points. It is recommended to specify more points at those positions where the first derivative fluctuates significantly.

To keep map1D\_B as versatile as possible, no assumptions are made as to the names of the columns in the GDF file specifying the data. The names of the columns in the GDF-file have thus to be specified on the commandline.

The data points specified in the GDF file **filename** need to be sorted in ascending z-order. Specifically for this 1D element the z-samples do not need to be equidistant.

Example:

```
map1D_B("wcs","z",1, "Bfield.gdf","z","Bz",5) ;
```

Where the file **bfield.gdf** is created from the ASCII file **bfield.txt**:

```

1. # Example Bfield. z in [mm] and Bz in [Gauss]
2.   z   Bz
3.   0    0
4.   1   10
5.   2   21
6.   3   33
7.   4   46
8.   5   60
9.   6   75
10.  7   91
11.  8  108
12. ...   ...

```

Conversion from ASCII to GDF format and conversion of the units to the MKS system used by GPT are done simultaneously by ASCII2GDF with the following command:

```
ascii2gdf -o bfield.gdf bfield.txt z 1e-3 Ez 1e-4
```

### 4.7.2 map1D\_E

**map1D\_E(ECS, filename, z, Ez, Efac) ;**

Reads a 1D table of Ez samples on-axis from the specified GDF file and extrapolates these to a cylindrical symmetric field map for the electric field.

<b>ECS</b>	Element Coordinate System.
<b>filename</b>	Filename of GDF file containing the Ez samples along the z-axis.
<b>z</b>	Name of array in the file specifying the z-coordinates.
<b>Ez</b>	Name of array in the file specifying the longitudinal electric field on-axis.
<b>Efac</b>	Multiplication factor for the electric field.

The fields generated by this element are derived from [13]:

$$E_r(r, z) = -\frac{1}{2} r E_z'(z)$$

$$E_z(r, z) = E_z(z) - \frac{1}{4} r^2 E_z''(z)$$

These fields are only correct near the **z**-axis of the element. The map25D\_E and map3D\_E elements can be used to specify off-axis field information.

A so-called ‘natural cubic spline’ is calculated from the given (**z**, **Ez**) points. It is recommended to specify more points at those positions where the first derivative fluctuates significantly.

To keep map1D\_E as versatile as possible, no assumptions are made as to the names of the columns in the GDF file specifying the data. The names of the columns in the GDF file have thus to be specified on the commandline.

The data points specified in the GDF file **filename** need to be sorted in ascending z-order, but do not need to be equidistant.

### 4.7.3 map1D\_TM

**map1D\_TM(ECS, filename, z, Ez, fac, phi, w) ;**

Reads a 1D table of Ez samples on-axis from the specified GDF file and extrapolates these to a cylindrical symmetric field map for a TM mode cavity.

<b>ECS</b>	Element Coordinate System.
<b>filename</b>	Filename of GDF file containing the Ez-samples along the z-axis.
<b>z</b>	Name of array in the file specifying the z-coordinates.
<b>Ez</b>	Name of array in the file specifying the longitudinal electric field on-axis.
<b>fac</b>	Multiplication factor for all fields.
<b>phi</b>	Phase factor: $\phi$ in radians.
<b>w</b>	Angular frequency: $\omega$ .

The fields generated by this element are derived from:

$$E_z(r, z) = E_z(z) \cos(\omega t + \phi)$$

$$E_r(r, z) = -\frac{1}{2} r E_z'(z) \cos(\omega t + \phi)$$

$$B_\phi(r, z) = \frac{r \omega}{2c^2} E_z(z) \sin(\omega t + \phi)$$

These fields are only correct near the **z**-axis of the element. The map25D\_TM element can be used to specify off-axis field information.

A so-called ‘natural cubic spline’ is calculated from the given (**z**, **Ez**) points. It is recommended to specify more points at those positions where the first derivative fluctuates significantly.

To keep map1D\_TM as versatile as possible, no assumptions are made as to the names of the columns in the GDF file specifying the data. The names of the columns in the GDF file have thus to be specified on the commandline.

The datapoints specified in the GDF file **filename** need to be sorted in ascending z-order, but do not need to be equidistant.

#### 4.7.4 Map2D\_B

**map2D\_B(ECS,mapfile.gdf,r,z,Br,Bz,Bfac) ;**

Reads a 2D cylindrical symmetric field map for the magnetic field from the specified GDF file.

<b>ECS</b>	Element Coordinate System.
<b>mapfile</b>	Filename of GDF file containing the fields.
<b>r</b>	Name of array in the file with the r-coordinates [m].
<b>z</b>	Name of array in the file with the z-coordinates.[m]
<b>Br</b>	Name of array in the file with the radial magnetic field [T].
<b>Bz</b>	Name of array in the file with the longitudinal magnetic field [T].
<b>Bfac</b>	Multiplication factor for the magnetic field.

To keep map2D\_B as versatile as possible, no assumptions are made as to the names of the columns in the GDF file specifying the data. The names of the columns in the GDF file have thus to be specified on the commandline.

The rows specified in the GDF file **filename** don't need to be in any particular order, because the complete set is first sorted in the **r**- and **z**-directions for convenient internal use. From this sorted data the grid characteristics, i.e. rmin, rmax, and rdelta, are calculated. It is verified that all the grid points are present and lie within a range of  $\pm\Delta 10^{-3}$  off their optimal position, where  $\Delta$  is the grid spacing in the corresponding direction.

To calculate the fields, first the four datapoints around the particle position are determined. They are numbered 1 to 4 as shown in Figure 4-16.

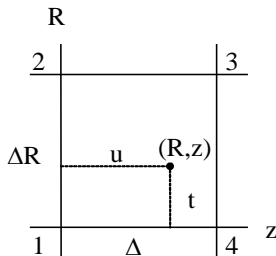


Figure 4-16: Datapoints around the particle position (R,z).

The relative distances  $t$  and  $u$  are calculated using:

$$t = \frac{(R - R_1)}{\Delta R}$$

$$u = \frac{(z - z_1)}{\Delta z}$$

Bilinear interpolation of the magnetic field yields:

$$B_r = (1-t)(1-u)Br_1 + t(1-u)Br_2 + tuBr_3 + (1-t)uBr_4$$

$$B_\phi = 0$$

$$B_z = (1-t)(1-u)Bz_1 + t(1-u)Bz_2 + tuBz_3 + (1-t)uBz_4$$

Within the element, the magnetic field is continuous in all directions.

#### 4.7.5 Map2D\_E

**map2D\_E(ECS,mapfile.gdf,r,z,Er,Ez,Efac) ;**

Reads a 2D cylindrical symmetric field map for the electric field from the specified GDF file.

<b>ECS</b>	Element Coordinate System.
<b>mapfile</b>	Filename of GDF file containing the fields.
<b>r</b>	Name of array in the file with the r-coordinates [m]
<b>z</b>	Name of array in the file with the z-coordinates [m].
<b>Er</b>	Name of array in the file with the radial electric field [V/m].
<b>Ez</b>	Name of array in the file with the longitudinal electric field [V/m].
<b>Efac</b>	Multiplication factor for the electric field.

To keep map2D\_E as versatile as possible, no assumptions are made as to the names of the columns in the GDF file specifying the data. The names of the columns in the GDFfile thus have to be specified on the commandline.

The rows specified in the GDF file **filename** don't need to be in any particular order, because the complete set is first sorted in the **r**- and **z**-directions for convenient internal use. From this sorted data the grid characteristics, i.e. rmin, rmax, and rdelta, are calculated. It is verified that all the grid points are present and lie within a range of  $\pm\Delta 10^{-3}$  off their optimal position, where  $\Delta$  is the grid spacing in the corresponding direction.

Bilinear interpolation of the electric field yields:

$$E_r = (1-t)(1-u)Er_1 + t(1-u)Er_2 + tuEr_3 + (1-t)uEr_4$$

$$E_\phi = 0$$

$$E_z = (1-t)(1-u)Ez_1 + t(1-u)Ez_2 + tuEz_3 + (1-t)uEz_4$$

Within the element, the electric field is continuous in all directions.

#### 4.7.6 Map2D\_Et

**Map2D\_Et(ECS, mapfile.gdf, r, z, Er, Ez, fac, tau) ;**

Reads a 2D electrostatic field-profile assuming linearly increasing amplitude as function of time.

<b>ECS</b>	Element Coordinate System.
<b>mapfile</b>	Filename of GDF file containing the fields.
<b>r</b>	Name of array in the file specifying the r-coordinates.
<b>z</b>	Name of array in the file specifying the z-coordinates.
<b>Er</b>	Name of array in the file specifying the electric field in the r-direction.
<b>Ez</b>	Name of array in the file specifying the electric field in the z-direction.
<b>fac</b>	Multiplication factor for the fields.
<b>tau</b>	Inverse slope [s].

The electromagnetic fields of this element are given by:

$$\mathbf{E}_{z,r}(z, r, t) = \mathbf{E}_{z,r}(z, r) \frac{t}{\tau}$$

$$\mathbf{B}_\phi(z, r, t) = \frac{1}{r c^2 \tau} \int_0^r r' E_z(z, r') dr'$$

where  $\mathbf{E}_{z,r}(z, r)$  is read from **mapfile** and interpolated analogous to the **map2D\_E** element. To prevent efficiency degradation, the magnetostatic field is pre-computed only once and stored in memory at the very beginning of the simulation.

Please note that a linear slope as function of time is the *only* time-dependent function that can be used as multiplication factor for an electrostatic field map.

The datapoints specified in the GDF file **filename** don't need to be in any particular order, because the complete set is first sorted in the **r**- and **z**-directions for convenient internal use. From this sorted data the grid characteristics, i.e. zmin, zmax, and zdelta, are extracted. It is verified that all the grid points are present and lie within a range of  $\pm\Delta 10^{-3}$  off their optimal position, where  $\Delta$  is the grid spacing in the corresponding direction.



### 4.7.7 Map2Dr\_E

**map2Dr\_E**(ECS, mapfile.gdf, x, z, Ex, Ez, L, Efac) ;

Reads a 2D field map in the zx-plane for the electric field from the specified GDF file.

<b>ECS</b>	Element Coordinate System.
<b>mapfile</b>	Filename of GDF file containing the fields.
<b>x</b>	Name of array in the file with the x-coordinates [m].
<b>z</b>	Name of array in the file with the z-coordinates [m]
<b>Ex</b>	Name of array in the file with the electric field in x-direction [V/m].
<b>Ez</b>	Name of array in the file with the electric field in z-direction [V/m].
<b>L</b>	‘Thickness’ of field map [m] in y-direction.
<b>Efac</b>	Multiplication factor for the electric field.

To keep **map2Dr\_E** as versatile as possible, no assumptions are made as to the names of the columns in the GDF file specifying the data. The names of the columns in the GDF file have to be specified on the commandline.

The rows specified in the GDF file **filename** don’t need to be in any particular order, because the complete set is first sorted in the **z**- and **x**-directions for convenient internal use. From this sorted data the grid characteristics, i.e. zmin, zmax, and zdelta. are calculated. It is verified that all the grid points are present and lie within a range of  $\pm\Delta \cdot 10^{-3}$  off their optimal position, where  $\Delta$  is the grid spacing in the corresponding direction.

The field map is only active when  $|y| < L/2$ . In that case, bilinear interpolation of the electric field yields:

$$E_x = (1-t)(1-u)Ex_1 + t(1-u)Ex_2 + tuEx_3 + (1-t)uEx_4$$

$$E_y = 0$$

$$E_z = (1-t)(1-u)Ez_1 + t(1-u)Ez_2 + tuEz_3 + (1-t)uEz_4$$

Within the element, the electric field is continuous in all directions.

### 4.7.8 Map2D\_V

**map2D\_V**(ECS, mapfile.gdf, r, z, V, Vfac, [Vtype]) ;

Reads a 2D cylindrical symmetric field map for the electric potential from the specified GDF file.

<b>ECS</b>	Element Coordinate System.
<b>mapfile</b>	Filename of GDF file containing the fields.
<b>r</b>	Name of array in the file with the r-coordinates [m]
<b>z</b>	Name of array in the file with the z-coordinates [m]
<b>V</b>	Name of array in the file with the electric potential [V].
<b>Vfac</b>	Multiplication factor for the electric potential.
<b>Vtype</b>	Interpolation method for <b>V</b> . Must be <b>lin</b> .

To keep **map2D\_V** as versatile as possible, no assumptions are made as to the names of the columns in the GDF file specifying the data. The names of the columns in the GDF file have to be specified on the commandline.

The rows specified in the GDF file **filename** don’t need to be in any particular order, because the complete set is first sorted in the **r**- and **z**-directions for convenient internal use. From this sorted data the grid characteristics, i.e. rmin, rmax, and rdelta, are calculated. It is verified that all the grid points are present and lie within a range of  $\pm\Delta \cdot 10^{-3}$  off their optimal position, where  $\Delta$  is the grid spacing in the corresponding direction.

When the interpolation type for the electric potential is ‘Lin’, a bilinear interpolation is performed. The source code allows other interpolation types to be implemented, but currently the only available interpolation type is ‘Lin’.

When the electric potential is specified, the electric field is calculated using

$$\mathbf{E} = -\nabla V = -\text{grad } V$$

which yields the following using the bilinear interpolation method for potential  $V$ :

$$E_r = \frac{(1-u)V_1 - (1-u)V_2 - uV_3 + uV_4}{\Delta R}$$

$$E_\phi = 0$$

$$E_z = \frac{(1-t)V_1 + tV_2 - tV_3 - (1-t)V_4}{\Delta z}$$

Please note that because the potential is interpolated linearly, its derivative  $\mathbf{E}$  is constant between the gridpoints. This results in discontinuities in the electric field. A higher-order interpolation is needed to produce a continuous electric field. Therefore it is currently more accurate to use the electric field in a simulation than the potential.

#### 4.7.9 Map25D\_E

**map25D\_E(ECS,mapfile.gdf,r,z,Er,Ephi,Ez,Efac) ;**

Reads a 2.5D cylindrical symmetric field map for the electric field from the specified GDF file.

<b>ECS</b>	Element Coordinate System.
<b>mapfile</b>	Filename of GDF file containing the fields.
<b>r</b>	Name of array in the file with the r-coordinates [m].
<b>z</b>	Name of array in the file with the z-coordinates [m].
<b>Er</b>	Name of array in the file with the radial electric field [V/m].
<b>Ephi</b>	Name of array in the file with the azimuthal electric field [V/m].
<b>Ez</b>	Name of array in the file with the longitudinal electric field [V/m].
<b>Efac</b>	Multiplication factor for the electric field.

To keep map25D\_E as versatile as possible, no assumptions are made as to the names of the columns in the GDF file specifying the data. The names of the columns in the GDF file have to be specified on the commandline.

The rows specified in the GDF file **filename** don't need to be in any particular order, because the complete set is first sorted in the **r**- and **z**-directions for convenient internal use. From this sorted data the grid characteristics, i.e. rmin, rmax, and rdelta, are calculated. It is verified that all the grid points are present and lie within a range of  $\pm\Delta 10^{-3}$  off their optimal position, where  $\Delta$  is the grid spacing in the corresponding direction.

Bilinear interpolation of the electric field yields:

$$E_r = (1-t)(1-u)Er_1 + t(1-u)Er_2 + tuEr_3 + (1-t)uEr_4$$

$$E_\phi = (1-t)(1-u)E\phi_1 + t(1-u)E\phi_2 + tuE\phi_3 + (1-t)uE\phi_4$$

$$E_z = (1-t)(1-u)Ez_1 + t(1-u)Ez_2 + tuEz_3 + (1-t)uEz_4$$

The electric field is continuous in all directions. The angular electric field is not chosen to be zero, as is the case when using map2D\_E.

#### 4.7.10 Map25D\_B

**map25D\_B(ECS,mapfile.gdf,r,z,Br,Bphi,Bz,Bfac) ;**

Reads a 2.5D cylindrical symmetric field map for the magnetic field from the specified GDF file.

<b>ECS</b>	Element Coordinate System.
<b>mapfile</b>	Filename of GDF file containing the fields.
<b>r</b>	Name of array in the file with the r-coordinates [m]
<b>z</b>	Name of array in the file with the z-coordinates [m]
<b>Br</b>	Name of array in the file with the radial magnetic field [T].
<b>Bphi</b>	Name of array in the file with the angular magnetic field [T].
<b>Bz</b>	Name of array in the file with the longitudinal magnetic field [T].
<b>Bfac</b>	Multiplication factor for the magnetic field.

To keep map25D\_B as versatile as possible, no assumptions are made as to the names of the columns in the GDF file specifying the data. The names of the columns in the GDF file have to be specified on the commandline.

The rows specified in the GDF file **filename** don't need to be in any particular order, because the complete set is first sorted in the **r**- and **z**-directions for convenient internal use. From this sorted data the grid characteristics, i.e. rmin, rmax, and rdelta, are calculated. It is verified that all the grid points are present and lie within a range of  $\pm\Delta \cdot 10^{-3}$  off their optimal position, where  $\Delta$  is the grid spacing in the corresponding direction.

Very similar, bilinear interpolation of the magnetic field yields:

$$B_r = (1-t)(1-u)Br_1 + t(1-u)Br_2 + tuBr_3 + (1-t)uBr_4$$

$$B_\phi = (1-t)(1-u)B\phi_1 + t(1-u)B\phi_2 + tuB\phi_3 + (1-t)uB\phi_4$$

$$B_z = (1-t)(1-u)Bz_1 + t(1-u)Bz_2 + tuBz_3 + (1-t)uBz_4$$

The magnetic field is continuous in all directions, but please note that if  $\nabla \cdot \mathbf{B} \neq 0$  in the original datafile, the effect of magnetic monopoles is simulated.

#### 4.7.11 map25D\_TM

**map25D\_TM(ECS, mapfile.gdf, r, z, Er, Ez, Bphi, ffac, k, phi, w)**

Reads a 2.5D cylindrical symmetric field map of a cavity in TM-mode from the specified GDF file.

<b>ECS</b>	Element Coordinate System.
<b>mapfile</b>	Filename of GDF file containing the fields.
<b>r</b>	Name of array in the file with the r-coordinates [m].
<b>z</b>	Name of array in the file with the z-coordinates [m].
<b>Er</b>	Name of array in the file with the radial electric field [V/m].
<b>Ez</b>	Name of array in the file with the longitudinal electric field [V/m].
<b>Bphi</b>	Name of array in the file with the angular magnetic field [T].
<b>ffac</b>	Multiplication factor for the electromagnetic field.
<b>k</b>	Longitudinal wavenumber k in [m <sup>-1</sup> ]. Must be zero for the simulation of a standing wave cavity.
<b>phi</b>	RF phase offset: $\phi$ .
<b>w</b>	Angular frequency: $\omega$ in [s <sup>-1</sup> ].

To keep map25D\_TM as versatile as possible, no assumptions are made as to the names of the columns in the GDF file specifying the data. The names of the columns in the GDF file have to be specified on the commandline.

The rows specified in the GDF file **mapfile** don't need to be in any particular order, because the complete set is first sorted in the **r**- and **z**-directions for convenient internal use. From this sorted data the grid characteristics, i.e. rmin, rmax, and rdelta, are calculated. It is verified that all the grid points are present and lie within a range of  $\pm\Delta \cdot 10^{-3}$  off their optimal position, where  $\Delta$  is the grid spacing in the corresponding direction.

Very similar to map25D\_B, bilinear interpolation of the electromagnetic field yields:

$$E_r = \cos(\omega t - kz + \phi) \left( (1-t)(1-u)Er_1 + t(1-u)Er_2 + tuEr_3 + (1-t)uEr_4 \right)$$

$$E_z = \cos(\omega t - kz + \phi) \left( (1-t)(1-u)Ez_1 + t(1-u)Ez_2 + tuEz_3 + (1-t)uEz_4 \right)$$

$$B_\phi = -\sin(\omega t - kz + \phi) \left( (1-t)(1-u)B\phi_1 + t(1-u)B\phi_2 + tuB\phi_3 + (1-t)uB\phi_4 \right)$$

FISH2GDF can be used to import fieldmaps created by the SUPERFISH set of codes. The converted file can subsequently be read using:

```
map25D_TM("wcs", "I", "fieldmap.gdf", "R", "Z", "Er", "Ez", "H", 1, 0, phi, 2*pi*freq) ;
```

#### 4.7.12 Map3D\_E

**map3D\_E(ECS, mapfile.gdf, x, y, z, Ex, Ey, Ez, Efac) ;**

Reads a 3D rectangular field map for the electric field from the specified GDF file.

<b>ECS</b>	Element Coordinate System.
<b>mapfile</b>	Filename of GDF file containing the fields.
<b>x</b>	Name of array in the file with the x-coordinates [m].
<b>y</b>	Name of array in the file with the y-coordinates [m].
<b>z</b>	Name of array in the file with the z-coordinates [m].
<b>Ex</b>	Name of array in the file with the electric field in the x-direction [V/m].
<b>Ey</b>	Name of array in the file with the electric field in the y-direction [V/m].
<b>Ez</b>	Name of array in the file with the electric field in the z-direction [V/m].
<b>Efac</b>	Multiplication factor for the electric field.

To keep map3D\_E as versatile as possible, no assumptions are made as to the names of the columns in the GDF file specifying the data. The names of the columns in the GDF file have to be specified on the commandline.

The rows specified in the GDF file **filename** don't need to be in any particular order, because the complete set is first sorted in the **x**-, **y**- and **z**-directions for convenient internal use. From this sorted data the grid characteristics, i.e. xmin, xmax, and xdelta, are calculated. It is verified that all the grid points are present and lie within a range of  $\pm\Delta 10^{-3}$  off their optimal position, where  $\Delta$  is the grid spacing in the corresponding direction.

To calculate the fields, first the eight datapoints around the particle position are determined. They are numbered 1 to 8 as shown in Figure 4-17.

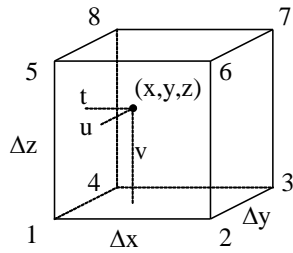


Figure 4-17: Datapoints around the particle position (x,y,z).

The relative distances  $t$ ,  $u$  and  $v$  are calculated using:

$$t = \frac{(x - x_1)}{\Delta x}$$

$$u = \frac{(y - y_1)}{\Delta y}$$

$$v = \frac{(z - z_1)}{\Delta z}$$

Bilinear interpolation of the electric field yields:

$$E_x = (1-t)(1-u)(1-v)Ex_1 + t(1-u)(1-v)Ex_2 + tu(1-v)Ex_3 + (1-t)u(1-v)Ex_4 + (1-t)(1-u)vEx_5 + t(1-u)vEx_6 + tuvEx_7 + (1-t)uvEx_8$$

$$E_y = (1-t)(1-u)(1-v)Ey_1 + t(1-u)(1-v)Ey_2 + tu(1-v)Ey_3 + (1-t)u(1-v)Ey_4 + (1-t)(1-u)vEy_5 + t(1-u)vEy_6 + tuvEy_7 + (1-t)uvEy_8$$

$$E_z = (1-t)(1-u)(1-v)Ez_1 + t(1-u)(1-v)Ez_2 + tu(1-v)Ez_3 + (1-t)u(1-v)Ez_4 + (1-t)(1-u)vEz_5 + t(1-u)vEz_6 + tuvEz_7 + (1-t)uvEz_8$$

The electric field is continuous in all directions.

#### 4.7.13 Map3D\_TM

**map3D\_TM(ECS, mapfile.gdf, x, y, z, Ex, Ey, Ez, Bx, By, Bz, ffac, phi, w) ;**

Reads a 3D rectangular field map for a standing electromagnetic wave pattern from the specified GDF-file.

**ECS** Element Coordinate System.

<b>mapfile</b>	Filename of GDF-file containing the fields.
<b>x</b>	Name of array in the file specifying the x coordinates.
<b>y</b>	Name of array in the file specifying the y coordinates.
<b>z</b>	Name of array in the file specifying the z coordinates.
<b>Ex</b>	Name of array in the file specifying the electric field in the x direction.
<b>Ey</b>	Name of array in the file specifying the electric field in the y direction.
<b>Ez</b>	Name of array in the file specifying the electric field in the z direction.
<b>Bx</b>	Name of array in the file specifying the magnetic field in the x direction.
<b>By</b>	Name of array in the file specifying the magnetic field in the y direction.
<b>Bz</b>	Name of array in the file specifying the magnetic field in the z direction.
<b>ffac</b>	Multiplication factor for the field.
<b>phi</b>	Phase offset: $\varphi$ .
<b>w</b>	Angular frequency: $\omega$ .

The electromagnetic fields of this element are given by:

$$\mathbf{E} = \cos(\omega t + \varphi) \mathbf{E}_{\text{int}}$$

$$\mathbf{B} = -\sin(\omega t + \varphi) \mathbf{B}_{\text{int}}$$

Where  $\mathbf{E}_{\text{int}}$  and  $\mathbf{B}_{\text{int}}$  are obtained by trilinear interpolation of the fields specified in **mapfile**. Please see **map3D\_E** and **map3D\_B** for a description of the interpolation equations.

To keep map3D\_TM as versatile as possible, no assumptions are made as to the names of the columns in the GDF-file specifying the data. Therefore the names of the columns in the GDF-file have to be specified on the commandline.

The datapoints specified in the GDF-file **filename** don't need to be in any particular order, because the complete set is first sorted in the **x**, **y** and **z** directions for convenient internal use. From this sorted data the grid characteristics, i.e. minimum, maximum and spacing are extracted. Then it is made sure that all the grid points are present and lie within a range of  $\pm\Delta 10^{-3}$  off their optimal position, where  $\Delta$  is the grid spacing in the corresponding direction.

Example:

```
Map3D_TM("wcs","z",1, "EBmap.gdf",
        "x","y","z","Ex","Ey","Ez","Bx","By","Bz",
        1.0, 0.0, 2998e6) ;
```

Where the file **EBmap.gdf** is created from the ASCII file **EBfield.txt**:

```
13. # Example EBfield. r in [mm], E in [V/m] and B in [Gauss]
14. x   y   z   Ex   Ey   Ez   Bx   By   Bz
15. ... ..
16. ... ..
```

Conversion from ASCII to GDF format and conversion of the units to the MKS system used by GPT are done simultaneously by ASCII2GDF with the following command:

```
ASCII2GDF -o EBmap.gdf EBfield.txt x 1e-3 y 1e-3 z 1e-3 Ex 1 Ey 1 Ez 1 Bx 1e-4
By 1e-4 Bz 1e-4
```

#### 4.7.14 Map3D\_Ecomplex

```
map3D_Ecomplex(ECS,mapfile.gdf,x,y,z,Exre,Eyre,Ezre,Exim,Eyim,Ezim,ffac,phi,w)
;
```

Reads a 3D rectangular field map for an oscillating electric field from the specified GDF-file.

<b>ECS</b>	Element Coordinate System.
<b>mapfile</b>	Filename of GDF-file containing the fields.
<b>x</b>	Name of array in the file specifying the x coordinates.
<b>y</b>	Name of array in the file specifying the y coordinates.
<b>z</b>	Name of array in the file specifying the z coordinates.
<b>Exre</b>	Name of array in the file specifying the real part of the electric field in the x direction.
<b>Eyre</b>	Name of array in the file specifying the real part of the electric field in the y direction.

<b>Ezre</b>	Name of array in the file specifying the real part of the electric field in the z direction.
<b>Exim</b>	Name of array in the file specifying the imaginary part of the electric field in the x direction.
<b>Eyim</b>	Name of array in the file specifying the imaginary part of the electric field in the y direction.
<b>Ezim</b>	Name of array in the file specifying the imaginary part of the electric field in the z direction.
<b>ffac</b>	Multiplication factor for the field.
<b>phi</b>	Phase offset: $\phi$ .
<b>w</b>	Angular frequency: $\omega$ .

The electric fields of this element are given by:

$$\mathbf{E} = \cos(\omega t + \phi) \mathbf{E}_{\text{re}} - \sin(\omega t + \phi) \mathbf{E}_{\text{im}}$$

Where  $\mathbf{E}_{\text{re}}$  and  $\mathbf{E}_{\text{im}}$  are obtained by trilinear interpolation of the fields specified in **mapfile**. Please see **map3D\_E** and **map3D\_B** for a description of the interpolation equations.

To keep **map3D\_Ecomplex** as versatile as possible, no assumptions are made as to the names of the columns in the GDF-file specifying the data. Therefore the names of the columns in the GDF-file have to be specified on the commandline.

The datapoints specified in the GDF-file **filename** don't need to be in any particular order, because the complete set is first sorted in the **x**, **y** and **z** directions for convenient internal use. From this sorted data the grid characteristics, i.e. minimum, maximum and spacing are extracted. Then it is made sure that all the grid points are present and lie within a range of  $\pm\Delta \cdot 10^{-3}$  off their optimal position, where  $\Delta$  is the grid spacing in the corresponding direction.

#### 4.7.14.1 CST MW-Studio

Fields calculated by the Eigenmode solver of CST Microwave Studio can be imported in GPT with a trivial modification. The procedure for the **E** field is as follows:

In CST MW-Studio:

- Select the desired eigenmode in the Navigation Tree, under 2D/3D Results/Mode  $n$ .
- Typically, only a small part of the calculation domain is relevant for tracking. The desired subvolume to be exported can be defined under Properties.../Specials.../Subvolume...
- Export the fields in the subvolume with File/Export/Plot data (ASCII). The step width must be fixed, but it does not need to be equal in all directions.

With an ASCII editor capable of handling large files:

- The first two lines of the ASCII file produced by MW-Studio are typically

```
x [mm]      y [mm]      z [mm]      ExRe [V/m]      EyRe [V/m]      EzRe [V/m]      ExIm [V/m]      ...
-----
```

- These two lines must be changed into the following single line, where spacing is irrelevant

```
x y z ExRe EyRe EzRe ExIm Eyim Ezim
```

In GPT:

- Before this ASCII file can be used as a field-map in a GPT inputfile, it must be converted to the GDF format. Assuming the ASCII filename is **mapE.txt**, and assuming the dimensions are in mm, this can be done in a (GPT) batch file with

```
asci2gdf -o mapE.gdf mapE.txt x 1e-3 y 1e-3 z 1e-3
```

- It is good practice to check the produced field map by opening it in GPTwin and just plotting a few 2D projections, such as z-Ezre, x-y, etc.
- The field map can subsequently be positioned in a GPT inputfile with:

```
zpos=1.3 ; # z-position of z=0 in the field-map
fac=1 ;
w=2*pi*2998e6 ;
phi=0 ;
map3D_Ecomplex("wcs", "z",zpos, "mapE.gdf", "x","y","z",
"Exre","Eyre","Ezre", "Exim","Eyim","Ezim", fac,phi,w) ;
```

The procedure for importing the **H** field is fully analogous, where it is noted that the two field-map elements are imported on top of each other in the GPT inputfile. This is by design; GPT automatically adds all fields, and the combination of the **E** and **B** fields is the desired total field.

#### 4.7.15 Map3D\_Hcomplex

```
map3D_Hcomplex(ECS,mapfile.gdf,x,y,z,Hxre,Hyre,Hzre,Hxim,Hyim,Hzim,ffac,phi,w)
;
```

Reads a 3D rectangular field map for an oscillating magnetic field from the specified GDF-file.

<b>ECS</b>	Element Coordinate System.
<b>mapfile</b>	Filename of GDF-file containing the fields.
<b>x</b>	Name of array in the file specifying the x coordinates.
<b>y</b>	Name of array in the file specifying the y coordinates.
<b>z</b>	Name of array in the file specifying the z coordinates.
<b>Hxre</b>	Name of array in the file specifying the real part of the electric field in the x direction.
<b>Hyre</b>	Name of array in the file specifying the real part of the electric field in the y direction.
<b>Hzre</b>	Name of array in the file specifying the real part of the electric field in the z direction.
<b>Hxim</b>	Name of array in the file specifying the imaginary part of the electric field in the x direction.
<b>Hyim</b>	Name of array in the file specifying the imaginary part of the electric field in the y direction.
<b>Hzim</b>	Name of array in the file specifying the imaginary part of the electric field in the z direction.
<b>ffac</b>	Multiplication factor for the field.
<b>phi</b>	Phase offset: $\phi$ .
<b>w</b>	Angular frequency: $\omega$ .

The electromagnetic fields of this element are given by:

$$\mathbf{B} = \mu_0 \cos(\omega t + \phi) \mathbf{H}_{\text{re}} - \mu_0 \sin(\omega t + \phi) \mathbf{H}_{\text{im}}$$

Where  $\mathbf{H}_{\text{re}}$  and  $\mathbf{H}_{\text{im}}$  are obtained by trilinear interpolation of the fields specified in **mapfile**. Please see **map3D\_E** and **map3D\_B** for a description of the interpolation equations.

To keep **map3D\_Hcomplex** as versatile as possible, no assumptions are made as to the names of the columns in the GDF-file specifying the data. Therefore the names of the columns in the GDF-file have to be specified on the commandline.

The datapoints specified in the GDF-file **filename** don't need to be in any particular order, because the complete set is first sorted in the **x**, **y** and **z** directions for convenient internal use. From this sorted data the grid characteristics, i.e. minimum, maximum and spacing are extracted. Then it is made sure that all the grid points are present and lie within a range of  $\pm\Delta 10^{-3}$  off their optimal position, where  $\Delta$  is the grid spacing in the corresponding direction.

#### 4.7.16 Map3D\_V

```
map3D_V(ECS,mapfile.gdf,x,y,z,V,Vfac,[Vtype]) ;
```

Reads a 3D rectangular field map for the electric potential from the specified GDF file.

<b>ECS</b>	Element Coordinate System.
<b>mapfile</b>	Filename of GDF file containing the fields.
<b>x</b>	Name of array in the file with the x-coordinates.
<b>y</b>	Name of array in the file with the y-coordinates.
<b>z</b>	Name of array in the file with the z-coordinates.
<b>V</b>	Name of array in the file with the electric potential.
<b>Vfac</b>	Multiplication factor for the electric potential.
<b>Vtype</b>	Interpolation method for <b>V</b> . Must be "lin".

To keep **map3D\_V** as versatile as possible, no assumptions are made as to the names of the columns in the GDF file specifying the data. The names of the columns in the GDF file have to be specified on the commandline.

The rows specified in the GDF file **filename** don't need to be in any particular order, because the complete set is first sorted in the **x**-, **y**- and **z**-directions for convenient internal use. From this sorted data the grid characteristics, i.e. xmin, xmax, and xdelta, are calculated. It is verified that all the grid points are present and lie within a range of  $\pm\Delta 10^{-3}$  off their optimal position, where  $\Delta$  is the grid spacing in the corresponding direction.

When the interpolation type for the electric potential is "**lin**", a bilinear interpolation is performed. The source code allows other interpolation types to be implemented, but currently the only available interpolation type is "**lin**".

When the electric potential is specified, the electric field is calculated using

$$\mathbf{E} = -\nabla V = -\text{grad } V$$

which yields the following using the bilinear interpolation method for potential  $V$ :

$$E_x = \left[ (1-u)(1-v)V_1 - (1-u)(1-v)V_2 - u(1-v)V_3 + u(1-v)V_4 + (1-u)vV_5 - (1-u)vV_6 - uvV_7 + uvV_8 \right] / \Delta x$$

$$E_y = \left[ (1-t)(1-v)V_1 + t(1-v)V_2 - t(1-v)V_3 - (1-t)(1-v)V_4 + (1-t)vV_5 + tvV_6 - tvV_7 - (1-t)vV_8 \right] / \Delta y$$

$$E_z = \left[ (1-t)(1-u)V_1 + t(1-u)V_2 + tuV_3 + (1-t)uV_4 - (1-t)(1-u)V_5 - t(1-u)V_6 - tuV_7 - (1-t)uV_8 \right] / \Delta z$$

Please note that because the potential is interpolated linearly, its derivative  $\mathbf{E}$  is constant between the gridpoints. This results in discontinuities in the electric field. A higher-order interpolation is needed to produce a continuous electric field. Therefore it is currently more accurate to use the electric field in a simulation than the potential.

#### 4.7.17 Map3D\_B

**map3D\_B(ECS,mapfile.gdf,x,y,z,Bx,By,Bz,Bfac) ;**

Reads a 3D rectangular field map for the magnetic field from the specified GDF file.

<b>ECS</b>	Element Coordinate System.
<b>mapfile</b>	Filename of GDF file containing the fields.
<b>x</b>	Name of array in the file with the $x$ -coordinates.
<b>y</b>	Name of array in the file with the $y$ -coordinates.
<b>z</b>	Name of array in the file with the $z$ -coordinates.
<b>Bx</b>	Name of array in the file with the magnetic field in the $x$ -direction.
<b>By</b>	Name of array in the file with the magnetic field in the $y$ -direction.
<b>Bz</b>	Name of array in the file with the magnetic field in the $z$ -direction.
<b>Bfac</b>	Multiplication factor for the magnetic field.

To keep map3D\_B as versatile as possible, no assumptions are made as to the names of the columns in the GDF file specifying the data. The names of the columns in the GDF file have to be specified on the commandline.

The rows specified in the GDF file **filename** don't need to be in any particular order, because the complete set is first sorted in the **x**-, **y**- and **z**-directions for convenient internal use. From this sorted data the grid characteristics, i.e. xmin, xmax, and xdelta, are calculated. It is verified that all the grid points are present and lie within a range of  $\pm\Delta 10^{-3}$  off their optimal position, where  $\Delta$  is the grid spacing in the corresponding direction.

Very similar, bilinear interpolation of the magnetic field yields:

$$B_x = (1-t)(1-u)(1-v)Bx_1 + t(1-u)(1-v)Bx_2 + tu(1-v)Bx_3 + (1-t)u(1-v)Bx_4 + (1-t)(1-u)vBx_5 + t(1-u)vBx_6 + tuvBx_7 + (1-t)uvBx_8$$

$$B_y = (1-t)(1-u)(1-v)By_1 + t(1-u)(1-v)By_2 + tu(1-v)By_3 + (1-t)u(1-v)By_4 + (1-t)(1-u)vBy_5 + t(1-u)vBy_6 + tuvBy_7 + (1-t)uvBy_8$$

$$B_z = (1-t)(1-u)(1-v)Bz_1 + t(1-u)(1-v)Bz_2 + tu(1-v)Bz_3 + (1-t)u(1-v)Bz_4 + (1-t)(1-u)vBz_5 + t(1-u)vBz_6 + tuvBz_7 + (1-t)uvBz_8$$



The magnetic field is continuous in all directions, but please note that if  $\nabla \cdot \mathbf{B} \neq 0$  in the original datafile, the effect of magnetic monopoles is simulated.

#### 4.7.18 Map3D\_remove

**map3D\_remove** (**ECS**, **mapfile.gdf**, **x**, **y**, **z**, **R**) ;

Reads a 3D rectangular map indicating if a particle must be removed or not.

<b>ECS</b>	Element Coordinate System.
<b>mapfile</b>	Filename of GDF file containing the fields.
<b>x</b>	Name of array in the file with the x-coordinates.
<b>y</b>	Name of array in the file with the y-coordinates.
<b>z</b>	Name of array in the file with the z-coordinates.
<b>R</b>	Name of array in the file containing either 1 or 0, where 1 indicates that all particles at that location must be removed.

To keep map3D\_remove as versatile as possible, no assumptions are made as to the names of the columns in the GDF file specifying the data. The names of the columns in the GDF file have to be specified on the commandline.

The rows specified in the GDF file **filename** don't need to be in any particular order, because the complete set is first sorted in the **x**-, **y**- and **z**-directions for convenient internal use. From this sorted data the grid characteristics, i.e. **xmin**, **xmax**, and **xdelta**, are calculated. It is verified that all the grid points are present and lie within a range of  $\pm \Delta 10^{-3}$  off their optimal position, where  $\Delta$  is the grid spacing in the corresponding direction.

Particles are removed if the bilinar interpolated value of all corners of the enclosing box is larger than 0.5.

## 4.8 Spacecharge

This section describes the built-in space-charge routines of GPT. Please see section 1.5 for a brief comparison between the different routines.

4.8.1	Spacecharge3Dmesh.....	188
4.8.2	spacecharge3Dtree.....	196
4.8.3	Spacecharge3D.....	198
4.8.4	Spacecharge3Dclassic.....	199
4.8.5	SetTotalCharge.....	199
4.8.6	Spacecharge2Dcircle.....	199
4.8.7	Setcharge2Dcircle.....	201
4.8.8	Spacecharge2Dline.....	201

It is possible to write new and/or more efficient space-charge models for specific situations. The procedure to develop such custom space-charge models is given in the GPT Programmer's Reference.

GPT uses the concept of macro-particles: Every particle in the simulations represents a (large) number of elementary particles. In the case of simulations of granularity/stochastic effects, every particle in the simulations must represent exactly one elementary particle. In other words,  $Q_{\text{tot}} = N \cdot q$ , where  $Q_{\text{tot}}$  is the total charge,  $N$  the number of particles and  $q$  the charge of an elementary particle. The simplest method is to set the total charge based on the number of particles (assuming electrons, and assuming  $\mathbf{n}$  is defined elsewhere):

```
Qtot = N*qe ;
setparticles ("beam", N, me, qe, Qtot)
```

Alternatively, it is possible to calculate the number of particles based on the total charge **Qtot** (assuming electrons, and assuming **Qtot** is defined elsewhere):

```
N = round(abs(Qtot/q)) ;
setparticles ("beam", N, me, qe, Qtot)
```

where the **round()** function rounds towards the nearest integer and where **abs** indicates the absolute value.

### 4.8.1 Spacecharge3Dmesh

```
spacecharge3Dmesh ([option,parameter(s)], ... ) ;
```

Mesh-based 3D space-charge routine.

We would like to express our thanks to Dr Gisela Pöplau from Rostock University, Germany for the development of the non-equidistant 3D multi-grid Poisson solver, tailor-made for this application.

#### 4.8.1.1 Syntax and options

The **sc3dmesh** element calculates 3D space-charge fields by solving Poisson's equations on a non-equidistant mesh adapted to the beam geometry. The model is very fast, allowing over a million particles to be tracked on a normal PC. The element scales almost linear with the number of particles in terms of CPU time. This element is not suitable for the simulation of the effect of short-range Coulomb interactions such as disorder induced heating. Please see section 4.8.2 for the correct approach for calculating point-to-point interactions.

The charge density is determined on a mesh in the rest frame of the bunch where no self-magnetic fields are present. A non-equidistant multi-grid technique is used to solve Poisson's equation to obtain the electrostatic potential. Interpolations and Lorentz transformations are used to transform the particle coordinates to the rest frame and to transform the calculated fields back to the laboratory frame.

Note: This element gives a poor estimate of the space-charge forces in bunches with a large energy spread, because particles still have relatively large velocities in the rest frame of the bunch. A warning is printed to inform the users when this is the case.

Option	Parameter(s)	Default	Description
"RestMaxGamma"	<b>Gmax</b>	2.0	Triggers a warning when particles have a Lorentz factor larger than <b>Gmax</b> in the zero-momentum frame of the bunch.

Option	Parameter(s)	Default	Description
"MeshNtotal"	[ <b>Nx</b> , <b>Ny</b> , <b>Nz</b> ]		Use a total of <b>Nx</b> , <b>Ny</b> and <b>Nz</b> meshlines in the x-, y- and z-direction respectively to fill the bounding box.
"MeshNbunch"	<b>Nx</b> , <b>Ny</b> , <b>Nz</b>		Slice the particle bunch in <b>Nx</b> , <b>Ny</b> and <b>Nz</b> meshlines in the x-, y- and z-direction respectively. Additional meshlines are added in all directions to fill the bounding box.
"MeshNfac"	<b>Alpha</b>	1	Automatically determine the total number of meshlines in the bunch using the following equation:
"MeshNpow"	<b>mpow</b>	1/3	$N_x=N_y=N_z=\alpha * N_{\text{particles}}^{\text{mpow}}$ . Can be used in combination with <b>MeshNtotal</b> without parameters to specify the total number of meshlines in the bounding box instead of in the bunch.
"MeshAdapt"	<b>Fn</b>	0.5	Sets the mesh adaptivity. The meshing algorithm ensures that the maximum difference in distance between neighboring meshlines is always kept less than the specified <b>fn</b> .
"MemOvershoot"	<b>n</b>	10	Percentage of memory overhead consumed by the memory management scheme. If set to 0, all block memory management is disabled resulting in the lowest memory consumption at the cost of a significant increase in page faults and CPU time.
"MeshBoxSize"	<b>Nstd</b>	5	Sets the minimum size of the bounding box in units of standard deviation for each dimension.
"MeshBoxAccuracy"	<b>macc</b>	0.3	Sets the minimum size of the bounding box, as a fraction of the effect of image charges in the walls of the box.
"MeshMaxAspect"	<b>A</b>	$\infty$	Enforces the maximum ratio between the largest and smallest mesh-spacing in each dimension to be less than <b>A</b> . Because this restriction is enforced by reducing the mesh adaptivity, using this option can result in a dramatic increase in the number of meshlines.
"SolverAcc"	<b>Verror</b>	0.01	Sets the accuracy of the multigrid Poisson solver.
"SolverMethod"	<b>"MGCG"</b>		Sets the method of the Poisson solver to any of the options listed below.
	<b>"MG"</b>		Multigrid algorithm.
	<b>"MGCG"</b>		Multigrid preconditioned cg-algorithm.
	<b>"CG"</b>		Preconditioned cg-algorithm.
	<b>"SOR"</b>		Use SOR procedure, for comparisons only.
"SolverStartZero"			Start from zero potential. If not specified, the solver starts from the previously obtained solution if the mesh size equal to mesh size of previous step.
"Cathode"			Simulates a flat cathode plane by setting a dirichlet boundary condition at z=0. Truncates the bounding box at all negative z-coordinates.
"BoundaryOpen"			Use open boundary conditions.
"BoundaryXperiodic"	<b>Xsize</b>		Use periodic boundary conditions in X. Not implemented yet.
"BoundaryYperiodic"	<b>Ysize</b>		Idem in Y.
"BoundaryZperiodic"	<b>Zsize</b>		Idem in Z.

Option	Parameter(s)	Default	Description
"BoundaryXYpipe"	<b>Xsize,Ysize</b>		Use Dirichlet boundary conditions on a beam-pipe with elliptical cross section in the xy-plane. Work in progress...
"Boundaries"	<b>String</b>	"DDD DDD"	Specify boundary conditions for each boundary individually, as a string in the following order: $x_{min}$ , $x_{max}$ , $y_{min}$ , $y_{max}$ , $z_{min}$ , $z_{max}$ . Options are several combinations of 'DAOPEN', see section 4.8.1.8.
"BeamScale"	<b>small, large</b>	$10^{-4}$ $10^{+4}$	Enforces the bunch aspect-ratio between <b>small</b> and <b>large</b> using a linear coordinate transform. The electromagnetic fields are adapted accordingly, but results will be incorrect when feature sizes in the bunch with an aspect ratio outside the specified range are present.
"Fieldfactor"	<b>scale</b>	1	Multiplication factor for all fields.
"MeshBoxXYmax"	<b>size</b>		Limits the transverse size of the mesh to given <b>size</b> .

The typical use of the `sc3dmesh` element is to use the default settings:

```
sc3dmesh() ;
```

To overwrite any of the default settings, the name of the option must be specified followed by one or more parameters. For example, to set a fixed number of 33 meshlines in all directions, the following line must be used:

```
sc3dmesh("MeshNtotal", 33, 33, 33) ;
```

The order of independent options is irrelevant. As a result, to combine a fixed number of meshlines with the simulation of a cathode plane at  $z=0$ , either one of the following lines can be used:

```
sc3dmesh("Cathode", "MeshNtotal", 33, 33, 33) ;
```

```
sc3dmesh("MeshNtotal", 33, 33, 33, "Cathode") ;
```

#### 4.8.1.2 Introduction to the algorithms

The chosen algorithm for this space-charge model in GPT is a mesh-based Poisson solver in the rest frame of the bunch. First the bunch is transformed to the frame with no average momentum. In this rest frame, only electrostatic forces are present as long as the velocities in this frame are non-relativistic. The bunch length in the rest frame is longer by the Lorentz factor  $\gamma$ .

Subsequently, a Cartesian mesh is generated in a box around the bunch. The distribution of the meshlines is non-equidistant and adapted to the projected charge density. To reduce the number of meshlines needed, an adaptive meshing technique is used. The purpose of this scheme is to both reduce 'wasted' CPU time in empty volume and reduce numerical errors by choosing more meshlines in regions with higher charge density.

The non-equidistant mesh is used to store an approximation of the charge density on the corners of the mesh. This information is obtained using a linear distribution of the charge of every particle over the eight corners of its enclosing meshbox.

The charge density on the mesh is fed into a Poisson solver to obtain the potential. A state-of-the-art multigrid Poisson solver has been constructed for the non-equidistant meshes described in subsection 4.8.1.8. It scales linearly in CPU time with the number of meshnodes. Selectable Dirichlet or open boundary conditions allow the simulation of bunches within pipes with rectangular cross section, bunches near a cathode and a bunch in open space.

The resulting potential is interpolated and differentiated using a 2<sup>nd</sup> order interpolation scheme to obtain the electric field in the rest frame of the bunch at all particle coordinates. This electric field is transformed back to the laboratory frame to obtain the electric and magnetic fields. The GPT kernel combines these fields with the external fields in the tracking engine.

The chosen algorithm implies that the velocity in the rest frame of the bunch is non-relativistic. This assumption is not always true for long bunches in the first stages of acceleration. Therefore, it is possible

that new electrons are emitted with an energy in the eV level while the front of the bunch has already been accelerated to relativistic velocities. This is a known limitation of the routine reducing the applicability.

#### 4.8.1.3 Rest frame

The first step in calculating the space-charge forces is the determination of a rest-frame velocity. This is the frame in which all particle velocities are (nearly) zero, resulting in an electrostatic field only. Because not all particles have equal velocity in a bunch with energy spread, a shared rest frame typically does not exist. The rest frame is then defined as the frame in which the total momentum is zero. The velocity  $\beta_o$  of this frame is defined by the average of all particle velocities, weighted by the Lorentz factor  $\gamma$ :

$$\beta_o = \frac{\overline{\gamma\beta}}{\overline{\gamma}} = \frac{\sum n_i \gamma_i \beta_i}{\sum n_i \gamma_i}$$

where  $n_i$  is the number of elementary particles represented by the macro-particle  $i$ . The normalized momentum  $\gamma_o \beta_o$  and the Lorentz factor  $\gamma_o$  of the rest frame are then given by:

$$\gamma_o \beta_o = \frac{\beta_o}{\sqrt{1 - \beta_o^2}}$$

$$\gamma_o = \sqrt{1 + \gamma_o^2 \beta_o^2}$$

When there is energy spread, the velocity of the rest frame is identical to the average velocity only when all velocities are non-relativistic.

The particle coordinates  $\mathbf{r}_i$  are different in the rest frame, denoted with a prime. They are a factor  $\gamma_o$  expanded in the direction of the velocity of the frame:

$$\begin{cases} \mathbf{r}_{i\perp}' = \mathbf{r}_{i\perp} \\ \mathbf{r}_{i\parallel}' = \gamma_o \mathbf{r}_{i\parallel} \end{cases} \Rightarrow \mathbf{r}_i' = \mathbf{r}_i + \frac{\mathbf{r}_i \cdot \gamma_o \beta_o}{\gamma_o + 1} \gamma_o \beta_o$$

The particle velocity  $\mathbf{u}_i$  hereby changes also:

$$\begin{cases} \mathbf{u}_{i\perp}' = \frac{\mathbf{u}_{i\perp}}{\gamma_o(1 - \beta_o \cdot \beta_o)} \\ \mathbf{u}_{i\parallel}' = \frac{\mathbf{u}_{i\parallel}}{(1 - \beta_o \cdot \beta_o)} \end{cases} \Rightarrow \mathbf{u}' = \frac{c}{\gamma_o \gamma_o - \gamma_o \beta_o \cdot \gamma_o \beta_o} \left[ \left( \frac{\gamma_o \beta_o \cdot \gamma_o \beta_o}{\gamma_o + 1} - \gamma_o \right) \gamma_o \beta_o + \gamma_o \beta_o \right]$$

It's more convenient to use the Lorentz factor given by:

$$\gamma_{u'} = \gamma_o \gamma_u (1 - \beta_o \beta_u)$$

Ideally, all velocities in the rest frame are well below the speed of light. If this is not the case, a warning is printed counting the number of particles with a Lorentz factor  $\gamma_{u'}$  larger than **Gmax**. The parameter **Gmax** can be set with the "**RestMaxGamma**" option.

#### 4.8.1.4 Bounding box

To calculate the electromagnetic potential, a Cartesian 3D mesh is used to store an estimate of the charge in the rest frame of the bunch. To solve the potential in free space, an infinite mesh is required. Because this is impractical, the actual mesh is truncated at a bounding box where the potential is assumed to be zero. The center of this bounding box is chosen as the average particle coordinate in the rest frame of the bunch. The effect of a bounding box (with Dirichlet boundary conditions) is similar to the effect of image charges.

Choosing a too large box is a waste of CPU time and memory, while choosing a too small box violates the assumption that the potential at the edges of the bounding box is zero. A combination of several options is available to set the correct size of the bounding box. The minimum size of the bounding box is always **nstd** times the standard deviation in each dimension, as can be set with the "**MeshBoxSize**" option. For low and high aspect ratio bunches this sets a too small box for the transverse and longitudinal dimensions respectively. The "**MeshBoxAccuracy**" option can be used to increase the box based on the maximum ratio of the actual fields divided by the fields produced by the image charges. This essentially makes the box sufficiently large to mimic a free space calculation. However, in extreme cases, this can set a mesh that is larger than the physical size of the beam pipe. This gives unphysical results and it is also a waste of CPU time to zero a large mesh. The "**MeshBoxXYmax**" option can be used to limit to maximum transverse size of the mesh that

is used for the space-charge calculations. The size should be set to the actual size of the beam pipe where it should be noted that the pipe is assumed to have square cross section.

#### 4.8.1.5 Number of meshlines

The bounding box is divided by a number of Cartesian meshlines. The meshlines form the edges of rectangular boxes filling the calculation domain. As explained in subsequent sections, the corners of the boxes, the crossings of the meshlines, are used to store an estimate of the charge density and to calculate the electrostatic fields.

Figure 4-18 shows a schematic of a typical meshline distribution in one dimension. A number of meshlines within the bunch dimension,  $N_{\text{bunch}}$ , are positioned more closely together where more charge is present. The lower and upper parts of the bounding box are filled with  $N_{\text{low}}$  and  $N_{\text{upp}}$  meshlines respectively, where the spacing between the meshlines gradually increases near the edge of the bounding box. The total number of meshlines is  $N_{\text{total}}$ .

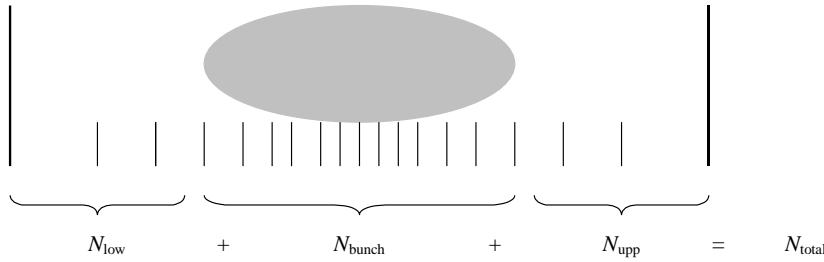


Figure 4-18: One-dimensional schematic of a typical meshline distribution.

By default, the number of meshlines in the bunch,  $N_{\text{bunch}}$ , is equal in all directions and chosen as a function of the number of particles  $N$ :

$$N_{\text{bunch}} = \text{alpha } N^{\text{mpow}}$$

where **alpha** and **mpow** can be set with the "**MeshNfac**" and "**MeshNpow**" options.

Alternatively, the number of meshlines slicing the bunch can be specified with the "**MeshNbunch**" option. Then, the number of meshlines in the bunch is fixed at **Nx**, **Ny** and **Nz** in the x-, y- and z-direction respectively and set independent on the number of particles in the bunch. In both cases, the space between the bunch and the edges of the bounding box is filled with as few additional meshlines as possible to save CPU and memory usage, see section 4.8.1.6.

A disadvantage of the options above is that an a-priori unknown number of meshlines are added to fill the bounding box. This can result in unpredictable memory usage and CPU time. To avoid this, the "**MeshNtotal**" option sets the total number of meshlines in the bounding box. When "**MeshNtotal**" is specified without further parameters, the total number of meshlines,  $N_{\text{total}}$ , is equal in all directions and given by:

$$N_{\text{total}} = \text{alpha } N^{\text{mpow}}$$

With parameters, the total number of meshlines is **Nx**, **Ny** and **Nz** in the x-, y- and z-direction respectively.

#### 4.8.1.6 Meshline positions

The positioning of the meshlines is an iterative process. To determine the position of the  $x'$ -lines, planes in the yz-plane, first a histogram of the  $x'$ -coordinates of the particles is created. To obtain a good trade-off between bin width and noise, the number of bins is taken equal to the square root of the number of particles, see Figure 4-19.

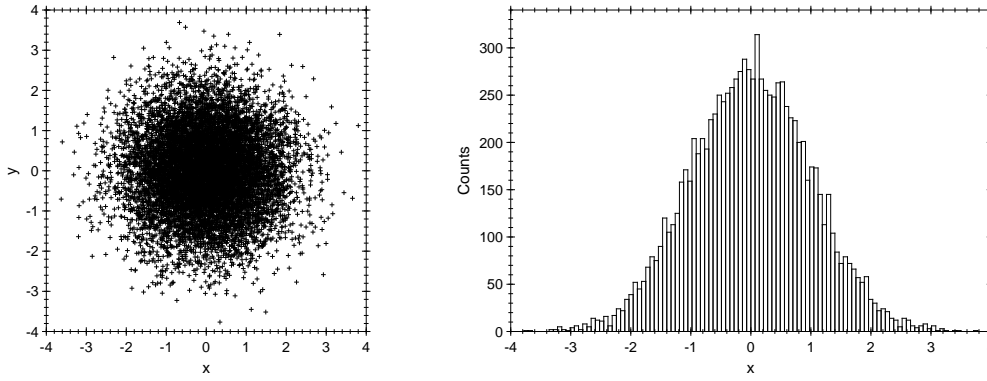


Figure 4-19: Particle positions in the xy-plane and a corresponding x-histogram for a Gaussian charge-density distribution. 10,000 sample particles are used for a Gaussian distribution with  $\sigma=1$ .

The next step approximates the Cumulative Density Function (CDF) by integrating the histograms. To compensate for the fact that we use three projections to adapt the meshline spacing to the charge density, the cubic root of the height of the histograms is used. This typically broadens the distribution. The inverse of this CDF is used to map  $N_x$  equidistantly spaced points to  $N_x$  meshline positions following the beam density.

The above procedure, however, cannot be used directly because it allows very large differences in neighboring mesh intervals, creating a non-optimal meshline distribution for the Poisson solver described in section 4.8.1.8. Therefore, the **fn** parameter is introduced to restrict the difference in spacing between neighboring meshlines. When **fn** is 0.25, this means that the difference in spacing between neighboring meshlines cannot vary by more than 25%. As an example, any mesh spacing of 1 mm with **fn**=0.25 enforces a spacing between 0.8 and 1.25 mm for its neighbours. The parameter **fn** can be set with the "**MeshAdapt**" option.

To span the mesh over the bounding box defined in section 4.8.1.4, additional meshlines are added left and right of the bunch. The spacing of these additional meshlines is increased towards the boundary, restricted to **fn**, to add as few lines as possible. If a fixed number of meshlines is chosen, the number of meshlines in the bunch decreases proportionally with the increase of meshlines between the edge of the bunch and the edge of the bounding box.

The addition of meshlines and the effect of **fn** is shown in **Error! Reference source not found.H**. When **fn**=0, the spacing between all neighboring meshlines is allowed to vary by 0%, creating an equidistant mesh. Such a mesh is most stable to solve for the Poisson solver, but it will create many empty meshboxes. On the other extreme, setting **fn**=0.5 results in dense sampling of the electron bunch and sparse sampling of the surrounding area.

#### 4.8.1.7 Charge on mesh

After the meshlines are positioned, the charge of all particles is distributed over the corners of the meshboxes using a trilinear interpolation technique. For every particle, the corresponding meshbox index ( $n_x, n_y, n_z$ ) is found by three separate bisection searches for the three dimensions. Then the relative distances  $t, u$  and  $v$  to the lower, left, bottom corner of the box are calculated from the meshlines positions  $l$ :

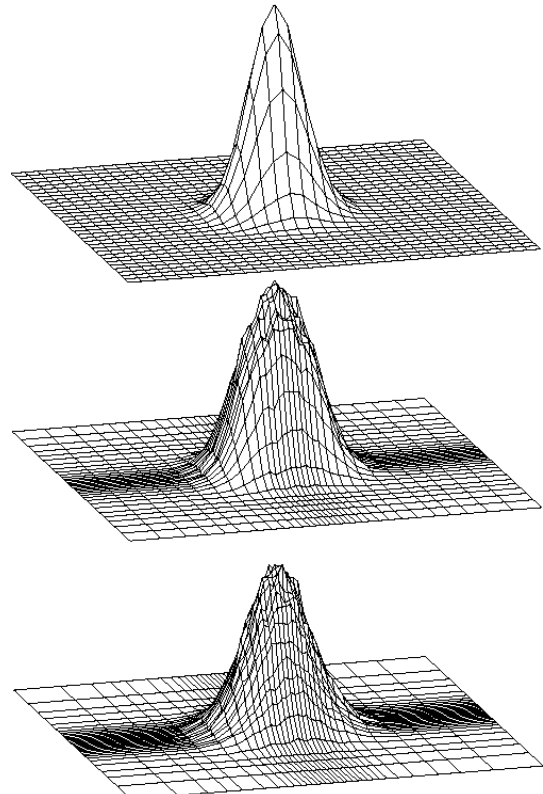


Figure 4-20: xy-meshline positions for a Gaussian charge density with **fn**=0 (top), **fn**=0.2 (middle) and **fn**=0.5 (bottom), with a bounding box of 5 sigma. The vertical axis shows the total charge in each meshbox, where the height of the top has been normalized in all plots individually.

$$\begin{aligned}
t &= (x_i - l_x(n_x)) / (l_x(n_x + 1) - l_x(n_x)) \\
u &= (y_i - l_y(n_y)) / (l_y(n_y + 1) - l_y(n_y)) \\
v &= (z_i - l_z(n_z)) / (l_z(n_z + 1) - l_z(n_z))
\end{aligned}$$

The charge  $Q_i$  of each particle  $i$  is distributed over all eight corners  $Q_{\text{mesh}}(n_x, n_y, n_z)$  of the enclosing meshbox as follows:

$$\begin{aligned}
Q_{\text{mesh}}(n_x, n_y, n_z) &= Q_i (t-1) (1-u) (1-v) \\
Q_{\text{mesh}}(n_x, n_y, n_z+1) &= Q_i (t-1) (1-u) v \\
Q_{\text{mesh}}(n_x, n_y+1, n_z) &= Q_i (t-1) u (1-v) \\
Q_{\text{mesh}}(n_x, n_y+1, n_z+1) &= Q_i (t-1) u v \\
Q_{\text{mesh}}(n_x+1, n_y, n_z) &= Q_i t (1-u) (1-v) \\
Q_{\text{mesh}}(n_x+1, n_y, n_z+1) &= Q_i t (1-u) v \\
Q_{\text{mesh}}(n_x+1, n_y+1, n_z) &= Q_i t u (1-v) \\
Q_{\text{mesh}}(n_x+1, n_y+1, n_z+1) &= Q_i t u v
\end{aligned}$$

#### 4.8.1.8 Solve potential

The electrostatic potential  $V$  in the rest frame of the bunch satisfies Poisson's equation:

$$-\nabla^2 V = \rho / \epsilon_0 \text{ in } \Omega,$$

where  $\rho$  is the charge density given in units of  $[\text{C}/\text{m}^3]$  and  $\Omega$  denotes the bounding box explained in section 4.8.1.4.

Possible boundary conditions are:

‘D’: Dirichlet boundary conditions with  $V=0$  on  $\partial\Omega$ .

‘A’: Dirichlet boundary conditions with an approximate value for the potential at the boundary based on the analytical expressions of a uniformly charged brick with equal RMS sizes.

‘O’: Open boundary conditions, which describe the decay of the potential of the bunch and ensure that  $\lim_{r \rightarrow \infty} V = 0$ .

‘P’: Periodic boundary condition. Not implemented yet.

‘E’: Elliptical boundary condition. Work in progress...

‘N’: Neumann boundary condition with  $\partial V / \partial n = 0$  on  $\partial\Omega$ .

Poisson's equation is discretized by means of second-order finite differences. The generation of the underlying mesh is described in section 4.8.1.6. The resulting linear system of equations  $AV_{\text{mesh}} = Q_{\text{mesh}}$  is solved by means of a multigrid (MG) technique adapted to non-equidistant grids. A more detailed description of this solver can be found in [17, 18].

The input of the Poisson solver are the meshline positions and the charge on all meshnodes  $Q_{\text{mesh}}(n_x, n_y, n_z)$ . The output is the potential on all meshnodes  $V_{\text{mesh}}(n_x, n_y, n_z)$ .

Two multigrid schemes are implemented: The most stable algorithm is the multigrid preconditioned conjugate gradient method (MGCG) that is set as default. For saving CPU time it is possible to choose the plain MG algorithm for bunches with ‘good’ behavior:

```
sc3dmesher("SolverMethod", "MG") ;
```

The number of multigrid iterations is determined by the option **"SolverAcc"** with the default setting  $10^{-2}$ . That means for the relative residual

$$\frac{|AV_{\text{mesh}}^{(n)} - Q_{\text{mesh}}|_{\text{max}}}{|Q_{\text{mesh}}|_{\text{max}}} \leq 10^{-2},$$

where  $V_{\text{mesh}}^{(n)}$  denotes the solution after  $n$  multigrid iterations. In our experience this solver accuracy suffices for most applications. A smaller number usually does not improve the result because all discretizations occurring in the simulation (this also applies to the tracking itself) restrict the accuracy that can be achieved. Furthermore the achievable accuracy is restricted by the noise that the charge density contains.



In cases the multigrid Poisson solver does not provide acceptable results, or does not even converge, several parameters can be changed:

#### ***Change the size of the bounding box***

In several cases enlarging the bounding box helps. This leads to a better approximation of the field near the surface of this bounding box (see section 4.8.1.4) in cases where the field of the bunch decays.

If the potential of the bunch has a decay of at least as  $1/r$ , the difference between simulations with Dirichlet or open boundaries is not essential. In case the stability of the algorithm turns out to be a problem Dirichlet boundary conditions should be preferred.

#### ***Change the Poisson solver algorithm***

Beside the multigrid algorithms two other Poisson solvers are implemented: A preconditioned conjugate gradient (CG) method with the diagonal of the matrix  $A$  as preconditioner and the SOR relaxation. The related commands are:

`sc3dmesh("SolverMethod","CG");` and `sc3dmesh("SolverMethod","SOR");` respectively.

Although both algorithms are much slower than the multigrid method (CG faster than SOR) they can be applied in order to verify that the problem is due to the solver (for instance no convergence).

#### ***Change the discretization:***

Problems with the Poisson solver are mostly caused by the discretization. As already mentioned in section 4.8.1.6 large differences in neighboring step sizes can be the underlying reason. Furthermore, the global aspect ratio  $h_{\max}/h_{\min}$  must not be too large. A smaller value for `fn`, which controls the step sizes of the mesh, therefore improves the discretization of Poisson's equation, e.g. `sc3dmesh("MeshAdapt",0.2);`

Another possibility to verify the mesh is to vary the number of meshlines (see section 4.8.1.5). A general advice cannot be given because an appropriate choice very much depends on the characteristics of the application. Note that a larger number of meshlines specified with `"MeshNtotal"` usually provides an undesired larger aspect ratio!

### **4.8.1.9 Interpolate $E'$ from $V'$**

The electric field in the rest frame of the bunch is given by the derivative of the potential:

$$\mathbf{E}' = -\nabla V$$

Centered differencing and a trilinear interpolation scheme are used to calculate this derivative at all particle positions. First, for every particle, the procedure described in 4.8.1.7 is again used to find the enclosing meshbox index  $(n_x, n_y, n_z)$ . To obtain the x-component of the electric field, first the electric fields interpolated at the left and at the right sides of the box, trilinear interpolated to the yz-position of the particle, are calculated using centered differencing:

$$E_{x,left} = \frac{((1-u)(1-v)V(-1,0,0) + (1-u)vV(-1,0,1) + u(1-v)V(-1,1,0) + uvV(-1,1,1)) - ((1-u)(1-v)V(+1,0,0) + (1-u)vV(+1,0,1) + u(1-v)V(+1,1,0) + uvV(+1,1,1))}{l_x(n_x+1) - l_x(n_x-1)}$$

$$E_{x,right} = \frac{((1-u)(1-v)V(0,0,0) + (1-u)vV(0,0,1) + u(1-v)V(0,1,0) + uvV(0,1,1)) - ((1-u)(1-v)V(2,0,0) + (1-u)vV(2,0,1) + u(1-v)V(2,1,0) + uvV(2,1,1))}{l_x(n_x+2) - l_x(n_x)}$$

The notation  $V(a,b,c)$  is used to represent the potential  $V$  at index  $(n_x+a, n_y+b, n_z+c)$ .

Linear interpolation is used to obtain the final x-component of the electric field at the particle position:

$$E_x = (1-t) E_{x,left} - left + t E_{x,right}$$

The equations for the y- and z-components of the electric field are fully analogous.

### **4.8.1.10 Aspect-ratio scaling**

Very low and very high aspect ratio bunches are difficult to simulate with the described mesh-based space-charge routine. For relatively uniform bunches, an option to increase the accuracy is to multiply the particle coordinates in one dimension such that the aspect ratio of the bunch falls in the range between 0.01 and 100.

Very high aspect ratio bunches ( $A > 100$ ) have nearly identical fields when the total charge is constant. From a physical point of view this is clear, because in the 'pancake' regime the bunch behaves as a surface charge

and the precise thickness of this surface does not affect the fields. As a result, it is safe to scale the longitudinal coordinate of all particles in a pancake bunch as long as it stays sufficiently flat. Symbolically:

$$\text{If } \begin{cases} stdz < stdx / S_{\text{large}} \\ stdz < stdy / S_{\text{large}} \end{cases} \Rightarrow \begin{cases} S = \frac{\min(stdx, stdy)}{S_{\text{large}} stdz} \text{ where } S_{\text{large}} \approx 100 \\ z_i \leftarrow S z_i \end{cases}$$

Clearly, this scaling can only be used when the features of interest in the bunch are ‘pancake’. If a ‘hotspot’ near a cathode has a radius of one-tenth of the radius of the bunch, the  $S_{\text{large}}$  parameter needs to be in the order of 1000 to allow scaling.

Scaling is also possible for very low aspect ratio bunches ( $A < 0.01$ ). These ‘cigar’-shaped bunches have equal transverse fields as long as the charge density remains constant. The longitudinal fields, except at the very edges, however scale inverse linear with the length. Therefore, the scaling recipe becomes:

$$\text{If } \begin{cases} stdz > stdx / S_{\text{small}} \\ stdz > stdy / S_{\text{small}} \end{cases} \Rightarrow \begin{cases} S = \frac{\max(stdx, stdy)}{S_{\text{small}} stdz} \\ z_i \leftarrow S z_i \\ E_x \leftarrow S E_x \\ E_y \leftarrow S E_y \\ E_z \leftarrow S^2 E_z \end{cases} \text{ where } S_{\text{small}} \approx 0.01$$

The parameters  $S_{\text{small}}$  and  $S_{\text{large}}$  can be set with the "**BeamScale**" option.

#### 4.8.1.11 Transform to rest frame

To obtain the actual electromagnetic 3D space-charge fields, the electric field  $\mathbf{E}'_i$  is transformed back to the laboratory frame. This is accomplished with the following Lorentz transformation:

$$\mathbf{E}_i = \gamma_0 \left[ \mathbf{E}'_i - \frac{\gamma_0}{\gamma_0 + 1} (\boldsymbol{\beta}_0 \cdot \mathbf{E}'_i) \boldsymbol{\beta}_0 \right]$$

$$\mathbf{B}_i = \frac{\gamma_0 \boldsymbol{\beta}_0 \times \mathbf{E}'_i}{c}$$

## 4.8.2 spacecharge3Dtree

**spacecharge3Dtree(theta)** ;

3D space-charge routine based on the Barnes-Hut hierarchical tree algorithm [19,20].

**theta** Overall accuracy parameter. The typical range is from 0.3 (publication quality) to 1.0 (quick and dirty).

The main use of **spacecharge3Dtree** is to calculate stochastic/granularity effects such as disorder-induced heating and Boersh effect efficiently: **spacecharge3Dtree** covers all Coulomb interactions from first principles, and therefore includes both space charge and stochastic effects.

The fields of relativistic bunches are calculated in a co-moving frame, fully analogous to the **spacecharge3Dmesh** element. This element is however substantially slower compared to the PIC method employed in **spacecharge3Dmesh**. Consequently, it is wise to use this element only when granularity effects are important.

A Barnes-Hut algorithm is used to efficiently compute the fields of many interacting particles. This is an  $\mathcal{O}(N \log N)$ -scheme based on hierarchical grouping of distant particles. The interaction between near neighbours is calculated individually, but distant charges are grouped together into a single-charge or multipole expression, leading to substantial savings in the number of interactions necessary to calculate the fields compared to the point-to-point method employed in **spacecharge3D**. Only in the case of excessive energy spread, when there is no co-moving frame with all velocities far below the speed of light, the fully relativistic **spacecharge3D** element should be considered.

To avoid field-discontinuities that slow down the integration of the equations of motion, each particle is represented as a Plummer sphere with smoothing length  $\mathbf{r}$ . The current implementation requires this radius

to be identical for all particles. It can be set with the **setmacrodist** keyword as described in section 4.2.1.12:

```
setmacrodist(set,"u",R,0) ;
```

where **set** is the particle set, for example **"beam"**.

If each particle in the simulation represents one elementary particle, the smoothing length **R** must be chosen much smaller than the typical distance between the particles. In the case where each particle represents a large number of elementary particles, **R** is a tradeoff between unphysical disorder-induced heating and underestimation of space-charge forces. The ‘correct’ value for this case is in the order of the typical distance between the macro-particles. However, in that case we strongly recommend benchmarking against the PIC model of **spacecharge3Dmesh**.

The charge density, electrostatic field and potential of the particles are respectively given by:

$$\begin{aligned}\rho(r) &= \frac{q}{4\pi} \frac{3R^2}{(r^2 + R^2)^{5/2}} \\ \mathbf{E}_r(r) &= \frac{q}{4\pi\epsilon_0} \frac{\mathbf{r}}{(r^2 + R^2)^{3/2}} \\ V(r) &= \frac{q}{4\pi\epsilon_0} \frac{1}{\sqrt{r^2 + R^2}}\end{aligned}$$

The integrated charge density equals the total charge  $q$ . The limiting cases for  $r \gg R$  are the well-known equations for point charges:

$$\begin{aligned}\mathbf{E}_r(r) &= \frac{q}{4\pi\epsilon_0} \frac{\mathbf{r}}{r^3} \\ V(r) &= \frac{q}{4\pi\epsilon_0 r}\end{aligned}$$

The algorithm calculates near-neighbour interactions individually, and all other particles are grouped in increasingly larger clusters as function of distance. The dimensionless parameter **theta** sets the accuracy of the calculations by indirectly defining the number of particles that are grouped together. It is defined as the threshold for the ratio between the size of a distant cluster and its distance. For a detailed explanation of **theta**, see [21]. A smaller value for **theta** results in a higher accuracy at the expense of CPU time. Typical values are in the range 0.3 to 2.0, with a recommended range between 0.5 and 1.0. In the extreme case **theta**=0, the algorithm does not use any grouping and calculates all  $N^2$  interactions individually.

Quadrupole moments of the charge distribution are taken into account in the calculation as it increases the accuracy at fairly modest computational costs. If the particle distribution contains both negative and positive charge also the dipole moment is taken into account.

#### 4.8.2.1 Lorentz transformations for relativistic bunches

All particle interactions are calculated in the rest frame of the bunch, fully analogous to the **spacecharge3Dmesh** method. The rest frame is defined as the frame with zero total momentum. It has a velocity  $\beta_0$  and accompanying Lorentz factor  $\gamma_0$  of respectively:

$$\begin{aligned}\beta_0 &= \frac{\sum n_i \gamma_i \beta_i}{\sum n_i \gamma_i} \\ \gamma_0 &= 1/\sqrt{1-\beta_0^2}\end{aligned}$$

The particle coordinates  $\mathbf{r}_i$  are different in the rest frame, denoted with a prime. They are a factor  $\gamma_0$  expanded in the direction of the velocity of the frame:

$$\begin{cases} \mathbf{r}'_{i\perp} = \mathbf{r}_{i\perp} \\ \mathbf{r}'_{i\parallel} = \gamma_0 \mathbf{r}_{i\parallel} \end{cases} \Rightarrow \mathbf{r}'_i = \mathbf{r}_i + \frac{\mathbf{r}_i \cdot \gamma_0 \beta_0}{\gamma_0 + 1} \gamma_0 \beta_0$$

Ideally, all velocities in the rest frame are well below the speed of light. A warning is printed if the Lorentz factor of a particle *as measured in the rest frame* exceeds the value of 2. The calculated electric field  $\mathbf{E}'_i$  is Lorentz transformed back to the laboratory frame to get the required  $\mathbf{E}$  and  $\mathbf{B}$  fields for the tracking:

$$\mathbf{E}_i = \gamma_0 \left[ \mathbf{E}'_i - \frac{\gamma_0}{\gamma_0 + 1} (\boldsymbol{\beta}_0 \cdot \mathbf{E}'_i) \boldsymbol{\beta}_0 \right]$$

$$\mathbf{B}_i = \frac{\gamma_0 \boldsymbol{\beta}_0 \times \mathbf{E}'_i}{c}$$

#### 4.8.2.2 Image charges

The **spacecharge3Dtree** model cannot be used directly to calculate the effect of image charges because the fields are singular at the cathode plane. Nevertheless, stochastic Coulomb interactions can be simulated while also taking into account the bulk effect of image charges. The recipe is combining three different spacecharge lines in the GPT inputfile as follows:

```
spacecharge3Dtree(theta) ;
spacecharge3Dmesh("Cathode") ;
spacecharge3Dmesh("Fieldfactor",-1) ;
```

This works because image charges are, by definition, the fields of the bunch including the (cathode) boundary condition, minus the fields of the bunch in free space. This can be simulated with two different **spacecharge3Dmesh** lines on top of the tree-based stochastic space charge model.

### 4.8.3 Spacecharge3D

```
spacecharge3D([zmin,zmax]) ;
```

Instructs GPT to take 3D space-charge effects into account using a point-to-point method.

**zmin**                    z-position [m] from where to calculate the space-charge fields. If not specified,  $-\infty$  is assumed.  
**zmax**                    z-position [m] unto where to calculate the space-charge forces. If not specified,  $\infty$  is assumed.

The fields generated by the **spacecharge3D** routine are calculated directly from relativistic particle-particle interaction. For each particle-particle contribution both particles have to be within the range **zmin** < z < **zmax**. Retardation and radiation effects are not taken into account. The advantage of this method is that no approximations are made; the disadvantage is the price in terms of CPU time. Particle-particle interactions are  $N^2$  processes, where  $N$  is the number of traced macro-particles.

To calculate the fields generated by particle  $j$  at the position of particle  $i$ , first both particle coordinates are transformed to the rest frame of particle  $j$ . Due to Lorentz contraction, the distance between the two particles thereby changes:

$$\mathbf{r}_{ji} = \mathbf{r}_i - \mathbf{r}_j$$

$$\mathbf{r}'_{ji} = \mathbf{r}_{ji} + \frac{\gamma_j^2}{\gamma_j + 1} (\mathbf{r}_{ji} \cdot \boldsymbol{\beta}_j) \boldsymbol{\beta}_j$$

where  $\mathbf{r}_{ji}$  is the distance measured in the lab frame and  $\mathbf{r}'_{ji}$  is the distance in the rest frame.

Within the rest frame of particle  $j$ , only an electric field is present. This coulomb field is given by

$$\mathbf{E}'_{j \rightarrow i} = \frac{1}{4\pi\epsilon_0} \frac{Q\mathbf{r}'_{ji}}{(\mathbf{r}_{ji}^2 + R^2)^{3/2}}$$

where  $R$  is the Plummer sphere radius. This extra term in the denominator is to prevent rare divisions by zero, and it slightly increases tracking speed. It can be set with the keyword **setmacrodist** described in section 4.2.1.12. To prevent an unrealistic drop in field amplitude, the radius  $R$  should be set smaller than the typical distance between two particles.

Transforming this electric field back to the lab frame and summing over all particles yields the electromagnetic fields at the position of particle  $i$ :

$$\mathbf{E}_i = \sum_{j \neq i} \gamma_j \left[ \mathbf{E}'_{j \rightarrow i} - \frac{\gamma_j}{\gamma_j + 1} (\boldsymbol{\beta}_j \cdot \mathbf{E}'_{j \rightarrow i}) \boldsymbol{\beta}_j \right]$$

$$\mathbf{B}_i = \sum_{j \neq i} \frac{\gamma_j \boldsymbol{\beta}_j \times \mathbf{E}'_{j \rightarrow i}}{c}$$

#### 4.8.4 Spacecharge3Dclassic

**spacecharge3Dclassic**([**zmin**,**zmax**]) ;

Instructs GPT to take 3D non-relativistic space-charge effects into account using a point-to-point method.

**zmin**                      z-position [m] from where to calculate the space-charge fields. If not specified,  $-\infty$  is assumed.

**zmax**                      z-position [m] unto where to calculate the space-charge forces. If not specified,  $\infty$  is assumed.

The fields generated by the **spacecharge3Dclassic** routine are calculated directly from non-relativistic particle-particle interaction. For each particle-particle contribution both particles have to be within the range **zmin** < z < **zmax**. Retardation, relativistic and radiation effects are not taken into account.

The coulomb field generated by particle *j* at the position of particle *i* is given by

$$\mathbf{r}_{ji} = \mathbf{r}_i - \mathbf{r}_j$$

$$\mathbf{E}_{j \rightarrow i} = \frac{1}{4\pi\epsilon_0} \frac{Q \mathbf{r}_{ji}}{(\mathbf{r}_{ji}^2 + R^2)^{3/2}}$$

where *R* is the Plummer sphere radius. This extra term in the denominator is to prevent rare divisions by zero, and it slightly increases tracking speed. It can be set with the keyword **setmacrodist** described in section 4.2.1.12. To prevent an unrealistic drop in field amplitude, the radius *R* should be set smaller than the typical distance between two particles.

#### 4.8.5 SetTotalCharge

**settotalcharge**(**set**,**Q**) ;

Sets the total charge of all particles in a set.

**set**                      Particle set.

**Q**                      Total charge [C] of the set.

This element can be used to specify the total charge of a set, analogue to the **Q** parameter of the **setparticles** function. It can only be used after all particles are added to the specified **set**.

#### 4.8.6 Spacecharge2Dcircle

**spacecharge2Dcircle**([**zmin**,**zmax**]) ;

Calculates 2D space-charge fields using charged circles.

**zmin**                      z-position [m] from where to calculate the space-charge forces. If not specified,  $-\infty$  is assumed.

**zmax**                      z-position [m] upto where to calculate the space-charge forces. If not specified,  $\infty$  is assumed.

The **spacecharge2Dcircle** element can be used to calculate the space-charge effect of cylinder-symmetric beams by representing every particle as a homogeneously charged circle. Because every particle represents a complete circle, the amount of particles needed to obtain correct statistics is much less when compared to the point-to-point calculations. The influence of the transverse velocity on the space-charge field is neglected.

For the calculation of the total fields working on particle  $i$  due to the space charge, first the parameters of the circle representing particle  $j$  are obtained. The radius  $R_j$ , charge density  $\lambda_j$  and center position  $\mathbf{C}_j$  are defined by:

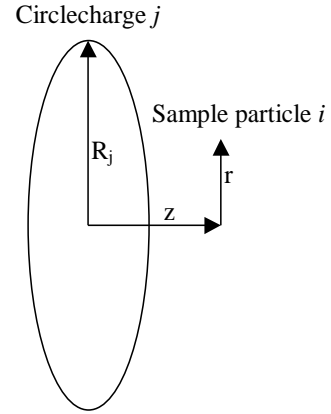
$$R_j = \sqrt{x_j^2 + y_j^2}$$

$$\lambda_j = Q_j / 2\pi R_j$$

$$\mathbf{C}_j = (0, 0, z_j)$$

The velocity of the circle is the longitudinal velocity of particle  $j$ . Therefore, the Lorentz factor  $\gamma_j$  of the circle must be:

$$\gamma_j = 1 / \sqrt{1 - \beta_{z,j}^2}$$



In the rest frame of the circle, there is only an electrostatic field<sup>4</sup>. This field is derived from the electrostatic potential (in polar coordinates):

$$\begin{aligned} V'_j(r, \theta) &= \frac{\lambda_j R}{4\pi\epsilon_0} \int_0^{2\pi} \frac{1}{\sqrt{R^2 + r^2 - 2Rr \sin(\theta) \cos(\phi)}} d\phi \\ &= \frac{Q_j}{2\pi^2 \epsilon_0} \frac{K\left(\frac{4Rr \sin(\theta)}{a^2 + r^2 + 2Rr \sin(\theta)}\right)}{\sqrt{R^2 + r^2 + 2Rr \sin(\theta)}} \end{aligned}$$

Using the definition<sup>5</sup>:

$$K(k) = \int_0^{\pi/2} \frac{1}{\sqrt{1 - k \sin(\theta)}} d\theta$$

The resulting electric field in the rest frame is calculated from  $\mathbf{E}' = -\nabla V'$ . Calculating the gradient and converting from polar to cylindrical coordinates yields<sup>6</sup>:

$$\begin{aligned} E'_r &= \frac{Q}{4\pi^2 \epsilon_0 r \sqrt{d^2 + 4Rr}} \left( K(\alpha) - \frac{R^2 - r^2 + z^2}{d^2} E(\alpha) \right) \\ E'_z &= \frac{Qz E(\alpha)}{2\pi^2 \epsilon_0 d^2 \sqrt{d^2 + 4Rr}} \end{aligned}$$

where  $E(k) = \int_0^{\pi/2} \sqrt{1 - k \sin(\theta)} d\theta$ ,  $d^2 = (R - r)^2 + z^2$  and  $\alpha = 4Rr / (d^2 + 4Rr)$ . Due to Lorentz contraction in the laboratory frame,  $z = \gamma_j (z_i - z_j)$ . No relativistic effects occur in the transverse direction because the circle is assumed to have a longitudinal velocity component only.

Transforming this field back to the lab frame and adding the contributions of all particles  $j$  yields:

$$\begin{aligned} E_x &= \sum_{j \neq i} \gamma_j E'_{x,j} & B_x &= \sum_{j \neq i} -\gamma_j \beta_{z,j} E'_{y,j} / c \\ E_y &= \sum_{j \neq i} \gamma_j E'_{y,j} & B_y &= \sum_{j \neq i} +\gamma_j \beta_{z,j} E'_{x,j} / c \\ E_z &= \sum_{j \neq i} E'_{z,j} & B_z &= 0 \end{aligned}$$

Currently, it is not allowed to start particles at  $x=y=0$  while using the **spacecharge2Dcircle** element. Because this element assumes cylindrical symmetry anyway, it is best to fill only the positive x-axis as shown in the following example.

<sup>4</sup> Actually, a  $\beta_{\phi,j}$  term could be interpreted as a rotation of the circle, and a  $dR/dt$  term as expansion and contraction. Both terms result in a magnetic field in the rest frame of the circle, but their contributions are neglected here.

<sup>5</sup> Please note that the argument  $k$  of the elliptic functions is sometimes written as  $k^2$  in the literature.

<sup>6</sup> Actually, we use the Carlson elliptic functions:  $K(k) = R_F(1 - k^2)$  and  $E(k) = R_F(1 - k^2) - \frac{1}{3} k^2 R_D(1 - k^2)$  to avoid the singularity at  $r=0$ .

Example: Start a 100 pC beam with a radius of 1 mm, optimally distributed for spacecharge2Dcircle. The optional **setphidist** can be specified after **setxdist** to fill the entire xy-plane.

```
1. nps = 1000 ;          # Start 1000 particles
2. Qtot = -100e-12 ;    # Total charge 100 pC
3. R = 1e-3 ;           # Beam radius of 1 mm
4. setparticles( "beam", nps, me, qe, Qtot ) ;
5. setxdist("beam","u",R/2,R) ;
6. setphidist("beam","u",0,2*pi) ;
7. setcharge2Dcircle("beam",Qtot) ;
8. spacecharge2Dcircle() ;
```

#### 4.8.7 Setcharge2Dcircle

**setcharge2Dcircle(set,Q) ;**

Sets the total charge of a particle set for the rz space-charge models.

**set**                      Particle set.  
**Q**                        Total charge of the particle set [C].

The number of elementary particles represented by each macro-particle,  $n_i$ , is calculated. In contrast to **setparticles** and **settotalcharge**, the  $n_i$ 's are not constant but a linear function of the distance of the particle to the z-axis. The total charge of all the particles in the specified **set** sums to **Q**.

When a point-to-point space-charge model is used, the optimal initial particle distribution is uniform in the xy-cross section for a uniform beam. This results in more particles at a larger radius, each representing the same number of elementary particles. However, when an rz space-charge model like **spacecharge2Dcircle** is used, it is better to distribute the particles equidistantly in  $r$ . This implies that particles further off-axis should carry more charge, linear with this distance. Thus each particle should represent  $n$  elementary particles as specified by:

$$n_i = \frac{Q \sqrt{x_i^2 + y_i^2}}{\sum_i q_i \sqrt{x_i^2 + y_i^2}}$$

where  $q_i$  is the elementary charge of particle  $i$ . For a uniform distribution in  $x$  of identical particles, the equation reduces to:

$$n_i = \frac{2\sqrt{x_i^2 + y_i^2} Q}{N R q}$$

#### 4.8.8 Spacecharge2Dline

**spacecharge2Dline([zmin,zmax]) ;**

Calculates 2D space-charge fields using infinitely long line charges [22].

**zmin**                    z-position [m] from where to calculate the space-charge forces. If not specified,  $-\infty$  is assumed.  
**zmax**                    z-position [m] unto where to calculate the space-charge forces. If not specified,  $\infty$  is assumed.

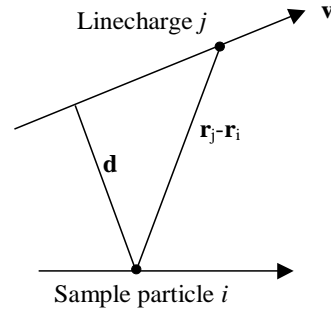
The **spacecharge2Dline** element can be used to provide a quick estimate for space-charge forces in continuous beams or very long bunches. Every particle is represented as a moving line charge, directed in the particle's velocity. Because every particle represents a complete line, the amount of particles needed to obtain correct statistics is much less when compared to the point-to-point calculations in **spacecharge3D**.

To calculate the fields at the position of particle  $i$ , generated by the moving line charge representing particle  $j$ , first the distance  $\mathbf{d}$  between the point  $i$  and the line  $j$  is calculated by:

$$\mathbf{d}_{ji} = (\mathbf{r}_j - \mathbf{r}_i) - [(\mathbf{r}_j - \mathbf{r}_i) \cdot \hat{\mathbf{v}}_j] \cdot \hat{\mathbf{v}}_j$$

The total charge ( $Q_{tot}$ ) parameter of **setparticles** is interpreted as the beam current [A] when **spacecharge2Dline** is used. Therefore, each particle  $j$  represents a current  $i_j$  [A] and charge density  $\lambda_j$  [C/m] given respectively by:

$$i_j = \frac{Q_{tot}}{N}, \quad \lambda_j = \frac{i_j}{v_j}$$



The total electromagnetic field, at the position of particle  $i$ , is the sum of the contributions of the individual line charges  $j$ . The magnetic contribution is due to the current  $i_j$ , the electrical contribution due to the charge density  $\lambda_j$ .

$$\mathbf{E}_i = \sum_{j \neq i} \frac{i_j}{|v_j|} \frac{1}{2\pi \epsilon_0 d_{ji}^2} \cdot -\mathbf{d}_{ji}$$

$$\mathbf{B}_i = \sum_{j \neq i} \frac{i_j}{|v_j|} \frac{\mu_0}{2\pi d_{ji}} \cdot (\mathbf{d}_{ji} \times \mathbf{v})$$

These equations are relativistically correct, even though no Lorentz transformation is applied. The transverse distribution is not restricted in any way.

When **setrmacrodist** is used, the line charges have a radius  $R$ . Within this radius, the equations reduce to:

$$\mathbf{E}_i = \sum_{j \neq i} \frac{i_j}{|v_j|} \frac{1}{2\pi \epsilon_0 R^2} \cdot -\mathbf{d}_{ji}$$

$$\mathbf{B}_i = \sum_{j \neq i} \frac{i_j}{|v_j|} \frac{\mu_0}{2\pi R} \cdot (\mathbf{d}_{ji} \times \mathbf{v})$$

Because every particle represents a line, the simulation must be started with a thin disk of particles. When the longitudinal dimensions of the disk become too large due to energy spread, the accuracy of the model diminishes rapidly.



## 4.9 Scattering

Despite the name of this section, it contains a description of both boundary and scatter elements. In combination, they can be used to generate particles scattered off a surface, as described in section 1.11. Arbitrary diffraction patterns can be simulated using the scatterbitmap element.

4.9.1	ForwardScatter .....	203
4.9.2	CopperScatter .....	203
4.9.3	ScatterBitmap .....	204
4.9.4	ScatterCone .....	205
4.9.5	ScatterIris.....	206
4.9.6	ScatterPipe.....	206
4.9.7	ScatterPlate.....	207
4.9.8	ScatterSphere.....	207
4.9.9	ScatterTorus.....	208

An aspect ratio of 1 is recommended when inspecting scattered trajectories. Without such an aspect-ratio all angles will be deformed, making interpretation much harder.

### 4.9.1 ForwardScatter

**forwardscatter** (**ECS**, **name**, **P**, [**nmin**]) ;

Scatter a particle in the forward direction with probability P.

<b>ECS</b>	Element Coordinate System.
<b>name</b>	Name of the surface.
<b>P</b>	Scatter probability.
<b>nmin</b>	Minimum nmacro.

A specularly reflected macro-particle is generated with the same energy as the incident particle in the forward direction. The new number of elementary particles this macro-particle represent is **P\*nmacro**. When this **P\*nmacro** < **nmin**, the new particle is not generated. Scatter output is written in the outputfile relative to the specified **ECS**.

One of the applications of the boundary elements is to remove particles using the **forwardscatter** element with a scattering probability of 0. This is demonstrated in the following example:

```
forwardscatter ("wcs", "I", "remove", 0) ;
scatteriris ("wcs", "z", 1, 0.5, 2 ) scatter="remove" ;
```

### 4.9.2 CopperScatter

**copperscatter** (**ECS**, **name**, **nmin**, **nmax**) ;

Scatter a particle from a copper surface.

The copperscatter element uses extrapolated data not yet experimentally confirmed.

<b>ECS</b>	Element Coordinate System.
<b>name</b>	Name of the surface.
<b>nmin</b>	Minimum nmacro, typically 1% of the initial nmacro.
<b>nmax</b>	Maximum nmacro, typically ignored by setting to 200% of the initial nmacro.

The probability for forward scattering is 1/3, the chance for backward is 2/3. The overall reflection chance is the product of the angle of incidence dependence and the dependence on the kinetic energy of the incident particle, as shown in Figure 4-21 and Figure 4-22. This overall reflection chance determines the **nmacro** of the reflected particle as calculated in **forwardscatter**. When the product of the scattering probabilities times the **nmacro** of the incident particle is below **nmin**, no new particle is generated. The total kinetic energy of the reflected particle varies uniformly between 45% and 95% of the kinetic energy of the incident particle.

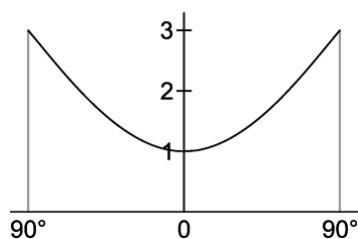


Figure 4-21: Reflection chance as function of angle of incidence. Zero angle corresponds to normal incidence.

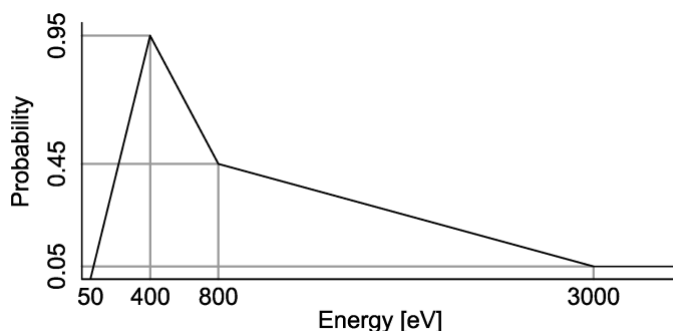


Figure 4-22: Reflection chance as function of incoming kinetic energy.

The simple function for the reflection chance as function of incoming kinetic energy comes from an extrapolation of the data from [23]. Custom scatter routines can be written, as is explained in the Programmer's Reference.

### 4.9.3 ScatterBitmap

**scatterbitmap**(ECS, name, filename, xres, yres) ;

Scatter a particle with an arbitrary distribution as specified in a bitmap.

<b>ECS</b>	Element Coordinate System.
<b>name</b>	Name of the surface.
<b>filename</b>	Filename of a grayscale bitmap file (.bmp) containing the desired momentum distribution.
<b>xres</b>	Normalized x-momentum change per pixel.
<b>yres</b>	Normalized y-momentum change per pixel.

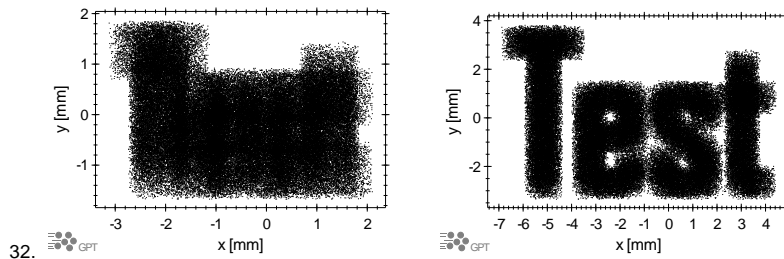
When a particle passes through a 'scatterbitmap' surface, the normalized horizontal and vertical momenta are changed according to the probability function given in **filename**. This can be used, for example, to model a diffraction process where the bitmap contains white-values representing the angular probability function for the diffraction process under investigation. In the example below, we use a simple bitmap containing the text 'test' in white.

Example: GPT inputfile diffracting a 1x1 mm square input beam off a 'test' bitmap.

```

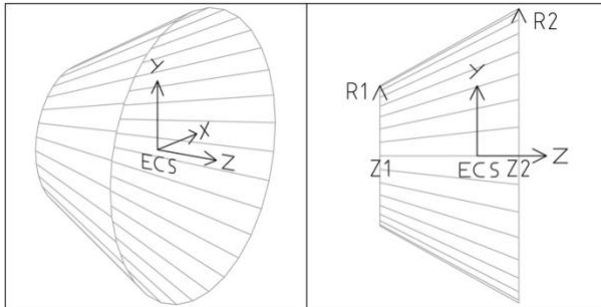
1. # setparticles("beam",10000,me,qe,0) ;
2.
3. setxdist("beam","u",0,1e-3) ;
4. setydist("beam","u",0,1e-3) ;
5.
6. setGdist("beam","u",1.2,0) ;
7.
8. scatterbitmap("wcs","I","diffract","test.bmp",0.001,0.001) ;
9. scatterplate("wcs","z",0.01,1,1) scatter="diffract" ;
10.
11. tout(0,1e-9,0.01e-9) ;
31.

```



#### 4.9.4 ScatterCone

**scattercone(ECS,z1,R1,z2,R2) scatter="sm" ;**  
 Cone-shaped scattering surface.



<b>ECS</b>	Element Coordinate System.
<b>z1</b>	z-position [m] of radius <b>R1</b> .
<b>R1</b>	Radius [m] of cone at <b>z=z1</b> position.
<b>z2</b>	z-position [m] of radius <b>R2</b> .
<b>R2</b>	Radius [m] of cone at <b>z=z2</b> position.
<b>sm</b>	Scatter model to be used.

New particles are generated when an incident particle passes through the infinitely thin cone surface. The particles are scattered according to the scattering model.

The equation for the cone boundary is given by:

$$x^2 + y^2 - \left( R1 + \frac{R2 - R1}{z2 - z1} (z - z1) \right)^2 = 0$$

Example: GPT inputfile with cone surface, 50% forward scattering probability. Plot zx.

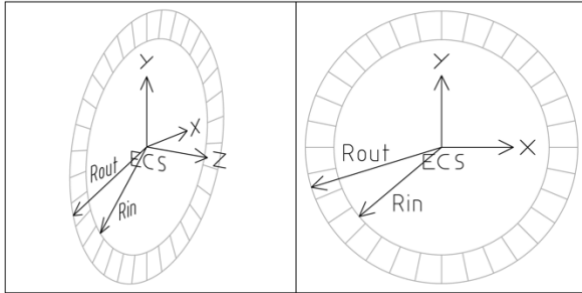
```

1. # Demonstration inputfile for cone scattering element
2. setstartline("beam",50, -2.5,0,0, 2.5,0,0, 0,0,1) ;
3.
4. forwardscatter("wcs","I","scat", 0.5) ;
5. scattercone("wcs","I", 1,0.5, 2.0,1.5 ) scatter="scat" ;
6.
7. tout(0, 6/c, 0.06/c) ;

```

### 4.9.5 ScatterIris

**scatteriris**(ECS,Rin,Rout) scatter="sm" ;  
Iris- or disk-shaped scattering surface.



**ECS** Element coordinate system.  
**Rin** Inner radius [m] of disk.  
**Rout** Outer radius [m] of disk.  
**sm** Scatter model to be used.

New particles are generated when an incident particle passes through the infinitely thin plate surface around the opening. The particles are scattered according to the scattering model. The normal of the disk is the z-axis.

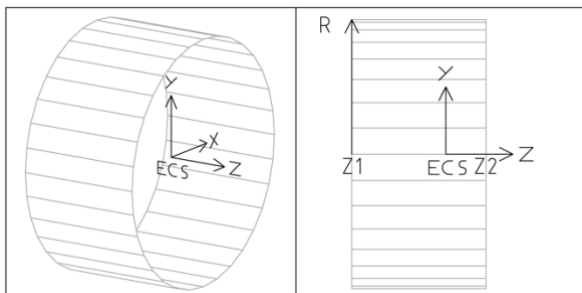
The description of the plate boundary is given by:  
 $z=0$  if  $r>Rin$  and  $r<Rout$ .

Example: GPT inputfile with iris surface, particles are removed. Plot zx.

```
1. # Demonstration inputfile for iris scattering element
2. setstartline("beam",50, -2.5,0,0, 2.5,0,0, 0,0,1) ;
3.
4. forwardscatter("wcs","I","remove", 0) ;
5. scatteriris("wcs","z", 1, 0.5,2 ) scatter="remove" ;
6.
7. tout(0, 4/c, 0.04/c) ;
33.
```

### 4.9.6 ScatterPipe

**scatterpipe**(ECS,z1,z2,R) scatter="sm" ;  
Pipe-shaped scattering surface.



**ECS** Element Coordinate System.  
**z1** z-position [m] where the pipe begins.  
**z2** z-position [m] where the pipe ends.  
**R** Radius [m] of pipe.  
**sm** Scatter model to be used.

New particles are generated when an incident particle passes through the infinitely thin pipe surface. The particles are scattered according to the scattering model.

The description of the cone boundary is given by:

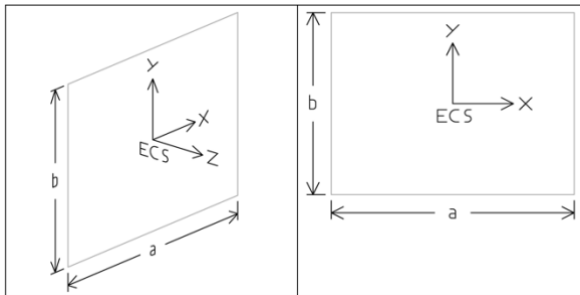
$$x^2 + y^2 - R^2 = 0$$

Example: GPT inputfile with pipe surface, 50% scattering probability. Plot xy.

```
1. # Demonstration inputfile for pipe scattering element
2. setstartline("beam",50, -2,2,0, 2,2,0, 0,-1,0) ;
3.
4. forwardscatter("wcs","I","scat", 0.5) ;
5. scatterpipe("wcs","I", -1,1, 1 ) scatter="scat" ;
6.
7. tout(0, 4/c, 0.04/c) ;
```

#### 4.9.7 ScatterPlate

**scatterplate(ECS,a,b) scatter="sm" ;**  
Plate-shaped scattering surface.



<b>ECS</b>	Element Coordinate System.
<b>a</b>	Total plate length in x-direction.
<b>b</b>	Total plate length in y-direction.
<b>sm</b>	Scatter model to be used.

New particles are generated when an incident particle passes through the infinitely thin plate surface. The particles are scattered according to the scattering model. The normal of the plate is the z-axis.

The description of the plate boundary is given by:

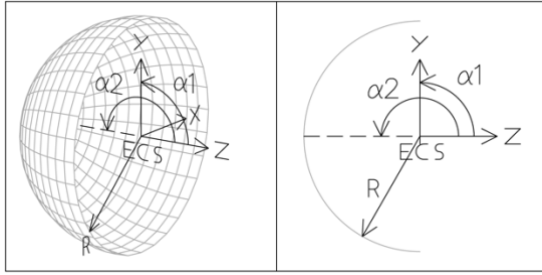
$$z=0$$

Example: GPT inputfile with plate surface, particles are removed. Plot xy.

```
1. # Demonstration inputfile for plate scattering element
2.
3. setparticles("beam",1000,me,qe,0.0) ;
4. setxdist("beam","u",0,2) ;
5. setydist("beam","u",0,2) ;
6. setGdist("beam","u",10,1) ;
7.
8. forwardscatter("wcs","I","remove", 0.0) ;
9. scatterplate("wcs","z",1, 1,1 ) scatter="remove" ;
10.
11. tout(2/c) ;
```

#### 4.9.8 ScatterSphere

**scattersphere(ECS,R,[a1,a2]) scatter="sm" ;**  
Sphere-shaped scattering surface.



<b>ECS</b>	Element Coordinate System.
<b>R</b>	Radius of sphere.
<b>a1</b>	Start angle [rad] measured ccw from the <b>z</b> -direction in the zR-plane.
<b>a2</b>	End angle [rad] measured ccw from the <b>z</b> -direction in the zR-plane.
<b>sm</b>	Scatter model to be used.

New particles are generated when an incident particle passes through the infinitely thin sphere surface. The particles are scattered according to the scattering model. The symmetry axis of the sphere is the z-axis.

The description of the sphere boundary is given by:

$$x^2 + y^2 + z^2 - R^2 = 0$$

Example: GPT inputfile with sphere surface, 50% scattering probability. Plot zx.

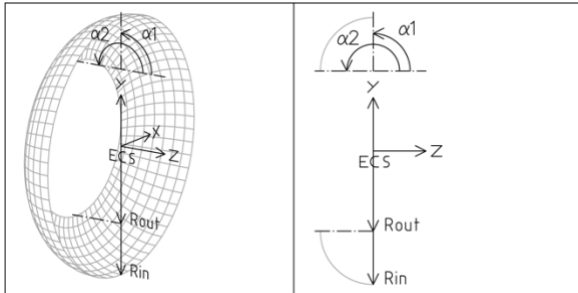
```

1. # Demonstration inputfile for an open sphere scattering element
2. setstartline("beam",50, 2,0,-2, 2,0,2, -1,0,0) ;
3.
4. forwardscatter("wcs","I","scat", 0.5) ;
5. scattersphere("wcs","I", 1, pi/2,pi ) scatter="scat" ;
6.
7. tout(0, 4/c, 0.04/c) ;

```

#### 4.9.9 ScatterTorus

**scattertorus(ECS,Rout,Rin,[a1,a2]) scatter="sm" ;**  
Torus-shaped scattering surface.



<b>ECS</b>	Element Coordinate System.
<b>Rout</b>	Outer radius [m] of torus.
<b>Rin</b>	Inner radius [m] of torus.
<b>a1</b>	Start angle [rad] measured ccw from the <b>z</b> -direction in the zr-plane.
<b>a2</b>	End angle [rad] measured ccw from the <b>z</b> -direction in the zr-plane.
<b>sm</b>	Scatter model to be used.

New particles are generated when an incident particle passes through the infinitely thin torus surface. The particles are scattered according to the scattering model.

The description of the torus boundary is given by:

$$a^4 - 2a^2(x^2 + y^2 - z^2 + b^2) + (x^2 + y^2 + z^2 - b^2)^2 = 0$$

where  $a$  is the outer radius and  $b$  is the inner radius of the torus.

Example: GPT inputfile with torus surface, 50% scattering probability. Plot zx.

```
1. # Demonstration inputfile for torus scattering element
2. setstartline("beam",50, 3,0,-2, 3,0,2, -1,0,0) ;
3.
4. forwardscatter("wcs","I","scat", 0.5) ;
5. scattertorus("wcs","I", 1.1,1.0, 0,pi/2 ) scatter="scat" ;
6.
7. tout(0, 4/c, 0.04/c) ;
```

## 4.10 Remove particles

The elements listed in this section remove particles when inside a specific volume. No scattered particles are generated.

4.10.1	Gminmax .....	210
4.10.2	Multislit.....	210
4.10.3	Rmax.....	210
4.10.4	StdXYZmax .....	210
4.10.5	XYmax.....	211
4.10.6	Zminmax.....	211

An alternative to these elements is to use the boundary elements of section 4.9 to define a boundary and use **forwardscatter** with a probability of 0 to remove the particle without generating a scattered particle.

### 4.10.1 Gminmax

**Gminmax** (**ECS**, **L**, **Gmin**, **Gmax**) ;

Removes all particles with a Lorentz factor outside the specified range.

<b>ECS</b>	Element Coordinate System.
<b>L</b>	Length of the element [m].
<b>Gmin</b>	Minimum Lorentz factor.
<b>Gmax</b>	Maximum Lorentz factor.

This element is only active when  $|z| < \frac{1}{2} \mathbf{L}$ . In that range, it removes all particles with a Lorentz factor outside the range bracketed by the specified **Gmin** and **Gmax**.

### 4.10.2 Multislit

**multislit** (**ECS**, **a**, **b**, **L**, **d**, **N**) ;

Removes a particle if it does not pass through an opening of a multiple slit.

<b>ECS</b>	Element Coordinate System.
<b>a</b>	Width of a slit opening [m] (in <b>x</b> -direction).
<b>b</b>	Height of a slit opening [m] (in <b>y</b> -direction).
<b>L</b>	Length of the element [m] (in <b>z</b> -direction).
<b>d</b>	Distance between the centers of two slit openings [m].
<b>N</b>	Number of slits.

This element simulates a multiple slit. The particles can only pass through the openings of the slit, all other particles are removed if  $|z| < \frac{1}{2} \mathbf{L}$ . This element is local.

### 4.10.3 Rmax

**rmax** (**ECS**, **R**, [**L**]) ;

Removes a particle when it is too far from the axis.

<b>ECS</b>	Element Coordinate System.
<b>R</b>	Maximum radius [m].
<b>L</b>	Length of the element [m]. If not specified, $\infty$ is assumed.

The particle is removed when:  $x^2 + y^2 > \mathbf{R}^2$  and  $|z| < \frac{1}{2} \mathbf{L}$ .

Although **L** can be specified, this element is global.

### 4.10.4 StdXYZmax

**stdxyzmax** (**Nstdx**, **Nstdy**, **Nstdz**) ;

Removes particles too far off the center of the bunch.



<b>Nstdx</b>	Allowed number of standard deviations in x. Ignored when zero.
<b>Nstdy</b>	Allowed number of standard deviations in y. Ignored when zero.
<b>Nstdz</b>	Allowed number of standard deviations in z. Ignored when zero.

Every particle located at least **Nstdx**, **Nstdy** or **Nstdz** standard deviations away from the average  $x$ -,  $y$ - or  $z$ -coordinate of the bunch is removed.

This element is intended to ‘clean up’ the simulation by removing all outliers, all the particles located too far from the center of the bunch. This can be used to solve the following problems:

- Outliers can affect the GDFA data analysis routines and cause unrealistic values for bunch length, energy spread etc.
- Outliers can significantly increase the simulation time for a variety of reasons.

Typical values for **Nstdx**, **Nstdy** and **Nstdz** are between 4 and 6.

Particle  $i$  is removed if one of the following conditions is true:

$$\mathbf{Nstdx} \neq 0 \wedge (x_i < \bar{x} - \mathbf{Nstdx} \, stdx \vee x_i > \bar{x} + \mathbf{Nstdx} \, stdx)$$

$$\mathbf{Nstdy} \neq 0 \wedge (y_i < \bar{y} - \mathbf{Nstdy} \, stdy \vee y_i > \bar{y} + \mathbf{Nstdy} \, stdy)$$

$$\mathbf{Nstdz} \neq 0 \wedge (z_i < \bar{z} - \mathbf{Nstdz} \, stdz \vee z_i > \bar{z} + \mathbf{Nstdz} \, stdz)$$

where

$$stdx = \sqrt{(x - \bar{x})^2}$$

$$stdy = \sqrt{(y - \bar{y})^2}$$

$$stdz = \sqrt{(z - \bar{z})^2}$$

#### 4.10.5 XYmax

**xymax** (**ECS**, **a**, **b**, [**L**]) ;

Removes a particle when it is too far from the axis.

<b>ECS</b>	Element Coordinate System.
<b>a</b>	Maximum $x$ -deviation [m].
<b>b</b>	Maximum $y$ -deviation [m].
<b>L</b>	Length of the element [m]. If not specified, $\infty$ is assumed.

The particle is removed when:  $|x| > \frac{1}{2} \mathbf{a}$  or  $|y| > \frac{1}{2} \mathbf{b}$  if  $|z| < \frac{1}{2} \mathbf{L}$ .

Although **L** can be specified, this element is global.

#### 4.10.6 Zminmax

**zminmax** (**ECS**, **zmin**, **zmax**) ;

Removes all particles in front of **zmin** or behind **zmax**.

<b>ECS</b>	Element Coordinate System.
<b>zmin</b>	Minimum $z$ -coordinate [m].
<b>zmax</b>	Maximum $z$ -coordinate [m].

The particle is removed when  $z < \mathbf{zmin}$  or  $z > \mathbf{zmax}$ .

## 4.11 Miscellaneous

This section contains all built-in elements not easily placed in any of the other categories.

4.11.1	CCS.....	212
4.11.2	CCSflip .....	212
4.11.3	Collision.....	212
4.11.4	Drift.....	213
4.11.5	Gravity .....	213
4.11.6	Overlaptest.....	213
4.11.7	Randomize .....	213
4.11.8	Run.....	214
4.11.9	SetRlimit .....	214
4.11.10	Viscosity .....	214

### 4.11.1 CCS

**ccs (ECS, CCSname) ;**

Defines a Custom Coordinate System.

**ECS**                      The coordinate system transform.  
**CCSname**                The name of the Custom Coordinate System.

See section 1.4.3 for the description of Custom Coordinate Systems.

### 4.11.2 CCSflip

**ccsflip (ECS, CCSname) ;**

Refer all particles to another axis.

**ECS**                      The coordinate system transform.  
**CCSname**                The name of the Custom Coordinate System to transfer the particle to.

All particles coordinates are referred to the axis named **CCSname** when  $z > 0$  in the specified ECS.

See section 1.4.3 for the description of Custom Coordinate Systems.

### 4.11.3 Collision

**collision() ;**

Detect particle-particle collisions and start a new 'combined' particle.

At the end of every successful timestep collisions between two particles are detected when:

$$|\mathbf{r}_i - \mathbf{r}_j|^2 < R_j^2$$

When a collision is detected, both particles are removed and a new particle is created. The new position is equal to the mass-weighted average position. The new momentum is the sum of the moments of the initial particles:

$$\mathbf{r}_{new} = (n_i m_i \mathbf{r}_i + n_j m_j \mathbf{r}_j) / (n_i m_i + n_j m_j)$$

$$\mathbf{p}_{new} = \mathbf{p}_1 + \mathbf{p}_2 \Rightarrow \gamma \beta_{new} = (n_i m_i \gamma \beta_i + n_j m_j \gamma \beta_j) / (n_i m_i + n_j m_j)$$

The new mass and charge are the sum of the mass and charge of the original particles as given by:

$$n_{new} = n_i + n_j$$

$$q_{new} = (n_i q_i + n_j q_j) / n_{new}$$

$$m_{new} = (n_i m_i + n_j m_j) / n_{new}$$

#### 4.11.4 Drift

**drift(ECS,L,[R]) ;**

Drift section.

**ECS** Element Coordinate System.

**L** Length of the drift section [m].

**R** Radius [m]. When this parameter is specified, the particle is removed when  $x^2 + y^2 > R^2$ .

This element is ‘active’ when  $|z| < \frac{1}{2}L$ . It does nothing except optionally remove a particle when it is too far from the axis. If your set up has large sections without elements it is recommended to use **drift**. It can speed up calculation time because all the other local elements on the axis don't have to be checked each timestep.

Although this element can be replaced by a **rmax**, it is recommended to use **drift** when possible because it is local and therefore faster.

#### 4.11.5 Gravity

**gravity(gx,gy,gz) ;**

Calculates uniform relativistic gravity force

**gx** Gravitational acceleration [m/s<sup>2</sup>] in x-direction.

**gy** Gravitational acceleration [m/s<sup>2</sup>] in y-direction.

**gz** Gravitational acceleration [m/s<sup>2</sup>] in z-direction.

For non-relativistic velocities, the gravitational field is simply given by:

$$\mathbf{F} = m\mathbf{g}$$

where **g** is the gravitational acceleration. For relativistic particles however, the more complicated equation from the general theory of relativity must be used:

$$\mathbf{F} = \gamma m [(1 + \beta^2) \mathbf{g} - (\beta \cdot \mathbf{g}) \beta]$$

The equation is derived from the relativistic gravity force of a spherically symmetric object with mass *M* given by:

$$\mathbf{F} = -GM \frac{E}{c^2} \frac{(1 + \beta^2) \mathbf{r} - (\beta \cdot \mathbf{r}) \beta}{|\mathbf{r}|^3}$$

where *G* is the gravitational constant and *E* is the particle energy  $\gamma mc^2$ . When the particle displacement is much smaller than *r*, the spherical field can be approximated by a uniform field using  $\mathbf{g} = -GM\mathbf{r}/|r|^3$ .

#### 4.11.6 Overlaptest

**overlaptest() ;**

Tests if local elements overlap on-axis.

As described in section 1.4.1, the GPT kernel does not allow local elements to overlap beyond neighbouring centers. This element can be added to the inputfile to run an on-axis test to see if local elements erroneously overlap. In case of a modeling error, an error with detailed information is printed and GPT does not start tracking.

When GPT is run with the *-v* option, this element prints the boundaries of all local elements.

#### 4.11.7 Randomize

**randomize([seed]) ;**

Initialize the GPT random-number generator.

**seed** Number indicating the starting point in the sequence of random numbers generated by GPT. The system time is used when omitted.

Without randomization, all pseudorandom sequences will reproduce from run to run. Using `randomize` you can specify a different `seed` for a different, but reproducing, sequence. When `seed` is not specified, the system time is used to assure every GPT run uses a different sequence.

When `randomize` is used in combination with the random-ordering specification (`~`) of the initial particle distributions, please make sure it appears before the corresponding `set...dist` element(s).

### 4.11.8 Run

```
run(program, [param1, param2, ...]) ;
```

Runs an external command.

**program**            Command to be executed.

**paramN**            Optional parameter(s).

Using `run`, any external program can be executed that doesn't require interactive (keyboard) input. When additional parameters are specified, they are separated by spaces and passed to the program. For example, the following lines will delete the file `filename` in the current directory.

```
run("del", "filename") ; # Windows
```

```
run("rm" , "filename") ; # Linux
```

Variables, expressions and the redirection operators `<`, `|` and `>` work as usual. For example the following code fragment runs `program -2 3.141592653589793 /options` and writes the output to the file `program.log`.

```
1. a = -2 ;
2. b = pi ;
3. run("program ",a,b, "/options", ">program.log")
```

Obviously, when specific Linux or DOS commands are specified, the GPT inputfile is not portable anymore. Furthermore, only command-line programs are supported by the GPTwin graphical user interface.

### 4.11.9 SetRlimit

```
setrlimit(resource,soft,hard) ;
```

Limits the use of system resources.

**resource**            Must be any of: `"CORE"` (maximum size of the core file [bytes]), `"CPU"` (Time limit in [s]), `"DATA"` (maximum size [bytes] of the data segment) or `"FSIZE"` (largest size [bytes] for any file written).

**soft**                The soft limit for the **resource**, implemented for the resource `"CPU"` only.

**hard**                The hard limit for the **resource**, implemented for all resources.

This element limits the use of system resources, in particular CPU time. It is primarily used to prevent GDFMGO/GDFSOLVE from wasting CPU time on unrealistic input parameters. This element is only implemented for the Linux/Mac version of GPT.

Setting the `"CPU"` limit instructs GPT to try to finish the current timestep and close all outputfiles after the **soft** limit is reached. When the **hard**-limit is reached for any **resource**, the program is terminated regardless of the state of the outputfile. This may result in corrupt and unreadable outputfiles. The following example sets a soft limit of 1000 and a hard limit of 1200 seconds:

```
setrlimit("CPU",1000,1200) ;
```

The implementation of `setrlimit` is a 1:1 mapping to the `setrlimit` function of the underlying operating system. Please consult your system documentation for technical details as they tend to differ slightly.

### 4.11.10 Viscosity

```
viscosity(eta) ;
```

Calculates viscosity forces.

**eta** viscosity [Pa s]:  $\eta$ .

This element adds a linear viscosity force as function of particle velocity. The viscosity force acts on all particles and is given by:

$$\mathbf{F} = -6\pi\eta R \boldsymbol{\beta} c$$

The radius of the particles  $R$  can be set using the **setrmacrodust** keyword. Typical **eta** values are  $17.1 \cdot 10^{-6}$  for air and  $1.00 \cdot 10^{-3}$  for water at standard pressure and room temperature.

## 4.12 Free Electron Laser (FEL), Wakefields, and CSR

This section describes elements for particle-radiation interaction, i.e. the simulation of Free Electron Lasers (FELs), wakefields and Coherent Synchrotron Radiation (CSR) effects.

4.12.1	Gauss00mf .....	216
4.12.2	Undueqfo .....	219
4.12.3	Unduplan.....	219
4.12.4	Wakefield.....	220

The FEL module allows multi-mode, multi-pass FEL simulations, with emphasis on phase-space evolution of the electron bunch during passage through the undulator. This is an expert element for expert users. If you plan to use GPT for serious design work on FELs, please contact us for additional advice.

The wakefield element calculates the fields of longitudinal and transverse wakefields in a 1D approximation. The wakefunctions are read from an external tabulated file and this file needs to be precomputed using other software. The implementation for the wakefields is not based on a series of kicks, but the wakefields themselves are added to the equations of motion. This is more natural and more accurate in a time-domain code, but please note that the units of the wakes are different compared to most other codes.

The CSR module is a full-featured CSR model based on 1D segmentation of the bunch in 3D space. The fields are directly evaluated from the Liénard–Wiechert potentials, based on the stored history of the bunch. This allows for example for microbunching studies in a series of magnets close together where the entrance and exit effects are crucial. There is an embargo on this element for a specific use case. Please contact us for details.

### 4.12.1 Gauss00mf

**gauss00mf**(ECS, w0, L, fmin, fmax, Nm, Ain, dz, alpha, LVset) ;

Multiple first order Gaussian modes in free space.

<b>ECS</b>	Element Coordinate System.
<b>w0</b>	Radius of waist [m].
<b>L</b>	Total cavity length [m].
<b>fmin</b>	Minimum frequency [Hz].
<b>fmax</b>	Maximum frequency [Hz].
<b>Nm</b>	Number of modes to be included in the simulation.
<b>Ain</b>	Initial field amplitude [V/m] for all modes.
<b>dz</b>	Initial translation of center pulse [m].
<b>alpha</b>	Damping [s <sup>-1</sup> ].
<b>LVset</b>	Name of the set containing ‘Litvinenko’ particles. To disable this option, an empty string "" must be specified.

The **gauss00mf** element of GPT models a radiation pattern consisting of a (large) number of first-order Gaussian waves propagating in free space [24]. Both the effect of the waves on the particle trajectories and the effect of the particles on the wave amplitudes and phases are included.

There is a separate GPT version that includes an updated version of this element including transverse modes and MPI capabilities. Please contact us for details.

#### 4.12.1.1 Equations

The Gaussian waves included in the simulation are all assumed to have a polarization in the x-direction. The total electromagnetic fields of all modes  $j$ , each with amplitude  $A_j$  and phase  $\phi_j$ , is then given by:

$$E_x = \sum_j A_j \frac{w_0}{w_j(z)} e^{-\frac{r^2}{w_j^2(z)}} \cos\left(\omega_j t - k_j z - \frac{k_j r^2 z}{2(z^2 + z_{0,j}^2)} + \arctan\left(\frac{z}{z_{0,j}}\right) + \phi_j\right)$$

$$B_y = E_x / c$$

where

$$w_j(z) = w_0 \sqrt{1 + z^2 / z_{0,j}^2}$$

$$z_{0,j} = \frac{1}{2} k_j w_0^2$$

$$\omega_j = k_j c$$

$$k_j = (n\pi - \arctan(2L^2 / n\pi w_0^2)) / L$$

and  $n$  is the mode number,  $r$  is the radial position of a particle and  $z$  the longitudinal position. The sign of both the electric and the magnetic field is reversed for all particles in the Litvinenko set.

The total stored energy of mode  $j$  in length  $L$  is given by:

$$W_j = \frac{1}{2} A_j^2 \pi \epsilon_0 w_0^2 L$$

The differential equations for the amplitudes and phases of all modes are derived by first separating each wave  $j$  in two orthogonal waves with amplitudes  $u$  and  $v$ :

$$E_{x,j} = u_j T_j \cos(\theta_j) - v_j T_j \sin(\theta_j)$$

where

$$u_j = A_j \cos(\varphi_j)$$

$$v_j = A_j \sin(\varphi_j)$$

$$T_j = \frac{w_0}{w_j(z)} e^{-\frac{r^2}{w_j^2(z)}}$$

$$\theta_j = \omega_j t - k_j z - \frac{k_j r^2 z}{2(z^2 + z_{0,j}^2)} + \arctan(z / z_{0,j})$$

The total number of modes  $N_{\text{all}}$  in the specified frequency range **fmin** to **fmax** is given by:

$$N_{\text{all}} = \frac{2L}{c} (\mathbf{fmax} - \mathbf{fmin})$$

In the simulation only a specified limited number of modes **Nm** is included. The mode spacing  $\Delta N$  can be calculated from:

$$\Delta N = \frac{N_{\text{all}}}{\mathbf{Nm}}$$

The most accurate simulation, with  $\Delta N=1$ , includes all modes in the simulation. When  $\Delta N$  is 2, every other mode is included. In other words, every simulated mode represents not only itself but also its neighboring mode. With typical FEL parameters with high frequencies and large cavities, a  $\Delta N$  parameter of more than one thousand is normal, indicating that every simulated mode represents over a thousand actual modes.

The mode numbers  $n_j$  used in the simulation are uniformly distributed between the specified frequencies by:

$$n_j = \frac{2L \mathbf{fmin}}{c} + (j - \frac{1}{2}) \Delta N, \quad j = 1 \dots \mathbf{Nm}$$

Because both  $\Delta N$  and  $n$  must be integers, the specified **Nm** is adapted to model the simulated frequency range properly between **fmin** and **fmax**.

The energy lost by each macro-particle  $i$ , with charge  $Q_i$ , contributes to an increase in stored energy in all  $\Delta N$  modes represented by mode  $j$ :

$$\frac{dW_j}{dt} = -\Delta N \sum_i Q_i \mathbf{v}_i \cdot \mathbf{E}_j$$

The differential equations solved by this element can be derived from the orthogonality of the modes and conservation of energy. An additional frequency independent damping term is added to account for outcoupling and mirror losses. The equations are solved for each mode individually and given by:

$$\frac{du_j}{dt} = -\sum_i \frac{Q_i \Delta N}{\epsilon_0 \pi w_0^2 L} v_{x,i} T_j \cos(\theta_j) - \alpha u_j$$

$$\frac{dv_j}{dt} = +\sum_i \frac{Q_i \Delta N}{\epsilon_0 \pi w_0^2 L} v_{x,i} T_j \sin(\theta_j) - \alpha v_j$$

The sign of the first term, not the damping, is reversed for all particles in the Litvinenko set.

The boundary conditions of the differential equations, the amplitudes and phases of all modes at  $t=0$ , are given by:

$$A_{j,t=0} = \mathbf{Ain} \Delta N$$

$$\varphi_{j,t=0} = k_j \mathbf{dz}$$

The initial pulse is created in the center of the cavity. In order to overlap the radiation pulse with an electron bunch, the  $\mathbf{dz}$  parameter can be used to translate the initial pulse. For example, for a cavity between  $z=0$  and  $z=L$  the pulse at  $t=0$  can be moved to  $z=0$  by specifying  $\mathbf{dz}=-L/2$ .

#### 4.12.1.2 Frequency domain output

At every time output of GPT, the **G00mf** element writes the amplitude, phase, frequency and wavelength of each mode in the GPT outputfile:

<b>A00</b>	Array of amplitudes of all modes [V/m]. Can be plotted as function of phase, frequency or wavelength.
<b>phi00</b>	Array of phases of all modes [rad].
<b>freq00</b>	Array of frequencies of all modes [Hz].
<b>lam00</b>	Array of wavelengths of all modes [m].

The amplitude and phase of mode  $j$  written in the GPT outputfile are calculated from:

$$\mathbf{A00}_j = A_j / \Delta N = \sqrt{u_j^2 + v_j^2} / \Delta N$$

$$\mathbf{phi00}_j = \arctan\left(\frac{v_j}{u_j}\right)$$

The division by  $\Delta N$  for the amplitude compensates the multiplication by  $\Delta N$  in the interaction strength. This makes the amplitude of the output spectrum independent of the number of modes.

The total energy in the pulse is also written in the outputfile:

**w00** Total energy in the pulse [J].

$$\mathbf{W00} = \frac{\pi \epsilon_0 w_0^2 L}{2 \Delta N} \sum_j A_j^2$$

The total energy in the pulse is equal to the energy lost by the particles:

$$W_{00} = \Delta \gamma mc^2 \frac{Q_{tot}}{q_e}$$

#### 4.12.1.3 Time-domain output

When **Nm**≠1, at every time output of GPT, the **G00mf** element writes the time-structure of the Gaussian modes to the GPT outputfile in the following arrays:

<b>At00</b>	Array of amplitudes [V/m], to be plotted as function of <b>t00</b> .
<b>Pt00</b>	Array of power [W], to be plotted as function of <b>t00</b> .
<b>t00</b>	Array for the time-axis [s].

The time-domain output is defined by the Fourier transform of the frequency domain. When all modes are included in the simulation,  $\Delta N=1$ , the time-domain output repeats itself after round-trip time  $2L/c$ . A mode spacing of  $\Delta N$  in frequency domain is equivalent to  $N$  identical pulses in the round-trip time. As a result, all relevant time output is defined in the interval  $\Delta t$  given by:

$$\Delta t = \frac{2L}{c \Delta N}$$



The time-structure is calculated by the discrete Fourier transformation of the frequency spectrum at  $z=0$  using:

$$\begin{aligned} \mathbf{t00}_k &= t_k = \left\{ -\frac{1}{2}\Delta t, dt - \frac{1}{2}\Delta t, 2dt - \frac{1}{2}\Delta t, \dots, \frac{1}{2}\Delta t \right\} \\ \mathbf{At00}_k &= A_{t_k + \text{offset}} = \sum_j A_j \cos(\omega_j t_k + \varphi_j) \\ \mathbf{Pt00}_k &= \frac{1}{2} \pi \varepsilon_0 \omega_0^2 c \mathbf{At00}_k^2 \end{aligned}$$

where the spacing in time domain  $dt$  is given by:

$$dt = \frac{1}{7 \mathbf{fmax}}$$

To ease the interpretation of the results,  $\text{offset}$  is chosen such that the pulse is centered around  $t=0$ . This is implemented by a robust minimalization of  $\sigma$  from:

$$\sigma = \sum_k |A_{t_k + \text{offset}}| \cdot |t_k|$$

All arrays for both frequency and time output can be visualized directly with GPTwin, or analyzed with the standard GPT analysis tools like GDFA.

#### 4.12.2 Undueqfo

**undueqfo**(ECS, Nu, lamu, Bu, trim1, trim2) ;

Double focusing undulator with equal focusing in  $x$  and  $y$ .

<b>ECS</b>	Element Coordinate System.
<b>Nu</b>	Total number of undulator periods.
<b>lamu</b>	Undulator period [m]
<b>Bu</b>	Undulator field amplitude [T].
<b>trim1</b>	First matching coefficient (usually ¼).
<b>trim2</b>	Second matching coefficient (usually ¾).

The **B** field generated by this element is given by:

$$\mathbf{B} = \mathbf{Bu} F_s \begin{pmatrix} \sinh\left(\frac{k_u}{\sqrt{2}} x\right) \sinh\left(\frac{k_u}{\sqrt{2}} y\right) \sin(k_u z) \\ \cosh\left(\frac{k_u}{\sqrt{2}} x\right) \cosh\left(\frac{k_u}{\sqrt{2}} y\right) \sin(k_u z) \\ \sqrt{2} \cosh\left(\frac{k_u}{\sqrt{2}} x\right) \sinh\left(\frac{k_u}{\sqrt{2}} y\right) \cos(k_u z) \end{pmatrix}$$

where  $k_u = \frac{2\pi}{\text{lamu}}$  and  $F_s = \text{trim1}, \text{trim2}, 1, 1, \dots, 1, 1, \text{trim2}, \text{trim1}$  for each half undulator period.

To import realistic undulator fields, please see the **MAP3D\_B** element.

#### 4.12.3 Unduplan

**unduplan**(ECS, Nu, lamu, Bu, trim1, trim2) ;

Planar undulator.

<b>ECS</b>	Element Coordinate System.
<b>Nu</b>	Total number of undulator periods.
<b>lamu</b>	Undulator period [m].
<b>Bu</b>	Undulator field amplitude [T].
<b>trim1</b>	First matching coefficient (usually ¼).
<b>trim2</b>	Second matching coefficient (usually ¾).

The **B** field generated by this element is given by:

$$\mathbf{B} = \mathbf{Bu} F_s \begin{pmatrix} 0 \\ \cosh(k_u y) \sin(k_u z) \\ \sinh(k_u y) \cos(k_u z) \end{pmatrix}$$

where  $k_u = \frac{2\pi}{\lambda_{mu}}$  and  $F_s$  is the shaping function for the first and the last half undulator period.

The dimensionless undulator strength  $K$  can be obtained using:

$$K = \left| \frac{qB\lambda_{mu}}{\sqrt{8}\pi mc} \right|$$

To import realistic undulator fields, please see the **MAP3D\_B** element.

#### 4.12.4 Wakefield

**wakefield(ECS,L,b1,wakefile.gdf,z,Wx,Wy,Wz,[options,...]) ;**

Include 1D longitudinal and/or transverse wakefield(s)

<b>ECS</b>	Element coordinate system.
<b>L</b>	Length of element [m]
<b>b1</b>	Fringe parameter [ $m^{-1}$ ]
<b>wakefile.gdf</b>	Filename containing the wake potentials
<b>z</b>	Name of the column containing the lag [m]. All coordinates must be positive.
<b>Wx</b>	Name of the column containing the transverse x-wake [ $V/C/m^2$ ]. Can be an empty string.
<b>Wy</b>	Name of the column containing the transverse y-wake [ $V/C/m^2$ ]. Can be an empty string.
<b>Wz</b>	Name of the column containing the longitudinal wake [ $V/C/m$ ]. Can be an empty string.
<b>options</b>	A list of further options that affect the model, see below.

This element includes 1D transverse and longitudinal wakefields in the range  $-L/2 < z < L/2$ . The wakes are a convolution of the 1D current profile of the bunch with the specified wake function(s). The fields are defined by:

$$E_x(z) = A(z) \int_{z'=z}^{\infty} B(z') I(z') W_x(z' - z) \bar{x}(z') dz'$$

$$E_y(z) = A(z) \int_{z'=z}^{\infty} B(z') I(z') W_y(z' - z) \bar{y}(z') dz'$$

$$E_z(z) = A(z) \int_{z'=z}^{\infty} B(z') I(z') W_z(z' - z) dz'$$

where a 1D longitudinal segmentation of the beam is used to estimate the line-current  $I(z)$  and the average transverse positions  $\bar{x}(z)$  and  $\bar{y}(z)$ . The additional shape functions  $A(z)$  and  $B(z')$  are described below.

Wakefields can be interpreted as upstream particles *emitting* a wake that is subsequently *received* by the downstream particles. The wake functions  $W_x(z)$ ,  $W_y(z)$  and  $W_z(z)$  define the amount of interaction as function of the distance between the emitting and receiving particles. All wakefields scale linearly with the amount of charge of the emitting particles, and the transverse wakes also scale linearly with the transverse offset of the receiving particles.

The  $A(z)$  function describes the  $z$ -range for the *receiving* particles, and this range coincides with the location of this element: The function  $A(z)$  is unity in range  $-L/2 < z < L/2$  and zero elsewhere, where for performance reasons a smooth transition region must be specified by the **b1** parameter. The exact equation for  $A(z)$  is an Enge function given by:

$$A(z) = \frac{1}{1 + e^{b1(-z-L/2)}} + \frac{1}{e^{b1(+z-L/2)}} - 1$$

where we note that the dimensions of **b1** are inverse meter and where  $\int_{-\infty}^{\infty} A(z) dz = L$ .

Default  $B(z) = 1$  and this implies that *emitting* particles can contribute to the wake even if they are outside the boundaries of this element. When this is not desired, the "**LimitZemission**" option can be used to limit the range of emission to the same range as the location of this element, including the transition region. Setting this option implies  $B(z) = A(z)$ .

The segments of the 1D profile are calculated using anisotropic meshing analogous to the **spacecharge3Dmesh** and **CSR1D** models: Smaller segments are created at higher line charge density, but

such that low charge regions will not result in excessively large segments. The wake function(s) are user defined in the file **wakefields.gdf**, tabulated using the **z**, **Wx**, **Wy** and **Wz** columns. If one of these columns is not present, or not desired, an empty string must be specified.

Please note that the convolution is over the *longitudinal* coordinate, and the column specifying the lag behind the test-particle must be given in units of meters, not seconds. This matches a time-domain simulation code such as GPT, but it is not following the usual convention for how wakes are specified. Another difference with some codes is that GPT calculates *fields* over the entire element, not an integrated effect at the very end. To aid debugging wakefields, the normal time output of GPT can be used to plot these fields.

The code is implemented using a combination of openMP and MPI and performs well on both multi-core and/or multi-node machines. Further options to affect the meshing and to adjust the fields are given below.

Option	Default	Description
"MeshNfac", <b>Nfac</b>	1	The total number of segments $N_{\text{seg}}$ in the 1D profile is given by the equation $N_{\text{seg}} = \text{Nfac} * N^{\text{Npow}}$ where $N$ is the total number of particles.
"MeshNpow", <b>Npow</b>	0.5	
"MeshAdapt", <b>adapt</b>	0.5	The length of the 1D-segments is adjusted to 1D line charge density raised to the power <b>adapt</b> . Consequently, setting <b>adapt</b> to 0 creates segments of equal length while a value of 1 gives segments that are two times longer when the current is half.
"FieldFactorWx", <b>fac</b>	1	Multiply transverse x-wakes by <b>fac</b>
"FieldFactorWy", <b>fac</b>	1	Multiply transverse y-wakes by <b>fac</b>
"FieldFactorWz", <b>fac</b>	1	Multiply longitudinal wakes by <b>fac</b>
"Gminmax", <b>Gmin</b> , <b>Gmax</b>	1, $\infty$	Only consider emitting particle having a Lorentz factor between <b>Gmin</b> and <b>Gmax</b> .
"LimitZemission"	false	Only consider emitting particles that are within the range of this element.

#### 4.12.4.1 Example:

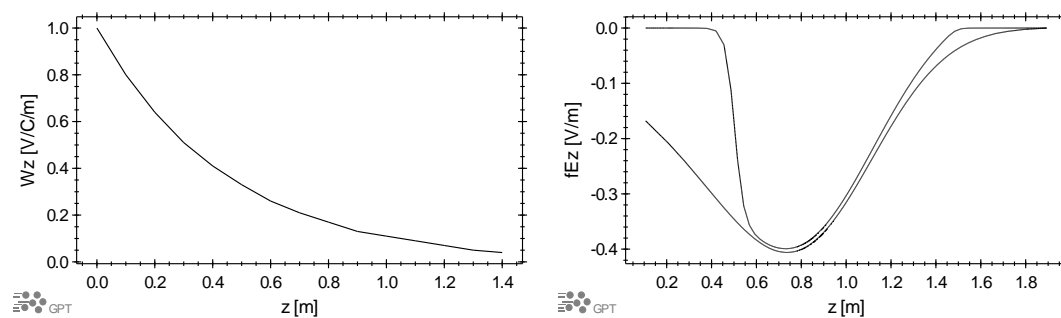
Below is an example, admittedly a bit fabricated, to visualize the effect of the overall length of the structure. We show the effect of a longitudinal wake with exponential decay on a Gaussian bunch, where the bunch is in the center of the structure at  $z=1$  m. The decay of the wake is of the order of the length of the structure, and so is the bunchlength. This leads to the following inputfile:

```

1. # Set particles
2. setparticles("beam",10000,me,qe,-1) ;
3. setzdist("beam","g",1,.3,3,3) ;
4.
5. # Wakefield
6. wakefield("wcs","z",1, L,50, "testwaves.gdf", "z","","","Wz") ;
7.
8. # Output
9. tout(0) ;

```

The results for  $L=1$  and  $L=10$  m are shown below. Due to the nature of wakefields, the maximum field amplitude trails behind the peak in line density at  $z=1$  m. However, the shorter structure reduces the interaction with the front and back of the bunch in two ways: Firstly, particles upstream the end of the structure have reduced interaction, leading to a lower overall field amplitude. Secondly, particles downstream the end of the structure observe lower fields. These are two different effects, caused by the two different  $A(z)$  expressions in the field equations.



Left: Longitudinal wake with exponential decay, read using an ASCII table and converted to GDF using GDF2A. Right: Longitudinal electric field of a Gaussian test-bunch, centered at  $z=1$  m with  $\sigma=0.3$  m. The two different lines represent a structure with an overall length of 1 and 10 meter.

## 4.13 Obsolete elements

This section contains variables and elements maintained for backward compatibility. Please use the indicated alternatives when creating a new GPT inputfile.

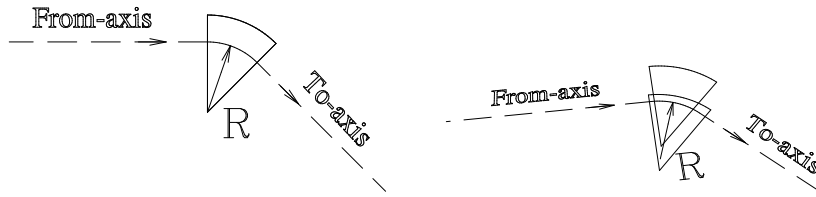
4.13.1	Bend.....	223
4.13.2	Bz.....	223
4.13.3	Ezcell.....	224
4.13.4	m.....	225
4.13.5	q.....	225
4.13.6	SetCathode.....	225
4.13.7	Setmacro.....	225
4.13.8	StartCathode .....	226
4.13.9	Start .....	227
4.13.10	Startcyl.....	227
4.13.11	Startgrid .....	229
4.13.12	Startpar .....	229
4.13.13	StartpGB .....	229

### 4.13.1 Bend

**bend**(**fromCCS**,**toCCS**,**R**,**Bfield**) ;

Bending magnet.

Obsolete element, please use **sectormagnet** instead.



<b>fromCCS</b>	Name of the CCS the particles start on.
<b>toCCS</b>	Name of the CCS the particles are bent to.
<b>R</b>	Radius of the bend [m].
<b>Bfield</b>	<b>B</b> field in the bending magnet [T]. Normally this is $\pm mc\gamma\beta/qR$ .

This element is an idealized bending magnet with a **B** field perpendicular to the **z**-directions of both the **fromCCS** and **toCCS**. The geometry is that of a wedge with the two straight sides perpendicular to the **z**-directions of the axes. When the axes do not intersect or when they are parallel, this element can not be used.

We define **d** and **e** as the **z**-directions and **C** as the intersection of the **fromCCS** and **toCCS**. The **B** field generated by this element<sup>7</sup> is given by:

$$\mathbf{B} = \begin{cases} \mathbf{Bfield} \frac{\mathbf{d} \times \mathbf{e}}{|\mathbf{d} \times \mathbf{e}|} & \text{if } \mathbf{r} \cdot \mathbf{d} - \mathbf{C} \cdot \mathbf{d} > -\frac{|\mathbf{d} \times \mathbf{e}|}{1 + \mathbf{d} \cdot \mathbf{e}} R \text{ and } \mathbf{r} \cdot \mathbf{e} - \mathbf{C} \cdot \mathbf{e} > -\frac{|\mathbf{d} \times \mathbf{e}|}{1 + \mathbf{d} \cdot \mathbf{e}} R \\ 0 & \text{otherwise} \end{cases}$$

In other words: It is the CCS specification that defines the geometry of the magnet, not the magnetic field.

### 4.13.2 Bz

**bz**(**ECS**,**filename**,**I**) ;

Axial global Bz-field.

Obsolete element: Please use **map1D\_B** instead.

<b>ECS</b>	Element Coordinate System.
------------	----------------------------

<sup>7</sup> In reality, half a bending magnet is constructed on the **fromaxis** and the other half on the **toaxis**. When a particle leaves one half of the bending magnet it is placed on the other axis to go through the remaining part of the bend.

**filename** File with  $B_z$  samples of the **B** field along the **z**-axis in [T]. The file must have the following layout:

#	Comment	Optional
<b>N</b>		Number of given <b>Bz</b> samples
<b>z<sub>1</sub></b>	<b>Bz<sub>1</sub></b>	z: <b>z</b> positions of samples
<b>z<sub>2</sub></b>	<b>Bz<sub>2</sub></b>	Bz: <b>B</b> field in <b>z</b> direction at (0,0,z)
<b>z<sub>3</sub></b>	<b>Bz<sub>3</sub></b>	
<b>⋮</b>	<b>⋮</b>	
<b>z<sub>N</sub></b>	<b>Bz<sub>N</sub></b>	

**I** Multiplication factor for **B**.

The  $B_z$  samples along the **z**-axis are specified in an external file. The **B** field generated by this element is given by:

$$\mathbf{B} = \mathbf{I} \left( -\frac{x}{2} \frac{dB_z}{dz}, -\frac{y}{2} \frac{dB_z}{dz}, B_z \right)$$

These fields are only correct near the **z**-axis of the element. A so-called ‘natural cubic spline’ is calculated from the given (**z**,**Bz**) points. It is recommended to specify more points at positions where the first derivative fluctuates significantly.

### 4.13.3 Ezcell

**ezcell(ECS,filename,Ezef,phi,w) ;**

Standing wave resonant cavity.

Obsolete element: Please use **map1D\_TM** instead.

**ECS** Element Coordinate System.

**filename** File with  $E_z$  samples of the **E** field along the **z**-axis. The file must have the following layout:

#	Comment	Optional
<b>N</b>		Number of given <b>Ez</b> samples
<b>z<sub>1</sub></b>	<b>Ez<sub>1</sub></b>	z: <b>z</b> -positions of samples
<b>z<sub>2</sub></b>	<b>Ez<sub>2</sub></b>	Ez: <b>E</b> field in <b>z</b> -direction at (0,0,z)
<b>z<sub>3</sub></b>	<b>Ez<sub>3</sub></b>	
<b>⋮</b>	<b>⋮</b>	
<b>z<sub>N</sub></b>	<b>Ez<sub>N</sub></b>	

**Ezef** Multiplication factor.

**phi** Phase factor:  $\phi$  in radians.

**w** Angular frequency:  $\omega$  in  $[s^{-1}]$ .

This element can be used to simulate a standing wave resonant cavity where the actual  $E_z$  field is known. It has been designed to simulate a single-cell prebuncher.

The fields generated by this element in cylindrical coordinates are given by:

$$E_z = \mathbf{Ez} \mathbf{Ezef} \cos(\omega t + \phi)$$

$$E_r = -\frac{r}{2} \frac{d\mathbf{Ez}}{dz} \mathbf{Ezef} \cos(\omega t + \phi)$$

$$B_\phi = \frac{r\omega \mathbf{Ez}}{2c^2} \mathbf{Ezef} \sin(\omega t + \phi)$$

The fields are only correct near the **z**-axis of the element. A so-called ‘natural cubic spline’ is calculated from the given (**z**,**Ez**) points. It is recommended to specify more points at the positions where the first derivative fluctuates significantly.

Combining the Maxwell equations in vacuum  $\nabla \times \mathbf{E} = -\partial \mathbf{B} / \partial t$  and  $\nabla \times \mathbf{B} = \mu_0 \epsilon_0 \partial \mathbf{E} / \partial t$  imposes the following restriction on the sampled electric field profile on axis:  $\omega^2 \mathbf{Ez} + c^2 \mathbf{Ez}'' = 0$ . Previous implementations of **ezcell** used the second derivative to obtain the  $B_\phi$  field, producing less accurate results.

#### 4.13.4 m

**m=expression ;**

Specifies the mass of an elementary particle.

Obsolete element: Please use **setparticles** instead.

**expression** Particle mass in kg. If not specified, the mass of an electron,  $9.10953e-31$  kg, is taken..

#### 4.13.5 q

**q=expression ;**

Specifies the charge of an elementary particle.

Use **setparticles** instead.

**expression** Particle charge in Coulomb. If not specified, the charge of an electron,  $-1.6021892e-19$  C is taken.

#### 4.13.6 SetCathode

**setcathode(set,Ra,Rc,kT) ;**

Modify a particle set according to a spherical cathode.

Obsolete element: Please use the new particle-set functions instead.

**set** Particle set.  
**Ra** Aperture [m].  
**Rc** Curvature radius [m]. Specify zero for a flat surface.  
**kT** Temperature [eV], not yet implemented. Please use the general start elements.

This element modifies a particle distribution for the simulation of a spherical cathode as shown in Figure 4-23.

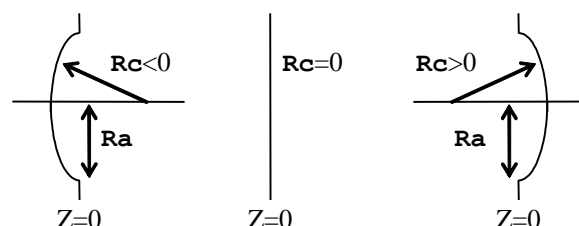


Figure 4-23: Spherical cathode for negative, zero and positive **Rc**.

The particle coordinates in real space are modified by:

$$z_i = z_i \pm \left( \sqrt{Rc^2 - r_i^2} - \sqrt{Rc^2 - Ra^2} \right)$$

where the + indicates a positive **Rc**, the – indicates a negative **Rc**. All particles with a radius larger than **Ra** are removed from the particle set.

The **startcathode** element must be used to generate the particles as function of time. When **startcathode** is not used, all particles will be started at  $t=0$ .

#### 4.13.7 Setrmacro

**setrmacro(set,radius) ;**

Sets the radius of the macro-particles in a set.

Obsolete element: Please use **setrmacrodists** instead.

**set** Particle set.  
**radius** Radius of particles [m].

This element can be used to specify the radius of the particles in a set.

### 4.13.8 StartCathode

**startcathode**(ECS, set, Ra, Rc, Lc, dzdt, dtmax) ;

Continuously add particles emerging from a spherical or flat surface during the simulation. For photo-cathode simulations, a curved laser front can be taken into account.

Obsolete element: Please use the new particle-set functions instead.

<b>ECS</b>	Element Coordinate System.
<b>set</b>	Particle set.
<b>Ra</b>	Aperture [m].
<b>Rc</b>	Cathode curvature radius [m]. Specify zero for a flat surface. When not zero, the <b>setcathode</b> element must be used before.
<b>Lc</b>	Laser curvature radius [m]. Specify zero for a flat laser front or when not applicable.
<b>dzdt</b>	Linear transformation between z-position and time in [m/s], may be negative.
<b>dtmax</b>	Maximum allowed extrapolation [s]. Specify 0 to start all particles one-by-one. A larger value speeds up the simulation, at the cost of accuracy.

This element can be used for the simulation of a spherical cathode or a continuous beam. It starts particles during the simulation according to a distribution, as defined using the regular start and set elements. However, the  $z$ -coordinate is used as time coordinate by dividing by **dzdt**. When simulating a spherical cathode, the previous element must be **setcathode**, with identical **Ra** and **Rc** parameters. When a photo-cathode is simulated, an optional curvature of the laser front, **Lc**, can be specified to account for the difference in arrival time between the center and the edge of the laser pulse on the cathode.

The 2.4 **spacecharge** routine should never be used in combination with **startcathode**. Instead, use **spacecharge3D** in the following way:

1. **setrmacro**(macro-particle-radius) ;
2. **spacecharge3D**() ;

For a flat surface and laser front, all particles emerge at the  $z=0$  plane of the ECS of **startcathode**, but only one particle is started at  $t=0$ . The other particles follow at later times  $t_i$ , depending on their  $z$ -distribution and **dzdt**, the transformation between position and time:

$$t_i = \frac{z_{\max} - z_i}{dzdt}$$

The energy of an individual particle will not influence the moment that it is added to the simulation. It is as if the previously specified bunch moves with constant longitudinal velocity **dzdt** towards the cathode. When a particle crosses the boundary, it emerges with the specified velocities. When a particle is added to the simulation, a small extrapolation is performed to compensate for the fact that timesteps normally don't coincide with precise plane boundaries:

$$\begin{aligned}\Delta t_i &= t - t_i \\ x_i &= x_i + \Delta t_i c \beta x_i \\ y_i &= y_i + \Delta t_i c \beta y_i \\ z_i &= \Delta t_i c \beta z_i\end{aligned}$$

Finally  $r$  and  $\beta r$  are transformed to the ECS of **startcathode**.

When the laser front is not flat, i.e. **Lc** is not zero, **startcathode** accounts for the different arrival time of the light, as shown in Figure 4-24. A positive **Lc** indicates that the center of the beam is illuminated first and a zero **Lc** indicates a flat laser front. The equations are modified accordingly:

$$t_i = \frac{z_{\max} - z_i}{dzdt} \mp \frac{\left( \sqrt{Lc^2 - r_i^2} - \sqrt{Lc^2 - La^2} \right)}{c}$$

The equations for a spherical cathode are analogous to those of a flat surface. The only difference is that particles are not positioned at the  $z=0$  plane of the ECS of **startcathode**, but at the spherical cathode boundary:



$$z_i = \pm \left( \sqrt{Rc^2 - Ra^2} - \sqrt{Rc^2 - r_i^2} \right)$$

$$t_i = \frac{(z_{\max} - z_i) \mp \left( \sqrt{Rc^2 - r_i^2} - \sqrt{Rc^2 - Ra^2} \right)}{dzdt} \mp \frac{\left( \sqrt{Lc^2 - r_i^2} - \sqrt{Lc^2 - La^2} \right) - \left( \sqrt{Rc^2 - r_i^2} - \sqrt{Rc^2 - Ra^2} \right)}{c}$$

where the signs of **Rc** and the final z-coordinates are identical, as shown in Figure 4-24.

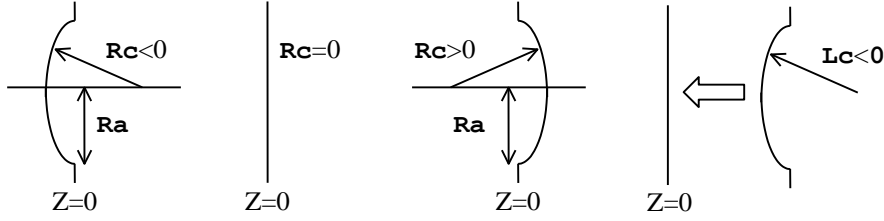


Figure 4-24: Spherical cathode for negative, zero and positive **Rc**.

### 4.13.9 Start

**start**(**ECS**,**startfile**) ;

Reads the initial coordinates of the macro-particles from a file. Particles are added to the particle set "**beam**".  
Obsolete element: Please use **setfile** instead.

**ECS** Element Coordinate System. The coordinates of the particles are interpreted relative to the ECS specified here. If no transformation is needed, the identity transformation must be specified: "**wcs**", "**I**".

**startfile** File with the initial coordinates of the particles. If the file is a GPT outputfile with a **tout(t)** ; statement, this group must be specified by a **time=t** ; statement above **start**. If the file is an ASCII file it must have the following layout:

#	Comment					Optional
<b>N</b>						Number of particles
<b>x<sub>1</sub></b>	<b>y<sub>1</sub></b>	<b>z<sub>1</sub></b>	<b>βx<sub>1</sub></b>	<b>βy<sub>1</sub></b>	<b>βz<sub>1</sub></b>	Particle 1
<b>x<sub>2</sub></b>	<b>y<sub>2</sub></b>	<b>z<sub>2</sub></b>	<b>βx<sub>2</sub></b>	<b>βy<sub>2</sub></b>	<b>βz<sub>2</sub></b>	Particle 2
<b>x<sub>3</sub></b>	<b>y<sub>3</sub></b>	<b>z<sub>3</sub></b>	<b>βx<sub>3</sub></b>	<b>βy<sub>3</sub></b>	<b>βz<sub>3</sub></b>	Particle 3
⋮	⋮	⋮	⋮	⋮	⋮	
<b>x<sub>N</sub></b>	<b>y<sub>N</sub></b>	<b>z<sub>N</sub></b>	<b>βx<sub>N</sub></b>	<b>βy<sub>N</sub></b>	<b>βz<sub>N</sub></b>	Particle N

The initial positions of the particles are read from an external file. This can be the outputfile of a previous run or an ASCII file. The position and velocity are interpreted relative to the specified Element Coordinate System.

The correct way to instruct GPT to restart using the outputfile of a previous run is shown in Listing 4-3 and Listing 4-4.

Listing 4-3: **file1.in**: First inputfile writing output at  $t=3$  to **file1.gdf**

```
1. startgrid( ... )
2. ...
3. tout(3) ;
```

Listing 4-4: **file2.in**: Second inputfile, reading the particle coordinates from **file1.gdf**

```
5. time=3 ;
6. start( "wcs", "I", "file1.gdf" ) ;
7. ...
```

Outputfiles created by MR can also be used. Either use MR again with exactly the same parameter sweep or specify **var=value** above **start** to specify which group has to be used.

### 4.13.10 Startcyl

**startcyl**(**ECS**,**nps**,**E0**,**Emod**,**sigE**,**R**,**div**,**divspr**,**Dmod**,**sigz/psi**, [**omega**])) ;

Specifies the initial distribution in real and velocity space of a cylindrical set of macro-particles. Particles are added to the particle set "**beam**".

Obsolete element: Please use the new particle-set functions instead.

<b>ECS</b>	Element Coordinate System.
<b>nps</b>	Number of macro-particles. <b>nps</b> is truncated to enable a smooth distribution in xy-space. Possible values are 1, 7, 19, 37, 61, 91, 127, 169, 217, 271, 331, 397, 469, 547, ...
<b>Eo</b>	Mean total energy in eV.
<b>Emod</b>	String that determines the energy distribution function. <b>Emod</b> can be "Uniform" or "Gaussian".
<b>sigE</b>	Energy spread in fraction of <b>Eo</b> . Total spread for a uniform distribution and 1/e for a Gaussian distribution.
<b>R</b>	Maximum beam radius.
<b>div</b>	Linear divergence with particle radius. A negative value is allowed.
<b>divspr</b>	Divergence randomly distributed among the particles.
<b>Dmod</b>	String that determines the density distribution function. <b>Dmod</b> can be "Uniform", "Gaussian" or "Class-C".
<b>sigz</b>	Bunch length: Total for a uniform distribution and 1/e for a Gaussian distribution.
<b>psi</b>	Half conduction angle for Class-C modulation.
<b>omega</b>	Modulation angular frequency for Class-C modulation.

The parameters represent a bunch as produced by an electron gun. The default gun orientation is in the z-direction but can be reoriented using the ECS.

The longitudinal velocity distribution can be chosen so that the energy distribution is either "Uniform" or "Gaussian". The corresponding probability density functions are respectively given by:

$$\text{Uniform}^8: \begin{cases} \frac{N}{\sigma_E} & \text{if } -\frac{1}{2}\sigma_E \leq E - E_0 \leq \frac{1}{2}\sigma_E \\ 0 & \text{otherwise} \end{cases}$$

$$\text{Gaussian: } \frac{N}{\sqrt{2\pi}\sigma} \exp\left(-\frac{z^2}{2\sigma^2}\right)$$

The transverse distribution in real space is a homogeneous cylinder with radius **R**.

The transverse distribution in velocity space consists of two independent divergences:

- A divergence **div** linear to the radius of the particle:  $vr = \mathbf{div}(\mathbf{R}/r)$ . It only rotates the phase-space ellipse and therefore does not contribute to the emittance.
- A divergence uniformly distributed in the range  $[0, \mathbf{divspr}]$  which is randomly assigned to the particles. The resulting bunch will have an emittance of **R divspr**.

The longitudinal spatial distribution can be "Uniform" (equidistant), "Gaussian" or "Class-C". The corresponding probability density functions are respectively given by:

$$\text{Uniform}^8: \begin{cases} \frac{N}{\sigma_z} & \text{if } -\frac{1}{2}\sigma_z \leq z \leq \frac{1}{2}\sigma_z \\ 0 & \text{otherwise} \end{cases}$$

$$\text{Gaussian: } \frac{N}{\sqrt{2\pi}\sigma_z} \exp\left(-\frac{z^2}{2\sigma_z^2}\right)$$

$$\text{Class-C}^9: \begin{cases} \frac{Nk_b(\cos(k_b z) - \cos(\psi))}{2(\sin(\psi) - \psi \cos(\psi))} & \text{if } -\frac{\psi}{k_b} \leq z \leq \frac{\psi}{k_b} \\ 0 & \text{otherwise} \end{cases}$$

$k_b = \omega_{gm} v_z$

This element does not position the particles (pseudo) randomly. The used algorithm positions the particles as homogeneous as possible in both real and phase space. Therefore much fewer particles are needed to obtain the same statistics as when using randomly distributed particles. This generally saves GPT a considerable amount of CPU time.

<sup>8</sup> Please note that the total distribution length is specified as  $\sigma$ .

<sup>9</sup> The bunch length can be calculated using  $L = 2\psi/k_b$ .

### 4.13.11 Startgrid

**startgrid**(ECS,Lx,dx,Ly,dy,Lz,dz,[Bx,By,Bz]) ;

Starts the macro-particles in a rectangular grid with equal velocity. Particles are added to the particle set "beam".

Obsolete element: Please use **setstartxyzgrid** instead.

<b>ECS</b>	Element Coordinate System. The coordinates of the particles are interpreted relative to the ECS specified here. If no transformation is needed, the identity transformation must be specified: "wcs", "I"
<b>Lx</b>	Length of array in <b>x</b> -direction. This length may be zero.
<b>dx</b>	Spacing in <b>x</b> -direction.
<b>Ly</b>	Length of array in <b>y</b> -direction. This length may be zero.
<b>dy</b>	Spacing in <b>y</b> -direction.
<b>Lz</b>	Length of array in <b>z</b> -direction. This length may be zero.
<b>dz</b>	Spacing in <b>z</b> -direction.
<b>Bx</b>	Velocities/c of the particles in <b>x</b> -direction. Default 0.
<b>By</b>	Velocities/c of the particles in <b>y</b> -direction. Default 0.
<b>Bz</b>	Velocities/c of the particles in <b>z</b> -direction. Default 0.

The particles start in a rectangular grid centered around the origin. The grid extends from  $-Lx/2, -Ly/2, -Lz/2$  to  $Lx/2, Ly/2, Lz/2$  with spacing **dx,dy,dz**. The orientation and origin can be modified using the ECS.

It is simple to instruct GPT to initialize billions of particles using this keyword. Since GPT has no built-in limit for the number of particles, it must rely on the operating system to indicate an 'out of memory' condition. On some virtual memory machines, this error message can come too late, causing either GPT or the complete system to crash.

### 4.13.12 Startpar

**startpar**(ECS,x,y,z,Bx,By,Bz) ;

Specifies the initial position and velocity of a single macro-particle. Particles are added to the particle set "beam".

Obsolete element: Please use **setstartpar** instead.

<b>ECS</b>	Element Coordinate System. The coordinates of the particle are interpreted relative to the ECS specified here. If no transformation is needed, the identity transformation must be specified: "wcs", "I".
<b>x</b>	x-coordinate of the particle.
<b>y</b>	y-coordinate of the particle.
<b>z</b>	z-coordinate of the particle.
<b>Bx</b>	Velocity/c of the particle in the <b>x</b> -direction.
<b>By</b>	Velocity/c of the particle in the <b>y</b> -direction.
<b>Bz</b>	Velocity/c of the particle in the <b>z</b> -direction.

The ECS is obsolete here because the **x,y,z** and **Bx,By,Bz** parameters are sufficient to specify any position and any velocity. It is introduced for compatibility with other **start** functions.

### 4.13.13 StartpGB

**startpargb**(ECS,x,y,z,GBx,GBx,GBz) ;

Specifies the initial position and velocity of a single macro-particle. Particles are added to the particle set "beam".

Obsolete element: Please use **setstartpar** instead.

<b>ECS</b>	Element Coordinate System. The coordinates of the particle are interpreted relative to the ECS specified here. If no transformation is needed, the identity transformation must be specified: "wcs", "I".
<b>x</b>	x-coordinate of the particle.
<b>y</b>	y-coordinate of the particle.
<b>z</b>	z-coordinate of the particle.

<b>GB<math>\mathbf{x}</math></b>	Momentum $\gamma\beta$ of the particle in the $\mathbf{x}$ -direction.
<b>GB<math>\mathbf{y}</math></b>	Momentum $\gamma\beta$ of the particle in the $\mathbf{y}$ -direction.
<b>GB<math>\mathbf{z}</math></b>	Momentum $\gamma\beta$ of the particle in the $\mathbf{z}$ -direction.

# References

---

- 1 H. Niederreiter, *Random Number Generation and Quasi-Monte Carlo Methods*, SIAM Philadelphia, 1992.
- 2 William H. Press, Brian P. Flannery, Saul A. Teukolsky and William T. Vetterling, *Numerical Recipes, The Art of Scientific Computing*, Cambridge University Press, 2nd edition, 1992.
- 3 Francis F. Chen, *Introduction to plasma physics and controlled fusion*, Plenum Press, New York, 1984, Section 2.3.3.
- 4 J.H. Billen, L.M. Young, POISSON SUPERFISH, Los Alamos National Lab. Report LA-UR-96-1834.
- 5 M. Borland, *A Self-Describing File Protocol for Simulation Integration and Shared Postprocessors*, Proceedings of the PAC 1995 Conference.
- 6 S. Ramo, J.R. Whinnery, T. van Duzer, *Fields and waves in communication electronics*, John Wiley & Sons, 2<sup>nd</sup> edition, 1984, pp. 493.
- 7 G. Saxon, Private communication.
- 8 J.D. Jackson, *Classical Electrodynamics*, John Wiley & Sons, New York, 3<sup>rd</sup> edition, 1998, pp 130.
- 9 J. Barnes, P. Hut, *A hierarchical  $O(N \log N)$  force-calculation algorithm*, Nature **324**, 1986, p. 446.
- 10 J.E. Barnes, *A modified tree code: Don't laugh; It runs*, J. Comp. Phys **87**, 1990, p. 161.
- 11 W.J. Duffin, *Electricity and magnetism*, McGraw-Hill Book Company, 4<sup>th</sup> edition, 1990, Chapter 7.10.
- 12 Bas van der Geer, Bruno Muratori, Marieke de Loos, *Tracking Through Analytic Quadrupole Fringe Fields With GPT*, EPAC 2015.
- 13 Ximen Jiye, *Aberration Theory in Electron and Ion Optics*, Academic Press, 1986, pp. 18.
- 14 M. Berz, B. Erdélyi, K. Makino, *Fringe field effects in small rings of large acceptance*, PRST-AB **3**, 2000, 124001 and references therein.
- 15 Thanks to Bruno Muratori, Daresbury Laboratory, UK.
- 16 J.D. Jackson, *Classical Electrodynamics*, John Wiley & Sons, New York, 2<sup>nd</sup> edition, 1975.
- 17 W.L. Briggs, H. van Emden and S. McCormick, *A Multigrid Tutorial*, SIAM Philadelphia, 2<sup>nd</sup> edition, 2000.
- 18 W. Hackbusch, *Multi-Grid Methods and Applications*, Springer, Berlin, 1985.
- 19 J. Barnes, P. Hut, *A hierarchical  $O(N \log N)$  force-calculation algorithm*, Nature **324**, 1986, p. 446.
- 20 J.E. Barnes, *A modified tree code: Don't laugh; It runs*, J. Comp. Phys **87**, 1990, p. 161.
- 21 P. Gibbon, G. Sutmann, *Long-Range Interactions in Many-Particle Simulation*, published in *Quantum Simulations of Complex Many-Body Systems: From Theory to Algorithms*, J. Grotendorst, D. Marx, A. Muramatsu (Eds.), John von Neumann Institute for Computing, Jülich, NIC Series, Vol. **10**, ISBN 3-00-009057-6, 2002, p. 467.
- 22 C.A.J. van der Geer, 'FELIX design and instrumentation', Thesis 1999, ISBN 90-386-0787-3, pp 23-25.
- 23 J.L.H. Jonker, Philips Res. Rep., 12, 1957, p. 249.
- 24 M.J. de Loos, C.A.J. van der Geer, S.B. van der Geer, A.F.G. van der Meer, D. Oepke, R. Wünsch, Proc. of the 24<sup>th</sup> Int. Free Electron Laser Conference 2002, Argonne, USA.



# Index

## A

abs ..... 121  
 accelerating structures ..... 147  
 acceptance ..... 139  
 accuracy ..... 25, 64, 140  
 acos ..... 121  
 acosh ..... 121  
 adaptive mesh ..... 193  
 addGoscillation ..... 133  
 addGzoscillation ..... 136  
 addXdiv ..... 137  
 addYdiv ..... 137  
 addZdiv ..... 137  
 addzoscillation ..... 130  
 and ..... 120  
 angle of incidence ..... 30  
 ASCII2GDF ..... 85, 174  
 ascii ..... 85  
 asin ..... 121  
 asinh ..... 121  
 aspect ratio ..... 195  
 associativity ..... 120  
 ASTRA ..... 86  
 ASTRA2GDF ..... 86  
 atan ..... 121  
 atanh ..... 121  
 AutoCAD ..... 51, 91  
 averages ..... 98  
 avg ..... 49  
 avgBx ..... 98  
 avgBy ..... 98  
 avgBz ..... 98  
 avgfBx ..... 98  
 avgfBy ..... 98  
 avgfBz ..... 98  
 avgfEx ..... 98  
 avgfEy ..... 98  
 avgfEz ..... 98  
 avgG ..... 98  
 avgp ..... 98  
 avgr ..... 98  
 avgt ..... 98  
 avgx ..... 98  
 avgy ..... 98  
 avgz ..... 98

## B

backtracking ..... 34  
 barmagnet ..... 159  
 batch file ..... 43  
 beamloading ..... 153  
 bend ..... 223  
 bitmap ..... 131  
 Bmultipole ..... 160  
 boundary conditions ..... 194  
 boundary elements ..... 29  
 bounding box ..... 191  
 bounding-box ..... 29

Broydens method ..... 35  
 buncher ..... 151, 152, 153, 224  
 Bx ..... 26, 142, 143, 144  
 By ..... 26, 142, 143, 144  
 bz ..... 223  
 Bz ..... 26, 142, 143, 144  
 bzsolenoid ..... 162

## C

c ..... 121  
 cathode ..... 126  
 cbrt ..... 121  
 ccs ..... 212  
 CCS ..... 13  
 ccsflip ..... 212  
 ceil ..... 121  
 circlecharge ..... 155  
 Coherent Synchrotron Radiation ..... *See* CSR  
 collector ..... 203  
   design with GPT ..... 29  
   scattering ..... *See* scatter  
 Collision ..... 212  
 concatenation ..... 120  
 cone ..... 204, 205  
 constants in inputfile ..... 121  
 coordinate systems  
   custom ..... 13  
   element ..... 12  
   world ..... 12  
 copperscatter ..... 203  
 cos ..... 121  
 cosh ..... 121  
 cosine distribution ..... 21  
 Courant Snyder parameters ..... 100  
 cputime ..... 27, 102  
   limit ..... 214  
 CSalphax ..... 100  
 CSalphay ..... 100  
 CSalphaz ..... 100  
 CSbetax ..... 100  
 CSbetay ..... 100  
 CSbetaz ..... 100  
 CSgammax ..... 100  
 CSgammay ..... 100  
 CSgammaz ..... 100  
 CSR ..... 216  
 CST MW-studio ..... 184  
 Ctrl-C ..... 11  
 curved  
   cathode ..... 126  
   laser front ..... 126  
 Custom Coordinate System.CCS

## D

dBx\_50 ..... 101  
 dBy\_50 ..... 101  
 dBz\_50 ..... 101  
 defined ..... 121

deg ..... 121  
 del ..... 214  
 Delta error indicator ..... 25  
 dipole ..... 165  
 Dirichle boundaries ..... 194  
 distribution  
   ascending order ..... 23  
   cosine ..... 21  
   descending order ..... 23  
   file ..... 21  
   full random order ..... 23  
   Gaussian ..... 19  
   Hammersley order ..... 23  
   linear ..... 20  
   quadratic ..... 20  
   random order ..... 23  
   sphere ..... 21  
   uniform ..... 19  
 drift ..... 213  
 dt\_50 ..... 101  
 dtmax ..... 141  
 dtmaxt ..... 141  
 dtmin ..... 141  
 dtstart ..... 141  
 dx\_50 ..... 101  
 DXF ..... 91  
 DXF export ..... 91  
 dy\_50 ..... 101  
 dz\_50 ..... 101

## E

e ..... 121  
 ECS ..... 12  
   specifying ..... 12  
 ecyl ..... 155  
 ehole ..... 156  
 Einzel lens ..... 156  
 electrostatic elements ..... 155  
 elegant ..... 144  
 element  
   accelerating structures ..... 147  
   field maps ..... 174  
   global ..... 12  
   local ..... 12, 213  
   miscellaneous ..... 212  
   obsolete ..... 223  
   start ..... 123  
   static electric ..... 155  
   static magnetic ..... 159  
 Element Coordinate System ECS  
 else ..... 120  
 emittance ..... 99  
 Enge function ..... 169  
 Enhanced Metafile ..... 51  
 environment variable ..... 122  
 eps0 ..... 121  
 erect ..... 157  
 erf ..... 121  
 erfc ..... 121  
 exp ..... 121

exp2.....121  
 expm1 .....121  
 exporting graphics .....51  
 ezcell .....224

**F**

factorial.....120  
 fBx .....26, 144  
 fBy .....26, 144  
 fBz.....26, 144  
 FEL .....216  
 fEx.....26, 144  
 fEy.....26, 144  
 fEz.....26, 144  
 field maps.....174  
 file distribution.....21  
 FINT .....169  
 FISH.....87  
 FISH2GDF.....87, 174  
 FISHFILE .....89  
 floor.....121  
 floorplan.....144  
 forwardscatter .....30, 203  
 Free Electron Laser.....*See* FEL  
 fringe fields.....169  
 functions in inputfile.....121, 122

**G**

G .....26, 142, 143, 144  
 gap.....168  
 gaussian modes.....216  
 gauss00mf.....216  
 Gaussian distribution .....19  
 GDF .....28  
 GDF2A .....45, 90  
 GDF2DXF .....91  
 GDF2GDF .....92  
 GDF2HIS .....93  
 GDF2SDDS .....94  
 GDF2VTP.....95  
 GDFA .....44, 50, 97  
   averages.....98  
   Courant Snyder parameters  
     .....100  
   Emittance.....99  
   Robust estimates.....101  
   standard deviations.....98  
 GDFFLATTEN.....103  
 GDFMGO .....31, 37, 59, 104  
   optimize.....106  
   options.....105  
   output.....107  
   variables.....106  
 GDFSELECT.....109  
 GDFsolve  
   optimizer.....36  
   root finder.....32  
 GDFSOLVE .....31, 55, 110  
   constraints.....111  
   optimize.....112  
   options.....111  
   output.....112  
   variables.....111  
 GDFTRANS .....44, 49, 114  
 Geer, S.B. van der.....ii  
 General Particle Tracer..*See* GPT

genetic optimization .....37  
 getenv .....122  
 Gminmax .....210  
 GPT  
   commandline.....9  
   equations of motion.....**Error!**  
     **Not a valid bookmark in**  
     **entry on page 24**  
   errors .....11  
   output .....**Error! Not a valid**  
     **bookmark in entry on**  
     **page 26**  
   Runge-Kutta.....**Error! Not a**  
     **valid bookmark in entry**  
     **on page 25**  
   running .....9  
   stopping.....11  
   verbose .....9  
   warnings .....11  
 GPT Datafile Format... *See* GDF  
 GPTLICENSE .....9, 44  
 GPTwin.....46  
 gravity.....213  
 grayscale.....131

**H**

*h* .....25, 141  
 Hammersley.....17  
 help .....46  
 Hessian .....36  
 Histograms.....93

**I**

ID .....26, 142, 143, 144  
 if statement .....120  
 image .....131  
 initial particle distribution .....16,  
 123  
 inputfile.....42  
 intersection point .....30  
 iris .....206  
 isectormagnet.....162

**J**

Jacobian .....34

**L**

laser front.....126  
 laser image.....131  
 lgamma .....121  
 license .....*See* GPTLICENSE  
 linac .....151, 152, 153  
 linear distribution.....20  
 linecharge .....157  
 linecurrent.....164  
 Litvinenko.....216  
 log .....121  
 log10.....121  
 log1p.....121  
 log2 .....121  
 longitudinal emittance .....99  
 Loos, M.J. de .....ii  
 Low discrepancy sequence .....17

**M**

m .....121, 225  
 ma .....121  
 MAD.....169  
 magdipole .....165  
 magline .....165  
 magnetic  
   charge.....159  
   scalar potential .....159  
 magnetostatic elements.....159  
 magnets.....159  
 magplate .....165  
 magpoint.....166  
 map1D\_B.....175  
 map1D\_E.....176  
 map1D\_TM .....176  
 map25D\_B.....180  
 map25D\_E.....180  
 map25D\_TM .....87, 181  
 map2D\_B.....87, 177  
 map2D\_E.....79, 82, 87, 177  
 map2D\_Er .....82  
 map2D\_Et.....178  
 map2D\_V .....179  
 map2Dr\_E .....79, 87, 179  
 map3D\_B.....186  
 map3D\_E.....181  
 map3D\_Ecomplex .....183  
 map3D\_Hcomplex.....185  
 map3D\_remove .....187  
 map3D\_TM .....182  
 map3D\_V .....185  
 max .....49  
 max-min.....49  
 me .....121  
 Mean.....101  
 medianBx.....101  
 medianBy.....101  
 medianBz.....101  
 mediant .....101  
 medianx .....101  
 mediany .....101  
 medianz .....101  
 mesh.....188  
   adaptive .....193  
   charge density .....193  
   number of lines .....192  
   position of lines.....192  
 Metafile .....51  
 mgorank.....107  
 mgoviolations .....107  
 Microwave studio .....184  
 min.....49  
 miscellaneous elements .....212  
 mp .....121  
 mpi.....104, 116  
 MR.....52, 115  
 mu0 .....121  
 multi-core .....104, 116  
 multi-dimensional.....*See* MR  
 multigrid .....188, 194  
 multiple run .....*See* MR  
 multislit.....210

**N**

N .....49



nemirrms ..... 102  
 nemix ..... **102**  
 nemix100 ..... **100**  
 nemix90 ..... **100**  
 nemixrms ..... **99**, 100, 136  
 nemiy ..... **102**  
 nemiy100 ..... **100**  
 nemiy90 ..... **100**  
 nemiyrms ..... **99**, 100, 136  
 nemiz100 ..... **100**  
 nemiz90 ..... **100**  
 nemizrms ..... **99**  
 Neumann boundaries ..... 194  
 Newton-Raphson ..... 32  
 normalization ..... 99  
 number ..... **122**  
 numpar ..... **102**

## O

obsolete elements ..... **223**  
 open boundaries ..... 194  
 operators in inputfile ..... **120**  
 optimization ..... 54, 55  
   genetic ..... 37  
   multi-objective ..... 59  
   root-finder ..... 57  
   scanning with MR ..... 58  
   single-objective ..... 55  
   using derivatives ..... 36  
 or ..... **120**  
 outliers ..... 211  
 output control ..... **139**  
 outputvalue ..... **141**  
 overlaptest ..... **213**

## P

PANDIRA ..... 87  
 parameter file ..... 115  
 parameter scan ..... 115  
 ParaView ..... 95  
 particle distribution ..... **16**, **123**  
 periodic boundaries ..... 194  
 photo-cathode ..... 74  
 photoemission ..... 131  
 pi ..... **121**  
 pipe ..... **206**  
 plate ..... **207**  
 platecharge ..... **157**  
 pointcharge ..... **157**  
 pointchargeset ..... **158**  
 Poisson ..... 188  
 POISSON ..... 87  
 pp ..... **141**  
 precedence of operators ..... **120**

## Q

q ..... **121**, **225**  
 Q ..... **102**  
 qe ..... **121**  
 quadratic distribution ..... **20**  
 quadrupole ..... 43, **166**

## R

radius ..... 129

random ..... **121**  
 randomize ..... **213**  
 Range ..... **101**  
 RAW2GDF ..... **117**, 174  
 rectcoil ..... **167**  
 rectmagnet ..... **168**  
 Remove particles ..... **210**  
 rest-frame ..... 188, 191  
 rm ..... 214  
 rmacro ..... 129  
 rmax ..... **102**, **210**  
 RMS Emittance ..... **99**  
 Robust estimates ..... **101**  
 root finder ..... 32, 57  
 round ..... **121**  
 run ..... 47, **214**  
 Runge-Kutta ..... 25  
 rxy ..... **26**

## S

S ..... **25**, 142  
 safety ..... 25, **142**  
 scan ..... 115  
 scat\_Ein ..... 30  
 scat\_Enet ..... 30  
 scat\_Eout ..... 30  
 scat\_inp ..... 30  
 scat\_nnd ..... 82, 89  
 scat\_nnE ..... 81, 82, 89, 102  
 scat\_nnEor ..... 82, 89  
 scat\_nnphi ..... 82, 89  
 scat\_nnQ ..... 81, 82, 89, 102  
 scat\_nnQor ..... 82, 89  
 scat\_nnr ..... 89  
 scat\_nnrphi ..... 89  
 scat\_nnx ..... 89  
 scat\_nny ..... 82, 89  
 scat\_nnz ..... 89  
 scat\_Qin ..... 30  
 scat\_Qnet ..... 30  
 scat\_Qout ..... 30  
 scat\_x ..... **30**  
 scat\_y ..... 30  
 scat\_z ..... 30  
 scatter ..... 203  
   angle ..... 30  
   boundaries ..... 29, 203  
   elements ..... 29, 30  
   FISHFILE ..... 89  
   GDFA statistics ..... 102  
   unrolled coordinates ..... 89  
 scatterbitmap ..... **204**  
 scattercone ..... **205**  
 scattering ..... 29  
 scatterInn ..... 82, **102**  
 scatteriris ..... **206**  
 scatterpipe ..... **206**  
 scatterplate ..... **207**  
 scatterplot ..... 47  
 scatterPnn ..... 82, **102**  
 scattersphere ..... **207**  
 scattertorus ..... **208**  
 screen ..... 52, **142**  
 SDDS ..... 94  
 sectormagnet ..... **168**  
 setcathode ..... **225**  
 setcharge2Dcircle ..... **201**

setcopy ..... **126**  
 setcurvature ..... **126**  
 setellipse ..... **133**  
 setextrapolate ..... **125**  
 setfile ..... 86, **124**  
 setGBphidist ..... **135**  
 setGBRxydist ..... **134**  
 setGBthetadist ..... **135**  
 setGBXdist ..... **134**  
 setGBXemittance ..... **135**  
 setGBYdist ..... **134**  
 setGBYemittance ..... **136**  
 setGBZdist ..... **134**  
 setGdist ..... **135**  
 setmove ..... **126**  
 setparticles ..... 43, **123**  
 setphidist ..... 43, **133**  
 setreduce ..... **128**  
 setrlimit ..... 108, **214**  
 setrmacro ..... **225**  
 setrmacrodist ..... **129**  
 setrxydist ..... 43, **133**  
 setscale ..... **125**  
 setshuffle ..... **128**  
 setstartline ..... **129**  
 setstartpar ..... **129**  
 setstartxyzgrid ..... **130**  
 setTcopy ..... **127**  
 setTdist ..... 75, **138**  
 settotalcharge ..... **199**  
 settransform ..... **125**  
 setXdist ..... **131**  
 setxydistbmp ..... **131**  
 setYdist ..... **132**  
 setZdist ..... **133**  
 sextupole ..... **171**  
 SF7 ..... 87  
 sin ..... **121**  
 Singular Value Decomposition  
   ..... *See* SVD  
 sinh ..... **121**  
 slit ..... *See* multislit  
 snapshot ..... 43, **142**  
 solenoid ..... 66, **172**  
 spacecharge ..... 14, **188**  
 spacecharge2Dcircle ..... **199**  
 spacecharge2Dline ..... **201**  
 spacecharge3D ..... **198**  
 spacecharge3Dclassic ..... **199**  
 spacecharge3Dmesh ..... **188**  
 spacecharge3Dtree ..... **196**  
 sphere ..... **207**  
 sphere distribution ..... **21**  
 spline ..... 175, 176  
 sqrt ..... **121**  
 standard deviations ..... 98  
 start ..... **227**  
 start elements ..... **16**, **123**  
 startcathode ..... **226**  
 startcyl ..... **227**  
 startgrid ..... **229**  
 startpar ..... **229**  
 startpgb ..... **229**  
 statistics ..... 48  
 std ..... 49  
 stdBx ..... **98**  
 stdBy ..... **98**  
 stdBz ..... **98**

stderr .....9  
 stdG.....**98**  
 stdin.....9  
 stdout.....9  
 stdt.....**98**  
 stdx.....**98**  
 stdxyzmax .....**210**  
 stdy.....**98**  
 stdz.....**98**  
 stepsize.....25  
 stop.....47  
 string .....**122**  
   concatenation.....**122**  
 sum.....49  
 SUPERFISH .....87, 89  
 SVD .....34

**T**

t .....26, 142  
 tan .....**121**  
 tanh .....**121**  
 tcontinue .....79, **143**  
 TE011cylcavity.....**147**  
 TE011gauss.....**147**  
 TE110gauss.....**148**  
 templates .....50  
 TErrectcavity.....**148**  
 TeX .....51

tgamma .....**121**  
 time .....**143**  
 time distribution.....74  
 timestep control .....**139**, 145  
 tlen .....79, 81, 102  
 TM010cylcavity .....**149**  
 TM010gauss .....**150**  
 TM110cylcavity .....**149**  
 TM110gauss .....**149**  
 tmax .....**143**  
 TMrectcavity .....**151**  
 torus .....**208**  
 tout .....**144**  
 trajectories .....49, 114  
 transverse emittance .....99  
 trunc .....**121**  
 trwcell .....**151**  
 trwlinac .....**152**  
 trwlinbm .....**153**

**U**

undueqfo .....**219**  
 unduplan .....**219**  
 uniform distribution.....**19**  
 unrolled coordinates .....80, 89

**V**

viscosity .....**214**  
 VTP export .....**95**

**W**

wakefield .....216, **220**  
 WCS .....**12**  
 Windows Metafile .....51  
 World Coordinate System . WCS  
 writeelegant .....**144**  
 writefloorplan .....**144**  
 writesteps .....**145**

**X**

x .....26, 142, 143, 144  
 xymax .....**211**

**Y**

y .....26, 142, 143, 144  
 YACC .....120

**Z**

z .....26, 142, 143, 144  
 Zcol.....79  
 zminmax .....**211**